Isolation and Characterization of Elicitors

from the Oral Secretion of Lepidoptera Larvae

Dissertation

for the obtainment of the academic degree

doctor rerum naturalium

(Dr. rer. nat.)

submitted to the Council of the Faculty of Chemistry and Geoscience of the
Friedrich-Schiller-Universität Jena

by Master

Huijuan Guo

born on 28.11.1983 in Datong, P.R.China

Gutachter:

1. Prof. Dr. Wilhelm Boland, Max Planck Institute for Chemical Ecology

2. Prof. Dr. Georg Pohnert, Friedrich-Schiller-University Jena

Tag der öffentlichen Verteidigung: 22.01.2014

For my parents

Table of Contents

1 General Introduction

1.1 Plant–insect interactions

Plant–insect interactions are a complex system, which involves multiple interactions between at least four players. Firstly, many insect species are herbivores feeding on plant. Secondly, plants can defend against harmful insects in many ways, for example, they can produce trichomes[1] and thorns as structural defenses. Furthermore, plants can produce chemical compounds that are poisonous to insects[2] as chemical defense, in order to avoid the further eating. Moreover, plants can produce special odors[3] to attract predatory insects. Thirdly, insects have developed ways to overcome plant defenses by coevolution. For example, insects can store and use chemicals from plants by "sequestration"[4], and they can eat toxic plants by filtering out and excreting the toxins by "filtration/resistance"[5]. Interestingly, there are many microorganisms living in the insect gut and there are also many endophyte microorganisms present in the plant. All of them might have significant contribution in the plant–insect interactions. The complex ecosystem involved in the plant–insect interactions is summarized in the **Scheme 1**, diverse chemical factors are involved in these process.
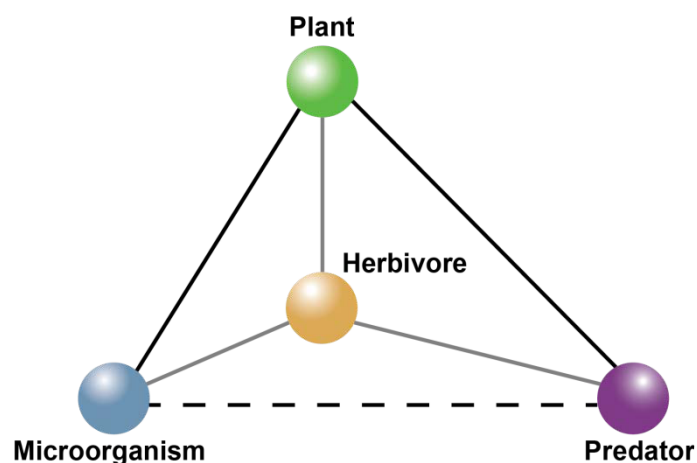
Scheme 1. Possible relationships in the ecosystem of feeding insect on plant

Feeding insects can trigger multiple plant defense responses (**Figure 1**)[6]. Plants directly respond to insect herbivory by inducing biochemical changes that impede pest growth and indirectly by promoting advantageous interactions with beneficial organisms through the release of volatile organic compounds[7,8] (VOC). In general, the earliest detectable signaling events in plant defense responses included plasma membrane depolarization and transmembrane ion

fluxes[9]. Membrane potential (V_m) changes have been found to be a common event when plants interact with different biotrophs and vary depending on the type and feeding habit of the insect. V_m is the result of an imbalance in the quantity of cations and anions across biological membranes, which might be caused by the conformational changes of ion channels[10], as well as formation of new ion channels or pores[11] by the compounds from oral secretions (OS). The V_m of the plasma membrane lies in the range of –120 to –200 mV in plant cell. It might shift either to more negative (hyperpolarization) or to more positive values (depolarization) in response to various biotic or abiotic stresses, following by a fast electrical signal that spreads through the entire plant starting from the wounding point. Recently, a new type of electrical long-distance signal that propagates systemically[12], i.e., from leaf to leaf, the "system potential" (SP) has been reported. It operates by stimulating the plasma membrane H^+-ATPase, which may hold and transport information systemically within the whole plant or at least in parts of the plants. Recently, the glutamate receptor-like gene was found to be involved the leaf-to-leaf wound signaling as a possible mechanism of long-distance wound signaling in plants.[13]
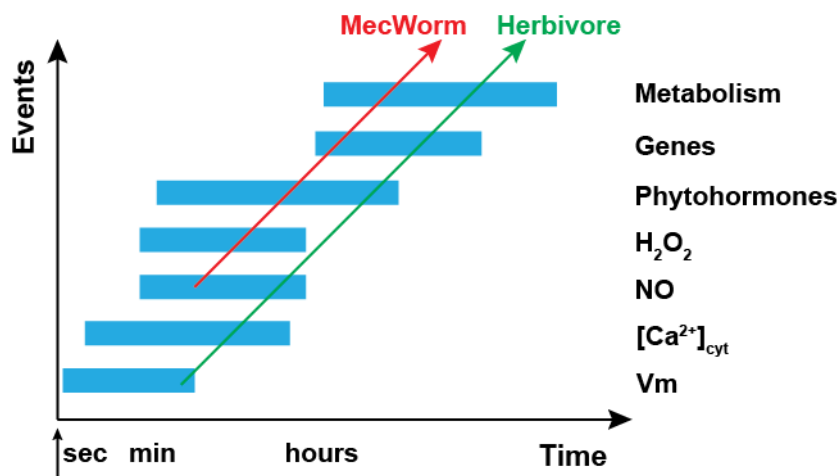
Figure 1. Consecutive events in plant tissues after insect feeding. (cited from ref. 7)

In plant cells Ca^{2+} ions play a physiologically key role as an intracellular second messenger. It is especially important for the maintenance of cellular homeostasis and signal transduction pathways[14]. Under normal condition, the cytosolic Ca^{2+} concentration is about 100 to 200 nM, which is 10^4 times less than that in the apoplastic fluid and 10^4 to 10^5 times less than that in cellular organelles. Ca^{2+} influx, which changes cytosolic Ca^{2+} concentration, is often involved in stress responses and developmental regulation. Herbivore damage induced a strong Ca^{2+} influx in regions 30 to 200 μm away from the damaged zones, which was higher than the mechanical wounding-elicited Ca^{2+} signal[9]. This suggests that an OS-recognition mechanism

plays a role in activating Ca^{2+} influxes. It is likely that herbivore-derived elicitors are bound to as-yet-unidentified receptors for Ca^{2+} influxes to be triggered.

Nitric oxide (NO) is a signaling molecule involved in disease resistance, abiotic stress, cell death, respiration, senescence, root development, germination, and hormone responses[15]. Until now the available information on NO accumulation in response to herbivory or wounding in general is limited and contradictory. For example, wounding tomato (*Lycopersicon esculenttum*) leaves did not cause an increase in NO production[16], whereas a significant amount of NO was produced after wounding of potato (*Solanum tuberosum*) or *Arabidopsis thaliana* plants[17]. Reactive oxygen species (ROSs) are also generated in plant tissues in response to herbivory[18]. In response to herbivores, H_2O_2 levels are likely elevated as long as the attacks persist. In soybean (*Glycine max*), a localized oxidative response in leaves could be detected by herbivore attacks[19]. ROS also represent second messengers that can trigger production of herbivore-induced volatile compounds[20].

The phytohormones often associated with mediating plant responses to insects are jasmonic acid (JA, **1**), salicylic acid (SA, **2**) and ethylene (E). JA (**1**) is the most important hormone that controls plant defense against herbivores. JA (**1**) and its derivatives collectively referred to as jasmonates, which are the key regulators of plant responses to damage and insect herbivory[21]. JA-Ile (**3** and **4**) (**Figure 2**) has been described as active form of JA (**1**), especially the minor component (+)-7-*iso*-JA-L-Ile (**4**) shows high bioactivity and is therefore considered the most important plant endogenous JA (**1**) metabolite[22], rather than (−)-JA-L-Ile (**3**). The precursor of JA (**1**) is *cis*-(+)-12-oxo-phytodienoic acid (*cis*-OPDA, **5**), which also involved into the downstream signal pathway. SA (**2**) is involved in systemic acquired resistance to biotrophic pathogens[23]. However, its role in herbivore-induced responses is less clear. When the crude OS of *S. littoralis* larva was applied on a damaged *A. thaliana* leaf, the elevation of these phytohormones could be detected as an important response to defense[24].
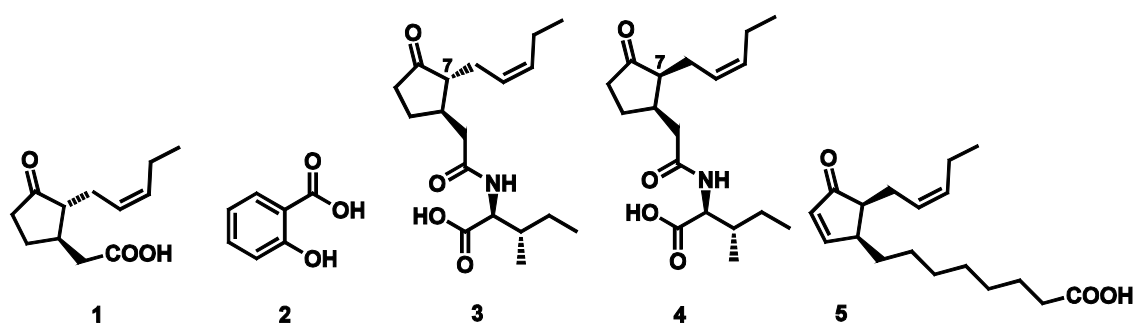
Figure 2. Structures of phytohormones: jasmonic acid (**1**), salicylic acid (**2**), (−)-JA-L-Ile (**3**), (+)-7-*iso*-JA-L-Ile (**4**) and *cis*-(+)-12-oxo-phytodienoic acid (**5**)

Numerous microarray studies analyzing global changes in gene expression after herbivory have confirmed the induced expression of many defensive genes. Moreover, the massive re-programming of gene expression observed in these studies suggested that herbivory results in a shift from growth-oriented to defense-oriented plant metabolism[25]. Plant gene expression induced by OS revealed up-regulation of a gene encoding calmodulin like protein, *CML42*. Most importantly, the *CML42* only responds to the insect OS, not to the mechanical wounding (MecWorm). Calmodulin like proteins (CMLs) are sensor relay proteins that are unique to plants, with 50 members in Arabidopsis. They are defined by the presence of two to six predicted Ca^{2+}-binding EF hand motifs. In plants, Ca^{2+} signaling plays a regulatory role in various developmental processes as well as in pathways involved in response to stimuli such as pathogen attack[26], drought, salinity[27], and temperature shock[28]. Among Ca^{2+}-binding proteins, the EF-hand is the most prevalent structural motif for Ca^{2+}-binding, thus the EF-hand Ca^{2+} sensors often play key roles in the transduction and amplification of cell signals[29]. In the model plant *A. thaliana*, CML42 acts as a CaM-related calcium sensor and plays the important role not only in trichome branching[30], but is shown to be involved as a negative regulator in herbivore deterrence; moreover it acts in UV irradiation protection and the reduction of transpiration[24]. Herbivore induced plant defense signaling is summed in **Figure 3**.[31]
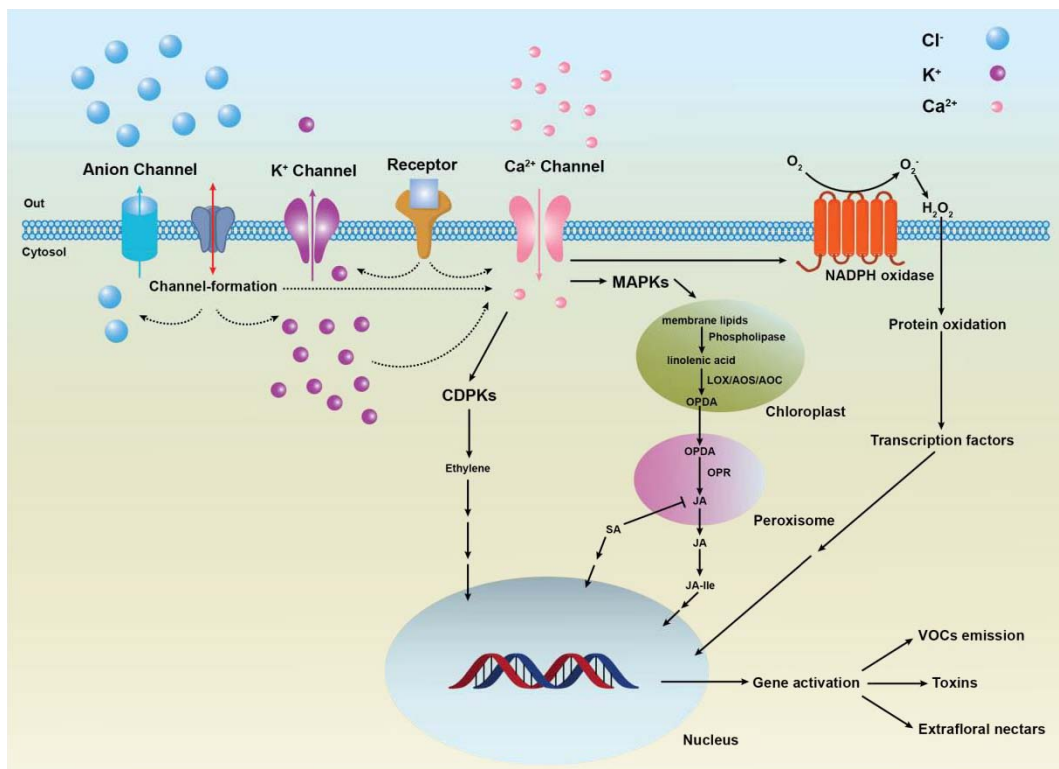
Figure 3. A brief summary of signaling events in a cell in an herbivore-attached leaf.

Leaves normally release small quantities of volatile chemicals, but when the plant was damaged by herbivorous insects, more volatiles are released after some time. The chemical identity of the volatile compounds depends on the plant species and the herbivorous insect species. These volatiles attract both parasitic and predatory insects that are natural enemies of the herbivores. The plants are able to differentiate between herbivore damage and a general wound response, suggesting the presence of elicitors associated with insect feeding that are absent in other types of leaf damage[32]. Typical defense volatile compounds produced by lima bean (*Phaseolus lunatus*) after *S. littoralis* feeding are octen-3-ol (**6**), *cis*-3-hexenyl acetate (**7**), β-ocimene (**8**), linalool (**9**), (*E*)–4,8–dimethyl-1,3,7-nonatriene (DMNT, **10**), $C_{11}H_{14}$ (**11**), methyl salicylic acid (**12**) and (*E,E*)–4,8,12–trimethyl–1,3,7,11–tridecatetraene (TMTT, **13**). The structures of **6–13** are presented in **Figure 4**.
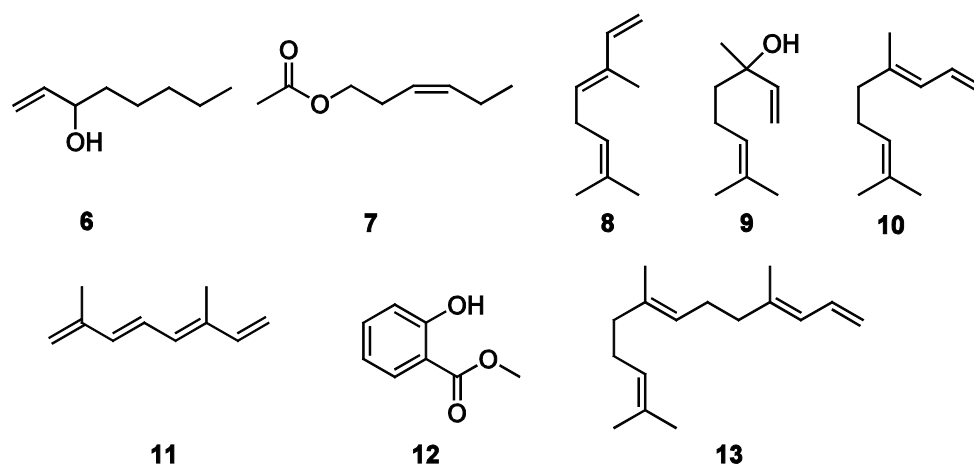
Figure 4. Structures of VOC (6–13): octen-3-ol (**6**), *cis*-3-hexenyl acetate (**7**), β-ocimene (**8**), linalool (**9**), (*E*)–4,8–dimethyl-1,3,7-nonatriene (DMNT, **10**), $C_{11}H_{14}$ (**11**), methyl salicylic acid (**12**) and (*E,E*) –4,8,12–trimethyl–1,3,7,11–tridecatetraene (TMTT, **13**)

Although the individual plant defense events have been widely investigated, only little has been known about the connections between them and their inter-dependence. Moreover, synergistic and antagonistic cross-talk among the signaling pathways is involved in helping the plant to choose the preferred defensive strategy against the attacker[33]. Previously, the fluxes of ions e.g. Na^+, K^+, Cl^- and Ca^{2+} usually result in temporary changes of cell membrane potentials. Recent research reported that, $[Ca^{2+}]_{cyt}$ might not be directly involved in V_m depolarization, rather the induced V_m depolarization appears to be associated to an increased voltage gated K^+ channel activity[34]. In lima bean, reactive oxygen species (ROS) (H_2O_2) release caused V_m depolarization involving Ca^{2+} channels[35]. However in *A. thaliana*, ROS seemed not to be involved in V_m depolarization. Therefore investigation of the connection between

different responses is very helpful to understand the cross-talk among the complex plant defense reactions.

1.2 Elicitors induced plant defense reactions

1.2.1 Plant damaged-self recognition

Insect herbivory on plant consist at least two aspects, the mechanical damage originating from the continuous biting, the chemical factors from the contribution of wounding plant tissue, or from factors in the insect oral secretions (OS). MecWorm is designed as a mechanical caterpillar in order to mimic the continuously mechanical wounding from caterpillars[36]. However this is still a complex process containing the physical damage and the contribution of damaged plant tissue. MecWorm treatment is sufficient to induce the VOC emission in lima bean qualitatively similar to that from real herbivore feeding, indicating that either the mechanical wounding or the elicitors from damaged leaves could trigger the plant defense. After continuously mechanical damage, some molecules are released from outside of cell protoplast and become exposed to enzymes that are localized in different compartments. These released molecules are signatures of "damage self" and might include elicitors of plant defense responses, so called "plant damaged-self recognition"[37]. Fragments of plant-derived molecules are among the first described defense elicitors, for example peptides such as systemin and oligosaccharides such as oligogalacturonides degraded from cell wall-derived pectins. The research therefore indicated that the plant itself contained the molecules that were required for defense induction. Accordingly, the application of leaf extract to slightly wounded lima bean leaves and flame wounding elicited almost the same gene transcriptional patterns as those elicited by JA (**1**)[38].

1.2.2 Elicitors from insect oral secretions

Despite the high number of known plant responses to herbivory, only a few known classes of insect-derived defense elicitors have been discovered. Due to the limited amount of OS and significant bioactivity, the discovery of new elicitors is an extremely challenging work.

The first claimed herbivore-derived elicitor was a β-glucosidase[39] from the gut regurgitant of *Pieris brassicae* caterpillar, which mainly fed on cabbage. It could induce the volatile compounds emission in order to attract the parasitic wasps (*Cotesia glomerata*) and was involved in the activation of the major classes of phytoanticipins: cyanogenic glucosides, benzoxazinoid glucosides, avenacosides and glucosinolates[40].

The fi rst completely characterized h erbivore-derived elicitor w as v olicitin (**14**), a h ydroxylated fatty a cid-amino acid c onjugate (FAC), which w as i dentified i n the o ral s ecretion o f beet armyworm (*Spodoptera exigua*). Volicitin (**14**) can induce the emission of volatile compounds from maize[41]. Later on, s everal an alogues (**15–24**) were d iscovered f rom t he o ral secretions of closely or distantly related *Spodoptera* sp. (Noctuidae) or other genera of herbivorous i nsects[42,43]. T he di versity o f FACs is linked t o the m odification o f fatty acid ch ains with glutamine and glutamic acid via an amide bond (**Figure 5**), leading to a s pecies specific ratio in the regurgitant.

14 R = NH₂, R' = OH (volicitin)
15 R = NH₂, R' = H   (18:3-Gln)
16 R = OH, R' = H   (18:3-Glu)

17 R = NH₂, R' = OH
18 R = NH₂, R' = H   (18:2-Gln)
19 R = OH, R' = H   (18:2-Glu)

20 18:1-Gln

21 16:1-Gln

22 16:0-Gln

23 14:1-Gln

24 14:0-Gln
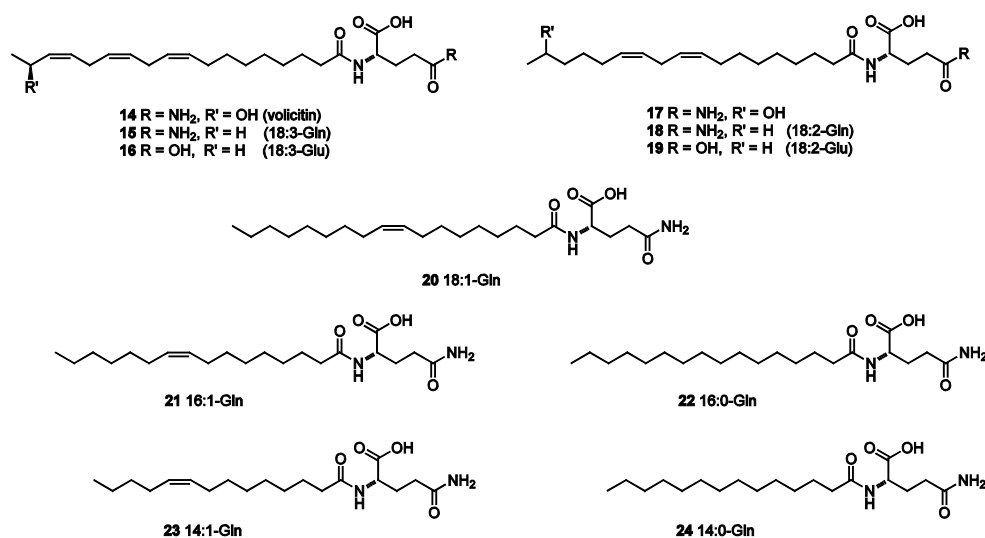
Figure 5. Chemical structures of volicitin analogues (14–24): volicitin (**14**), *N*-linolenoyl-L-glutamine (**15**), *N*-linolenoyl-L-glutamic acid (**16**), *N*-(17-hydroxylinolyl)-L-glutamine (**17**), *N*-linolyl-L-glutamine (**18**), *N*-linolyl-L-glutamic acid (**19**), *N*-oleyl-L-glutamine (**20**), *N*-palmitoleyl-L-glutamine (**21**), *N*-palmitoleyl-L-glutamic acid (**22**), *N*-myristoleyl-L-glutamine (**23**), *N*-myristoleyl-L-glutamic acid (**24**). (Gln: glutamine; Glu: glutamic acid).

Further s creenings o f the r egurgitant f rom le pidoteran l arvae (*S. exigua* and *S. frugiperda*) allowed t he d iscovery o f additional ox ygen-containing f atty acid m etabolites, in p articular dihydroxy fatty a cid (**25**) and e poxy fatty a cid (**26**)[44]. Furthemore, *N*-(17-acyloxy-acyl)-glutamines (**27–30**)[45] were identified as novel surfactants in the oral secretion of several lepidopteran larvae (*S. exigua, S. littoralis, S. frugiperda* and *H. virescens*) (**Figure 6**). The first backbone-phosphorylated f atty a cid de rivatives (**31**, **32**) i n n ature w ere identified f rom th e regurgitant of *S. exigua*[46].
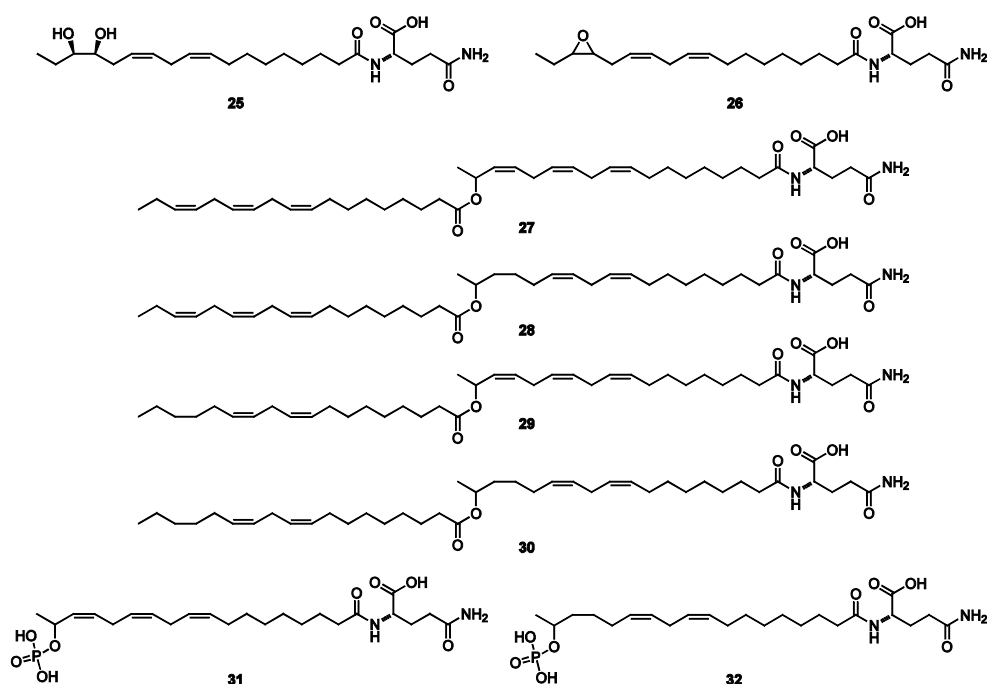
Figure 6. Chemical structures of volicitin analogues (25–32): *N*-(15,16-dihydroxylinoleo-yl)-glutamine (**25**), *N*-(15,16-epoxylinoleoyl)-glutamine (**26**), *N*-(17-linolenoyloxy-linoleno-yl)-glutamine (**27**), *N*-(17-linolenoyloxy-linoleoyl)-glutamine (**28**), *N*-(17-linoleoyloxy-lino-lenoyl)-glutamine (**29**), *N*-(17-linoleoyloxy-linoleoyl)-glutamine (**30**), *N*-(17-phosphonooxy-linolenoyl)-glutamine (**31**), *N*-(17-phosphonooxylinoleoyl)-glutamine (**32**).

Volicitin (**14**) is assumed to bind to a plasma membrane protein from *Zea mays*, which indicates that the initiation of plant defenses in response to herbivore damage can be mediated by a binding protein-ligand interaction [47]. *N*-acyl amino acid conjugates, such as *N*-acylornithines[48], *N*-acylserines[49] and *N*-acylisoleucines[50] are well known bacterial metabolites, mainly produced by *Streptomyces*, *Flavobacteria* and *Pseudomonas* species. Previous research about the biosynthesis of these conjugates has provided the first evidence that the amide bond between the plant derived fatty acid and L-glutamine can also be made by micro-organisms living in the fore- and midgut of the insect larvae[51]. This indicated that insect gut bacteria might be involved in the plant–insect interactions.

Fatty acid derivatives play an important role in plant defense reaction. Bruchins A–D (**33–36**), derived from pea weevil (*Bruchus pisorum* L.), are potential plant regulators causing neoplastic growth on pods of pea lines[52] (**Figure 7**). They are long-chain α,ω-diols, esterified at one or both hydroxyl groups with 3-hydroxypropanoic acid. Bruchin B (**34**) can up regulate a putative isoflavone synthase gene *CYP93C18*, leading to increase in the levels of pisatin, an isoflavone phytoalexin[53].
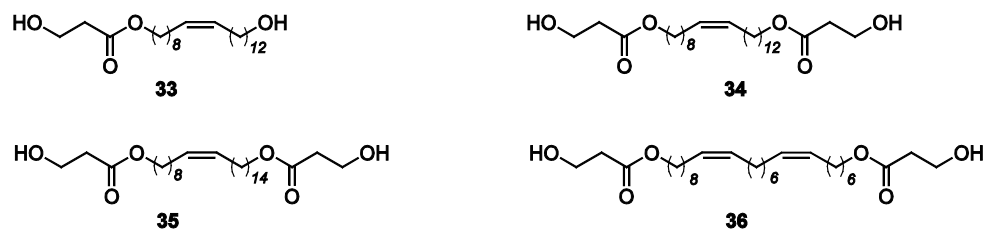
Figure 7. Chemical structures of Bruchins A–D (33–36)

Caeliferins[54] A16:1 (**37**), A16:0 (**38**), B16:1 (**39**) and B16:0 (**40**), disulfooxy fatty acids from the regurgitant of the American bird grasshopper *Schistocerca americana*, are known elicitors which trigger volatile compounds emission from damaged corn seedlings leaves (**Figure 8**). These are non-lepidopteran elicitors belonging to saturated and mono-unsaturated sulfated α-hydroxy fatty acids, whose total systhesis have been described recently[55].
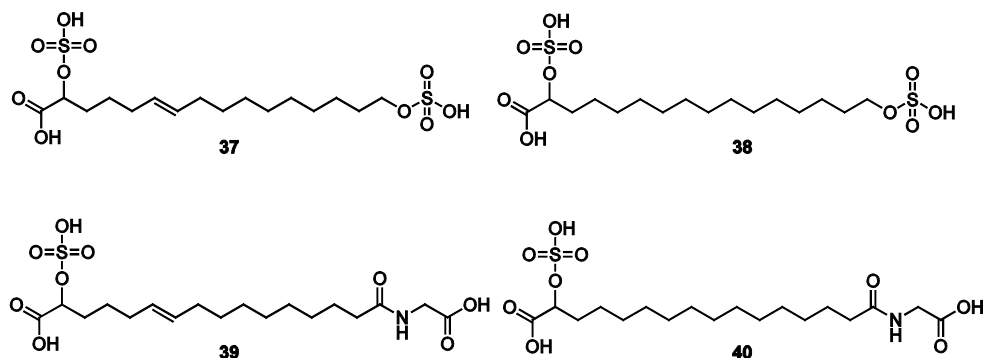
Figure 8. Chemical structures of Caeliferins (37–40)

Inceptin[56], a disulfide-bridged peptide (+ICDINGVCVDA-), isolated from *S. frugiperda* larval oral secretions, can promote cowpea ethylene production and trigger the increase of the defense-related phytohormones jasmonic acid (**1**) and salicylic acid (**2**). Inceptin (*Vu*-In) is a proteolytic fragment of chloroplastic ATP synthase γ-subunit (cATPC) regulatory region that mediates plant perception of herbivory through the induction of volatiles, or phenylpropanoids and protease inhibitor defenses. Three additional cATPC fragments[62] *Vu*-In^-A [+ICDINGV-CVD-], *Vu*-^GE+In [+GEICDINGVCVDA-] and *Vu*-^E+In [+EICDINGVCVDA-], especially *Vu*-^GE+In and *Vu*-^E+In are able to induce the ethylene production. It is highly possible that the inceptins are gut proteolysis products.

The past decade has included the discovery of multiple classes of insect-produced elicitors, so called herbivore-associated molecular patterns (HAMPs). The diversity of HAMPs consists of the type of herbivore and the corresponding plant species, the diversity of molecule type and multiple biochemical effects. Normally individual elicitors have been discovered by fol-

lowing a biochemical effect, for example the VOC emission or phytohormone elevation. However it is possible that the activity of an elicitor may show multiple biochemical effects, or depends on the plant species. Different elicitors may trigger the same biochemical effects, even in different plant species. One biochemical effect might need to be triggered by the combination of more than one elicitor. Phytohormone-based activity mapping of three different insect herbivore-produced elicitors indicated that the activity of individual elicitors on closely related plant species is highly idiosyncratic[57]. JA (**1**) and ethylene exist as highly conserved markers for plant defense. FACs represent the most broadly active elicitors examined in triggering of JA (**1**) elevation in certain plant species. These facts indicate the diversity of biochemical mechanisms mediating plant–herbivore recognition. They comprise multiple classes of elicitors, specific model systems and targeted biochemical plant response. The molecular interaction should be considered as a tuning control according to the different herbivore attact on the different plant species.

Insect OS is a pool of many different chemical substances. When the OS comes into contact with wounded plant leaves, different elicitors interact simultaneously with different signal compounds of the plant and trigger different plant reaction at the same time. Therefore plant defense response is an integral response of many OS elicitors and signal cascades. The discovery of new elicitors following certain plant defense events may simplify the complex response. Moreover an elicitor may act as a molecular sensor to evaluate the corresponding signal cascades in known plant defense events or leading to discover the unknown plant defense events. This will be a powerful way to understand the plant–insect interactions.

1.3 Membrane potential change

Ion channels are integral components of all membranes and they can be seen as dynamic ion transport systems coupled via membrane electrical activities. They do not only influence membrane voltage through the ionic currents they mediated, but also their activities can be regulated by membrane voltage. Ion channels are divided into four groups according to the gating mechanism[58]: ligand-gated, voltage-gated, stretch-activated and light-activated ion channels. They can be affected by biotic or abiotic stimuli and regulate diverse plant physiological processes involved in plant growth and plant defense. According to the ion selectivity, plant ion channels contain potassium channels, calcium channels and anion channels. In addition, ion transporters or carriers are involved in ion transporting.

As the very early event in plant–insect interaction, the membrane potential changes highly depend on the imbalance of ion distribution compared with the normal situation. The ion imbalance is triggered directly by the ion flux through the plant cell membrane and this is also the first step to connect the outside stimuli into the cell response. Induction of ion fluxes has been demonstrated for oral secretions of herbivores, but not for known elicitors from the regurgitant, such as volicitin (**14**) or inceptin. Given that ion fluxes through channels directly influence V_m, it seems reasonable to assume that unknown elicitors regulate the activities of various channels and thus, might be considered as important factors inducing electrical signals[59]. The ion flux could be affected either directly via channel formation processes or indirectly via receptor-mediated processes. The ion flux could be affected by another ion flux, which could be induced by the formation of additional pores into the cell membrane, mediated by channel-forming compounds. Normally these pores act as toxin leading to the cell lysis by changing the cell permeation to ions and small molecules. The ion flux could also be affected indirectly via receptor-mediated processes. Receptor-mediated ion flux is a complex process, either by direct interaction with the certain ion-channels or by activation of ion-channels associated with second signaling cascades. Detailed investigations in *A. thaliana* mutated line (*pdko3*) indicated that the induced V_m depolarization was associated to an increased voltage gated K^+ channel activity[34], triggered by the interaction between unknown elicitor from OS and an unknown receptor-like protein present on the cell membrane.

Receptor-mediated V_m change is a highly specific process. It not only depends on the elicitor from the insect OS, but also depends on the receptor present in the cell membrane. This might be highly specific to the certain cell types and plant species. Compared with receptor-

mediated V_m change, the direct channel formation on the cell membrane is a relatively general process, without the specific interaction with a certain receptor on the cell membrane.

1.4 Channel-forming compounds in nature

1.4.1 Channel-forming peptides/proteins

Channel-forming p eptides/proteins are know n f rom over 1 00 cu rrently r ecognized protein families, most of them restricted to prokaryotes or eukaryotes, but also a few ubiquitous ones. They e xhibit d iverse b iological a ctivities, ma inly a ntimicrobial[60] or c ytotoxic[61] activities. According t o t he s tructural features and bi ological f unctions, t hese pr oteins belong t o f our major cu rrently r ecognized cl asses (**Table 1**): (1) α-helix-type ch annels p resent in b acterial, archaeal and eukaryotic c ytoplasmic an d o rganellar membranes, (2) β-barrel-type por ins present in the outer membrane of Gram-negative bacterial, mitochondria and chloroplasts, (3) secreted pore-forming toxins, and (4) nonribosomally synthesized peptides[62].

The ion flux not only depends on the channel-forming peptides/proteins, but also relies on the 3D s tructures t riggered by self-assembling p rocesses. T he pores de rived from s oluble po re-forming proteins fall into two ma in classes[63]. Best described a re pores w ith t ransmembrane β-barrels, in which polypeptide strands weave back and forth across the lipid bilayer, with α-hemolysin (**41**) as a typical ex ample[64]. α-Hemolysin (**41**) is an ex tracellular protein secreted by most strains of pathogenic *Staphylococcus aureus*. T he mature protein c ontains 293 r esi-dues and has a molecular weight of 33 kDa. It is composed primarily of 65% β-sheets and 10% α-helices.[65] It is secreted as a water-soluble monomer, upon contacting with lipid bilayers the monomers assemble to form a heptameric pore with vestibule of 3 nm and a pore-diameter of 1.5 nm[66,67] (**Figure 9**).
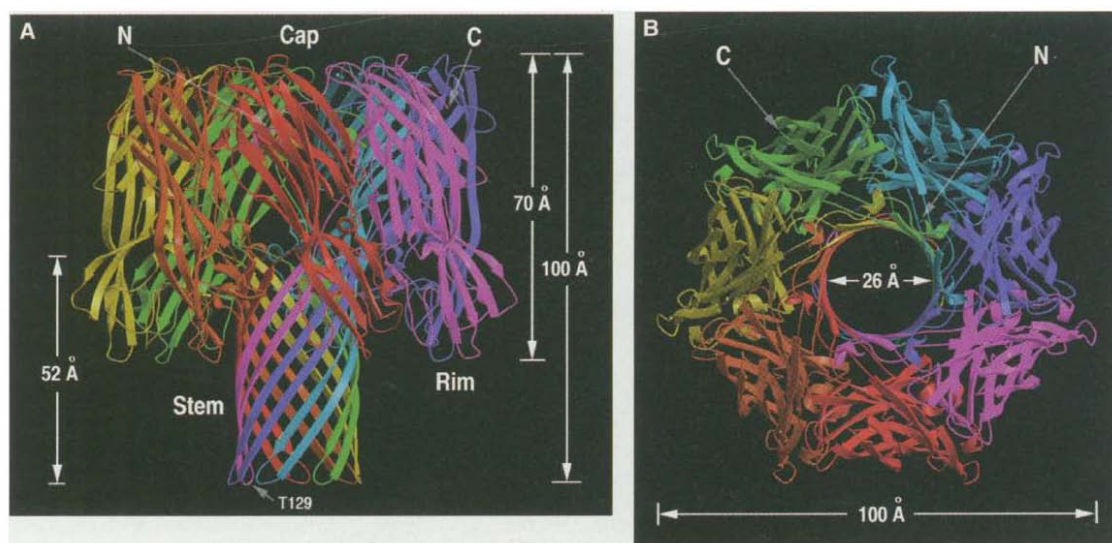
Figure 9. The Ribbon representations of the α-HL (41) heptamer with each monomer in a different color. (cited from ref. 63)

Table 1. Class of known channel-forming peptides/proteins

Channel type	Function	Distribution	Example
α-helix channels	ionic homeostasis; electrical communication	ubiquitous	voltage-gated ion channel
			chloride channel
		bacteria	small conductance mechanosensitive ion channel
		animals	glutamate-gated Ion Channel
			ATP-gated Cation Channel
			ligand-gated Ion Channel
		animal virus	Influenza virus matrix-2
		animals/yeast	nonselective cation channel2
		animals/plants	cytochrome b_{558}
		plants	chloroplast outer envelope solute channel
		yeast	yeast stretch-activated, cation-selective, Ca^{2+} channel
holins	protein export; cell suicide	bacteria	16 members
β-barrel porins	outer membrane permeation	bacteria	outer membrane protein
			general bacterial porin
			bacterial toxin export channel
			sugar porin
		eukaryotes	mitochondrial and plastid porin
pore toxins	biological warfare	bacteria	channel-forming colicin
			α-hemolysin toxin (**41**)
			hemolysin E (Hly E)
			colicin V
			nisin
		yeast	yeast killer toxin
		protozoans	amoebapore
		animals	whipworm stichosome porin
			cecropin
			melittin
			δ-toxin
			defensin
nonribosomal synthesized channel	biological warfare	bacteria	gramicidin
			syringomycin
			tolaasin
		fungi	alamethicin (**42**)

α-HL (**41**) pore allowed rapid ion flux[68,69,70] of K^+, Ca^{2+} and small peptides. It shows hemolytic activity and has a marked preference for rabbit red blood cells, induces demonecrosis and spastic muscle paralysis and is lethal to laboratory animals.

The second class comprises many pores that are thought to be formed from spiral polypeptide rodes, known as α-helices, for example cytolysin A (Cly A, also known as HlyE[71]). For some peptides like alamethicin (ALA, **42**), they could also form a bundle of α-helices[72]. In 1967, ALA (**42**) was discovered from culture broth of the fungus *Trichoderma viride*[73]. Final structure of ALA (**42**) was identified by Pandey et al. in 1977[74] (**Figure 10**). Structurally, ALA (**42**) belongs to the class of peptaibols with molecular weights around 2 kDa, containing non-proteinogenic amino acid residues like α-aminoisobutyric acid (Aib), amino alcohol (phenylalaninol) at the C-terminal residues. As an antimicrobial compound[75], ALA (**42**) was well studied for more than 50 years, and the channel-forming activity[76] was one of the major toxic mechanisms[77,78].
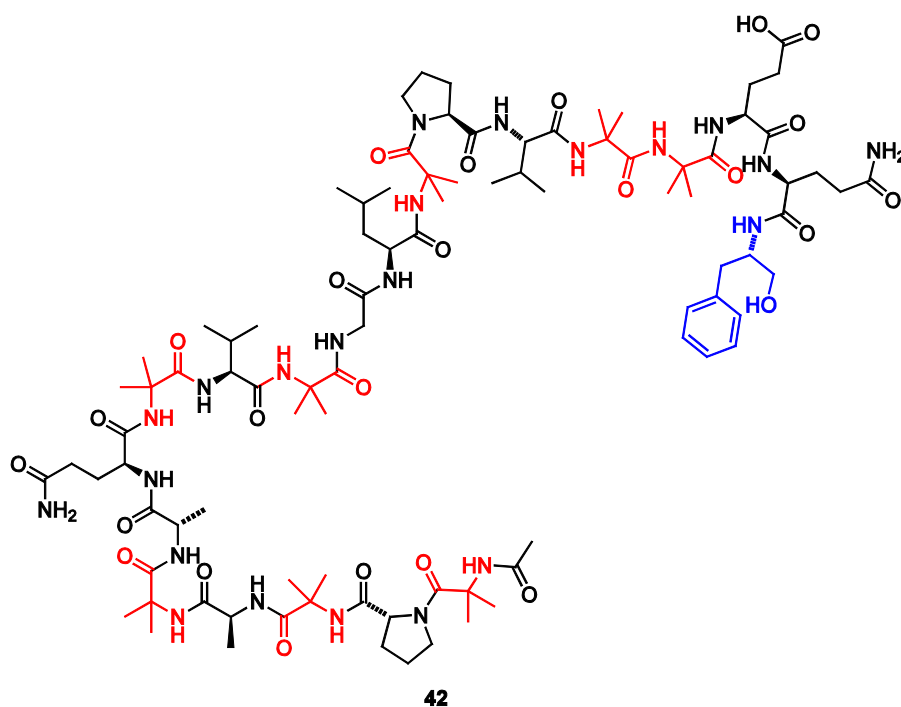
Figure 10. Structure feature of ALA (42). Red amino acid represented 2-amino-isobutyric acid (Aib), blue amino acid represented phenylalaninol (phenol).

Besides the antimicrobial activity, ALA (**42**) shows diverse physiological effects in plants[79,80]. Typical examples are the induction of DMNT (**10**), MeSA (**12**), and TMTT (**13**) emission in lima beans[80] (*P. lunatus*), together with 20- and 90-fold up-regulation of JA (**1**) and SA (**2**) biosynthesis respectively[11], and triggering membrane depolarization in *P. lunatus* and *Hordeum vulgare*[81]. Via the MEP-pathway ALA (**42**) induced the stimulation of DMNT (**10**)

biosynthesis[82], MeSA (**12**) emission in *A. thalinan* by u p-regulation of *AtBSMT1* gene[83], TMTT (**13**) emission through terpene synthesis pathway by up-regulation of terpene synthase 04 ge ne[84] (*TPS04*). R ecent r esearch indicated th at A LA (**42**) could t rigger h ypersensitive response (HR) like pathogen attack in *Arabidopsis*[85], for ex ample, active cell death, lesion in leaves, de position of c allose[86], p roduction of phe nolic c ompounds and t ranscription of the defense gene *PR2* and *PDF1.2*. ALA (**42**) is a very powerful model of channel-forming compounds to evaluate the plant defense mechanism induced by pathogenic fungi.

1.4.2 Non-peptide channel forming compounds

Besides t he l arge f amily of pe ptides/proteins, t here are many non -peptide c hannel f orming compounds. B eticolins[87], first isolated from the fungus *Cercospora beticola*, share the same polycyclic s keleton including a c hlorine atom an d partially hydrogenated anthraquinone a nd xanthone m oieties (beticolin 3, **43**). T hey s how br oad c ytotoxic a ctivities, while they can form voltage-independent and weakly selective ion channel in the membranes[88]. The polyene antibiotic amphotericin B (**44**), isolated from *Streptomyces nodosus*, has been a leading broad-spectrum antifungal antibiotic for more than fifty years[89]. The mode of action of amphotericin B (**44**) was determined as a complex formation with ergosterol in fungal membranes, followed by the self assembly of the complex to form transmembrane pores that lead to uncontrolled loss of ions and small molecules[90].
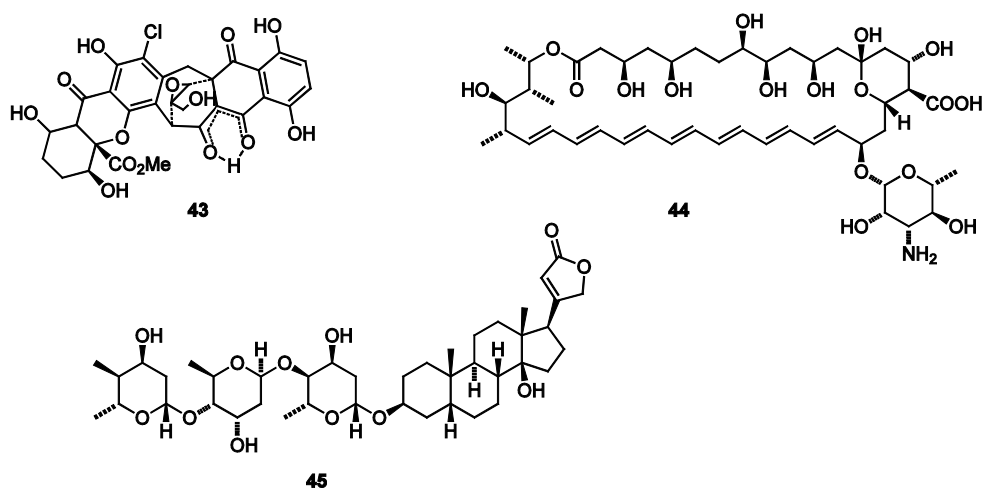
Figure 11. Chemical structures of typical non-peptide channel forming compounds: beticolin 3 (**43**), amphotericin B (**44**), digitoxin (**45**)

Digitoxin (**45**) obtained from *Digitalis purpurea*, belongs to cardiac glycosides, comprising a group of steroidal compounds[91] that possess cardiac activity and contain a five or six membered lactone ring (**Figure 11**). It is important that centuries-old drugs can still treat congestive heart failture, and acted as an antitumor agent. The new mode of action has been reported recently, and is based on the formation of transmembrane calcium channels for the calcium uptake[92].

2 Goal of This Study

Insect herbivory on plants is a complex interaction between several organisms consisting of various chemical factors and fine tuned plant signaling cascades. Herbivory-induced plant responses are mediated by elaborated signaling networks, the major events according to the measurable time schedule are known, but the cross-talk between different events are still under research. The trigger of plant physiological responses consists of at least three aspects: (1) the mechanical damage from insect biting, (2) the chemical factors from damaged plant tissue (especially cell wall) and (3) the chemical factors from insect oral secretions (OS). Chemical factors from plant and insect played critical roles in triggering the plant response. However until now only a limited number of these elicitors has been identified from the insect oral secretions, and only the late plant responses like phytohormone elevation and volatile emission have been investigated. Therefore this PhD work mainly focused on the discovery of new elicitor(s) involved in plant–insect interactions. Assay-guided purification from insect OS has been recognized as a powerful tool to facilitate the new elicitor discovery.

- In order to find the mode of action of the early events during plant–insect interactions, the elicitors from the insect OS which could induce the transmembrane ion flux had to be investigated. The hypothesis is based on the channel formation contributed to the transmembrane ion flux and V_m change. As a classic method to evaluate the channel-forming activity, black lipid bilayer membrane (BLM) assay[93,94] was used. The observation of ion flux due to OS in this artificial system confirmed the existence of such compounds. The elicitor should be identified and purified by the combination with multiple column chromatography methods guided by BLM activity.

- For the sake of finding the connection between transmembrane ion flux and the later defense events, the identified elicitor should be used to evaluate the further defense-related activities, like $[Ca^{2+}]_{cyt}$ increase, gene expression, phytohormone elevation and VOC emission. This will give us the information about the cross-talk among the complex plant–insect interactions. Thus a combination of OS and MecWorm, Spit-Worm had to be further investigated the cooperative action of chemical factors and mechanical damage in order to closely mimic the insect herbivore.

- The channel forming compounds contain many different types of molecules, the comparison between typical channel forming compounds in plant defense will provide

more information about their mode of action of the transmembrane ion flux in the plant–insect interactions.

- In order to better understand the chemical complexity of the insect OS, more compounds should be identified by chemical guided purification, especially from the BLM-inactive fractions. The chemical components present in the OS may come from the secretion of insect gland, the digestive products of food and the secretion of gut bacteria. The origin of channel formation elicitors should be investigated.

As a side project, the chemical composition of white secretion from pitcher plant *Nepenthes lowii* has been analyzed. *N. lowii* are carnivorous plants whose prey-trapping mechanism features a deep cavity filled with liquid known as a pitfall trap. However, some *N. lowii* plants are visited by tree shrews like *Tupaia montana* without trapping. *T. montana* feeds on the white secretion on the inner surface of the lid and defecates into the pitcher, which may provide additional nitrogen source to the pitcher plant. As the major "food" for *T. montana*, the white secretion provide the possibility to attract the special animals in order to obtain the nitrogen source. Investigation of the composition of this white secretion provides the opportunity to understand the interaction between *N. lowii* and *T. montana*.

3 Results and Discussion

3.1 BLM-guided purification of channel-forming compound from OS

3.1.1 Characteristic investigation of the BLM active compounds

In order to obtain the characteristics of channel-forming compounds in the OS, the crude OS sample was submitted to molecule cut-off separation and serie tests like heating, proteases digestion and organic solvent extraction, followed by the BLM activity evaluation.

3.1.1.1 Vivaspin molecule cut-off

For the sake of investigating the molecular size of channel-forming compounds, the crude OS sample was applied to Vivaspin 500 with different molecular weight cut-off (3 KD, 5 KD and 30 KD). After centrifugation, the sample was separated into two fractions, the remaining upper part, which can't pass through the membrane, contained molecules whose molecular weight (MW) was larger than the cutoff value.

The channel forming activity was determined with the BLM assay by measuring the current change across an artificial bilayer under voltage-clamp condition. Here the constant voltage +30 mV was applied to the lipid bilayer. When pore-forming compounds inserted into the bilayer, an observed current indicated the present of active compounds (**Figure 12**).

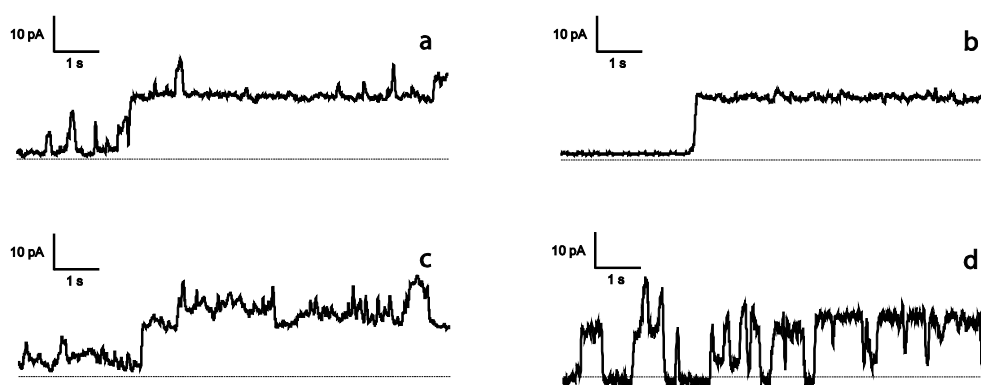**Figure 12. Currents generated by:** (a), crude OS of *S. littoralis*; (b), active fractions (up part) from Vivaspin 500 (3 KD); (c), active fractions from Vivaspin 500 (5 KD); (d), active fractions from Vivaspin 500 (30 KD) in BLM assay. Experimental conditions: Buffer (*cis/trans*): 200 mM KCl, 10 mM Tris/HCl, pH 9.2. 10 μL/mL of sample was applied to the *cis*-compartment of the membrane at +30 mV.

Different current profiles have been observed in OS and different active fractions. The variations might be due to the different stabilities of the pores or to different oligomers[95]. Multiple current steps (**Figure 12d**) indicated that simultaneous as well as consecutive openings of more than one channel happened. Negative control or inactive fractions did not trigger current production.

Due to the clear activity always in the remaining part of Vivaspin, the active compound should be the molecule (**Figure 12**) whose molecular weight is higher than 30 kDa.

3.1.1.2 Heat denaturation

With the purpose of investigating the stability after heating, the crude supernatant was kept at room temperature for 24 h or heated for 4 h at 100 $^{\circ}$C. After that the BLM activity has been tested to evaluate the channel-forming activity.

The channels were stable at room temperature for at least 24 h, however 100 $^{\circ}$C for 4 h destroyed the BLM activity (**Figure 13**). Combined with previous results, this indicated that the active compound(s) were heat-labile large molecule(s).
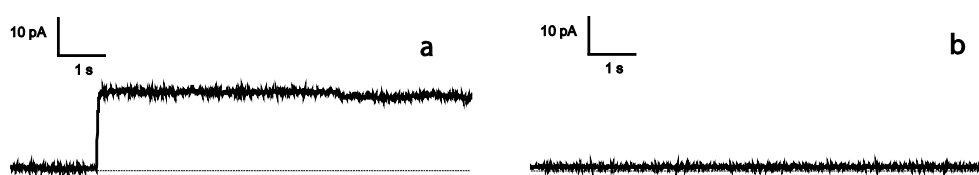
Figure 13. Currents generated by: (a), crude OS supernatant of *S. littoralis* at room temperature after 24 h; (b), after 100 $^{\circ}$C for 4 h treatment in BLM assay with KCl buffer.

3.1.1.3 Pronase digestion

In order to investigate whether a protein was the candidate for this heat-labile large molecule, the crude OS was treated by pronase. Pronase is a mixture of non-specific proteases, which comprised various types of endopeptideases (serine and metalloproteases) and exopeptidases (carboxypeptidases and aminopeptidases), isolated from *Streptomyces griseus*. Typically, neutral protease, chymotrypsin, trypsin, carboxypeptidase, and aminopeptidase are present, together with neutral and alkaline phosphatases. Their activities extend to both denatured proteins and native proteins leading to complete or nearly complete digestion into individual amino acids.

OS supernatant was treated with 1.0 mg/mL pronase at 37 $^{\circ}$C for 16 h, following the evaluation of the BLM activity of the digested product. The BLM activity of enzyme control

(**Figure 14b**) and the hydrolysis product (**Figure 14c**) may originate from the effect of 0.05% SDS existed in the reaction system. In order to avoid the effect from SDS, the crude supernatant was treated by the digestive system without SDS. A channel-forming activity of digested product was not detected (**Figure 14e**). This result indicated a protein as a possible candidate for the heating-labile large channel-forming compound(s).

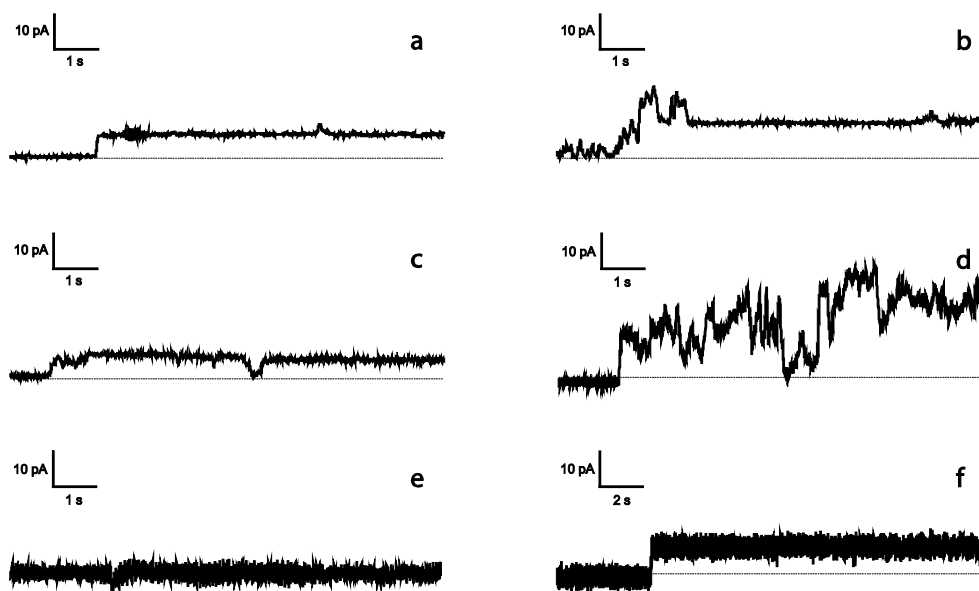**Figure 14.   Currents generated by:** (a), crude OS supernatant of *S. littoralis*; (b),pronase control with 0.05% SDS; (c), OS digestive product by pronase with 0.05% SDS; (d), pronase control without SDS; (e), OS digestive product by pronase without SDS; (f), 0.1% SDS in BLM assay with KCl buffer.

3.1.1.4 Organic solvent extract

In order to evaluate the polarity of channel-forming compound, the crude OS was extracted by CH_2Cl_2 followed by evaluation of BLM activity for the CH_2Cl_2 extract and the aqueous phase. Both CH_2Cl_2 extract and aqueous phase were BLM active, indicating that different active compounds existed in the organic layer (**Figure 15b**) and the aqueous phase (**Figure 15c**), respectively.

The activity detected from aqueous layer indicated that CH_2Cl_2 couldn't destroy the activity of large water-soluble active compound. However from measurement to measurement, the BLM activity from CH_2Cl_2 extract was not reproducible, but the aqueous phase showed stable BLM activity.

The above findings indicated that the BLM active compound was heat-labile with large molecular weight (> 30 kDa) with respect to Viva spin separation and heat treatment. In addition,

it was a pronase-labile compound. Combining all the informations, a channel forming protein was the most likely BLM active candidate. Therefore further purification was done to identify the channel-forming protein from insect oral secretions.
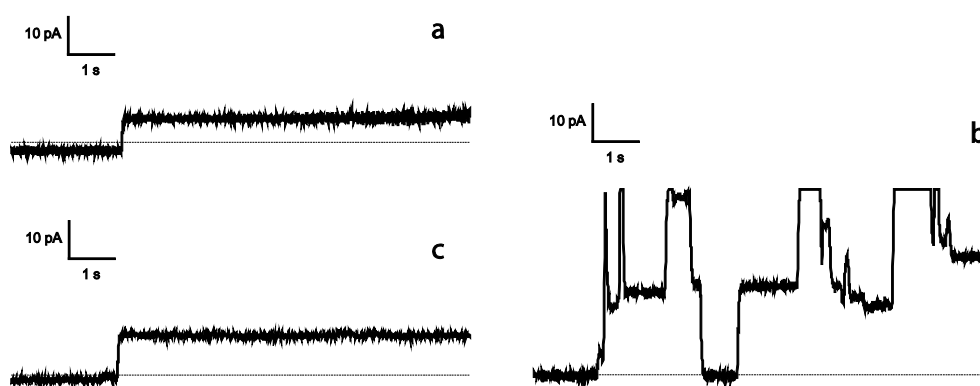

Figure 15. Currents generated by: (a), supernatant of *S. littoralis* OS; (b), CH₂Cl₂ extract; and (c), aqueous phase in BLM assay.

3.1.2 Identification of porin-like protein

For the sake of purifying the active compound(s), 10 mL of OS were collected from 500 larvae of *S. littoralis* (4th instar). The complex mixture of the OS was first extracted using CH_2Cl_2 and the aqueous layer was separated by a series of chromatographic procedures as described (**Scheme 2**).

The active fractions were submitted to electrophoresis, and the protein profile is shown in **Figure 16**. Altogether, 13 bands, representing fractions 3 to 7, were cut from the gel obtained from the active fraction after Sephadex G75 separation (**Figure 16a**) and subjected to the proteomic analysis. The protein hits were identified using stringent database searching (MASCOT) and homology-based database searching (MS BLAST). Besides several typical background proteins from the diet such as phaseolin and phytohemagglutinin from *Phaseolus vulgaris*, a protein matching the sequence of a desiccation-related protein from *A. thaliana* was found. Moreover, diverse serine proteases were identified by MASCOT and MS BLAST resembling entries from related insect species (e.g. *Spodoptera litura* and/or *Helicoverpa punctigera*) as well as an α-amylase from *H. armigera*, but these compounds were not channel-active. The protein from the bands 11 and 13 (**Figure 16a**) matched to a porin Gram-negative type protein from the Gram-negative *Ralstonia pickettii* 12J, and was named as porin-like protein (PLP). The molecular weight of this hit (38 kDa) corresponded well to the position of the protein in the SDS-gel.
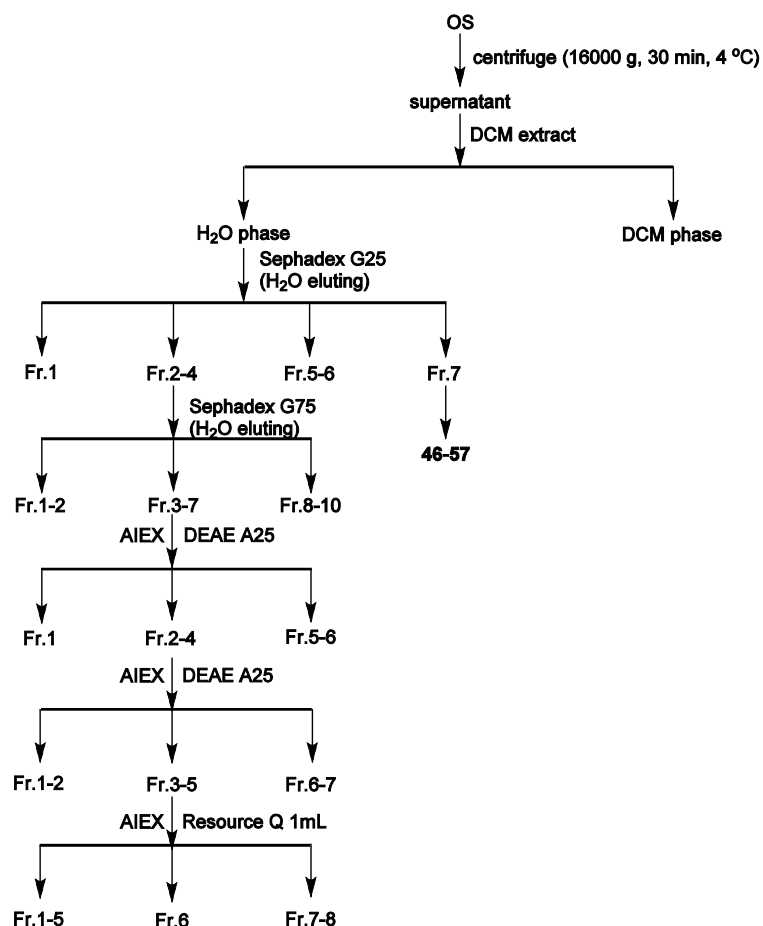
Scheme 2. Purification chart of channel-forming protein from OS
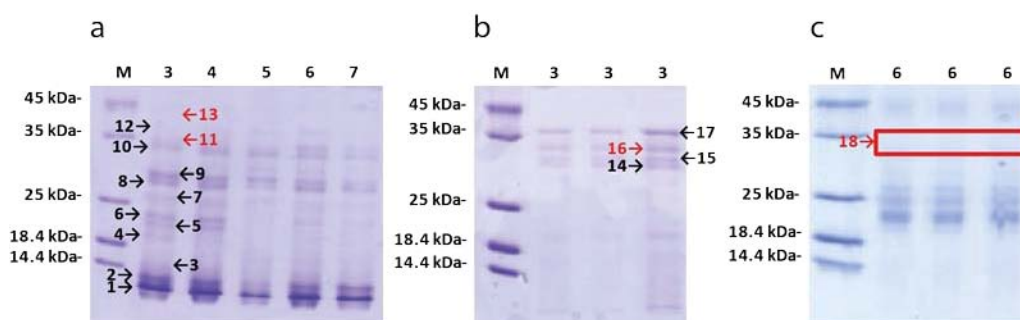
Figure 16. Gel electrophoresis of the active fractions obtained from the three purification experiments. Coomassie-stained protein bands subjected for proteomic analysis were highlighted with arrows (red arrows indicated the PLP-containing bands). (a), active fractions (Fr. 3-7) from Sephadex G75; (b), active fractions (Fr. 3) from 2nd DEAE A25; (c), final active fraction (Fr. 6) from ÄKTA AIEX Resource Q.

In the next separation step (anion exchange chromatography), we significantly improved the purification by reducing the number of serine proteases-like candidates. The dominant band 16 was identified in the molecular mass range of 35 kDa (**Figure 16b**) and also matched with

a porin type protein from *Ralstonia* (Gram-negative). Final purification of an active fraction was obt ained a fter f ractionation b y Ä KTA A IEX c hromatography.   The f ractions 3–5 (**Scheme 2**) were f inally p urified o ver a r esource Q b y gradient elution (**Figure 17**).   The same PLP hit could be also identified from SDS-PAGE gel (band 18, **Figure 16c**). A complete overview on the proposed protein candidates are given in **Tables S2**, **S3**, **and S4**.
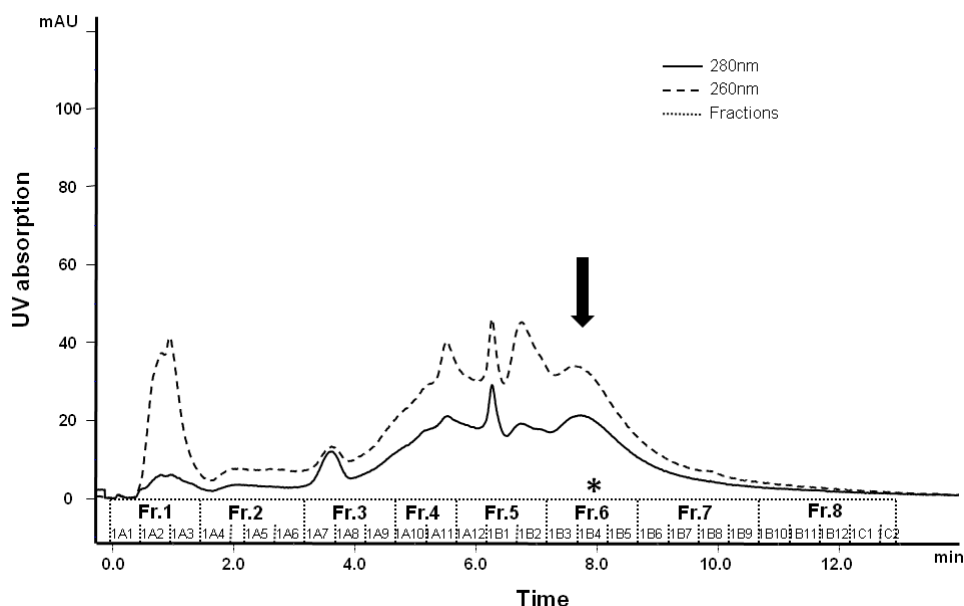
Figure 17. Chromatogram of final purification step by ÄKTA-AIEX Resource Q–1 mL.
1.0 mL combined sample of Fr. 3 to Fr. 5 from 2nd DEAE A25 was injected into ÄKTA, 1.0 mL-subfraction was automatically collected by a fraction collector. Eight fractions were produced by further combination of neighbor subfractions. After concentrating and desalting, only Fr. 6 was active in BLM assay.

The BLM activity of active fractions is presented in **Figure 18**. Due to the limited amount of the f inal a ctive f raction, f urther purification to obtain t he channel-forming p rotein a nd t he evaluation of the biological activities was not possible. A s several reports existed about the channel-forming activity of porins[62], we named this channel-forming protein in OS as porin-like protein (PLP) and s et out to prove its biological activity as an elicitor of plant defense reaction using a commercial sample. Since α-HL (**41**) (Sigma, H9395, CAS RN: 94716–94–6) exhibited comparable channel forming activity in BLM assay system with KCl buffer (**Figure 18f**), it could be used to mimic the porin-like protein to further evaluate the function of channel forming compounds in the plant–insect interactions.

Figure 18. Currents generated by: (a), H_2O as negative control; (b), crude OS of *S. littoralis* larvae; (c), active fractions from Sephadex G75; (d), active fractions from 2nd DEAE Sephadex A25; (e),final active fraction (Fr. 6) and (f), α-HL (**41**) in BLM assay.

3.1.3 Calcium ion-dependent BLM activity

With the purpose of investigating whether this PLP protein could perform the Ca^{2+} flux in artificial membrane, the Ca^{2+} flux was measured in BLM assay. This assay provided an artificial bilayer system without the interference of Ca^{2+} channels from the cell membrane. To evaluate the ion selectivity of the channel-forming compounds with respect to Ca^{2+} ions in the BLM assay system, the KCl buffer was replaced by $Ca(NO_3)_2$ and samples of OS, α-HL (**41**) and the PLP-fraction were added (**Figure 19**).

In contrast to the results with monovalent cations, no clear channel formation was obtained from OS sample. However, after extraction of the OS with CH_2Cl_2 the remaining aqueous phase was active with Ca^{2+} buffer. Recombination of the two phases generated an inactive sample, suggesting a still unknown interaction between the components from the two phases (**Figure 20**).
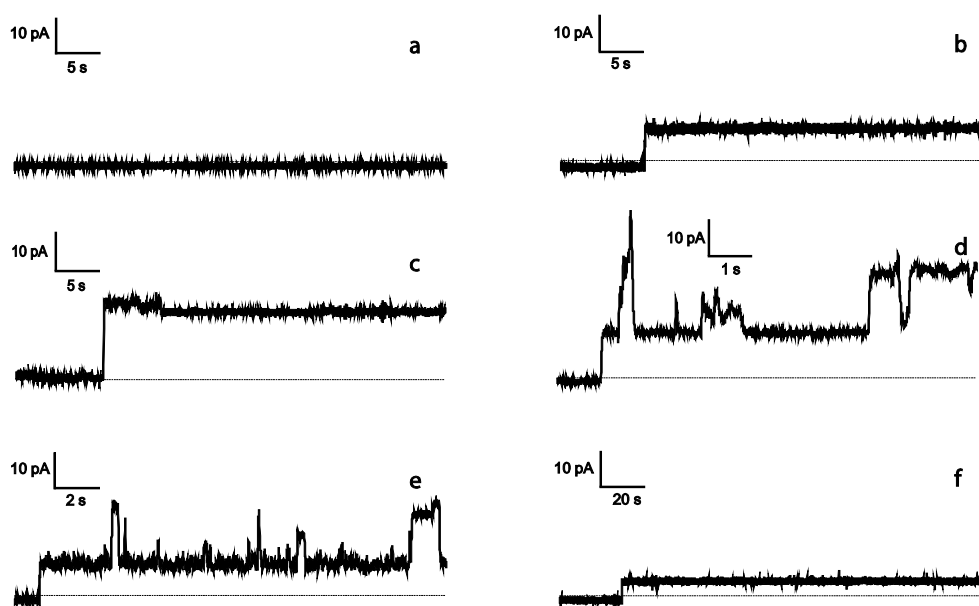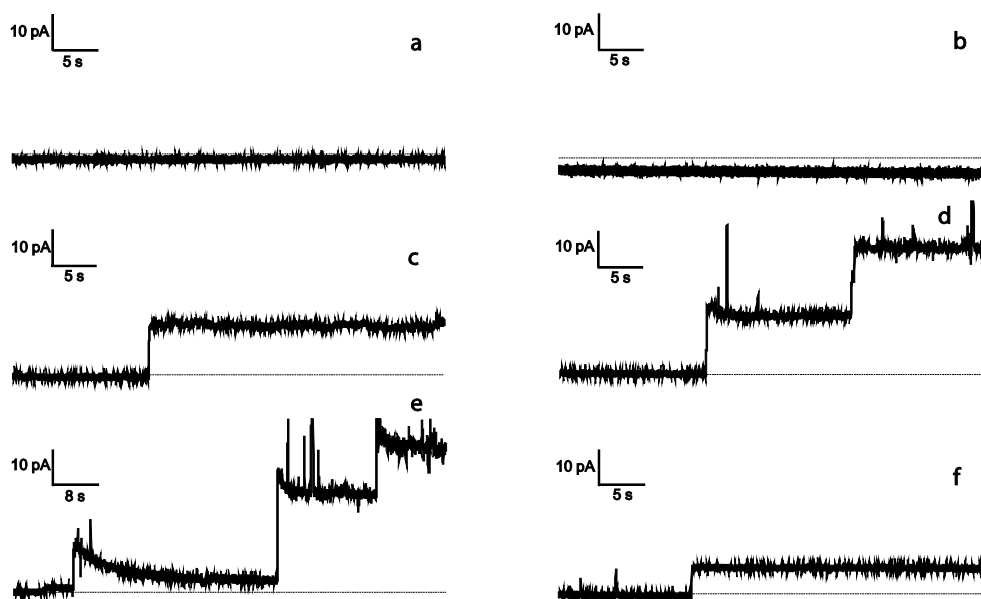
Figure 19. C urrents g enerated b y: (a), H_2O a s ne gative control; (b), crude O S o f *S. littoralis* larvae; (c), active f ractions f rom S ephadex G 75; (d), active f ractions f rom 2 [nd] DEAE S ephadex A 25; (e), final active fraction; (f), α-HL (**41**) in BLM assay. E xperimental conditions: B uffer (*cis/trans*): 100 m M C a(NO$_3$)$_2$, 10 m M T ris/HCl, pH 9.2. 10 µL/mL o f sample (except 20 µL/mL o f 0.1 mg/mL α-HL solution) w as applied to the *cis*-compartment of t he m embrane at +3 0 m V. Typical r ecording f rom t hree i ndependent ex periments w ere represented.
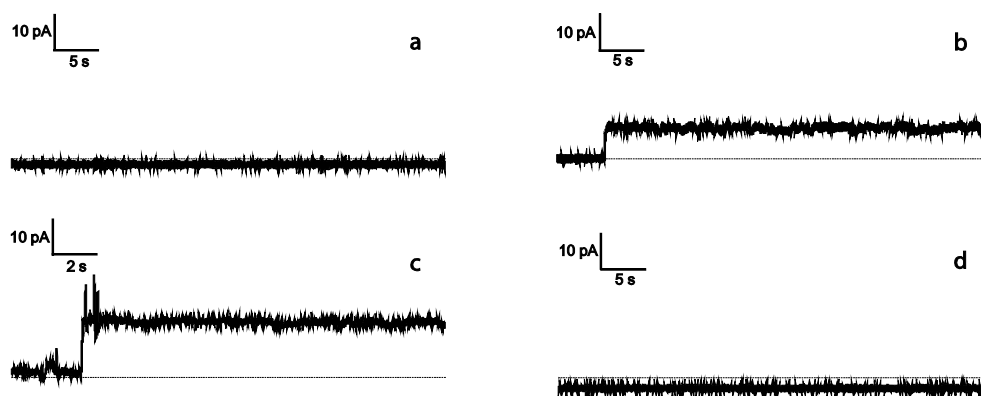
Figure 20. C urrents g enerated b y: (a), H_2O as ne gative control; (b), aqueous pha se a fter CH_2Cl_2 extract; (c), 10 mg/mL CH_2Cl_2 extract in H_2O; and (d), recombination of CH_2Cl_2 ex- tract with aqueous phase in BLM assay. Experimental conditions: Buffer (*cis/trans*): 100 mM Ca(NO$_3$)$_2$, 10 mM Tris/HCl, pH 9.2. 10 µL/mL of sample was applied to the *cis*-compartment of t he m embrane at +3 0 m V. Typical r ecording f rom t hree i ndependent ex periments w ere represented.

3.1.4 Measurements of cytosolic Ca^{2+} concentrations in soybean cell

To ev aluate Ca^{2+} ion flux elicited by crude OS, PLP-fraction and α-HL (**41**) *in vivo,* changes of c ytosolic C a^{2+} were measured b y us ing a s uspension of t ransgenic s oybean cells w hich

expressed the Ca^{2+} sensing protein aequorin[96]. In fact, crude OS induced the elevation of cytosolic Ca^{2+} concentrations. However neither the active fractions nor α-HL (**41**) induced a Ca^{2+} influx (**Figure 21**).

Figure 21. Changes of cytosolic Ca^{2+} concentration ($[Ca^{2+}]_{cyt}$) in soybean cell suspension cultures expressing the Ca^{2+} sensing aequorin system treated by: (a), 10 μL OS; (b), 5 μL aqueous phase after CH_2Cl_2 extraction; (c), 5 μL active fractions from G25; (d), 5 μL active fractions from G75; (e), 5 μL active fractions from 1st A25; and (f), 5 μL active fractions from 2nd A25. Red line represented sample, and black line represented negative control (H_2O). Typical recording from three independent experiments were presented.

This result indicated that the Ca^{2+} flux caused by active fractions and α-HL (**41**) is too low to be detected, however the effect from crude OS maybe the integral influence from different chemical components. The detergent activity observed in the aqueous phase (**Figure 21b**) indicated the possible active compounds present, however loss of the activity from further PLP-fractions indicated the PLP was not responsible for it.

Interestingly, the recombination of CH_2Cl_2 phase and aqueous phase triggered the Ca^{2+} influx *in vivo* (**Figure 22e**), although the recombined sample failed to induce Ca^{2+}-dependent channel-formation in the BLM-assay (**Figure 20d**).

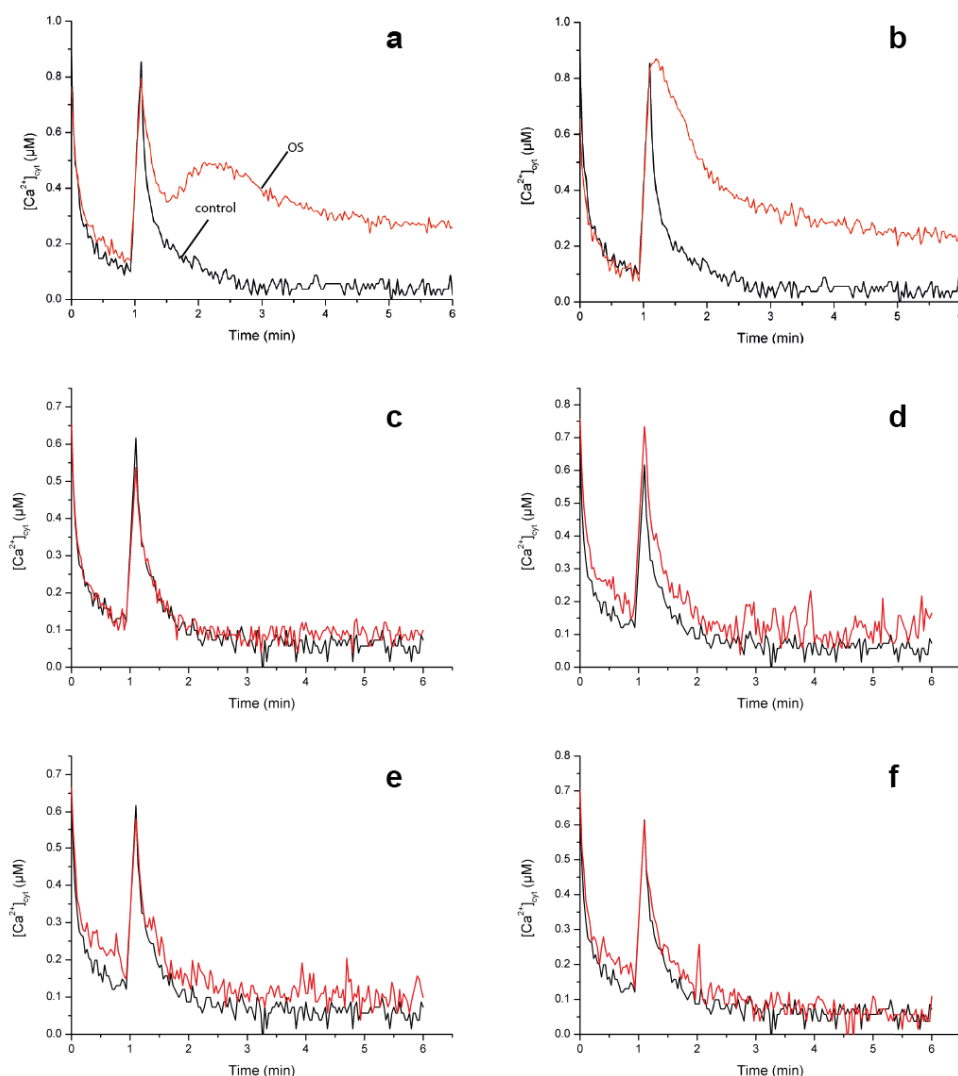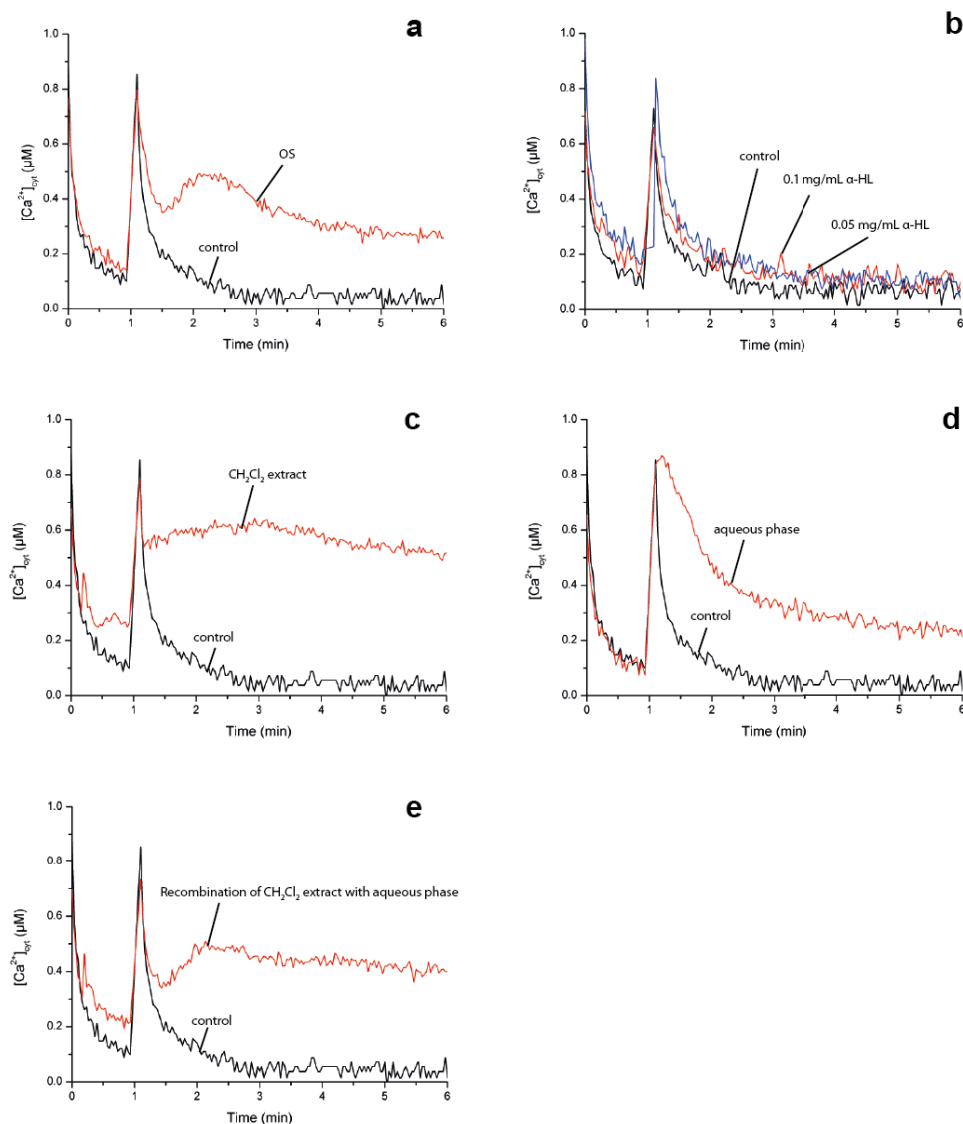**Figure 22. Changes of cytosolic Ca^{2+} concentration ($[Ca^{2+}]_{cyt}$) in soybean cell suspension cultures expressing the Ca^{2+} sensing aequorin system treated by:** (a), OS (H_2O as control); (b), α-HL (**41**) (10 mM Tris/HCl pH 8.0 a s control); and (c), 10 m g/mL C H_2Cl_2 extract o f crude OS suspended in H_2O (H_2O as control); (d), aqueous phase of c rude OS (H_2O as control); and (e), recombination of CH_2Cl_2 extract with aqueous phase (H_2O as control). Red line represented sample, and black line represented negative control. Typical recording from three independent experiments were represented.

This observation indicated th at th e evelation of Ca^{2+} concentrations of t he cytosol is highly dependent on the molecules present in the organic phase, either by direct or indirect activation of the Ca^{2+} channel. Channel-forming PLP, like α-HL (**41**) is not sufficient for Ca^{2+} elevation in soybean cell.

3.1.5 Measurement of cytosolic Ca²⁺ concentrations in *A. thaliana* leaf tissue

Additionally, the cytosolic Ca^{2+} concentration was measured in *A. thaliana* leaf which could express the Ca^{2+} binding protein aequorin[97]. The result showed that crude OS as well as CH_2Cl_2 extract of OS could induce Ca^{2+} elevation in cytosol, however α-HL (**41**) didn't show any activity (**Figure 23c**). This experiment has been done by Dr. Jyothilakshmi Vadassery.
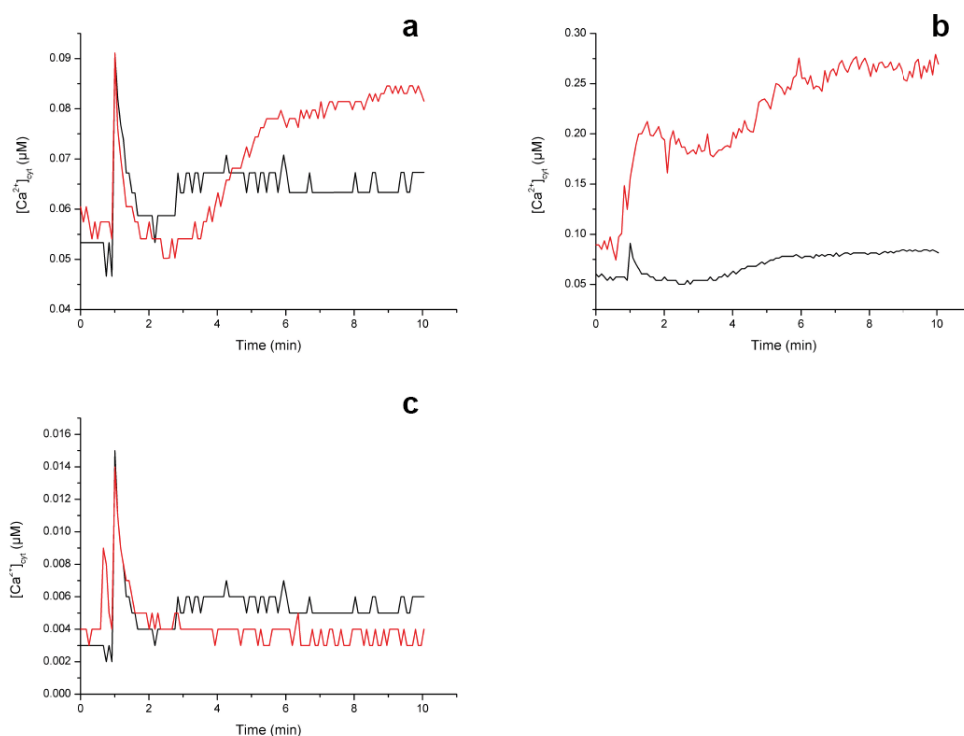
Figure 23. Changes of cytosolic Ca^{2+} concentration ($[Ca^{2+}]_{cyt}$) in *A. thaliana* leaf tissue expressing the Ca^{2+} sensing aequorin system treated by: (a), OS (H_2O as control); (b), CH_2Cl_2 extract (H_2O as control); and (c), 0.1 mg/mL α-HL (**41**) (10 mM Tris/HCl pH 8.0 as control). Red line represented sample, and black line represented control. 25 µL sample solution was applied in the assay respectively.

This observation suggested that the channel-forming PLP is not enough to trigger Ca^{2+} elevation in cytosol neither in *A. thaliana* nor in soybean. The compounds present in the organic phase may play more important role.

3.1.6 Measurement of apoplastic voltage

The OS-dependent generation of ion fluxes in lipid bilayers and plant membranes[93,94] as well as the elicitation of depolarization in leaf segments[9] prompted us to investigate whether single or repeated application of OS induce electrical signals in whole plants. Upon application of

OS from *S. littoralis* to wounded whole *Vicia faba* plants, an electrical signal was induced and could be detected as shown in **Figure 24**. When treatments and measurements were carried out on the same leaf, a depolarization was detected at a distance of 2.5 cm from the application site of OS. In addition, a delayed, long distance electrical signal was determined also on a non-treated, systemic leaf in a distance of about 25 cm. These results again indicated that an electrical signal transfer was initiated by unknown, presumable channel-forming compounds, which were present in the OS. This work has been operated by Dr. Jens B. Hafke from Justus-Liebig University in Giessen.
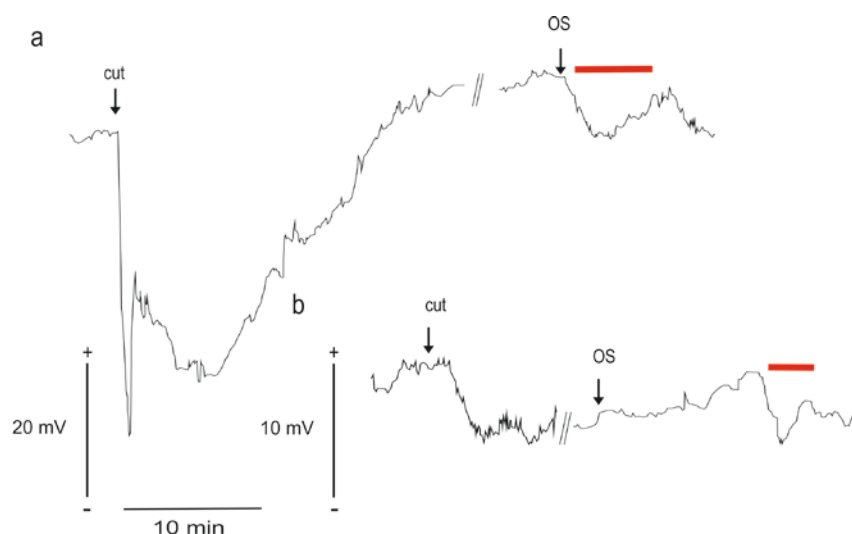
Figure 24. Measurements of electrical responses of *Vicia faba* plants to application of *S. littoralis* larvae-derived OS: (a), Local response. The distance between OS application site and the site of apoplastic voltage measurement was 2.5 cm on the same leaf; (b), Systemic response. The distance between OS application site on one leaf and the site of apoplastic voltage measurement on a different leaf was 25 cm. The hyperpolarization of the apoplast (indicated by the red bars) resembled depolarization of the symplast. Typical recordings (each out of four independent measurements) are showen.

3.1.7 Measurement of phytohormone level in *A. thaliana* leaf tissue

Crude OS could trigger the elevation of jasmonic acid (JA, **1**), salicylic acid (SA, **2**), (−)-JA-L-Ile (**3**), (+)-7-*iso*-JA-L-Ile (**4**) and *cis*-OPDA (**5**) in *A. thaliana* as an important response to defense.[24] However as the known elicitor from *S. littoralis* OS, volicitin (**14**) and *N*-linolenoly-Gln (**15**) couldn't induce the JA (**1**) elevation in *A. thaliana*.[57] It is very important to know whether the channel formation is the elicitor which results in the phytohormone elevation in crude OS.

With the purpose of evaluating the phytohormone elevation activity, 1 μg α-HL (**41**) dissolved in 20 μL 10 mM Tris/HCl pH 8.0 was applied on one damaged *A. thaliana* leaf. Leaf tissues were collected for the measurement of phytohormone after five time points (0 min, 30 min, 45 min, 60 min and 90 min) treatment (**Figure 25**).
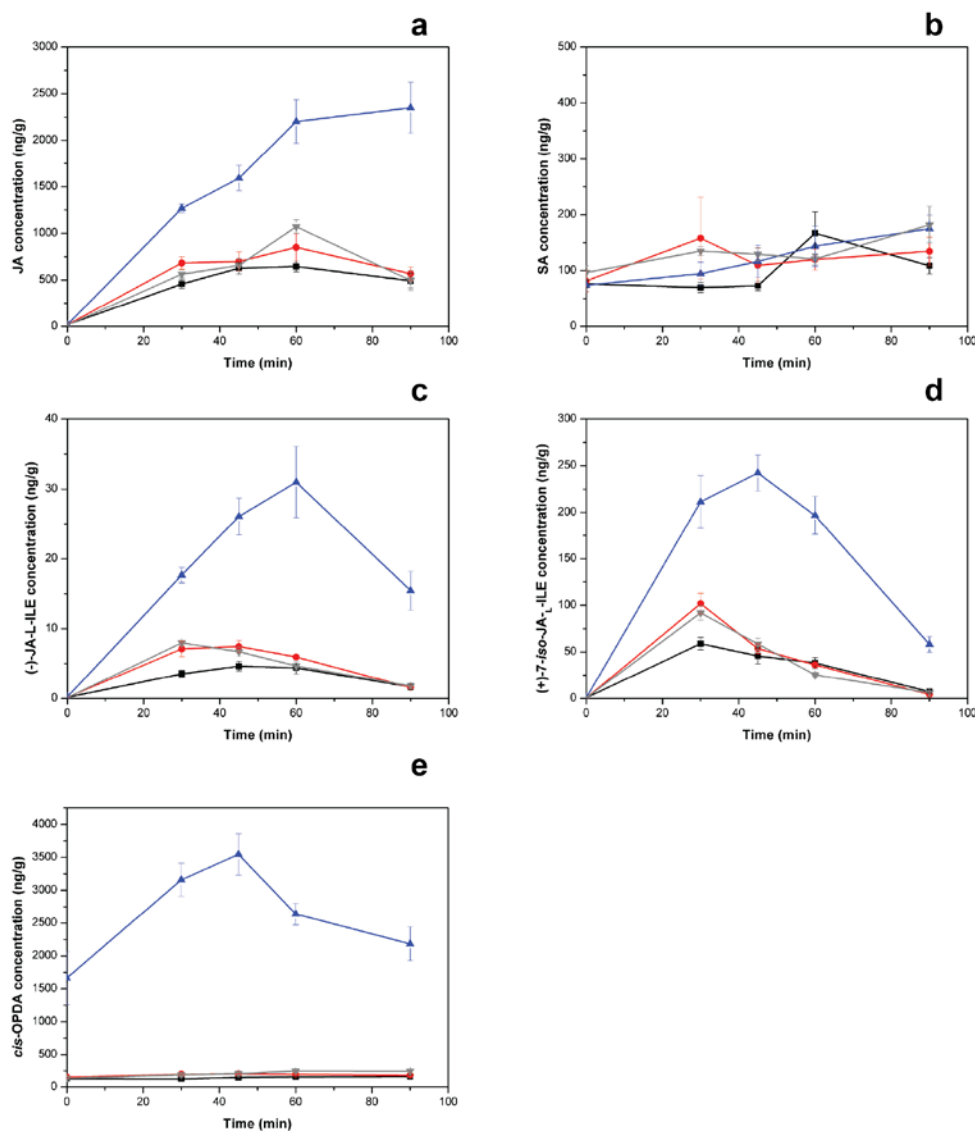
Figure 25. Activity of α-HL (41) on an induced phytohormone production time course in *A. thaliana* leaf tissue: plant treatment included damage plus water as negative control (black), crude OS as positive control (blue), buffer (red), and α-HL (**41**, grey) with average (n = 3, ± SEM) (a) JA (**1**) (ng/g FW), (b) SA (**2**) (ng/g FW), (c) (−)-JA-L-Ile (**3**) (ng/g FW), (d) (+)-7-*iso*-JA-L-Ile (**4**) (ng/g FW), and (e) *cis*-OPDA (**5**) (ng/g FW).

Crude OS was applied as positive control, buffer and H_2O were applied as negative control. The result showed that the positive control (crude OS) could induce significant increase of JA (**1**), (−)-JA-L-Ile (**3**), (+)-7-*iso*-JA-L-Ile (**4**) and *cis*-OPDA (**5**), however, α-HL (**41**) couldn't induce any elevation of measured phytohormones. This indicated that the channel-forming

PLP couldn't significantly trigger the elevation of phytohormone level in *A. thaliana* directly. Phytohormone elevation might result from other chemical factors present in the OS.

3.1.8 *CML42* up-regulation assay in *A. thaliana*

Wounded leaves of *A. thaliana* were treated with diluted OS, PLP-fractions, and α-HL (**41**), respectively (**Figure 26**).
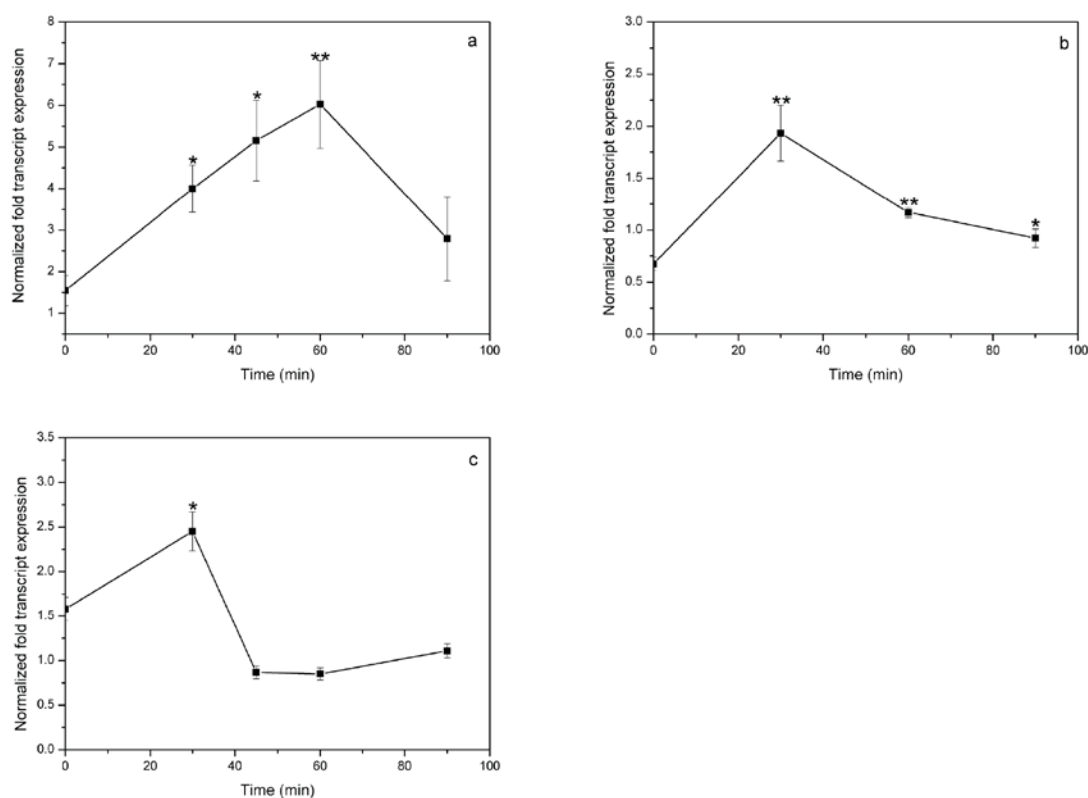
Figure 26. *CML42* **transcript levels in** *A. thaliana* **leaves treated by:** OS, final active fraction and α-HL (**41**), the fold change was calculated relative to control which was pattern wheel wounding plus 10 mM Tris buffer pH 8.0 (all samples were dissolved in 10 mM Tris buffer pH 8.0): (a) 20 μL 1:1 diluted crude OS of *S. littoralis* per leaf. Mean (± SE, n = 4), (b) 20 μL final active fraction per leaf. Mean (± SE, n = 3), and (c) 20 μL 0.05 mg/mL α-HL (**41**) per leaf. Mean (± SE, n = 4). Statistically significant differences between longer treatment time and 0 min were analyzed by t-test, *P≤0.05, **P≤0.001.

After 60 min treatment, the *Spodoptera*-derived OS up-regulated the expression of *CML42* sixfold, which was comparable to feeding larvae of *Spodoptera*. Both, the final active fraction and a dilution of α-HL (**41**) clearly induced after 30 min an up-regulation albeit to a lower extend than the OS. These results suggested that a porin-like protein was most likely one of the factors present in the OS that could trigger *CML42* up-regulation.

3.1.9 VOC emission assay collected by charcoal trap in *P. lunatus*

Emission of VOC from plants is an intensively studied example of an inducible and indirect defense response. It is employed in the attraction of carnivorous insects searching for their prey[7]. The insect feeding-induced VOC emission has been demonstrated for several plant species, for example maize[41], cotton[98] and lima bean[99].

In order to evaluate the VOC emission caused by channel-forming compound, freshly detached plantlets of lima bean (*P. lunatus*) were placed into a solution contained fresh OS, α-HL (**41**), and 1 mM JA (**1**) solution (1% MeOH) as positive control. Headspace VOC were collected during 24 h after treatment, and eluted from the charcal trap by CH_2Cl_2 for GC-MS analysis (**Figure 27**).
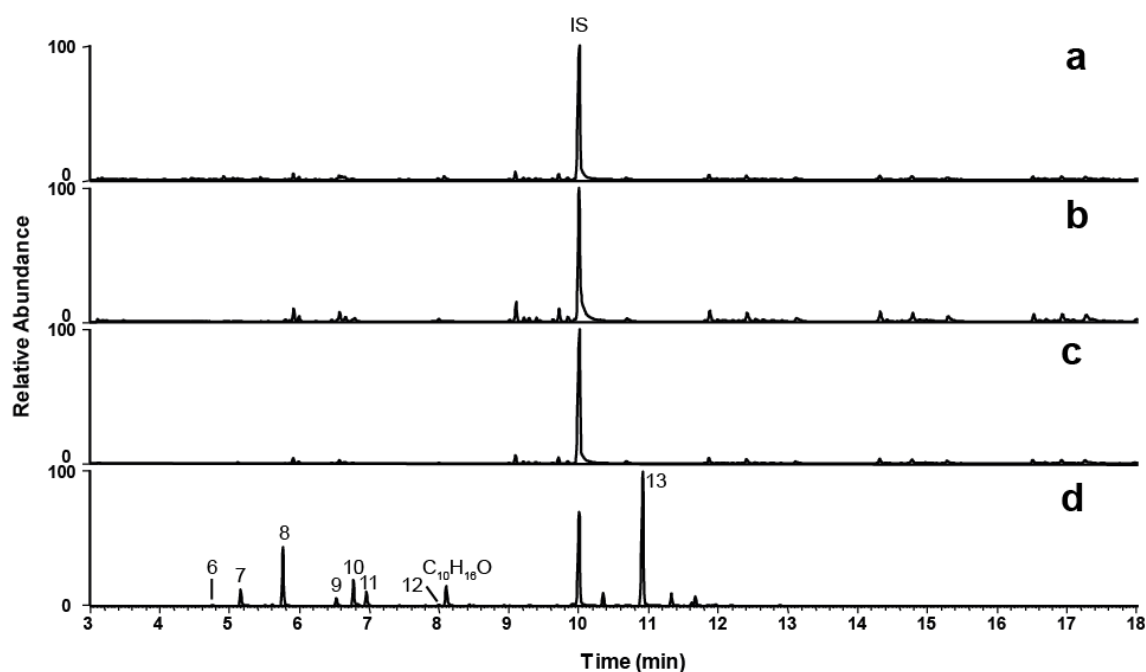
Figure 27. GC-MS profiles of induced VOC emitted from *P. lunatus* leaves treated by different sample solution. (a), 20 μL 10 mM Tris/HCl buffer pH 8.0 in 2 mL H_2O; (b), 20 μL crude OS in 2 mL H_2O; and (c), 20 μL 1.0 mg/mL α-HL (**41**) in 2 mL H_2O; (d), 1 mM JA (**1**) solution (1% MeOH in H_2O). IS, internal standard (1-bromodecane, 200 ng/mL).

In contrast to feeding experiments, OS solution couldn't induce strong VOC emission in lima bean. However the continuous mechanical wounding "MecWorm" was sufficient to elicit herbivory-related volatile emission, although the amount was not exactly the same as insect feeding[36]. This indicated that mechanical wounding played an important role in triggering of VOC emission, however the OS had unknown regulatory effect. The observation from α-HL

(**41**) treatment s uggested t hat t he ch annel-forming P LP is n ot s ufficient to e licit th e V OC emission.

3.1.10 VOC emission assay with SpitWorm and zNose in *P. lunatus*

In order to better mimic the insect feeding process, the SpitWorm was designed to combine the mechanical wounding and chemical factors from OS. The VOC emission assay was also modified with SpitWorm together with zNose[100] (**Figure 28**). With SpitWorm damage, the MecWorm part can produce continuous mechanical wounding and damaged leaf tissue. During damage, OS was continuously provided onto the damage site, and can directly contact with damaged leaf tissue. zNose allowed a continuous monitoring of the emission of volatiles from biological sources with high time resolution.
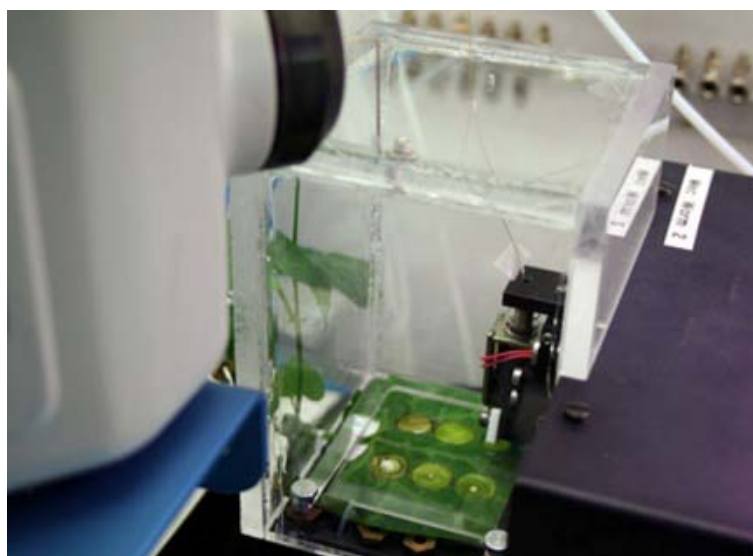
Figure 28. The setup of SpitWorm and zNose for the VOC detection

Ocimene (**8**), DMNT (**10**), MeSA (**12**) and TMTT (**13**) were typical VOC released during insect feeding. We focused on these four compounds to evaluate the effect of OS and α-HL (**41**). The instrument was calibrated by using standard compounds ocimene (**8**), DMNT (**10**), MeSA (**12**) and TMTT (**13**). Diurnal an d n octurnal d amage d ifferences[101] to in itiate V OC emission were involved in the experiment as well. During three days treatment, typical VOC emission was monitored with the zNose by recording the response every 10 min. The behavior of ocimene (**8**), DMNT (**10**), and MeSA (**12**) was quite similar among MecWorm, Spit-Worm-OS, and SpitWorm-α-HL (**41**) (**Figure 29**). This indicated that the emission of these three VOC is mainly induced by continuous mechanical damage, while OS and α-HL (**41**)

didn't show a significant contribution. TMTT (**13**) showed more emission in the SpitWorm treatment, compared with MecWorm treatment alone. This indicated that TMTT (**13**) biosynthesis was influenced by the chemical components present in OS.
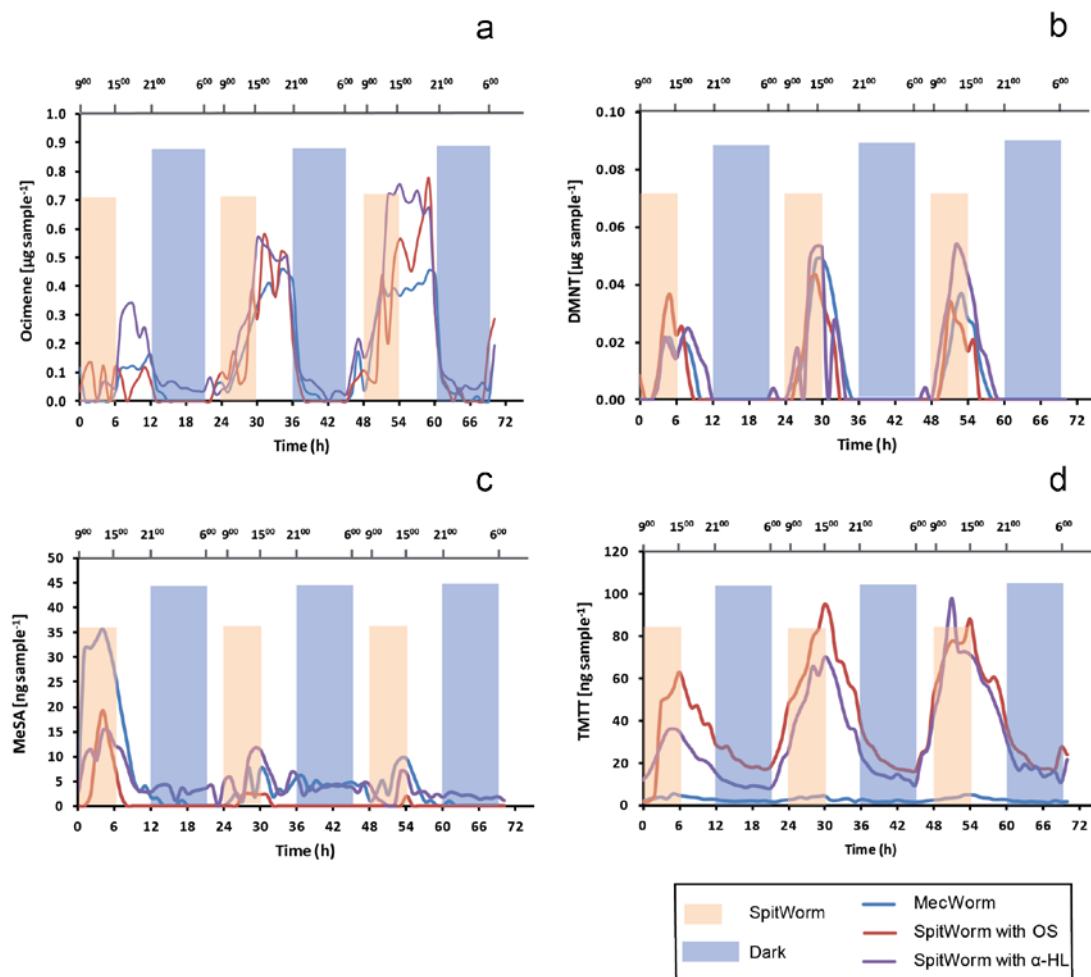
Figure 29. (a), Emission of ocimene (8); (b), emission of DMNT (10); (c), emission of MeSA (12), and (d), emission of TMTT (13) in SpitWorm-treated lima bean leaves: Headspace analyses were performed in triplicate and one typical example was present.

3.1.11 Summary of plant defense reactions induced by PLP and α-HL (41)

Channel-forming activity of OS was widespread among at least four different lepidopteran insect families, indicating a widespread phenomenon in the initial phase of plant–insect interaction. Since the collection of the OS from larvae of *S. littoralis* was time-consuming and laborious (20 μL OS per larva per harvest), it was difficult to get sufficient pure material from original OS. The combination of protein biochemistry and proteomic analysis provided an alternative and practical way to characterize the active candidates from the mixed sample.

The commercially available α-HL (**41**) was applied to mimic the channel-forming PLP, in order to further evaluate the function of channel-forming compounds in diverse plant defense reactions. The activities are summarized in **Table 2**.

Table 2. Summary of plant defense activities of OS, final active fraction (Fr.6) and α-HL (41)

Biological assay	*OS*	*Fr. 6*	*α-Hemolysin (41)*
BLM assay (K^+)	+	+	+ (30 nM)
BLM assay (Ca^{2+})	–	+	+ (60 nM)
Ca^{2+} assay (soybean cell)	+	–	– (0.5 μM)
Ca^{2+} assay (*A. thaliana* leaf)	+	–	– (0.6 μM)
Apoplastic voltage	+	–	–
Jasmonates (**1**, **3–5**)	+	n.d.	– (1.5 μM)
SA (**2**)	–	n.d.	– (1.5 μM)
CML42 gene expression	+	+	+ (1.5 μM)
VOC emission (charcoal)	–	n.d.	– (0.3 μM)
VOC emission (SpitWorm)	–	n.d.	– (3.0 μM)

The general screening for elicitors based on direct channel formation in the artificial membranes, and the BLM-guided purification was performed using KCl buffer. Conflicting results were obtained in the Ca^{2+} assay between crude OS and BLM active fractions: active fractions with PLP were active in the BLM-assay, while the crude OS was not (**Figure 19b**). Only after removal of the unknown component(s) by extracting the OS with CH_2Cl_2, the remaining aqueous phase triggered the Ca^{2+} flux**.** Strikingly, when the separated fractions were recombined, the Ca^{2+} flux was no longer observed (**Figure 20d**), suggesting a still unknown interaction between the compounds in the complex OS mixture.

The low response of α-HL (**41**) and the PLP-fraction in measurements of cytosolic Ca^{2+} can be easily explained if the plant cell wall hampered the mobility of the PLP and therefore the protein couldn't reach the cell membrane to form channels; or the Ca^{2+} increase took place but was simply too low to be detected. Alternatively, in the soybean cells, a receptor-mediated process might be responsible for the Ca^{2+} flux that can be initiated by yet not identified elicitors, which were absent after the first purification step. Considering the complexity of HAMPs[102,103], the data suggested that different biological active compounds existed in the crude OS which are responsible for the *in vivo* and *in vitro* Ca^{2+} flux and furthermore regulate the Ca^{2+} influx in plant cell.

Up-regulation of *CML42* by the insect-delivered PLP suggested that channel formation might be an important factor for the plant to balance its defenses against various herbivores. A possible mechanism for the onset of plant defense is the channel/pore formation by PLP-type proteins on the plant cell membrane triggering transmembrane ion fluxes and subsequent membrane depolarization. A receptor-mediated regulation of *CML42* by unknown compounds from the OS was also possible.

Previous research showed that the phytohormone responses to elicitors are similar. However activity was idiosyncratically distributed across angiosperm diversity. For example, in *A. thaliana*, only caeliferin A (**37**) was active, volicitin (**14**) and inceptin had no effect to the phytohormone elevation. A missing effect for the elevation of phytohormone by α-HL (**41**) and PLP suggestes that the channel formation might only effect on the early signaling, and does not contribute to the late plant responses. There must be other later signals which trigger the late signaling. However, crude OS contained diverse classes of elicitors targeting various biochemical mechanisms and inducing different plant responses. So it seems that only the combination of those different elicitors leads to the full spectrum of plant defense reactions.

No significant VOC emission was detected after treatment with α-HL (**41**) or crude OS. VOC emission by herbivore feeding could be started by continuously mechanical damage and tuned by the chemical factors from OS. However little is known about this fine regulatory relationship between mechanical damage and chemical elicitors. Metabolite induction is the very late defense event in the plant, which involves the accumulative signal cascades from the early events, and this process needs to be clarified in future.

3.1.12 Putative gut microbial origin of PLP

According to the proteomic analysis, the PLP hit matchs with the porin protein from bacterial *Ralstonia pickettii*. However this bacterium species couldn't be detected in the insect's microbe[104]. Considering the complex microbiota in the insect gut, they are the important members in the insect gut ecosystem and might contribute to the plant–insect interaction by secreting multiple metabolites into the regurgitant (OS). Therefore we tried to evaluate whether the gut bacteria could produce channel-forming activity, in order to further identify the channel-forming compound from gut microbial secretion. This observation will be used to prove the important role of gut microbes, and better understand the relationship among host plant, feeding insect and symbiotic bacteria.

Enterococcus mundtii and *Clostridium* sp. were the major bacterial species among the commensals in 4th instar *S. littoralis* larvae in which stage the OS was collected. *E. mundtii* derived mundticin[105] and *Clostridium* sp. derived Epsilon toxin[106] were typical channel forming peptides and proteins produced by these two species, suggesting that the gut microorganisms have to be considered as a rich source of channel-forming compounds. The fermentation of *E. mundtii* didn't show the channel-forming activity in BLM assay, however *C. cellulolyticum* could (**Figure 30**). Therefore we mainly focused on the investigation of *C. cellulolyticum* secreted channel-forming compound(s).
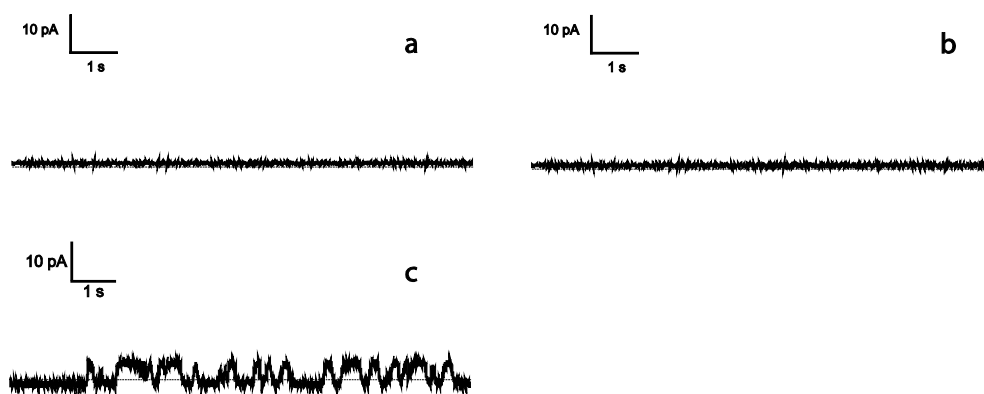

Figure 30. Currents generated by: (a), H_2O as negative control; (b), fermentation of *E. mundtii*; (c), fermentation of *C. cellulolyticum* in BLM assay with KCl buffer.

C. cellulolyticum is an anaerobic nonruminal Gram-positive bacterium that was isolated from decayed grass compost and was an important industrial strain as a result of its ability to degrade crystalline cellulose[107]. The reported secondary metabolites have been only identified under the induction by soil extracts. This indicated that the elicitor(s) from the soil extract could activate the "silent" gene expression and leading to a better survival in the environment. In order to mimic the gut environment, the wild type *C. cellulolyticum* was incubated together with certain amount of oral secretion. The secretion of channel-forming compound(s) was confirmed by test the BLM activity of induced liquid culture (**Figure 31a** and **Figure 31b**). However the activity was not quite stable, base on the observation of missing activity from measurement to measurement.

50 mL *C. cellulolyticum* fermentation induced with 200 μL OS was submitted to further investigation. In order to classify the type of this channel-forming compound(s), several treatments were applied to this sample. Heating at 100 °C for 15 min could destroy the BLM activity (**Figure 31c**), and Vivaspin 30 KD could keep the BLM activity on nonfiltrated part

(**Figure 31d**). T hese results indicated that the channel-forming proteins might be the poten-
tial candidate.
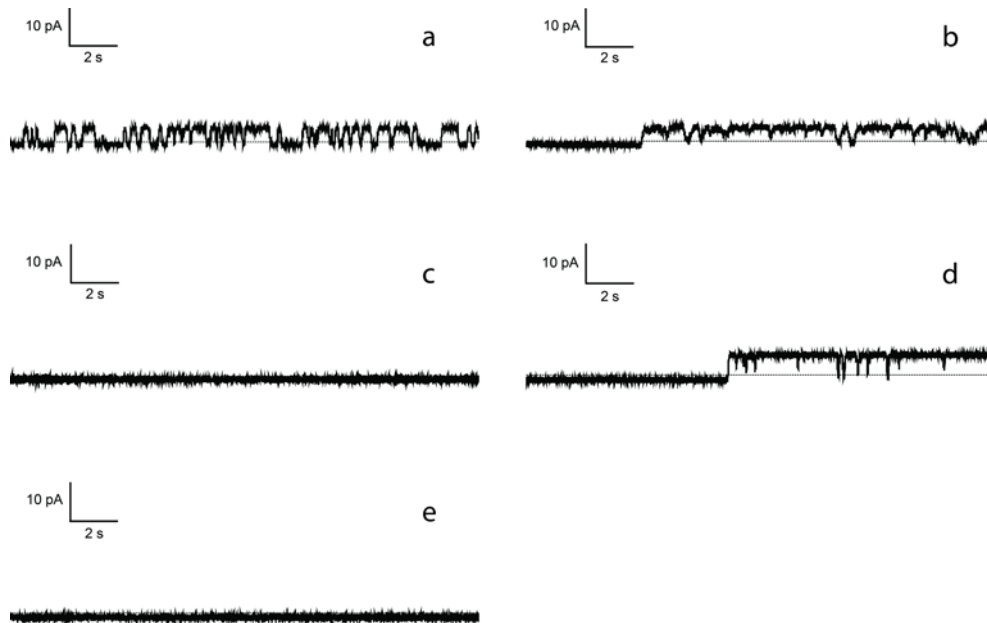
Figure 31. Currents generated by: (a), 50 mL WT *C. cellulolyticum* induced by 400 μL OS;
(b), 50 m L W T *C. c ellulolyticum* induced by 200 μL O S; (c), heating at 1 00 $^{\circ}$C; (d), 50 m L
WT *C. c ellulolyticum* induced by 200 μL O S after Vivaspin 30 KD separation; (e), nonfil-
trated part and filtrated part in BLM assay with KCl buffer.

After concentration b y Vivaspin 30 KD, t he s upernatants of WT *C. cellulolyticum* and i n-
duced *C. cellulolyticum* were submitted to the electrophoresis analysis by loading sample to
12% SDS-PAGE gel, following the Coomassie Staining (**Figure 32**).

**Figure 32. G el electrophoresis o f t he s upernatant f rom W T *C. cellulolyticum* and i n-
duced *C. cellulolyticum* concentrated by Vivaspin 30 KD.**

The significantly different protein profiles from WT and induced sample indicated the crucial
influence from added OS. Considering the complex digestive proteases present in the OS, the
"new" proteins in the induced sample might originate from the hydrolysis of WT proteins by

OS. Alternatively the chemical compounds present in the OS could induce new protein expression in order to adjust to the complex gut environment.
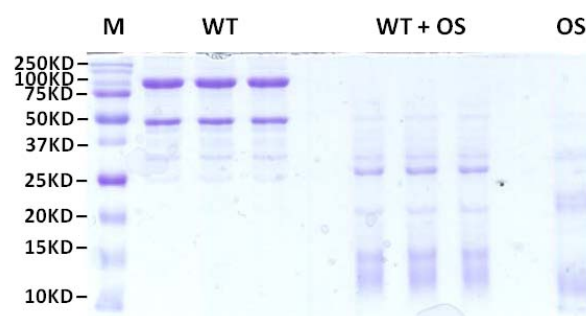
The concentrated supernatant from Vivaspin 30 KD filtrater was submitted to Superdex 75 coupled with ÄKTA FPLC system, eluted by BLM buffer (10 mM Tris/HCl, 200 mM KCl, pH 9.2). The elution profile is present in **Figure 33**. BLM active fraction B4 and B5 were submitted to in-solution proteomic analysis with MS^E data acquisition. The protein information is present in the **Table S5**.
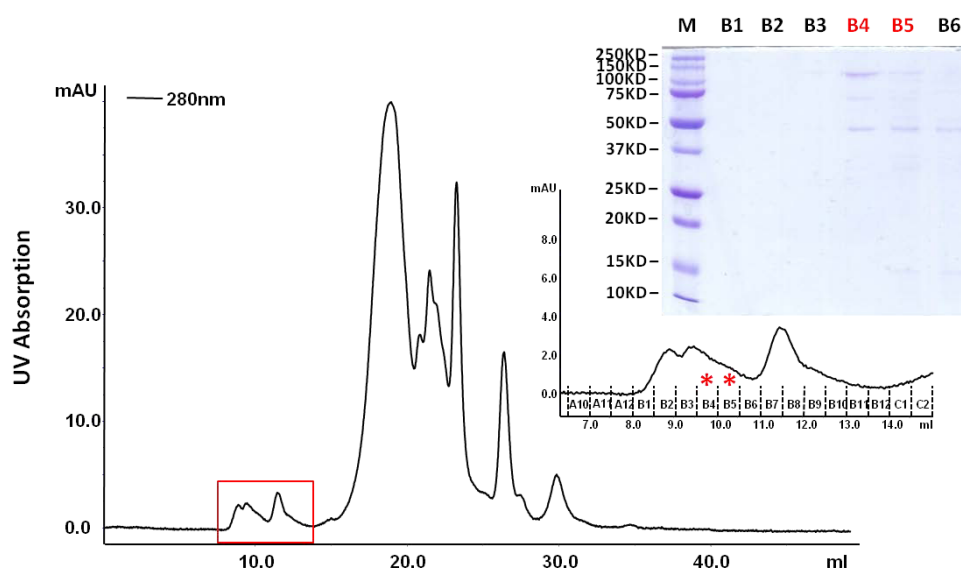
Figure 33. ÄKTA Superdex 75 chromatogram of concentrated supernatant by Vivaspin 30 KD, and corresponding electrophoresis of 12% SDS-PAGE gel (Fractions B4 and B5 were BLM active.)

3.1.13 Evaluation of the plant defense activities of alamethicin (42)

In order to further evaluate the plant response from different channel forming compound, the similar plant defense activies were evaluated from different type of channel-forming compounds. Here we focused on the channel forming peptaibol alamethicin (ALA, **42**), and tried to compare the plant defense activities between α-HL (**41**) and ALA (**42**) in *in vivo* Ca^{2+} assay, *CML42* gene expression level, and VOC emission treated by SpitWorm and detected with zNose.

3.1.13.1 Calcium ion-dependent BLM assay

In vitro ion permeation of ALA (**42**) in BLM assay has already been deeply investigated. ALA (**42**) exhibited a strong voltage-dependent conductance in membranes formed from 2.5%

sphingomyelin in tocopherol, from chloroform, from methanol (5:3:1, v/v/v) with 0.1 M NaCl solution[77], and from 1% lecithin in n-decane with 0.1 M KCl solution[108]. Additionally, there was a ratio of $P_{Ca}/P_{Cl} = 0.3$ from 1% phosphatidyl ethanolamine in n-decane[109]. However, little has been known about the Ca^{2+} permeation of ALA (**42**) in BLM system with an artificial membrane formed from lecithin in heptane. Because the lipid composition might have influence on the channel formation, it was necessary to evaluate BLM activity again using lecithin in heptane to form the artificial bilayer. Ca^{2+} permeation in the BLM system which contained 20 mg/mL lecithin in heptane was highly concentration-dependent, 100 μg/mL (50 μM) and 10 μg/mL (5 μM) ALA (**42**) could exhibit BLM activity, but a concentration of ALA (**42**) at 1 μg/mL (0.5 μM) was inactive in the BLM assay (**Figure 34**).
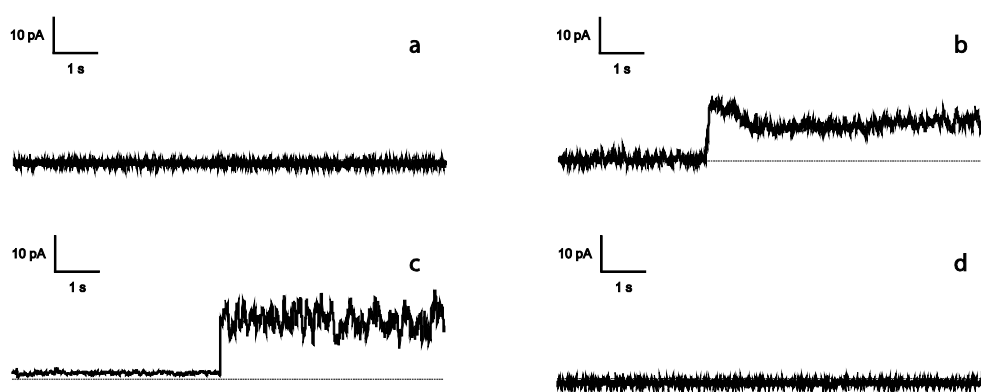
Figure 34. Currents generated by ALA (42) in BLM assay with Ca(NO₃)₂ buffer. (a), 1 μg/mL ALA (**42**) in 1% MeOH; (b), 10 μg/mL ALA (**42**) in 1% MeOH; (c), 100 μg/mL ALA (**42**) in 1% MeOH; (d), 1% MeOH as negative control.

3.1.13.2 *Measurement of the cytosolic Ca²⁺ concentration in vivo*

The ALA (**42**) channel could permeat the Ca^{2+}, Mn^{2+} and Ni^{2+} in bovine chromaffin cells at a concentration of 100 μg/mL[110]. Ca^{2+} permeation could be also detected in rabbit skeletal muscle sarcoplasmic reticulum vesicles, rat brain microsomes, and rat liver mitochondria at 3–7 μg/mL ALA (**42**)[111]. To evaluate Ca^{2+} ion flux elicited by ALA (**42**) in planta, changes of cytosolic Ca^{2+} were measured by using a suspension of transgenic soybean cells and *A. thaliana* whole leaves which expressed the Ca^{2+} sensing protein aequorin. Dose-dependent increase of $[Ca^{2+}]_{cyt}$ could be detected in the soybean cell system. While 10 μg/mL ALA (**42**) didn't show activity (**Figure 35**), 100 μg/mL ALA (**42**) was active either in soybean cell system or in *A. thaliana* leaf system (**Figure 36**).

Figure 35. Changes of cytosolic Ca^{2+} concentration ([Ca^{2+}]$_{cyt}$) in soybean cell suspension cultures expressing the Ca^{2+} sensing aequorin system treated by: (a), 10 µg/mL 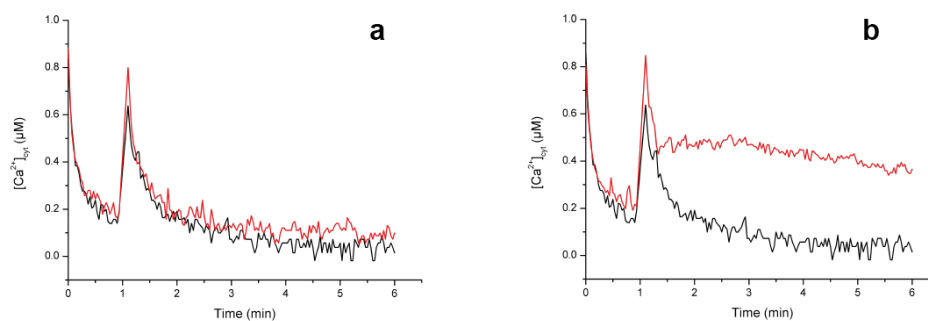ALA (**42**) in 1% MeOH (20 µL); (b), 100 µg/mL ALA (**42**) in 1% MeOH (20 µL). Red line represented ALA (**42**) sample, black line represented negative control (1% MeOH).
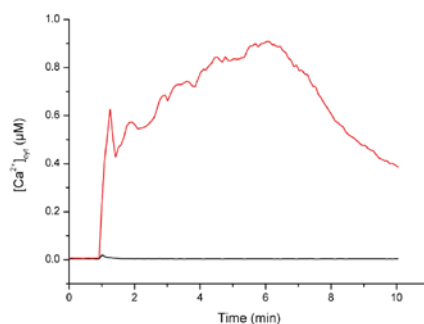
Figure 36. Changes of cytosolic Ca^{2+} concentration ([Ca^{2+}]$_{cyt}$) in *A. thaliana* leaf tissue expressing the Ca^{2+} sensing aequorin system treated by: 100 µg/mL ALA (**42**) (25 µL) in BLM assay.   Red line represented sample, black line represented negative control (1% MeOH).

Due to the complexity of the plant cell membrane, it was difficult to conclude that the increase of [Ca^{2+}]$_{cyt}$ was only dependent on the Ca^{2+} permeation through the ALA (**42**) channel. It was also possible that a specific Ca^{2+} channel was opened either by depolarization-activated or by receptor-activated signal pathway.

3.1.13.3 Defense-related gene CML42 up-regulation assay

In order to evaluate the activity of ALA (**42**) on the defense marker gene, the transcription level of *CML42* has been measured after treatment by 2 µg ALA (**42**) on damaged *A. thaliana* leaves (wild type Col-0) (**Figure 37**). ALA (**42**) could trigger the up-regulation of *CML42* with a maximum three folds value of up-regulation after 45 min treatment, which was later than the effect from α-HL (**41**) treatment (30 min).
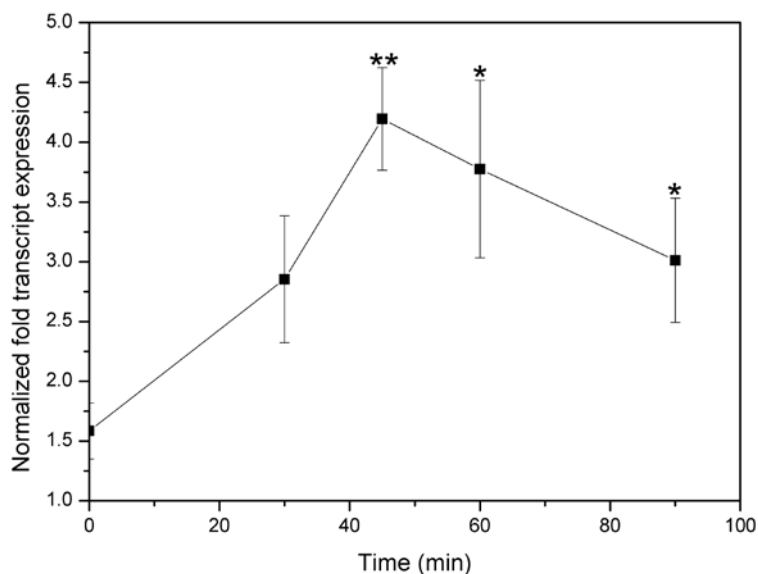
Figure 37. *CML42* transcript l evels i n *A. thaliana* leaves t reated w ith 2 µg ALA (**42**). The fold change was calculated relative to a control which was wounded by pattern wheel plus 1% MeOH per leaf. Mean (± SE, n = 4). Statistically significant differences between longer time of treatment and 0 min were analyzed by t-test, *P≤0.05, **P≤0.001.

As discussed be fore, *CML42* might b e a n egative r egulator dur ing pl ant de fense r eaction. However ALA (**42**) is a strong positive effector of plant defense. This indicated that *CML42* is a possible multi-functional defense-marker gene, however the signal cascades of ALA (**42**) and *CML42* need to be further investigated.

3.1.13.4 VOC emission assay with SpitWorm and zNose

Three defense-related VOC (DMNT (**10**), MeSA (**12**) and TMTT (**13**)) from lima bean plant were emitted strongly when the plant was immersed into a ALA (**42**) solution[80,100]. However, the emission kinetic was not investigated. Therefore, we would like to evaluate the effect of VOC emission of ALA (**42**) under the SpitWorm treatment with zNose detection (**Figure 38**).

Compared with the MecWorm treatment, ocimene (**8**) was produced less by SpitWorm treatment. DMTT (**10**), MeSA (**12**) and TMTT (**13**) were major VOC at 100 µg/mL ALA (**42**) treatment. This result i ndicated t hat onl y continuously mechanical d amage was e nough t o trigger the ocimene (**8**) emission, but the stronger emission of DMTT (**10**), MeSA (**12**) and TMTT (**13**) were induced by the ALA (**42**) treatment.
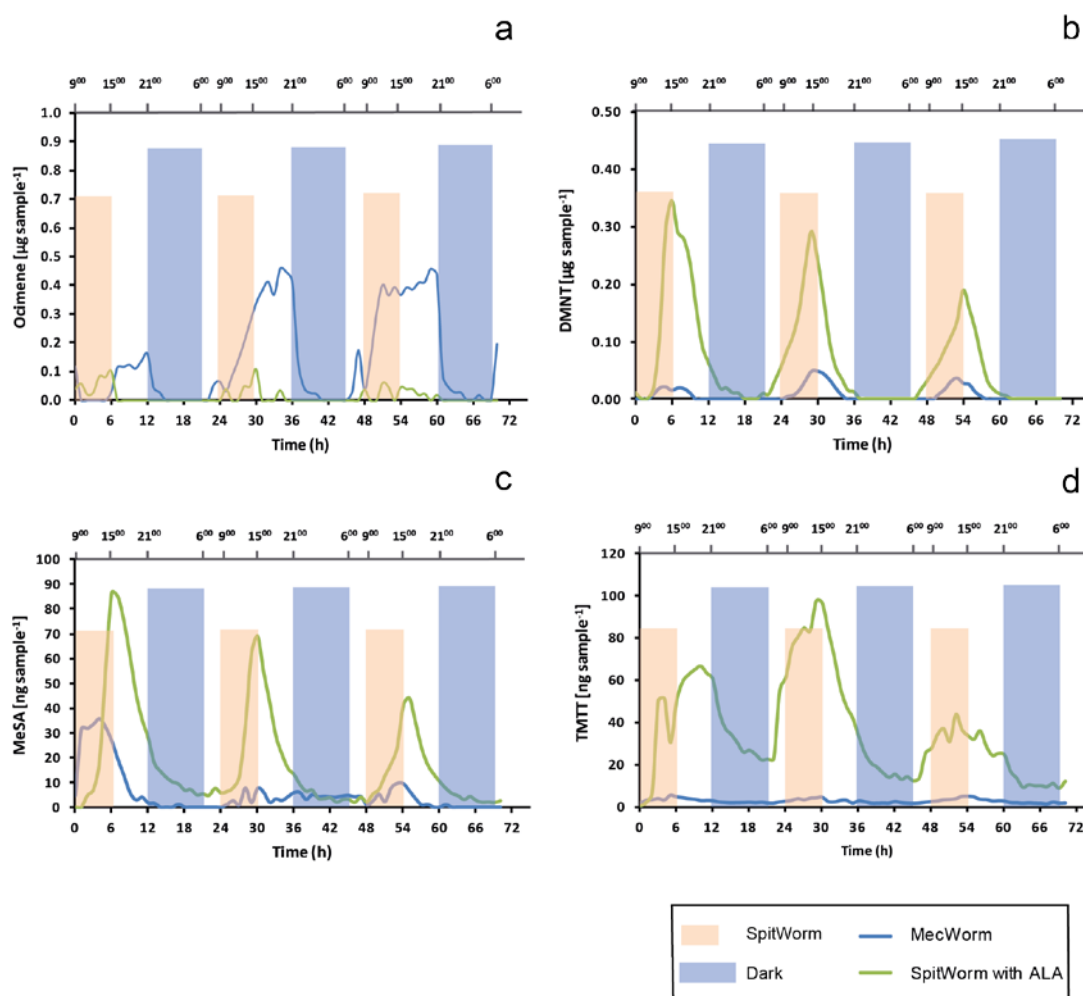
Figure 38.   (a), E mission of o cimene (8); (b), e mission of DMNT (10); (c), e mission of MeSA (12) a nd (d), e mission of TMTT (13) in Spi tWorm-treated lima b ean leaves: Headspace analyses were performed in triplicate and one typical example is presented.

3.1.13.5 Summary of plant defense activities after alamethicin (42) treatment

ALA (**42**) could trigger the elevation of $[Ca^{2+}]_{cyt}$, induce the long distance electrical signal[81], increase the transcription level of the defense-related gene *CML42* and activate phytohormone elevation and VOC emission (**Table 3**).

In line with the literature, some significant plant defense activities induced b y ALA (**42**) are summarized in **Table 4**. As a model for channel-forming compounds, ALA (**42**) was used to evaluate t he effect of por e-formation for plant defense response. M any different ch annel-forming compounds have been used in parallel to compare their effects, for example compari-son between channel-forming peptides and specific channel-forming peptaibols[79,80]. ALA (**42**) could exhibit mu lti-functions, others were either i nactive or low e fficient. There are at least two reasons for the action of ALA (**42**).

Table 3. Summary of plant defense activities induced by alamethicin (42)

Biological assay	Alamethicin (42)
BLM assay (K^+)	+
BLM assay (Ca^{2+})	+
Ca^{2+} assay (soybean cell)	+ (8.3 μM)
Ca^{2+} assay (*Arabidopsis* leaf)	+ (10 μM)
Apoplastic voltage	+ (25 nM)
JA (**1**)	+ (5.0 μM)
(−)-JA-L-Ile (**3**)	n.d.
(+)-7-*iso*-JA-L-Ile (**4**)	n.d.
cis-OPDA (**5**)	+ (5.0 μM)
SA (**2**)	+ (5.0 μM)
CML42 gene expression	+ (50 μM)
VOC emission (charcoal)	+ (5.0 μM)
VOC emission (zNose)	+ (50 μM)

Table 4. Summary of plant defense reactions induced by alamethicin (42)

Plant	Defense marker gene	Defense events and signaling	Mechanism
P. lunatus		JA elevation[11,80]	Octadecanoid pathway[11]
		VOC emission[11,80]	MEP-pathway[82]
		SA elevation	
		depolarization[81]	
Nicotiana tabacum		apoptosis	Permeable for small molecules[112]
A. thaliana	*AtBSMT1*	MeSA elevation[83]	carboxyl methyltransferase[83]
	TPS04/GES[84]	TMTT biosynthesis	geranyllinalool synthase (GES)
	At3g25180[113]	TMTT biosynthesis	P450 enzyme CYP82G1
	PR2[79]	Phenolic compounds	hypersensitive responses
	PDF1.2[79]	ROS intermediates	
		Callose deposition	
		DNA fragmentation	
		rRNA degradation[114]	
		Callose synthase[115]	Ca^{2+} elevation
	CML42		
Lotus japonicus	*LjEbOS*[116]	(*E*)-β-Ocimene	(*E*)-β-Ocimene synthase

The arrangement of the peptide as an octameric pore provides the ALA (**42**) specific biological activities. Normally peptaibols contain several α-aminoisobutyric acid (Aib) residues and carry an acetylated *N*-terminal residue and a *C*-terminal 1,2-aminoalcohol (phenylalaninol).

ALA (**42**) has more stability against enzymes of the peptaibol in planta due to its high content (37%) in Aib residues[79]. In addition, strong helicogenicity is also an important factor because Aib could support (α- or 3_{10}-) helical structures more effectively than normal amino acid due to typical $C^{\alpha,\alpha}$-dimethylation (Thorpe-Ingold effect)[117]. A minimal length is also a prerequisite for peptaibol activity in plants. Secondly, besides the channel-forming effect, it was also possible that some ligand recognition interactions with a receptor on the cell membrane may play an important role due to the specific amino acid sequence of ALA (**42**). ALA-induced plant defense was also a dose-dependent process, higher concentration effects and lower concentration effects may be associated with different active cellular events[79].

Besides the plant defense activities, alamethicin (**42**) also affects insect cells. ALA F30 induces tissue damage in larvae of mosquito *Culex pipiens*, with an LD_{50} value of 110 μg/mL after 48 h ALA (**42**) exposure[118]. A rapid efflux of intracellular K^+ through the plasma membrane of two insects, *S. frugiperda* and *Choristoneura fumiferana*, was induced by ALA (**42**) as a consequence of ion-channel formation[119]. ALA (**42**) also showed cytotoxicity in *in vivo* assay, with the LD_{50} value of 80 mg/kg after oral administration to mice[120].

3.1.13.6 Comparison of the plant defense activities between α-HL (41) and ALA (42)

α-HL (**41**) is a typical channel-forming protein secreted from bacteria, and alamethicin (**42**) is a typical channel-forming peptaibol secreted from saprophytic fungi. Both had significant channel-forming activity not only in an artificial membrane but also in real biomembranes. However, the effects are not identical. The major differences between α-HL (**41**) and ALA (**42**) are summarized in **Table 5**. And the difference of plant defense activities between α-HL (**41**) and ALA (**42**) are summarized in **Table 6**.

Table 5. Comparison of the channel-forming activities between α-HL (41) and ALA (42)

Channel property	*α-HL (41)*	*ALA (42)*
Molecular size	33 kDa	2 kDa
Conductance	90 pS (100 mM KCl) 450 pS (500 mM KCl)	8 nS (100 mM KCl)
Ion selectivity	$P_{Ca}/P_{Cl} = 0.05$ (pH 7.0) $P_K/P_{Cl} = 0.5$ (pH 7.0)	$P_{Ca}/P_{Cl} = 0.3$ $P_K/P_{Cl} = 2.7$ $P_{Na}/P_{Cl} = 1.6$
Pore diameter	1.5 nm (7 monomers)	2.6 nm (4-11 monomers)
Mechanism	14-stranded barrel	"Barrel-stave" model
Self-assemble	Seven monomers	3-12 monomers
Toxicity to insect	yes	yes

Table 6. Summary of plant defense activities from α-HL (41) and ALA (42)

Biological assay	OS	Fr. 6	α-HL (41)	ALA (42)
BLM assay (K^+)	+	+	+ (30 nM)	+
BLM assay (Ca^{2+})	–	+	+ (60 nM)	+
Ca^{2+} assay (soybean cell)	+	–	– (0.5 μM)	+ (8.3 μM)
Ca^{2+} assay (*Arabidopsis* leaf)	+	–	– (0.6 μM)	+ (10 μM)
Apoplastic voltage	+	–	– (3.0 μM)	+ (25 nM)
JA (1)	+	n.d.	– (1.5 μM)	+ (5.0 μM)
(–)-JA-L-Ile (3)	+	n.d.	– (1.5 μM)	n.d.
(+)-7-*iso*-JA-L-Ile (4)	+	n.d.	– (1.5 μM)	n.d.
cis-OPDA (5)	+	n.d.	– (1.5 μM)	+ (5.0 μM)
SA (2)	–	n.d.	– (1.5 μM)	+ (5.0 μM)
CML42 gene expression	+	+	+ (1.5 μM)	+ (50 μM)
VOC emission (charcoal)	–	n.d.	– (0.3 μM)	+ (5.0 μM)
VOC emission (zNose)	–	n.d.	– (3.0 μM)	+ (50 μM)

α-HL (41) induces the pore formation in planar lipid bilayer membranes[121], with conductance of 90 pS at 100 mM KCl[122], allowing a rapid efflux of K^+ and influx of Na^+, Ca^{2+} and small molecules in human keratinocytes[123,124,125]. Under neutral condition, α-HL shows weak anion selectivity, and theoretical studies confirm the weak anion selectivity[126]. However the pore can be voltage-dependently inhibited by divalent and trivalent cations[122]. α-HL (41) can also induce the Ca^{2+} influx in pheochromocytoma PC12 cells[69] and human airway epithelial S9 cell at high concentration[127].

Compared with α-HL (41), ALA (42) has a smaller molecular size. This might lead to more flexible transportation of ALA (42) in the biological tissue. The conductance of ALA (42) is quite flexible because it is voltage-dependent and concentration-dependent[78,109]. The smallest conductance substrate (20 pS in 1 M KCl) presumably resulting from a tetramer[128], is impermeable for Ca^{2+} or Cl^-, the maximum conductance could be until μS[109,129]. However the alamethicin (42) channel shows weak cation selectivity with the permeation ratio: $P_{Ca}/P_{Cl} = 0.3$, $P_{Na}/P_{Cl} = 1.6$, and $P_K/P_{Cl} = 2.7$[109]. The pore size of alamethicin (42) is quite flexible, dependent on the number of monomers. The different biological functions of these two channel-forming compounds may be based on the different channel characteristics.

The conductance of channel-forming compounds in crude OS was 340±19 pS at 100 mM KCl[93], however the conductance was concentration-dependent and membrane-dependent[108]. Crude OS exhibited cation selectivity with the permeation ratio of $P_K/P_{Cl} = 4.5$. Ion selectivi-

ty was pH dependent in α-HL (**41**) channel, the permeation ratio of P_K/P_{Cl} was 1.0 at pH 5.0, however at pH 7.0 the ratio was 0.5. Here a basic condition was applied in order to mimic the basic condition in the insect gut.

α-HL (**41**) was a reasonable candidate to mimic BLM active proteins in the crude OS due to (1) its coincidence with the bacterial porin hit from proteomic analysis, (2) it shows a comparable molecular size, and (3) a comparable although not identical BLM activity. Considering the diversity within the porin family in different organism, the PLP present in OS should share some common porin characteristics but very likely have diversely specific structure features. Due to the limited amount of final BLM-active fraction, it was difficult to get pure protein from original spit. Proteomic analysis provided a possibility to identify tiny amount of proteins in complex mixtures. The final aim is to get the pure BLM active protein for further biological tests, and molecular biology approaches are powerful tools to investigate the corresponding genes of the PLP. Heterologous expression provides a possible option to avoid the difficulty of sample collection. In addition, proteomic analysis indicated the bacterial origin of this porin-like protein, and the BLM-activity of exudates from *Clostridum* sp. confirmed this hypothesis. The regulating factor(s) present in the CH_2Cl_2 phase should be investigated in future, to understand the molecular interactions in the crude OS and furthermore for better understanding the signaling cascade in plant–insect interactions.

3.2 Saponins from crude OS

3.2.1 Identification of saponins

The fraction 7 from Sephadex G25 elution (**Scheme 2**) contained glucosides according to the typical neutral loss of sugar moieties in ESI-MS analysis. After 1-butanol extraction (**Figure 39**) followed by HPLC semi-preparative fractionation, two of the major compounds (**46** and **47**) were submitted to 1D and 2D NMR analysis. Combination of the ESI-MS fragmentation pattern and NMR spectra analysis revealed that these two compounds belonged to the olean-12-ene-type triterpene oligoglycosides. Finally 12 oleanene type saponins (**46–57**) were identified from Fr. 7 according to the specific neutral loss pattern of sugar moieties by comparison of the ESI-MS spectra with those of compound **46** and **47**. Olean-12-ene-type triterpene oligoglycosides are typical chemical constituents in beans, which originate from the artificial diet (beans powder). The structures of **46–57** are given in **Figure 40.** Here the structure elucidation of compound **46–57** is discussed in detail.
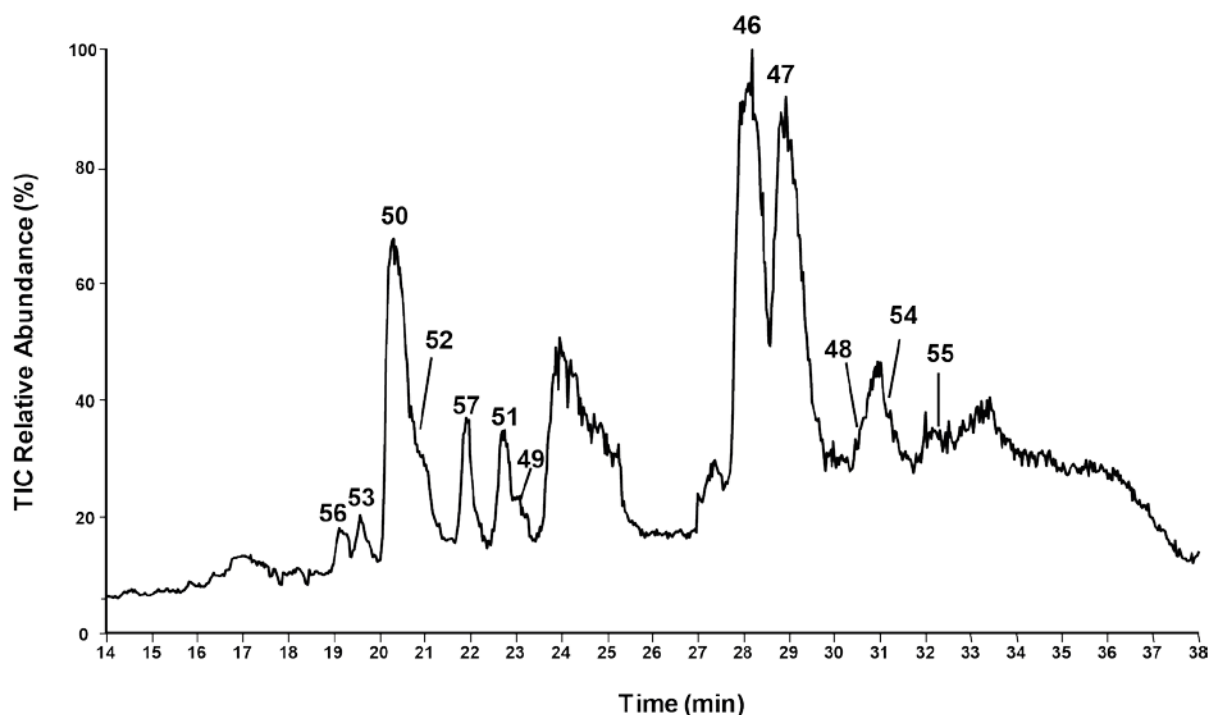

Figure 39. HPLC-ESI-MS total ion chromatogram of fraction 7 from Sephadex G25 fractionation
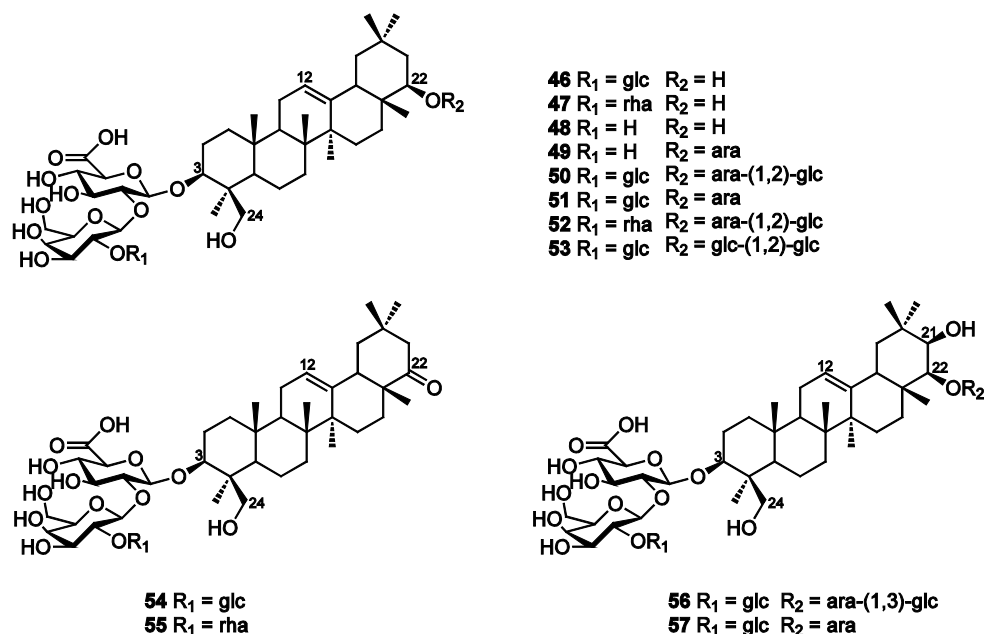
Figure 40. Structures of compounds 46–57

Compound **46** was obtained as a white powder after HPLC semi-preparation. The nominal mass of **46** was determined as M = 958 g/mol according to the ions at *m/z* 959 [M + H]$^+$ and *m/z* 1917 [2M + H]$^+$ (**Figure 41**).
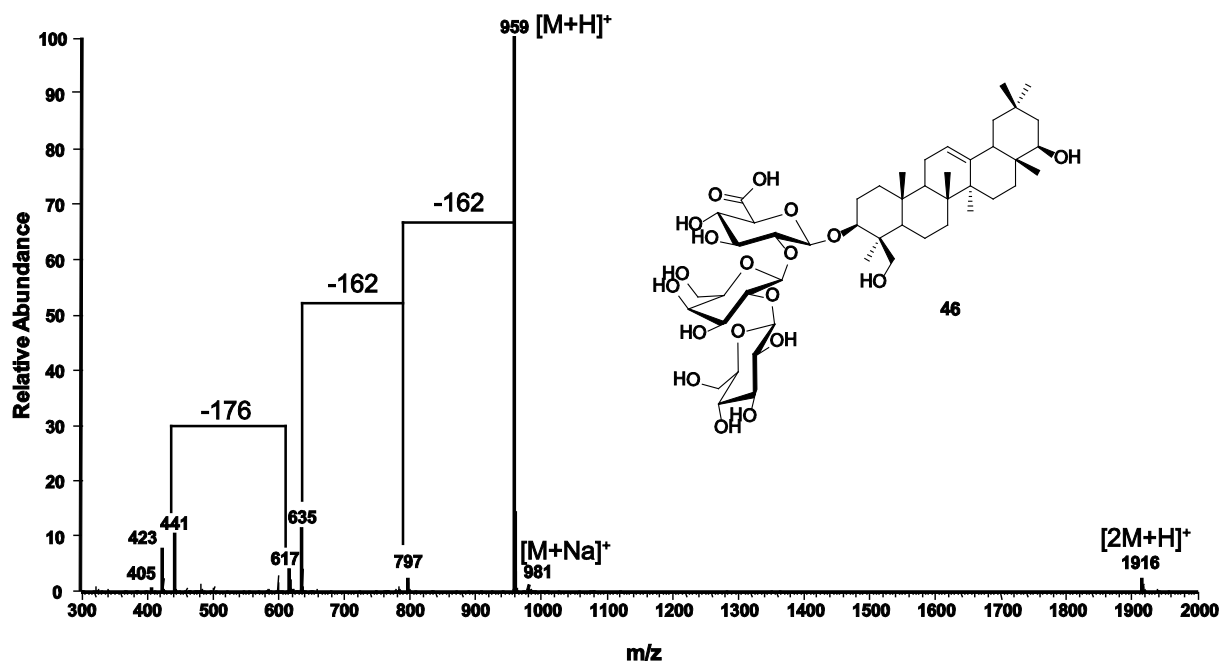

Figure 41. ESI-MS spectrum of soyasaponin V (46)

The molecular formula of **46** was determined to be $C_{48}H_{78}O_{19}$ (10 degrees of unsaturation) by HRESIMS analysis (*m/z* 959.52109 [M + H]$^+$, Δ +0.08 mDa). According to the typical fragment ions at *m/z* 797 [M – hexose + H]$^+$, *m/z* 635 [M – hexose – hexose + H]$^+$ and *m/z* 441 [M

– hexose – hexose – H_2O – hexuronic acid + H]$^+$, there must be two hexose and one hexuronic acid moiety in the molecule. Ions at *m/z* 441, 423, and 405 originated from the aglycone moiety. According to the ^{1}H NMR spectrum of **46** (**Figure 42**), seven singlet methyl groups (δ_H 0.77 ppm, 0.84 ppm, 0.85 ppm, 0.91 ppm, 0.95 ppm, 1.06 ppm, 1.17 ppm) were observed. Overlapping signals (δ_H 0.87–2.08 ppm) belong to methylene and methine protons of the triterpene moiety. The signal at δ_H 5.18 ppm (br s) corresponds to the C-12 olefinic proton of the aglycone. The aglycone moiety was assigned by careful analysis of the ^{1}H-^{1}H COSY, HSQC and HMBC NMR spectra of **46**. Overlapping signals (δ_H 3.10–3.77 ppm) in ^{1}H NMR indicated oxymethine groups in the sugar moiety, and three oxymethine signals at δ_H 4.83 ppm (br d, *J* = 8.5 Hz), 4.58 ppm (br d, *J* = 7.5 Hz) and δ_H 4.51 ppm (br d, *J* = 6.0 Hz) corresponded to the anomeric protons of the sugar moieties. The sugar moieties were assigned as galactose, glucose and glucuronic acid based on the typical chemical shift. The relatively large coupling constants of the anomeric protons indicated the β configuration. The sequence of the sugar chain was assigned as β-glucopyranosyl(1→2)-β-galactopyranosyl(1→2)-β-glucuronopyrano-syl by the observation of HMBC correlations of H2′ with C1″, H2″ with C1‴, H1″ with C2′, and H1‴ with C2″. Additional HMBC correlations of H1′ with C3 and H3 with C1′ indicated that the sugar chain was connected with C3.
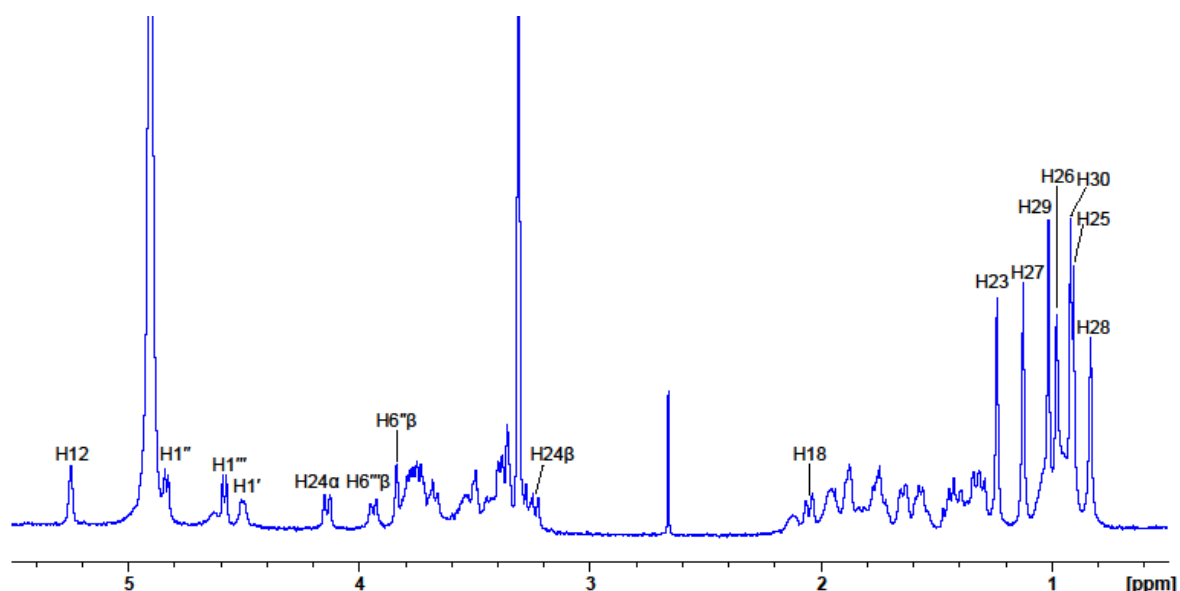
Figure 42. ^{1}H NMR spectrum of soyasaponin V (46, 500 MHz, CD$_3$OD-d_4)

The relative configuration of **46** was assigned according to the 2D ROESY NMR experiment (**Figure 43**). ROESY correlations of H23 with H3 and H5, H9 with H5 and H27, H27 with H9 and H19, H19 with H27 and H30 indicated they located on the same side of the aglycone plane, correlations of H25 with H24, H18 with H26 and H28 suggested they located on the

opposite side of the aglycone plane. Finally the structure was determined as soyasaponin V identified in haricot bean *P. vulgaris* after comparing the NMR data with literature[130].
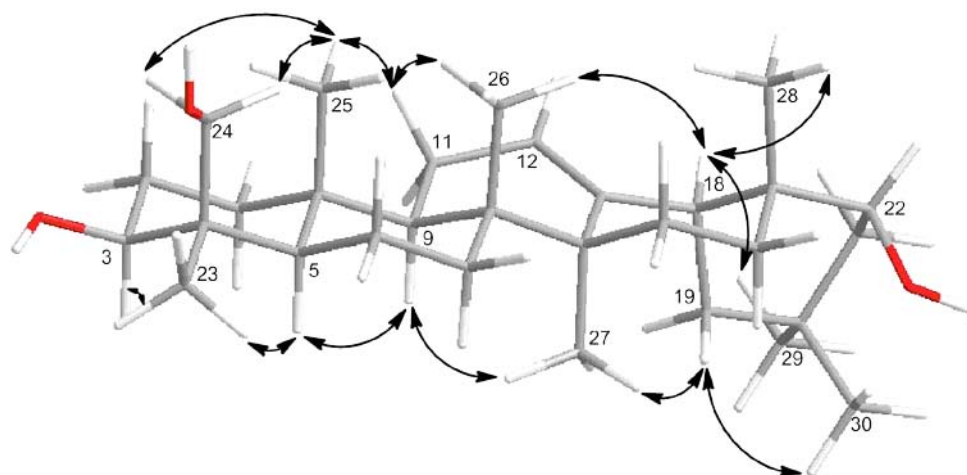
Figure 43. Key ROESY correlations of the soyasaponin V (46) aglycone

Compound **47** was obtained as a white powder after HPLC semi-preparative fractionation. The nominal mass of **47** was determined as M = 942 g/mol according to the ions at *m/z* 943 [M + H]$^+$ and 1885 [2M + H]$^+$ (**Figure 44**).

Figure 44. ESI-MS spectrum of soyasaponin I (47)

The molecular formula of **47** was determined to be $C_{48}H_{78}O_{18}$ (10 degrees of unsaturation) by HRESIMS analysis (*m/z* 943.52661 [M + H]$^+$, Δ +0.52 mDa). Comparison of the ESI-MS spectrum of **47** with **46** showed that the major fragment ions were identical, except for the

quasimolecular ion signal at m/z 943 $[M + H]^+$. This indicated that the difference between these two compounds was the terminal sugar. Due to the difference of 16 Da and the HRMS data, a deoxy sugar was 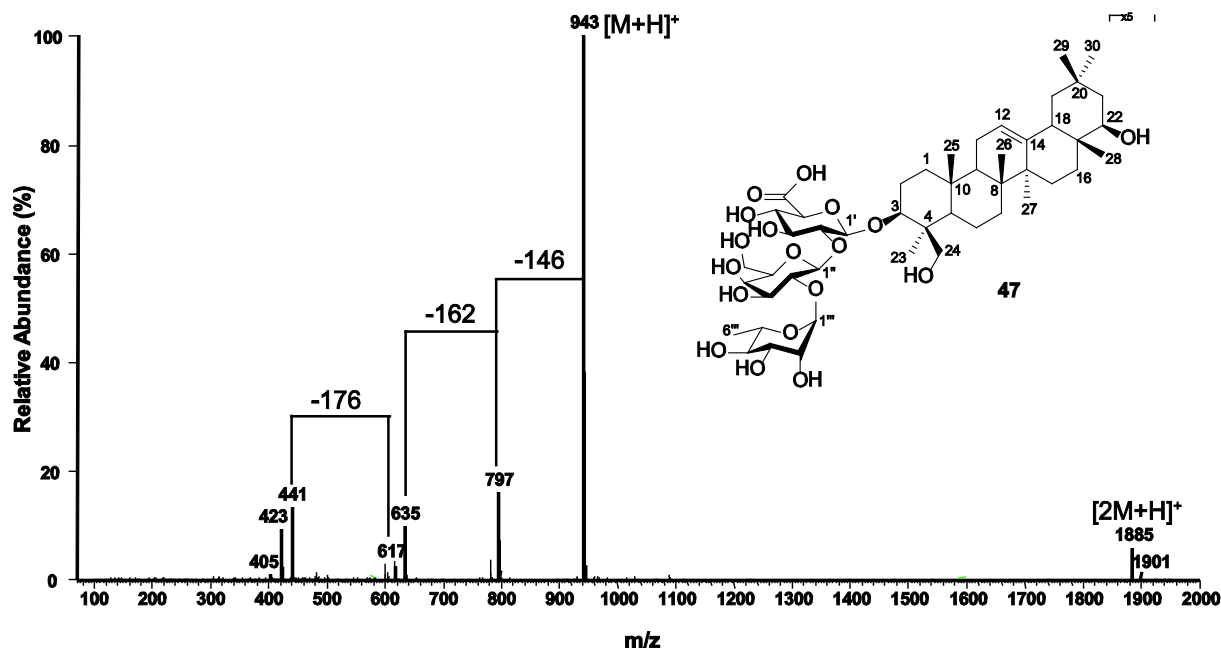the possible option. Detailed analysis of the ^{1}H NMR data, an additional methyl signal at δ_H 1.21 (d, $J = 6.35$ Hz) corresponded to the methyl group of terminal sugar (**Figure 45**). In parallel, one of the anomeric proton shifted from δ_H 4.58 (br d, $J = 7.5$ Hz) in **46** to δ_H 5.13 (br s) in **47**, indicated the terminal sugar was rhamnose, and the configuration can be assigned as α based on the relatively small coupling constant of anomeric proton.
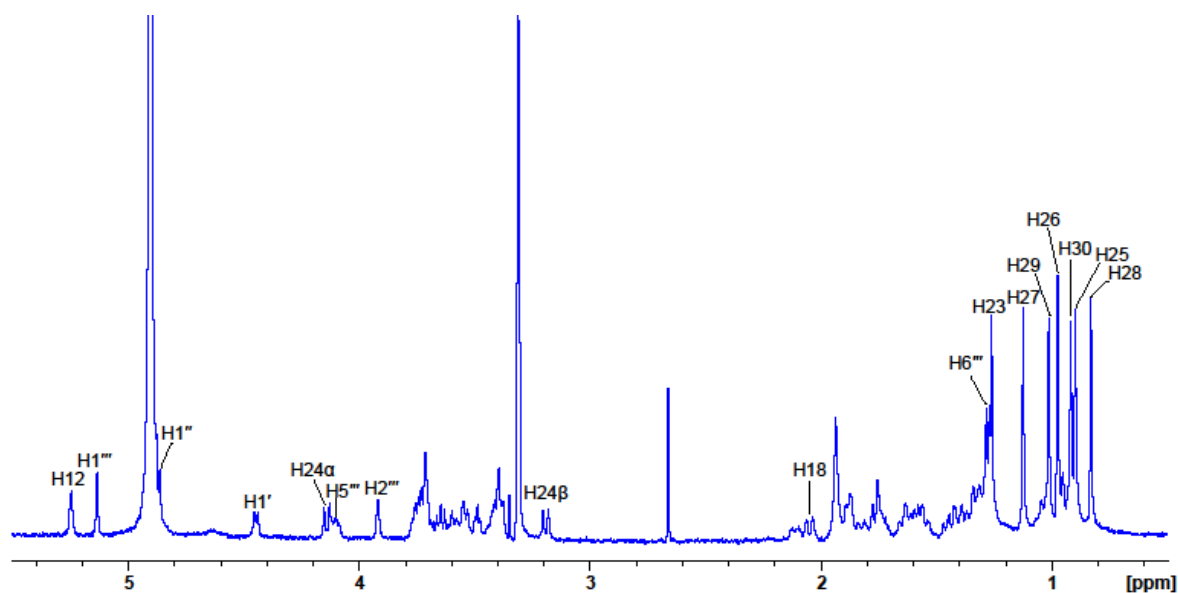

Figure 45. ^{1}H NMR spectrum of soyasaponin I (47, 500 MHz, CD$_3$OD-d_4)

The relative configuration of **47** was assigned according to the 2D ROESY NMR experiment. ROESY correlations of H23 with H3 and H5, H9 with H5 and H27, H27 with H9 and H19, H19 with H27 and H30 indicated they located on the same side of the aglycone plane, correlations of H25 with H24 and H26, H18 with H26 and H28 suggested they located on the another side of the aglycone plane. The structure of **47** was assigned as soyasaponin I[131,132] by detailed analysis of the ^{1}H-^{1}H COSY, HSQC and HMBC NMR data, and the structure was confirmed by comparison of the NMR spectra with those of an anthetic standard soyasaponin I obtained from Sigma.

Compound **48** was obtained as a white powder. Due to the limited amount, the structure of **48** was proposed based on the comparison of ESI-MS fragment patterns with **46** and **47** (**Figure 46**). Detailed analysis of the ESI-MS spectrum indicated the nominal mass of **48** was M = 796 g/mol due to the ions at m/z 797 $[M + H]^+$ and 1593 $[2M + H]^+$. The molecular formula of **48** was determined to be C$_{42}$H$_{68}$O$_{14}$ (nine degrees of unsaturation) by HRESIMS analysis

(*m/z* 797.46744 [M + H]$^+$, Δ −0.74 mDa). Detailed comparison of the mass spectra with **46** and **47** revealed that most of the fragment ions were identical except for the quasimolecular ion peaks observed at *m/z* 797 [M + H]$^+$, which was present in **46** and **47** as a fragment ion contain two sugar units. The two sugar moieties were proposed as β-galactopyranosyl(1→2)-β-glucuronopyranosyl and attached on 3-OH of aglycone cone based on the biosynthetic consideration. This connection was always present in the soyasaponins which may be generated by the same glycoside enzyme. The final structure of **48** was proposed as soyasaponin III[132] after comparison with literature.

The structure of compound **49** was assigned in mixture due to the limited available amount and insufficient separation. The nominal mass of **49** was determined to be M = 928 g/mol based on the ions at *m/z* 929 [M + H]$^+$ and 951 [M + Na]$^+$. The same fragment ions at *m/z* 441, 423, 405 indicated the same aglycone as compound **46** (**Figure 46**). Ions at *m/z* 797 [M − 132]$^+$ and 635 [M − 132 − 162]$^+$ indicated one deoxypentose unit and one hexose unit, however the ions at *m/z* 767 [M − 162]$^+$ and 635 [M − 162 − 132]$^+$ suggested that both of two sugar units were terminal, which can be cleavage simultaneously. Ions at *m/z* 617 [M − 162 − 132 − 18]$^+$ and 635 [M − 162 − 132]$^+$ indicated the same glucuronic acid moiety as in **46**. Considering the biosynthesis of soyasaponins, the 2nd sugar moiety on the sugar chain attached on 3-OH was always β-galactose. The 2nd sugar chain was attached on 22-OH due to the space crowd when the sugar chain was attached on 24-OH. The first sugar unit attached on 22-OH was always arabinose. Therefore arabinose moiety and galactose moiety were the two terminal sugar moiety attached on two sugar chains simultaneously. The structure of **49** was proposed as 3 -*O*-[β-galactopyranosyl(1→2)-β-glucuronopyranosyl]-22-*O*-arabinopyranosyl] soyasapogenol B.

441 —176— 617 —18— 635 —162— 797 —162— 959   **46**

441 —176— 617 —18— 635 —162— 797 —146— 943   **47**

441 —176— 617 —18— 635 —162— 797   **48**

441 —176— 617 —18— 635 —162— 797 —132— 929   **49**
                              └—132— 767 —162—┘

441 —176— 617 —18— 635 —162— 797 —162— 959 —132— 1091 —162— 1253   **50**
                              └—132— 929 —162—┘

441 —176— 617 —18— 635 —162— 797 —162— 959 —132— 1091   **51**
                              └—132— 929 —162—┘

441 —176— 617 —18— 635 —162— 797 —146— 943 —148— 1091 —146— 1237   **52**
                              └—132— 1075 —162—┘

441 —176— 617 —18— 635 —162— 797 —162— 959 —162— 1121 —162— 1283   **53**

439 —176— 615 —18— 633 —162— 795 —162— 957   **54**

439 —176— 615 —18— 633 —162— 795 —146— 941   **55**

457 —176— 633 —18— 651 —162 x 2— 975 —132— 1107 —162— 1269   **56**
                       └—132— 783 —162— 945 —162—┘

457 —176— 633 —132— 765 —18— 783 —162— 945 —162— 1107   **57**
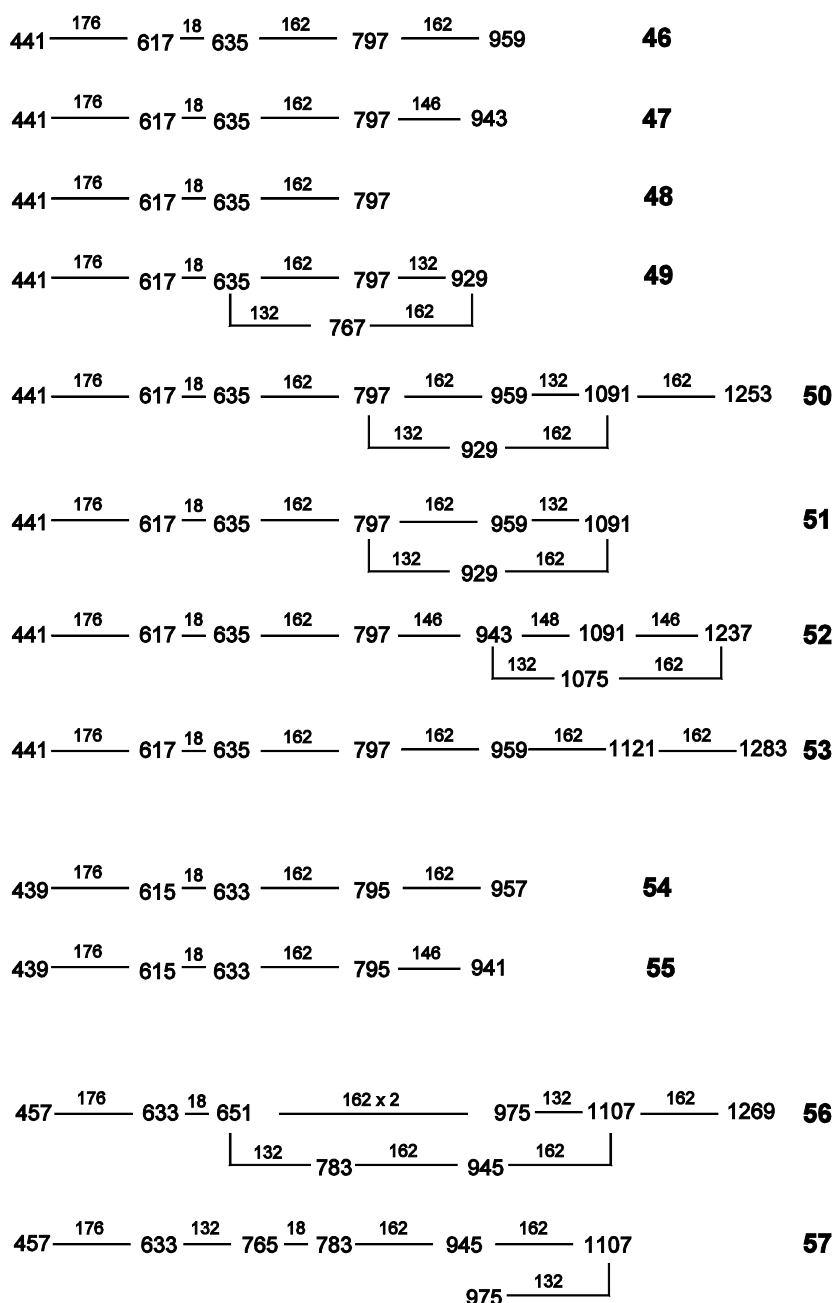   975 —132—┘

Figure 46. Summary of neutral loss pattern from compounds 46–57.

The s tructure of compound **50** was a ssigned m ainly ba sed on the analysis o f the ESI-MS spectrum. T he nominal mass of **50** was d etermined t o be M = 1252 g/mol a ccording to the ions at *m/z* 1253 [M + H]$^+$ and 1275 [M + Na]$^+$. D etailed comparison o f ESI-MS fragment pattern with those of **46** (**Figure 46**), two additional sugar mo ieties mu st be attached on the structure, due to the observation of ions at *m/z* 1091 [M − 162]$^+$ and *m/z* 959 [M − 162 − 132]$^+$. Additionally the ion at *m/z* 929 [M − 162 − 162]$^+$ indicated that **50** contained two sugar chains, with the terminal sugar unit being hexose. Due to the same biosynthetic consideration as be-fore, the additional sugar moieties were suggested as arabinose and glucose connected to each

other by 1→3 linkage as 2nd sugar chain attached on 22-OH at arabinose moiety. Finally, the structure of **50** was proposed as phaseoside I[133] after comparison with literature.

The structure of **51** was assigned in mixture by comparison the ESI-MS fragment pattern with those of **50** (**Figure 46**). The nominal mass was determined to be M = 1090 g/mol based on the ions at m/z 1091 $[M + H]^+$ and 1113 $[M + Na]^+$. Detailed comparison of the spectrum with **50** determinated that the only difference of these two compounds was the quasimolecular ion of m/z 1091 for **51** and m/z 1253 for **50**. The loss of terminal glucose was concluded because of mass loss of 162 Da. The fragment ions at m/z 959 $[M − 132]^+$ and 929 $[M − 162]^+$ indicated that the arabinose and glucose were two terminal moieties. The observation further suggested that the lost glucose moiety came from the 22-O-Glc(-Ara). Finally the structure of **51** was proposed as 3 -O-[β-glucopyranosyl(1→2)-β-galactopyranosyl(1→2)-β-glucurono-pyranosyl]-22-O-arabinopyranosyl soyasapogenol B.

The structure of **52** was determined in mixture. Detailed analysis of the ESI-MS fragment pattern of **52** indicated the same fragment ions below to m/z 943 as **47** (**Figure 46**). The fragment ions at m/z 1075 $[M − 162]^+$ and m/z 1091 $[M − 146]^+$, indicating hexose and deoxyhexose moieties as terminal sugar units, suggested a 2nd sugar substituent in compound **52**. Therefore **52** was the additional glucoside product of **47**. The ion at m/z 943 $[M − 162 − 132]^+$ suggested that the additional sugar chain contained one hexose and deoxypentose. Considering the biogeneration of soyasaponins, arabinose was highly possible present in the 2nd sugar chain always as 22-O-[arabinopyranosyl(1→2)glucopyranosyl]. Finally the structure of **52** was proposed as sophoraflavoside I[134] by comparison with reported MS data.

The structure of **53** was analyzed in mixture. Analysis of the ESI-MS fragment pattern of **53** indicated the same fragment ions below to m/z 959 as **46** (**Figure 46**), suggesting the similar structure features as **46**. The ion at m/z 959 $[M − 162 − 162]^+$ indicated that the additional sugar chain contained two hexose moieties. Therefore **53** was the further glycoside product of **46**, which contained 2nd sugar chain as 22-O-[glucopyranosyl(1→2)-glucopyranosyl]. The structure of **53** was proposed as 3 -O-[β-glucopyranosyl(1→2)-β-galactopyranosyl(1→2)-β-glucuronopyranosyl]-22-O-[β-glucopyranosyl (1→2)-β-glucopyranosyl] soyasapogenol B.

The structure of **54** was assigned by analysis of ESI-MS fragment pattern and comparison with other structure analogues. The nominal mass of **54** was determined to be M = 956 g/mol according to ions at m/z 957 $[M + H]^+$, 979 $[M + Na]^+$ and 995 $[M + K]^+$. Having two mass units less than compound **46** suggested that **54** is an oxidation product of **46** (**Figure 46**).

Detailed analysis of the fragment ions at m/z 795 $[M - 162]^+$, 933 $[M - 162 - 162]^+$ and 439 $[M - 162 - 162 - 18 - 176]^+$ indicated the identical fragment pattern as **46**, with the same sugar moieties as **46**. Two mass units less of ions at m/z 421 and 439 in **54** than the ions at m/z 423 and 441 in **46** suggested that the aglycone is oxidized. According to the literature[135], sando-saponin A and sandosaponin B were possible candidates. Considering the biological origin, 22-OH is oxidized and the structure of **54** was proposed as sandosaponin A. The aglycone of **54** belonged to soyasapogenol E (**60**), which is the oxidation product of soyasapogenol B (**59**).

The structure of **55** was assigned by comparison of ESI-MS fragment pattern with those of **47** and **54**. The nominal mass of **55** was determined to be M = 940 g/mol based on ions at m/z 941 $[M + H]^+$, 963 $[M + Na]^+$ and 981 $[M + K]^+$. After comparison of the neutral loss pattern (**Figure 46**), there were two mass units less than **47** and 16 Da less than **54**. The same fragment ions at m/z 421 and 439 as **55** indicated the same aglycone moiety of **55** as **54**. The fragment ion at m/z 795 $[M - 146 + H]^+$ indicated the similar terminal sugar group as **47**. As a result, compound **55** is the oxidation product of **47**. After comparison with literature ta[136,137], the structure of **55** was finally assigned as dehydrosoyasaponin I. Both compound **54** and **55** were based on soyasapogenol E (**60**) as aglycone moiety.

The structure of compound **56** was assigned in mixture by comparison of the ESI-MS fragment pattern with **46** (**Figure 46**). The nominal mass of **56** was determined to be M = 1268 g/mol according to ions at m/z 1269 $[M + H]^+$ and 1291 $[M + Na]^+$. The ion at m/z 1107 $[M - 162 + H]^+$ indicated a terminal hexose moiety along with a deoxypentose moiety. Ions at m/z 975 $[M - 162 - 132 + H]^+$ and 945 $[M - 162 - 162 + H]^+$ indicated that **56** had two terminal hexose moieties and the deoxypentose moiety was connected to one terminal hexose moiety. The aglycone fragment ions at m/z 421, 439 and 457 suggested the correspondingly hydrox-ylated aglycone structure, comparing with the aglycone moiety of **46** (m/z 405, 423, 441). The hydroxylation of C-21 matched with the aglycone type called soyasapogenol A (**58**). The final structure of **56** was proposed as soyasaponin A_1[138] after comparison with the literature.

The structure of compound **57** was assigned in mixture by comparison of the ESI-MS fragment pattern with **56** (**Figure 46**). The same fragment ions at m/z 421, 439 and 457 con-firmed the soyasapogenol A (**58**) type aglycone as in **56**. The mass difference of quasimole-cular ion at m/z 1107 $[M + H]^+$ in **57** and 1269 $[M + H]^+$ in **56** indicated the loss of one hex-ose moiety from **56**. Ions at m/z 975 $[M - 132 + H]^+$ and 945 $[M - 162 + H]^+$ indicated the two terminal sugar groups in **56**. Ions at m/z 783 $[M - 132 - 162 + H]^+$, 633 $[M - 132 - 162 - 162 - 18 + H]^+$ and 457 $[M - 132 - 162 - 162 - 18 - 176 + H]^+$ suggested a similar structural

feature as **56**, except for the different 2nd sugar chain attached on the 22-OH in line with the loss of one hexose moiety. As a result, the structure of **57** was assigned as desglucosylsoyasaponin A$_1$[139] by comparison with the literature.

Saponins are very abundant and important plant secondary metabolites comprising one or more mono- or oligosaccharide moieties attached to an aglycone which had a steroidal or triterpenoid structure feature. Olean-glucuronide is one of the triterpene saponins characterized by an olean-12-ene-type triterpenes with a C-28 methyl group and a glucuronic acid moiety linked at the 3-OH of the triterpene[140]. They are widely distributed in leguminous plants, including many species of beans. Soyasaponins are a group of oleanane triterpenoids found in soy and other legumes. Normally they can be detected from different organs. However they are highly concentrated in seed, leaves and root hairs[141]. They are amphiphilic molecules, with polar water soluble sugar moieties attached to a nonpolar, water insoluble pentacyclic ring structure. They are classified into two main groups according to the aglycones (soyasapogenols A (**58**), B (**59**) and E (**60**)) and the attachment of sugar moieties at positions 3-OH and 22-OH. Group A are bidesmosidic saponins with two glycosylation sites at 3-OH and 22-OH on the oleanane ring structure. Group A is divided into two subgroups, knowns as acetylated and deacetylated forms[142] respectively. Group B soyasaponins are further classified into two subcategories known as 2,3-dihydro-2,5-dihydroxy-6-methyl-4H-pyran-4-one (DDMP) and non-DDMP conjugated molecules. There is a third soyasaponin aglycone known as group E, which had a ketone at C-22 and had been reported as artifact formed during extraction process[143]. The structures of aglycones are shown in **Figure 47**.
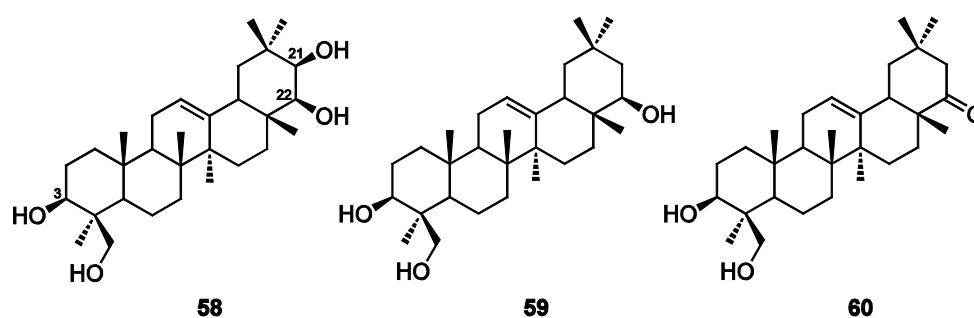

Figure 47. Chemical structures of three types of aglycone: soyasapogenol A (**58**), B (**59**), and E (**60**)

Generally, plants stored saponins as glycosides, typically in the bidesmosidic form, which could be hydrolyzed to the monodesmosidic forms and followed by the enhancement of the bioactivity of saponins[144]. Most soyasaponins are thermally labile, polar and non-volatile

compounds and are present in only trace amounts in the plant. Techniques having been used recently to analyze saponins include HPLC, TLC, MS and GC for corresponding aglycones released by acid hydrolysis. Applying LC-MS to structural and analytical problems involving organic molecules had become increasingly common over the last few decades, and ESI-MS as a soft ionization method has been extensively used to characterize saponins and confirm their structures. MS fragmentation provided unique structural information to support the fast identification of saponins and the determination of the sugar sequences[145].

3.2.2 Metabolism of saponins in the insect gut

According to the literature[146], soyasaponin I (**47**) can be metabolized to soyasaponin III (**48**) and even soyasapogenol B (**59**) by human gut microorganisms. The sugar moieties of soya-saponins are hydrolyzed sequentially to yield smaller and more hydrophobic and more active metabolites. Acetylated soyasaponin Ab could be metabolized by human fecal suspensions[147]. It has been reported that ingested soyasaponins are hydrolyzed to aglycones by nonspecific glycosidases of the fecal microflora in chicks, rats and mice[148]. This indicated that mamma-lian gut microbial enzymes exhibit the ability to hydrolyze various glycosidic bonds in soya-saponins. Human intestinal bacteria, especially *Lactobacilli*, *Bacteroides* and *Bifidobacteria* species, possess glycosidase and β-glucuronidase activities[149]. Considering the complex gut microbiota and diverse digestive enzymes present in the gut of *S. littoralis*, the food-derived saponins might be metabolized by the gut bacteria.

In order to investigate the digestion of saponins in the insect gut, the extract of artificial diet, crude oral secretion and the extract of feces were analyzed under the same LC-MS condition. The comparison of metabolite profile is shown in **Figure 48** and **Table 7**.
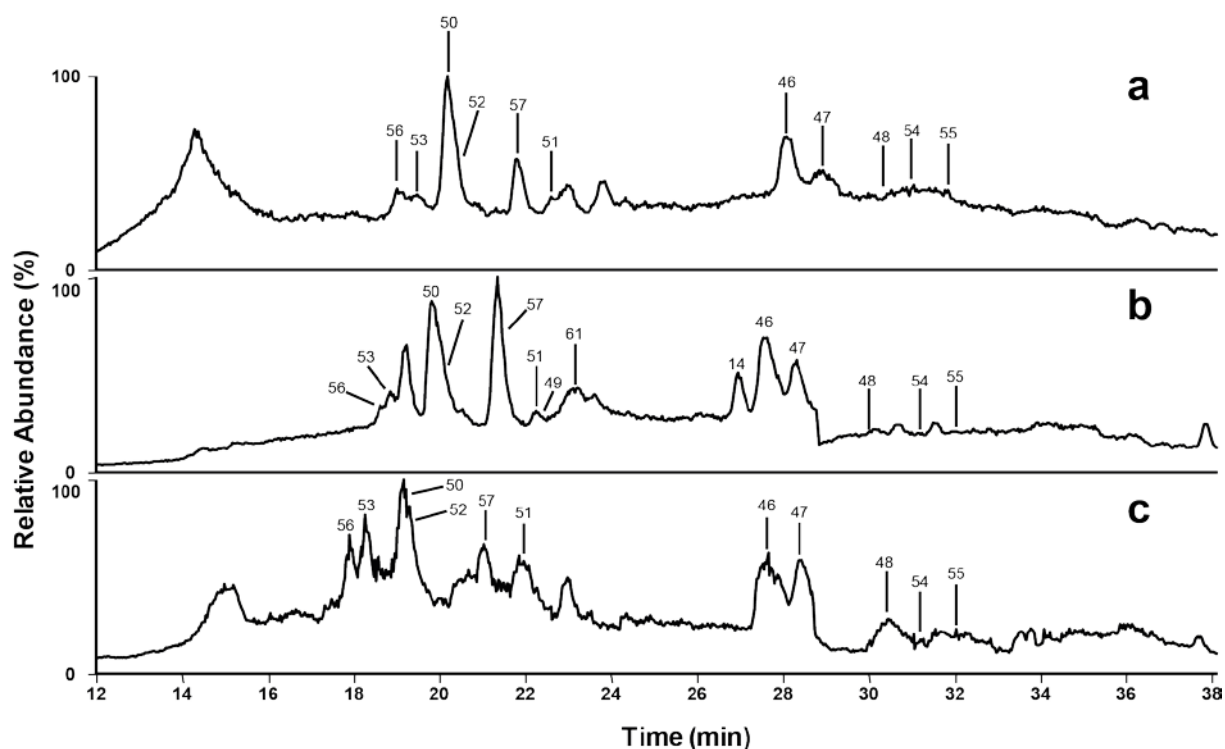
Figure 48. Comparison of HPLC-ESI-MS total ion chromatograms: (a), H_2O extract of artificial diet; (b), supernatant of crude oral secretion; (c), MeOH extract of feces.

Table 7. Saponins and aglycones from the extract of artificial diet, crude oral secretion, and the extract of feces

Compound name	Extract of diet	Crude OS	Extract of feces
Soyasaponin V (**46**)	+	+	+
Soyasaponin I (**47**)	+	+	+
Soyasaponin III (**48**)	trace	trace	trace
Compound **49**	trace	trace	trace
Phaseoside I (**50**)	+	+	+
Compound **51**	+	+	+
Sophoraflavoside I (**52**)	+	+	+
Compound **53**	+	+	+
Sandosaponin A (**54**)	trace	+	+
Dehydrosoyasaponin I (**55**)	trace	+	+
Soyasaponin A1 (**56**)	+	+	+
Desglucosylsoyasaponin A1 (**57**)	+	+	+
Aglycones			
Soyasapogenol A (**58**)	–	–	–
Soyasapogenol B (**59**)	–	–	–
Soyasapogenol E (**60**)	–	–	–

In all samples, five penta-oligosaccharide saponins (**50**, **52**, **53**, **56**, and **57**) were detected as major components. Tri-oligosaccharide saponins (**46** and **47**) were detected from all samples, however **49** was only detected in trace amount in all samples. **54** and **55** as oxidized product of **46** and **47** showed higher concentration in oral secretions and extract of feces. According to the literature, **54** and **55** might be artificial products during the extraction process. Because of the higher amount of these two compounds in OS and feces, it is also possible that **54** and **55** might be the oxidized products in the insect gut. Di-oligosaccharide saponin (**48**) and tetra-oligosaccharide saponin (**51**) were present in the similar amounts in all samples. All in all, the saponin profiles between crude OS and feces were quite similar, indicating a low metabolic effect by the insect gut microbiota.

Three aglycones (**58–60**) were hardly detected from any of the samples under the chosen conditions. It is possible that this analytic approach is not suitable for the aglycone detection. Another possible explanation is that insect gut microflora couldn't digest the saponins from food completely similar to the mammalian gut microflora. According to the literature, only mammalian gut microorganism showed the ability to metabolize the saponins from food. Anaerobic incubation of the pure saponin with insect gut microflora is a possible way to investigate the digestive pathway of saponins in the future.

3.2.3 Possible biological functions of saponins in plant–insect interaction

Soyasaponins are olean-type triterpenoid glycosides with one or two oligosaccharide chains mainly present in legumes[150]. The physiological functions are not fully recognized until now. Soyasaponin I (**47**) acts as an inhibitor for glycolate oxidase from *Spinacia oleracea* which is involved in photorespiration, but the aglycone and methyl ester were inactive[151]. Since many soyasaponins showed potent antifungal activity, they might serve as phytoprotectants against fungal attack[152].

Recently, the possible physiological functions of soyasaponins in insect have been widely investigated. Soyasaponins administered to *Spodoptera littoralis* in the larval diet caused prolongation of the larval and pupal stages, retarded growth, increased mortality, and reduced fecundity and fertility[153]. The higher activity of hederagenin (aglycone) in comparison to its glycoside indicated that glycosylated saponins exerted insecticidal activity only when they were hydrolyzed by insect gut glycosidases and liberated to the active aglycone form[153]. On the other hand, glycosidation might render the apolar aglycones water-solubility and thereby

facilitate their ingestion. This would explain why soyasapogenol B **(59)** was less active in *S. littoralis* than soyasaponin I **(47)**[153].

Here 12 soyasaponins were detected in the oral secretion. The metabolic pathways should be investigated further, and the possible functions in plant–insect interactions should be analyzed. According to previous research[154], exogenously applied methyl jasmonate (MeJA) stimulated soyasaponin biosynthesis in cultured cells of *Glycyrrhiza glabra* by up-regulation of the mRNAs of oxidosqualene cyclase and squalene synthase which responsed to the oleanane-type triterpene aglycone biosynthesis. In addition, enzyme activity of glucuronosyltransferase, which performed the first glycoside reaction of the aglycone, was also up-regulated.   This might indicate that the soyasaponins are involved in plant defense by JA induced pathway.

3.3 Volatile compounds from crude OS of *S. littoralis* larva

Crude OS of *S. littoralis* larva contained numerous chemical components, including volatile and non-volatile compounds. Previous studies mainly focused on identification and characterization of the non-volatile compounds, however little has been known about the volatiles from crude OS.

The headspace volatile compounds from *S. littoralis* OS were collected using SPME technique equipped with polydimethlsiloxan (PDMS) fiber for 30 min at room temperature, and further submitted to GC-MS analysis. The major compounds were long-chain alkanes, especially pentadecane (**61**) with tiny amount tetradecane (**62**) and heptadecane (**63**). Their structures were confirmed by comparison of the retention times with authentic alkane mixtures (C_8–C_{20}) under the same GC-MS condition (**Figure 49**).
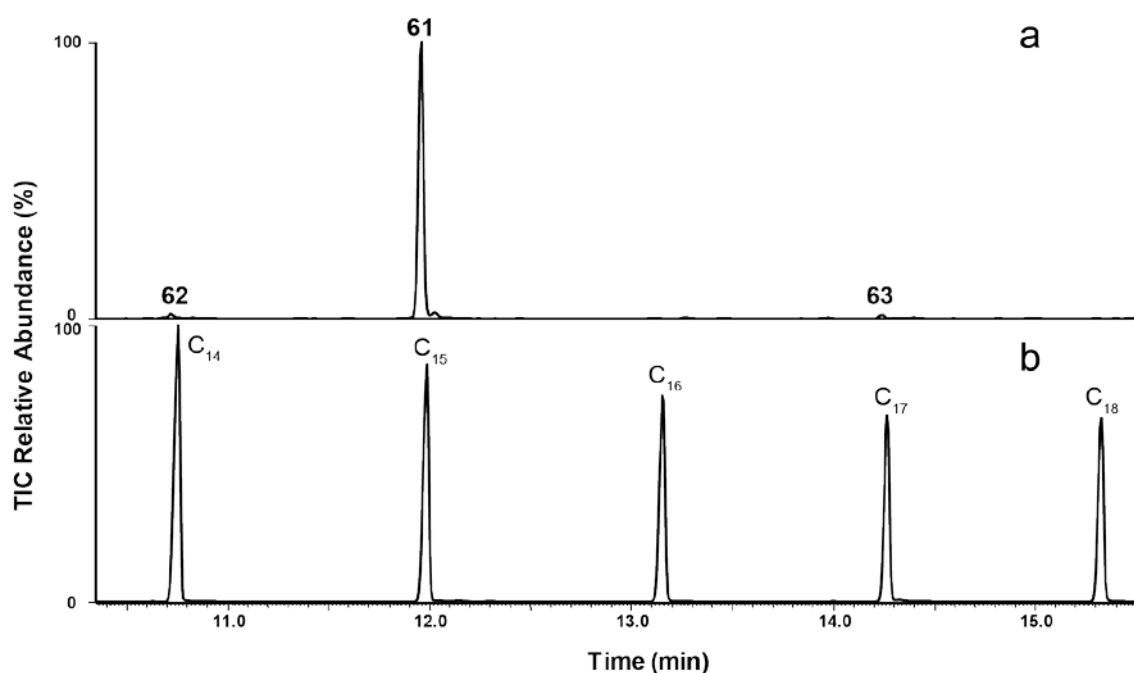
Figure 49. GC-MS chromatograms of volatile compounds from fresh OS and authentic alkanes C_8–C_{20}: (a), volatiles profile of OS; (b), authentic alkanes C_8–C_{20}. Pentadecane (**61**), Tetradecane (**62**), Heptadecane (**63**)

The headspace volatiles from artificial diet and the living larva were collected and measured under the same condition (**Figure 50**). The three alkanes (**61–63**) were hardly detected in diet or the whole larva, but were typical for fresh OS. This observation suggested that the alkanes might be secreted by insect glands and were present in higher concentration in the OS, but quite low in the whole larva.
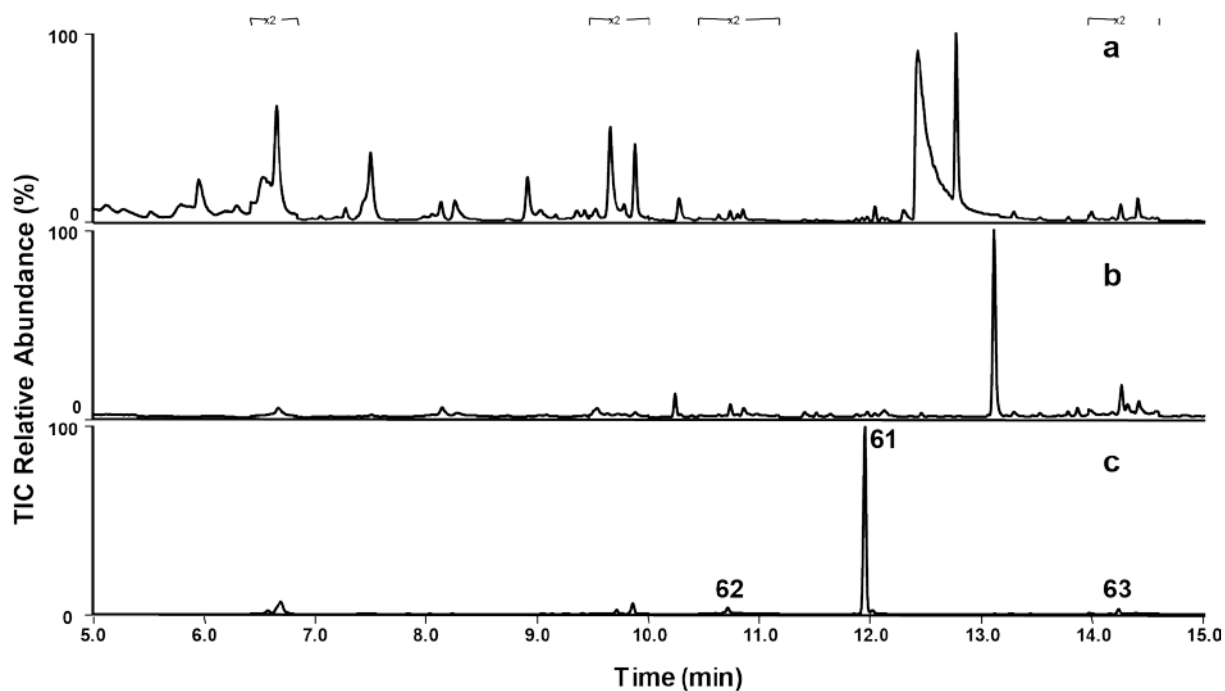
Figure 50. GC-MS analysis of volatile compounds collected by SPME: (a), from artificial diet; (b), from living larva; (c), from fresh OS. Pentadecane (**61**), Tetradecane (**62**), Heptadecane (**63**)

It has been reported that pentadecane (**61**) was the major compound from the whole hexane extract of *S. litura* larvae. In further biological tests, pentadecane (**61**) revealed the ability to elicit prey-locating behavior[155] by the predatory stink bug, *Eocanthecona furcellata*. Pentadecane (**61**) was also discovered as the major volatile component of ventral eversible gland secretions of *S. frugiperda* larva[156]. Recent studies have shown that bacterial volatiles which contained pentadecane (**61**) played an important role in bacterium–plant interactions[157]. Pentadecane (**61**) could promote plant growth in *A. thaliana*. However it couldn't trigger typical defense response, like production of ethylene and reactive oxygen species (ROS). These results suggested that pentadecane (**61**) might act as plant growth promoter and an effector to inhibit the plant's defense response. The biological functions of pentadecane (**61**) and other alkanes need to be investigated in different plant species (eg. lima bean) in future, in order to clarify their significance and functions in the plant–insect interactions.

3.4 Chemical investigations on the white secretion of the pitcher *Nepenthes lowii*

Figure 51. *Tupaia montana* "licking" on an aerial pitcher[161] of *Nepenthes lowii* (left) and an upper pitcher with visible white secretion on the inner surface of the lid (right, cited from wikipedia)

3.4.1 Tree shrew "lavatories"

Carnivorous plants occur in habitats that are deficient in key nutrients, such as nitrogen and phosphorus[158]. Evolutionaly, they are adapted to these deficiencies by producing highly modified leaf organs that serve to attract, trap, retain and digest animals to obtain nitrogen and phosphorus. Diverse arrays of trapping strategy were evolved, including snap-traps (*Dionaea muscipula*), sticky traps (*Drosera* spp.), vacuum traps (*Utricularia* spp.) and pitfall traps (*Nepenthes* spp.)[158]. Pitcher plants produce passive, gravity-operated pitfall traps that comprise an upper portion which possess elaborate structures to entice visiting animals into a precarious position. Visiting animals that lost their footing, drop into the fluid-filled lower portion of the trap, where they are retained and digested[159].

Most *Nepenthes* species use a combination of epicuticular wax crystals, viscoelastic fluids and slippery persistomes to capture and retain prey[160]. However some species produce very large pitchers and are able to trap vertebrates. Immature *N. lowii* produces terrestrial pitchers as typical traps for arthropod. But in mature plants, the aerial pitcher is different from other carnivorous plants, in that the pitchers lack the features normally associated with arthropod prey capture. Previous observations indicated that several pitchers at Mesilau (Malaysian Borneo) contained tree shrew faeces as a remarkable nitrogen sequestration strategy[161]. This research discovered that mountain tree shrews (*Tupaia montana*) defecate into the pitcher

while feeding on exudates secreted by glands on the inner surface of the pitcher lid (**Figure 51**, left). Further research revealed that the structure of *N. lowii* aerial pitchers facilitated both the feeding of *T.montana* on the lid exudates and defaecation into the pitchers. The thickened tendrils and robust pitchers could support adult *T.montana* without breaking. This phenomenon was observed in three giant montane pitcher plant species, *N. lowii, N. rajah* and *N. macrophylla*[162].

The white exudates strongly attracted our interests, because they might play an important role in enticing animals to the upper pitcher and may induce the laxation of animals. Previously, the identity of white exudates has been the subject of some debate. In the 1960s, these white beads were suggested by J. Harrison to be snail eggs that the tupaias came to eat[163]. However the observation of these "white beads" from cultivated *N. lowii* showed that they were plant derived. The substance (**Figure 51**, right) has been described as having a sugary taste[159], a slightly disagreeable odour[164], and "buttery-like substance"[161]. Here the composition of these exudates is investigated.

3.4.2 Analysis of white secretion from *N. lowii* in mixture

The crude white secretion was dried completely and the residue was dissolved in CD_3OD-d_4 for NMR measurement. Detailed analysis of the ^1H NMR spectrum of crude white secretion (**Figure 52a**) revealed that the major signals were observed between δ_H 3.3 ppm to 4.2 ppm which indicated the oxymethines from sugar moieties. The signals at δ_H 0.9 ppm, 1.2 ppm, 1.6 ppm, 2.0 ppm and 2.4 ppm indicated methyl and methylene protons from fatty acids. The signal at δ_H 5.4 ppm indicated alkenyl moieties. No other signals could be detected in the low field. These observations suggested that the white secretion was a mixture of sugar and fatty acid derivatives.

After solvent extraction of the 50% aqueous MeOH solution with hexane and CH_2Cl_2, the hexane phase and CH_2Cl_2 phase were combined as the organic extract and the residue as aqueous phase. The organic extract and aqueous phase were completely dried, and submitted to ^1H NMR analysis. Detailed analysis of the ^1H NMR spectrum data of the aqueous phase (**Figure 52b**) indicated the signals at δ_H 3.3–4.2 ppm corresponding to oxymethylene and oxymethine of sugars, the signals at δ_H 4.48 ppm ($J = 7.93$ Hz) and δ_H 5.11 ppm ($J = 3.49$ Hz) indicated the anomeric protons of free β- and α-glucose. The signal between δ_H 3.45 ppm and 3.50 ppm could be attributed to the proton signals originated from fructose. The signal at δ_H

5.39 ppm (J = 3.84 Hz) indicated the proton signals originated from free sucrose. Detailed analysis of ^{1}H NMR spectrum of the organic extract (**Figure 52c**) revealed signals at δ_H 0.9 ppm indicating terminal methyl groups, overlapping signals from δ_H 1.2 to 1.6 ppm belong to methylene moieties, a signal at δ_H 2.0 ppm belongs to an allylic methylene group, and a signal at δ_H 2.4 ppm indicated the methylene groups attached to the carboxyl group. A signal at δ_H 5.4 ppm belongs to alkenyl moieties, indicating that unsaturated fatty acids are present in the white secretion. Additional signals at δ_H 4.0–4.4 ppm suggested oxymethylene and oxyme- thine moieties corresponding to substituted glycerol moieties. These signals suggested that the organic extract comprised fatty acids and glyceride derivatives.
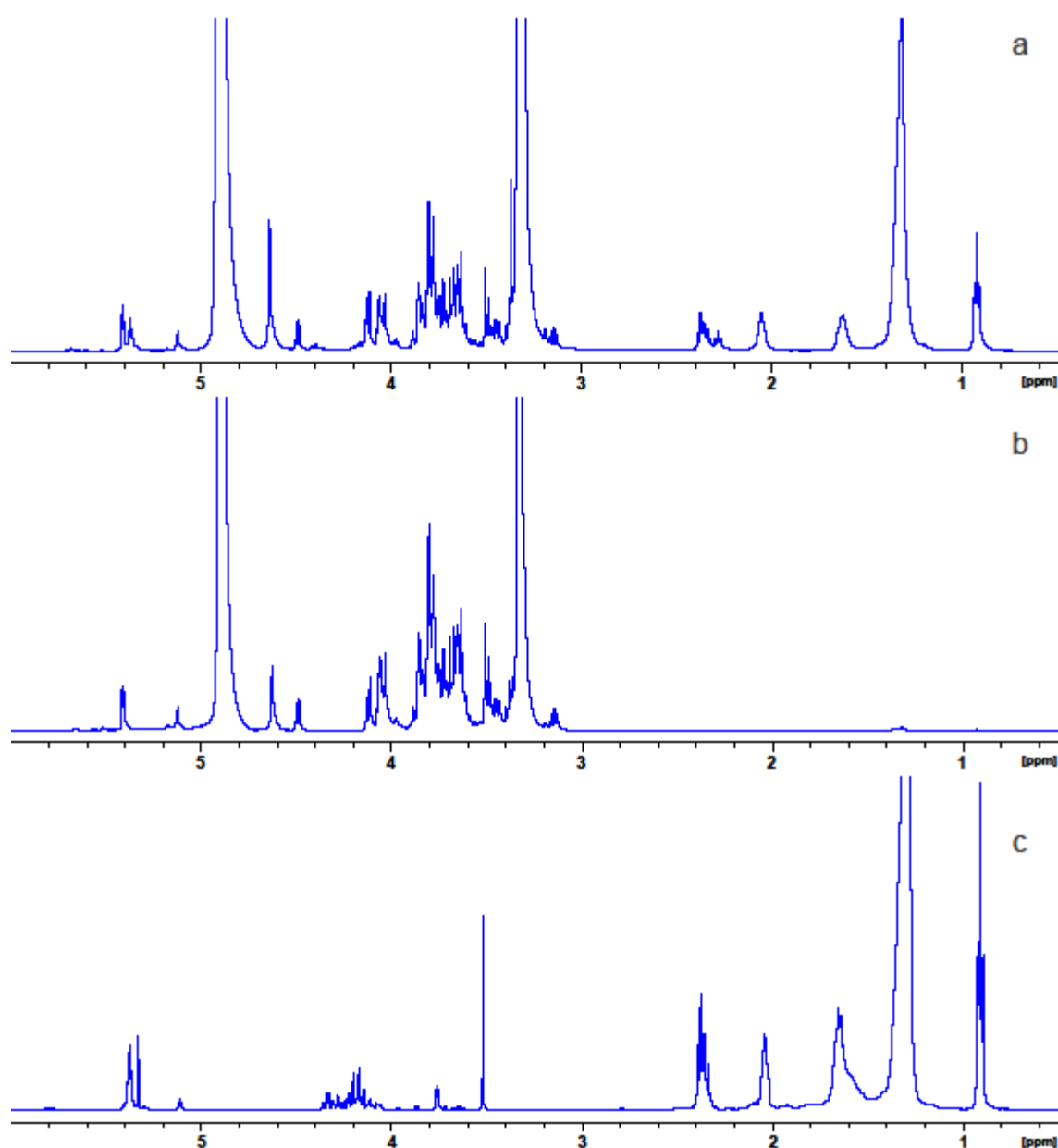
Figure 52. ^{1}H NMR spectra of crude white secretion in CD$_3$OD-d_4 (a), aqueous phase in CD$_3$OD-d_4 (b) and organic extract in CDCl$_3$-d_1 (c)

3.4.3 Analysis of the aqueous phase of white secretion

According to the ^{1}H NMR analysis (**Figure 52b**) of the aqueous phase sample, the major components in aqueous phase were glucose, fructose and sucrose, and the ^{1}H NMR spectrum was matched to D-(+)-glucose (**64**), D-(−)-fructose (**65**), D-(+)-sucrose (**66**). The trimethylsilyl (TMS) ethers were prepared by MSTFA derivatisation and submitted to GC-MS analysis (**Figure 53**), and their retention times and their EI-MS spectra were matched with TMS derivatives of authentic compounds (**Figure 54**). Due to the tautomeric effect, D-glucose and D-fructose display an equilibration mixture of at least five different conformations: α-fura, β-fura, α-pyro, β-pyro, and open-ring form (keto form for D-fructose). This could be used to explain the multiple peaks in ^{1}H NMR spectra and GC-MS chromatogram.
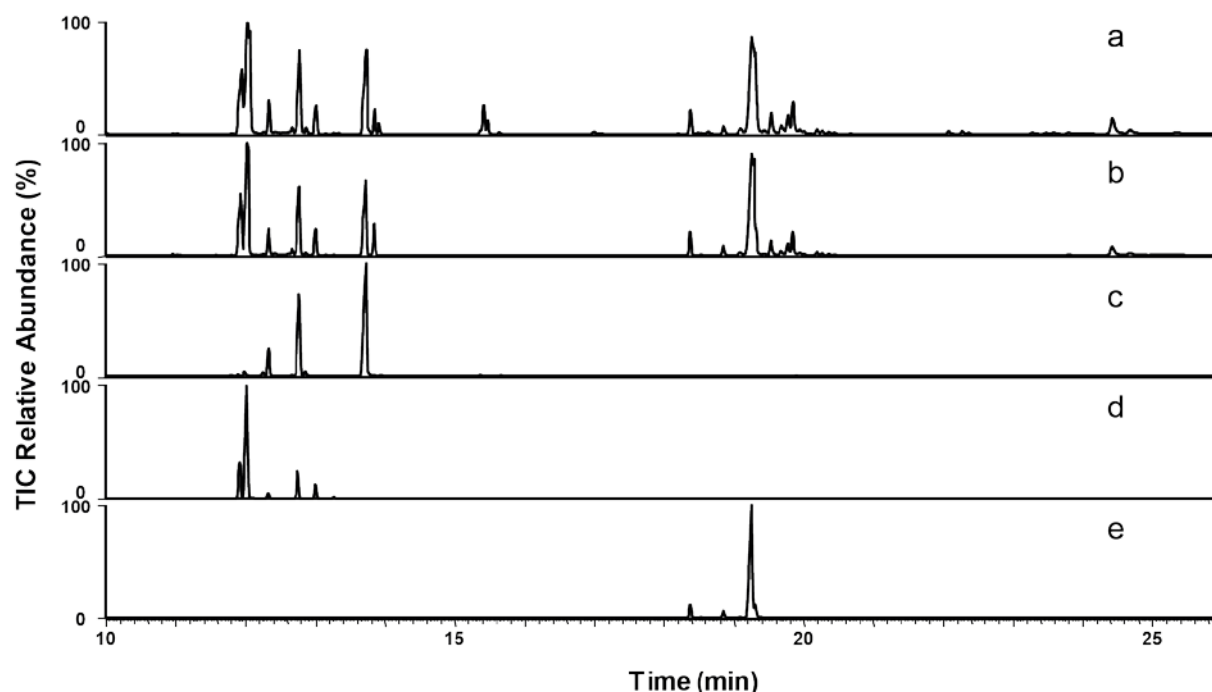
Figure 53. GC-MS chromatogram (total ion current) of aqueous phase of white secretion after MSTFA derivatisation: (a), crude white secretion; (b), aqueous phase of white secretion; (c), standard D-(+)-glucose (**64**); (d), standard D-(−)-fructose (**65**); (e), standard D-(+)-sucrose (**66**).
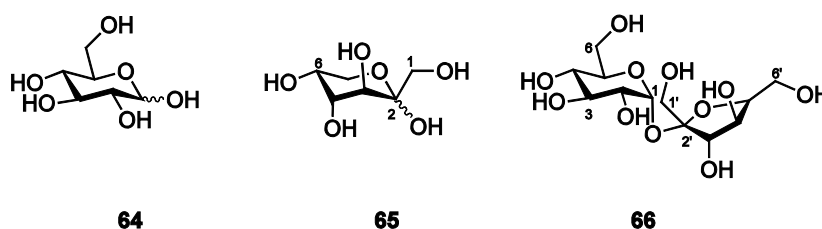
Figure 54. The structures of D-(+)-glucose (64); D-(−)-fructose (65); D-(+)-sucrose (66)

3.4.4 Analysis of the organic extract of the white secretion

Compound identification in the organic extract was based on detailed analysis of their EI-MS spectra of the corresponding TMS derivatives after GC separation (**Figure 55**). The trimethylsilyl (TMS) ethers were prepared by MSTFA derivatisation, 48 compounds were identified including 15 fatty acids, 11 mono-, 18 di- and three triglyceride esters (**Figure 56**).
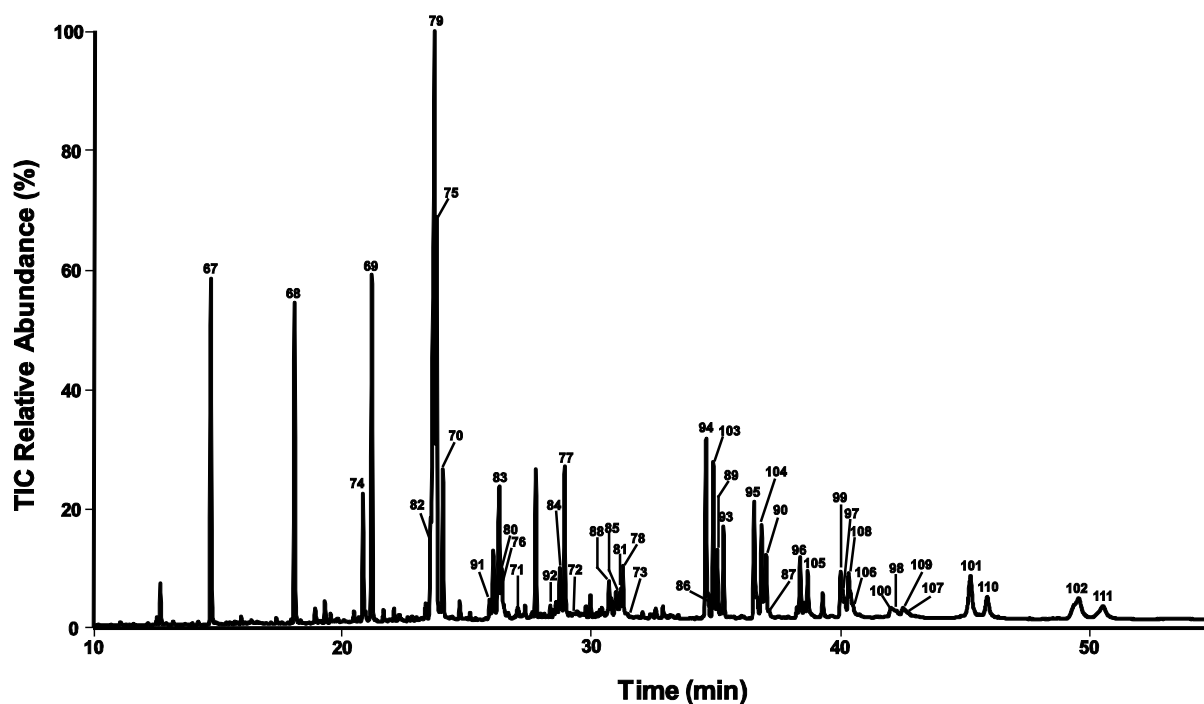

Figure 55. GC-MS chromatogram (total ion current) of the organic extract of white secretion after MSTFA derivatisation

Saturated fatty acids varing from C_{12}–C_{24} (**67**–**73**) were identified by analysis of their EI-MS spectra showing typical molecular and fragment ions. The structures were finally confirmed by comparison of their retention times with those of authentic references. The position of double bonds in unsaturated fatty acids (**74**–**82**) was determined by chemical ionization iontrap mass spectrometry with acetonitrile (ACN-CI-MS) as a reagent gas[165,166,167] by analyzing the corresponding fatty acid methyl ester(s) (FAMEs) obtained by CH_2N_2 derivatisation. The fatty acids methyl esters were assigned by EI-MS and CI-MS (**Figure 57**).
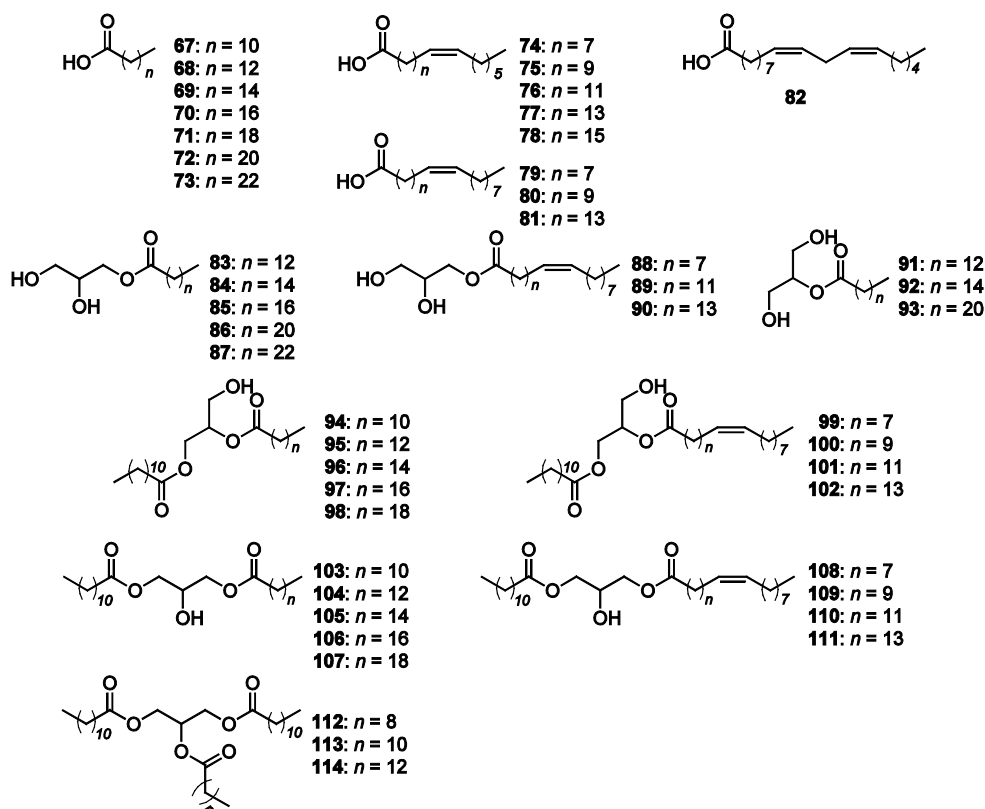
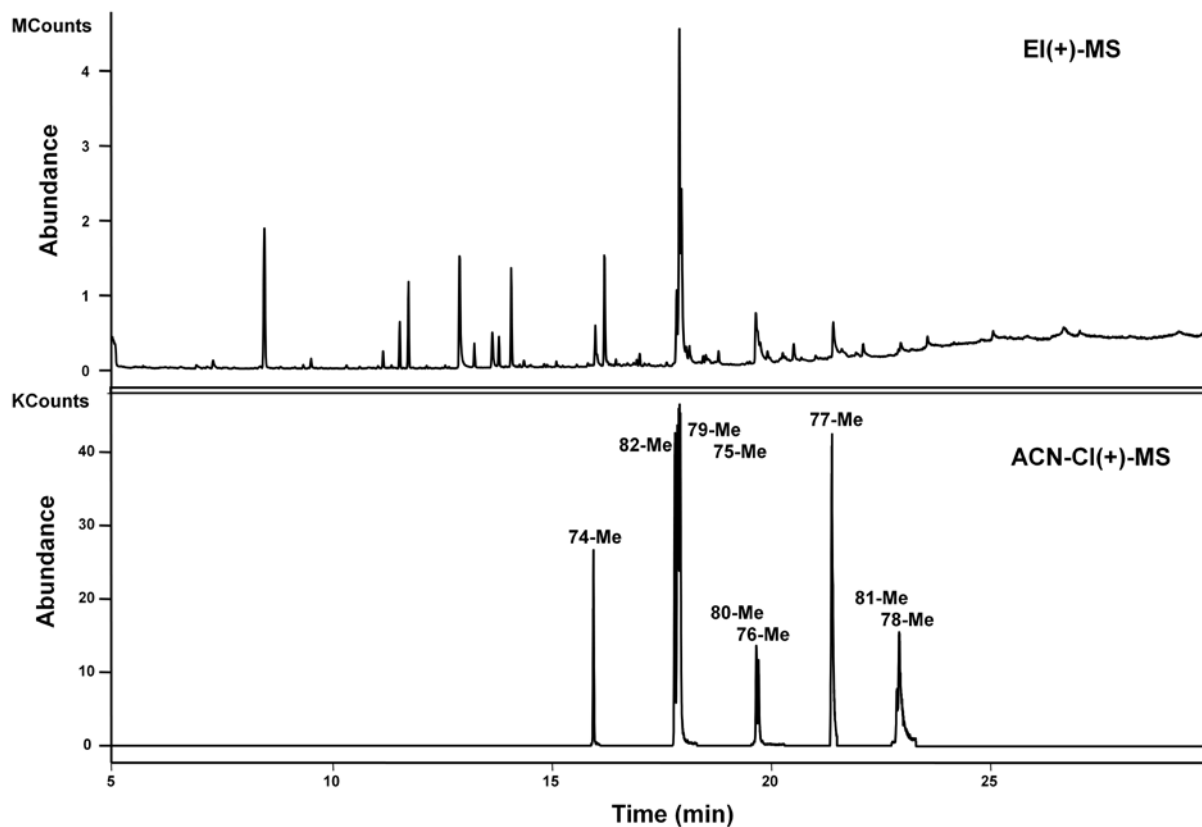**Figure 56. Compounds (67–114) present in the organic extract of the white secretion**

Figure 57. GC-MS chromatogram (total ion current) of the methyl esters of the organic extract of the white secretion

In ACN-CI-MS, the diagnostically useful $[C_3H_4N]^+$ ion identified as 1-(methyleneimino)-1-ethenylium (MIE), was formed from an ion/molecule reaction between $[C_2H_2N]^+$ (*m/z* 40) and neutral acetonitrile, followed by a loss of HCN. MIE covalently added cross analyte double bonds to yield a series of $[M + 54]^+$ ions. Upon collision induced dissociation (CID) of $[M + 54]^+$ as precursor ions, the loss of methanol is observed as $[M + 54 - 32]^+$ ions. Additionally, two diagnostic fragment ions are produced: the α ion contained the methyl ester end of the FAME, and the ω ion which contained the hydrocarbon end of FAME, were produced. Monoenes undergo bond cleavage at the allylic carbon of the double bond (**Figure 58a**), but the dienes undergo bond cleavage at the vinylic carbon of the double bonds (**Figure 58b**). These diagnostic ions were highly specific for unsaturated FAME and allowed unambiguous assignment of double bond positions (**Table 8**).
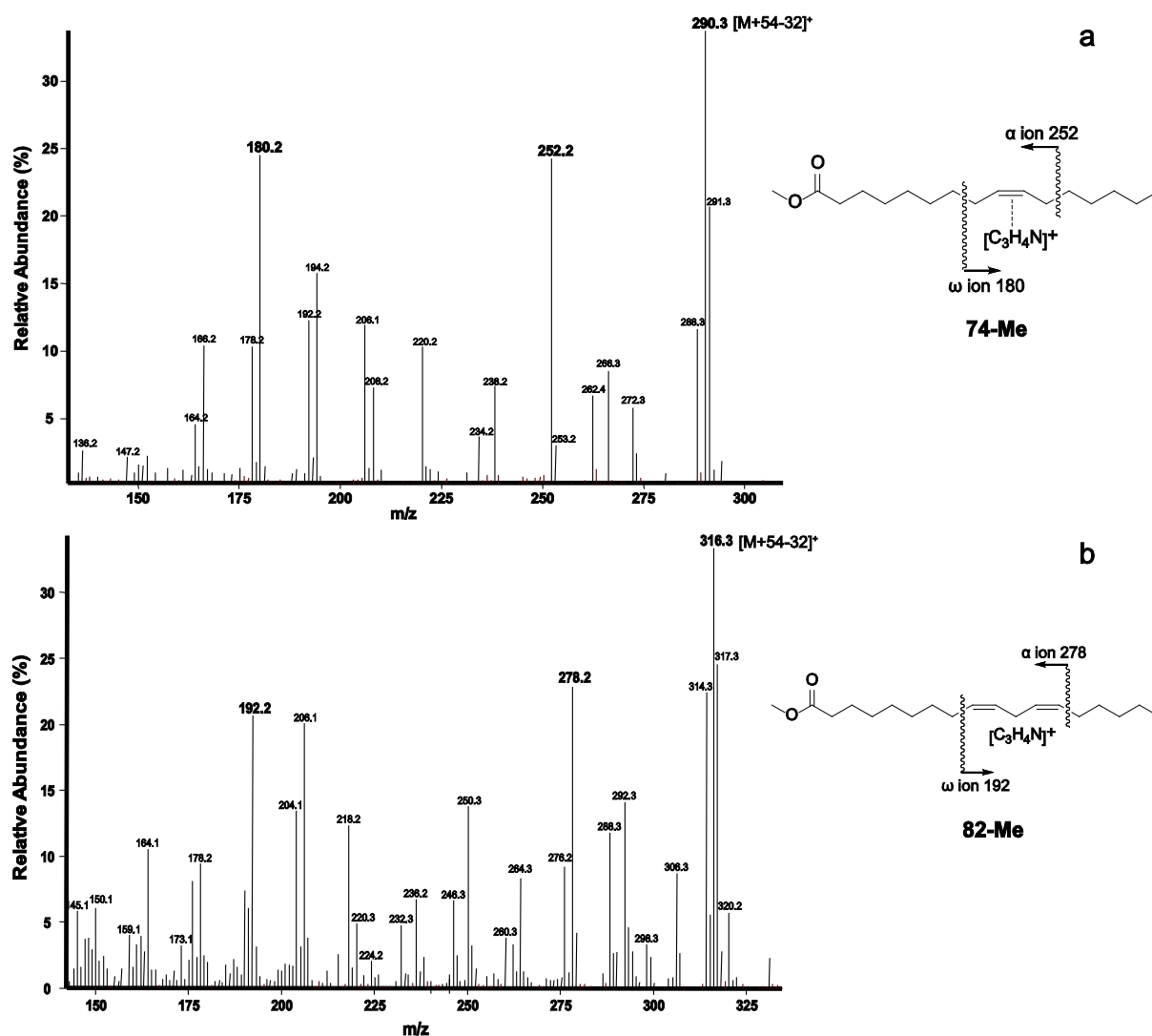
Figure 58. ACN-CI-MS/MS spectra of: (a), *m/z* 322 of methyl-palmitoleic acid (**74**-Me, C16:1, *n*-7); (b), *m/z* 348 of methyl-linoleic acid (**82**-Me, C18:2, *n*-6)

The *cis/trans* geometry of double bond was derived from detailed analysis the HSQC NMR spectra of the organic extract. The ^{13}C signal at δ_C 27.2 ppm correlated with one ^1H signal at δ_H 2.0 ppm corresponding to the allylic group in unsaturated fatty acid moieties. The upfield ^{13}C signal (δ_C 27.2 ppm) of the allylic group supported the *cis* configuration of the double bond, comparing with δ_C 32.7 ppm for *trans* configuration.[168] In *cis* configuration, two allylic carbons shield each other because of steric effects, providing upfield ^{13}C chemical shift.

Table 8. List of ACN-CI-MS/MS diagnostic ions from [M + 54]$^+$ CID fragmentation

Compound	FAME [M]$^+$	Precursor ion [M + 54]$^+$	Diagnostic fragment ions α	ω	Inferred Double bond position
74 (C16:1)	268	322	252	180	*n*-7
75 (C18:1)^a	296	350	280	180	*n*-7
76 (C20:1)^a	324	378	308	180	*n*-7
77 (C22:1)	352	406	336	180	*n*-7
78 (C24:1)^a	380	434	364	–	*n*-7
79 (C18:1)^b	296	350	252	208	*n*-9
80 (C20:1)^b	324	378	280	208	*n*-9
81 (C24:1)^b	380	434	336	208	*n*-9
82 (C18:2)	294	348	278	192	*n*-6

^{a}: later eluting isomer with longer retention time
^{b}: earier eluting isomer with shorter retention time

The structures of monoglycerides were determined based on analysis of the EI-MS spectra of their TMS ethers. The typical fragmentation pattern provides the structure information of the different monoglycerides (**Figure 59**).

The mass of **83**-TMS was calculated to be 446 according to the typical ion at *m/z* 431 [M − 15]$^+$ originating from the loss of a methyl group of the TMS moiety, while the molecular ion [M]$^{+\cdot}$ exhibited very low intensity. The attached fatty acid chain was further identified by fragment ions signal at *m/z* 211 [$C_{13}H_{27}CO$]$^+$ and 285 [$C_{13}H_{27}CO + 74$]$^+$. In addition, many observed ions correspond to the glycerol TMS ether and its rearrangement ions, for example, *m/z* 103, 117, 129, 147 and 203 (**Figure 59**). The predominant ion in trimethylsilyl ethers of 1-monoglycerides (α-monoglycerides) is [M − 103]$^+$, which arises from the cleavage between C-2 and C-3 of the glycerol moiety[169]. The base peak at *m/z* 343 was assigned as [M − 103]$^+$, and the final structure of **97** was determined as glycerol 1-myristate (**Figure 60**). Furthermore the structure was confirmed by comparison of the EI-MS data with the literature[170]. Other 1-monoglyceride homologs and derivatives (**84–90**) were assigned by comparison of their EI-MS spectra with that of **83**.
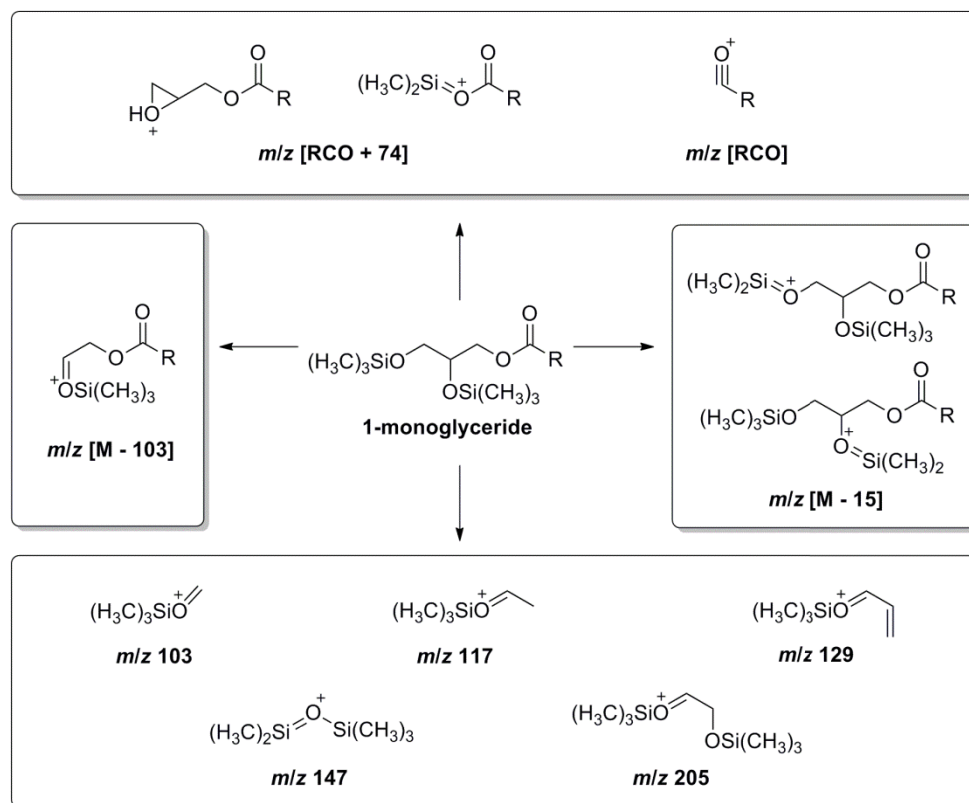
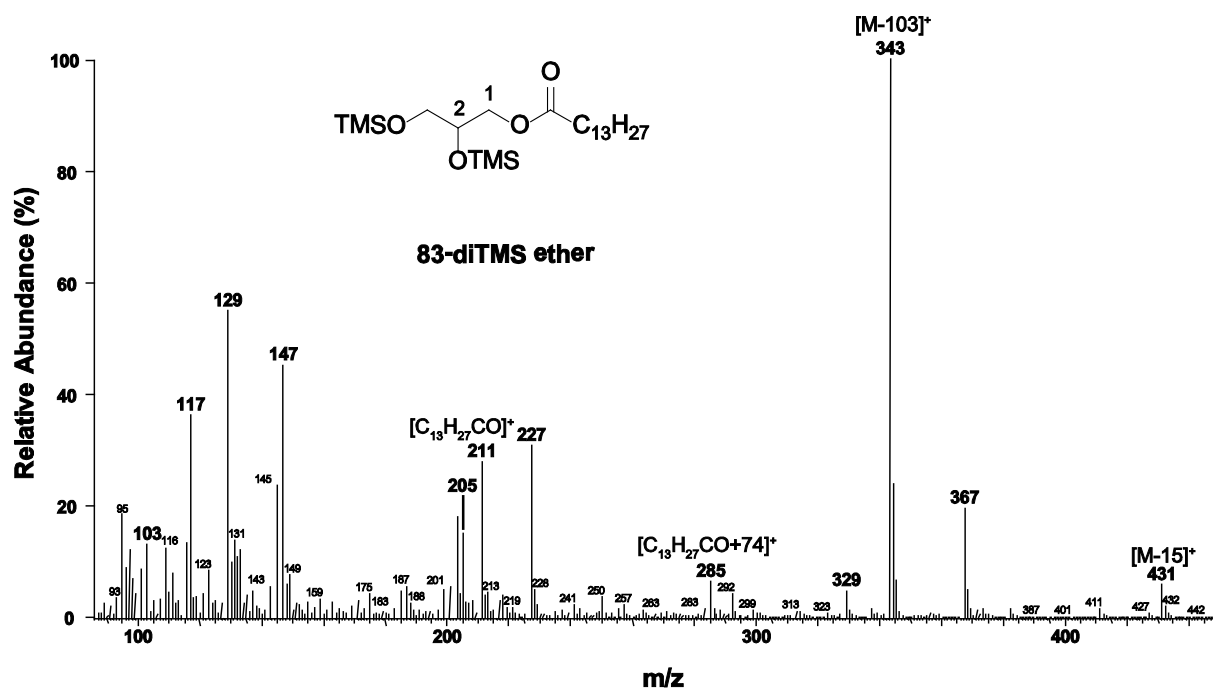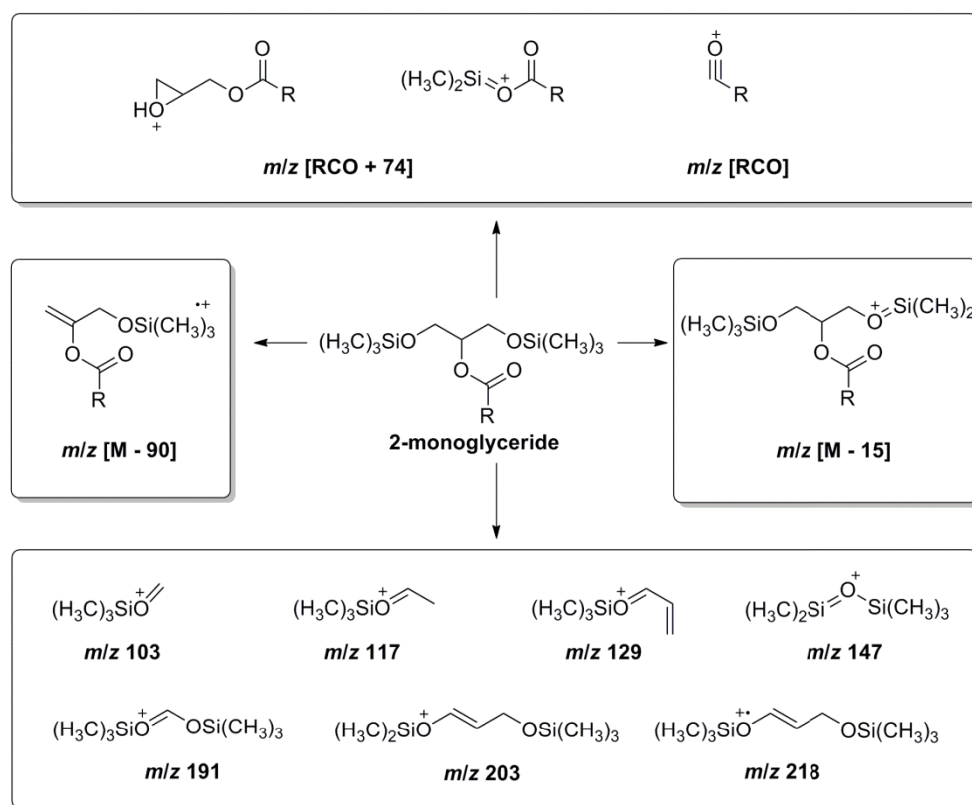**Figure 59. Principal fragmentation of the diTMS ether of 1-monoglycerides**

Figure 60. EI-MS spectrum of the diTMS ether of glycerol 1-myristate (83)

The mass of **91**-TMS was determined to be 446 based on the typical ions at *m/z* 431 $[M - 15]^+$ and 356 $[M - 90]^+$, which were derived from the loss of a methyl group from a TMS moiety and the whole TMS ether respectively. T he attached fatty acid chain was further confirmed by typical ions at *m/z* 211 $[C_{13}H_{27}CO]^+$ and 285 $[C_{13}H_{27}CO + 74]^+$. The ions at *m/z* 103, 129, 147, 191, 203 a nd 218 (**Figure 61**) were observed as corresponding glycerol TMS ether rearrangement ions. Especially, the ion at *m/z* 218, which arises from the elimination of the acyloxy group f rom t he m olecular i on, w as t ypically more favoured i n t he s pectra of 2 - monoglyceride (β-monoglyceride) than in 1-monoglyceride[169]. Finally the structure of **91** was assigned as glycerol 2-myristate (**Figure 62**), in agreement with MS data fro m literature[170]. Other 2-monoglyceride homologues and derivatives (**92** and **93**) were determined by comparison of their EI-MS spectra with that of **91**.

Figure 61. Principal fragmentation pattern of the diTMS ether of 2-monoglycerides
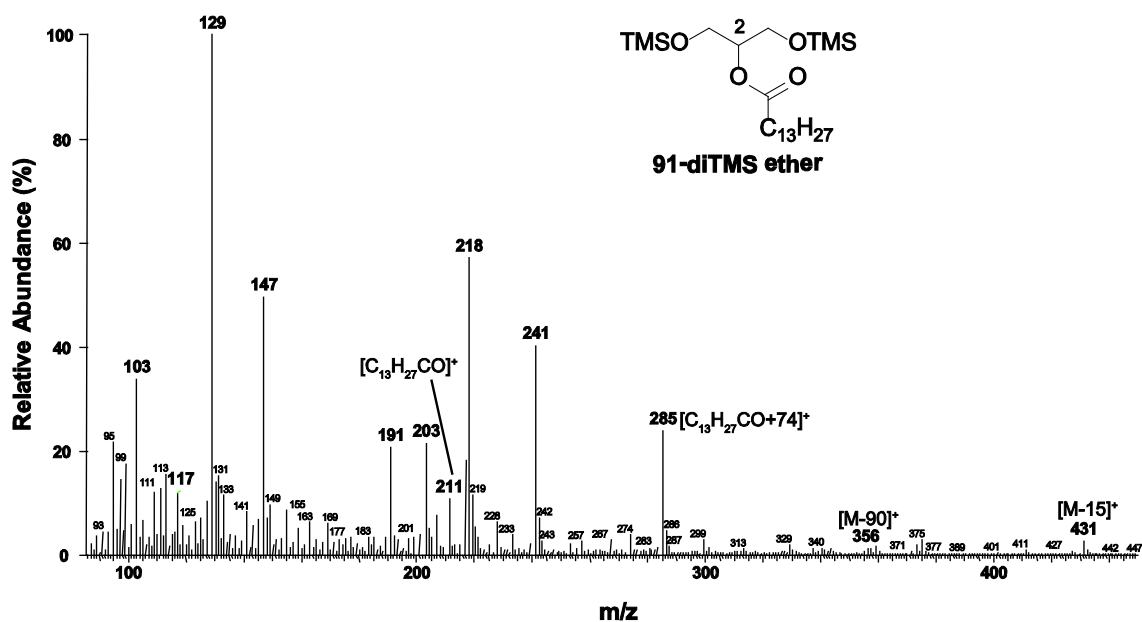
Figure 62. EI-MS spectrum of the diTMS ether of glycerol 2-myristate (91)

The structures of diglycerides were determined by analysis of the EI-MS spectra of their TMS ethers. The mass of **95**-TMS was assigned to be 556 according to ions at m/z 541 $[M - 15]^+$ and 466 $[M - 90]^+$. Ions at m/z 183 $[C_{11}H_{23}CO]^+$, 257 $[C_{11}H_{23}CO + 74]^+$ and 273 $[C_{11}H_{23}CO + 90]^+$ indicated that one of the attached fatty acid chain was -$C_{11}H_{23}COOH$ (**Figure 63**).
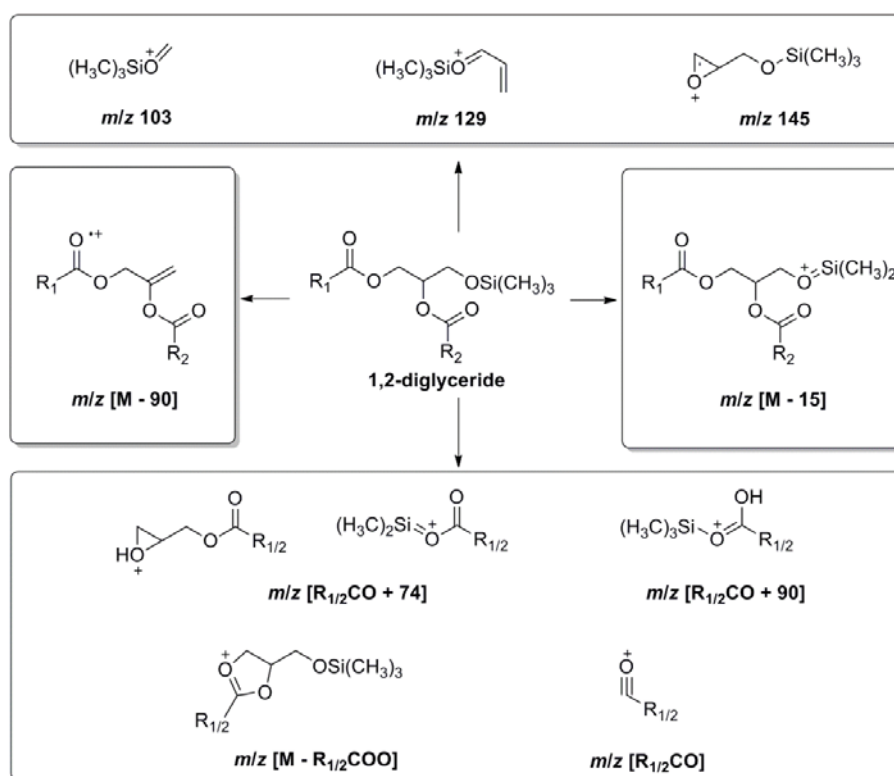

Figure 63. Principal fragmentation pattern of the TMS ether of 1,2-acyl glycerides

Similarly, another attached fatty acid chains was determined as -$C_{13}H_{27}COOH$, by typical ions at m/z 211 $[C_{13}H_{27}CO]^+$, 285 $[C_{13}H_{27}CO + 74]^+$ and 301 $[C_{13}H_{27}CO + 90]^+$. This conclusion was co nfirmed b y t he observation of i ons a t m/z 329 $[M - C_{13}H_{27}COO]^+$ and 357 $[M - C_{11}H_{23}COO]^+$, which originated from t he l oss of an acyloxy radical. D ue t o t he r elatively higher abundance of ions at m/z 257 $[C_{11}H_{23}CO + 74]^+$ and 285 $[C_{13}H_{27}CO + 74]^+$, compound **95** was d etermined as t he 1,2-isomer. A ccording to th e lite rature[171,172,173,174], t he r elatively higher abundant of ion at $[RCO + 74]^+$ indicated the 1,2-isomer when compared with the 1,3-isomer. The C_{12} fatty acid moiety was supposed to be attached on C-1 and the C_{14} fatty acid moiety attached on C -2, due t o t he r elatively higher a bundant i ons at m/z 329 $[M - C_{13}H_{27}COO]^+$ than m/z 357 $[M - C_{11}H_{23}COO]^+$. The fatty a cid moiety attached o n C -2 of glycerol was easier to be cleavaged than those attached on C-1 and C-3, therefore the relative-ly higher abundance of $[M - R_2COO]^+$ was expected for the C-2 substitutents. There is also a report that the ion at $[RCO]^+$, $[RCO + 74]^+$ and $[RCO + 90]^+$ may exhibit the higher intensity when it attached on C-2 of glycerides, however here the difference is not so significant to lead a conclusion. If the fatty acid chain at C-2 is saturated, the ratio of $[M - R_2COO]^+$ with $[M - R_1COO]^+$ is reported as 2, how ever i f an unsaturated fatty aci d chain is attached at C-2, the ratio is reported as 10–20. F inally, the structure of **95** was assigned to be glycerol, 1-laurate-2-myristate (**Figure 64**). The structure analogues of **94**, **96–98** were determined by compari-son of the EI-MS spectra with that of **95**, mainly based on the typical ions at m/z $[M - 15]^+$, $[RCO + 74]^+$ and $[M - RCOO]^+$, including the r atio of $[M - R_2COO]^+$ with $[M - R_1COO]^+$ from d ifferent f atty acid ch ains. In c ompounds **99–102**, t he u nsaturated f atty acid w as a t-tached on C-2, due to the observation of the higher abundance ion at m/z 329 $[M - R_2COO]^+$.
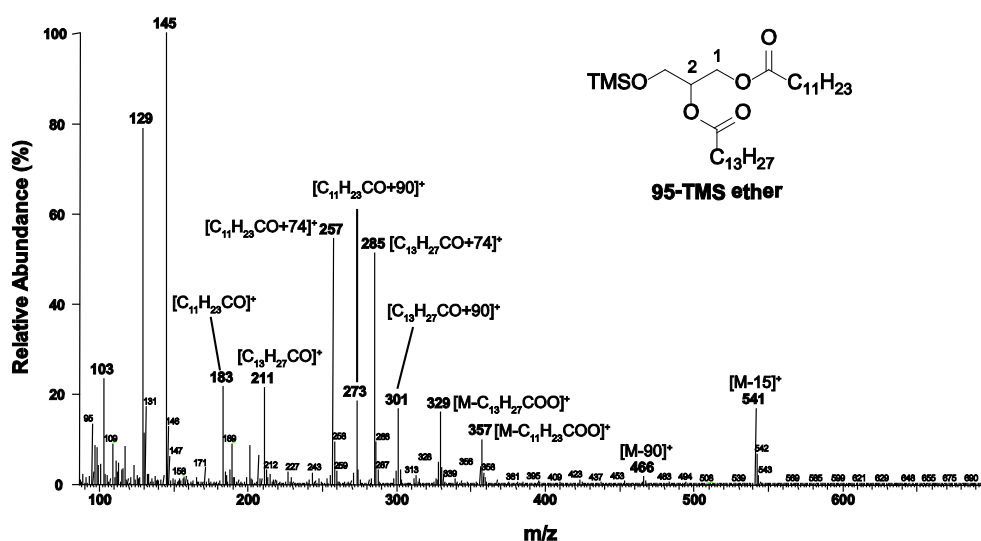

Figure 64. **EI-MS spectrum of the TMS ether of glycerol, 1-laurate-2-myristate (95)**

The mass of **104** was determined to be 556 based on the ions at m/z 466 $[M - 90]^+$ and 541 $[M - 15]^+$. The ions at m/z 183 $[C_{11}H_{23}CO]^+$, 211 $[C_{13}H_{27}CO]^+$, 257 $[C_{11}H_{23}CO + 74]^+$, 285 $[C_{13}H_{27}CO + 74]^+$, 329 $[M - C_{13}H_{27}COO]^+$ and 357 $[M - C_{11}H_{23}COO]^+$ (**Figure 65**) were observed in EI-MS spectrum of **95** and indicated the identical fatty acid moieties as in **104**. The 1,3-diglyceride isomer was supported by the observation of the most abundant ions at m/z 315 $[M - C_{13}H_{27}COOCH_2]^+$ and 343 $[M - C_{11}H_{23}COOCH_2]^+$, which originated from the loss of acyloxymethylene radical from the molecular ion[174]. Therefore the structure of **104** was assigned as glycerol, 1-laurate-3-myristate (**Figure 66**), in agreement with spectra data from literature[170]. The structures of 1,3-diglyceride homologues and derivatives (**103, 105–111**) were assigned by comparison of their EI-MS spectra with that of **104**.
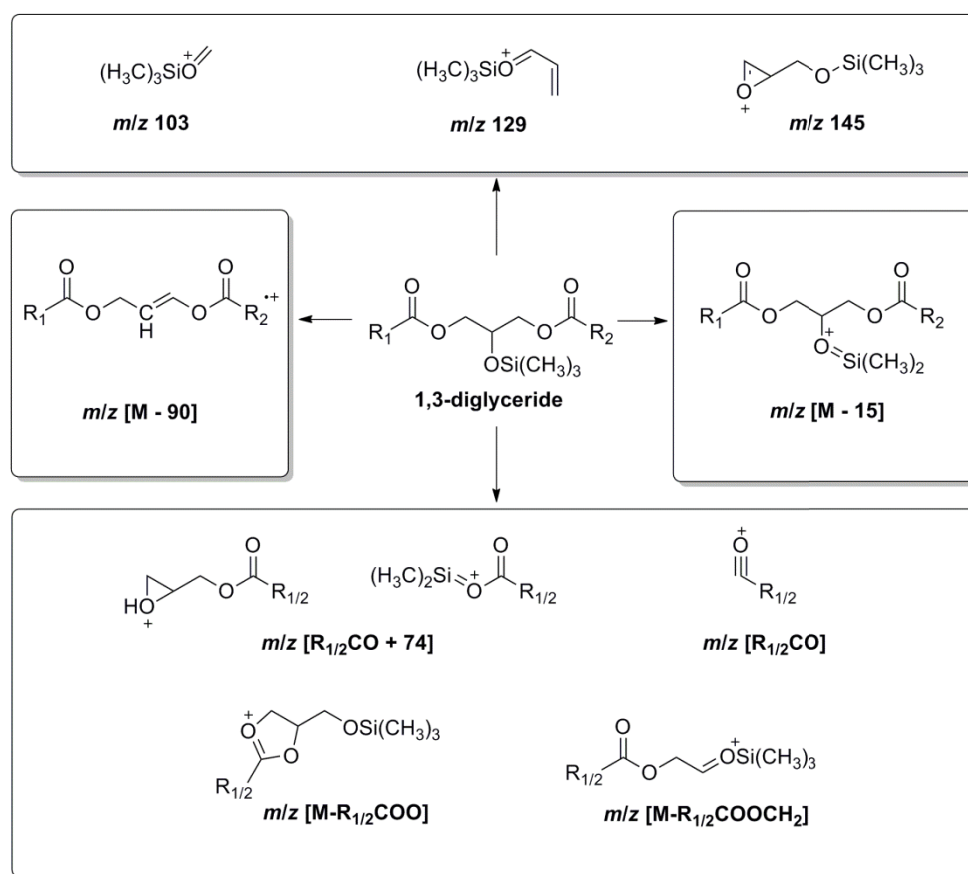

Figure 65. Principal fragmentation of the TMS ether of 1,3-acyl glycerides
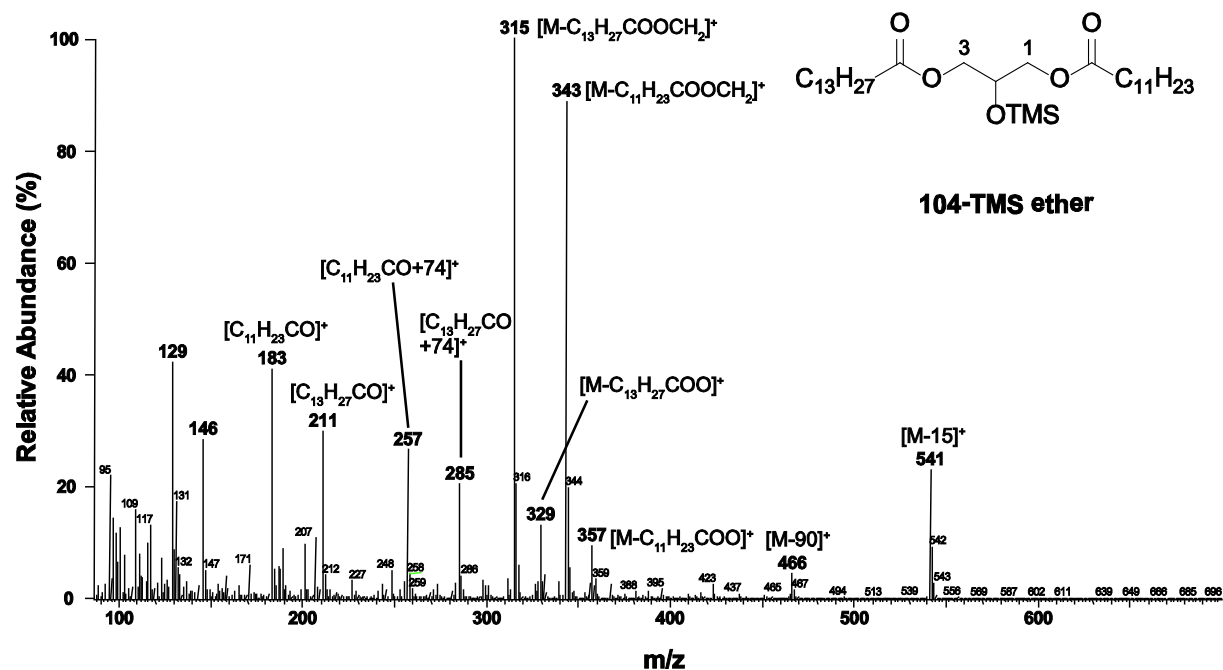
Figure 66. EI-MS spectrum of the TMS ether of glycerol, 1-laurate-3-myristate (104)

The triglycerides were identified by analysis of their EI-MS spectra (**Figure 67**). The molecular mass was difficult to determine due to very low abundance of molecular ion $[M]^+$. However, the attached fatty acid chains were assigned by the observation of the fragment ion $[M - RCOO]^+$ due to the loss of acyloxy chain and the corresponding ions $[RCO]^+$ and $[RCO + 74]^+$, together with ion $[RCO + 128]^+$ caused also by rearrangement with entire glycerol. The attached position of fatty acid chain on the glycerol skeleton is assigned according to the ion $[M - RCOOCH_2]^+$ originating from the loss of acyloxymethylene radical from the position 1 and 3[175,176].
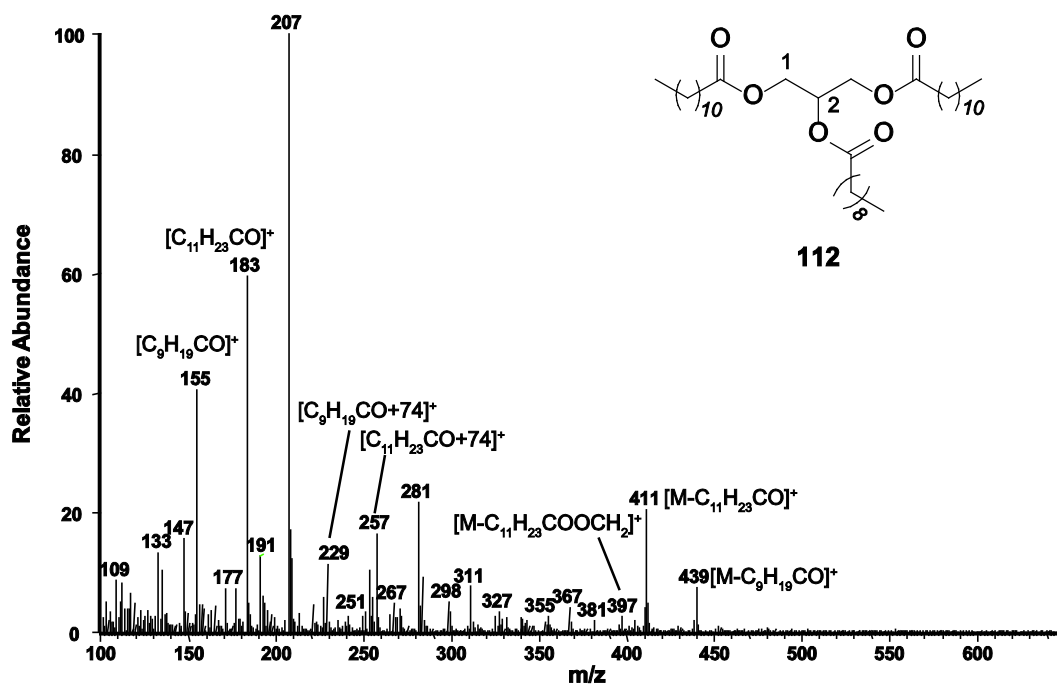
Figure 67. EI-MS spectrum of glycerol, 1-laurate-2-caprate-3-laurate (112)

3.4.5 Possible biological function of the white secretion

The copious exudates were produced by the glands on the inner side of pitcher lids of *N. lowii*, *N. macrophylla* and *N. rajah*. In comparison with other *Nepenthes* pitchers, the exudates of *N. lowii* are described as "white and buttery" in texture. However, the secretions of the lid glands of *N. macrophylla* are less copious and of thinner consistency. In *N. rajah*, the lid gland secretions are clear and watery in texture and do not seem to accumulate on the pitcher lids. It is unclear whether this is a result of rapid consumption by *T. montana* or run-off as a consequence of their low viscosity[162]. Based on detailed analysis by GC-MS and NMR, the major chemical components of white secretion of *N. lowii* were free sugars, fatty acids, monoglycerides, diglycerides and triglycerides. These compounds may be used to test some biological activities involved into the effect to the animal behavior, in order to understand the interaction of pitcher plants and feeding animals. According to the behavior of *T.montana*, they are highly frugivorous, specializing in crushing fruits to extract the sugary juices[177]. Therefore it might be considered potentially as preadapted to feeding on the sugar-rich secretions of *N. lowii*. But whether or not the identified compounds cause laxative effects in *T. Montana*, as speculated in earlier studies, is still an open question.

In literature, certain monoglycerides were found in extracts of plant roots, seeds and other parts.[178,179] These compounds showed several biological activities. For example, linolenic acid together with glycerol 1-laurate (**83**) exhibit strongly antimicrobial activity against *Bacillus cereus* and *Staphylococcus aureus*[180]. The monoglyceride 1-C18:1 (**101**) can induce selective apoptosis in human leukemic cells[181], and monoacylglycerol-oleic acid showed significant antioxidant activity in a mouse model[182]. Some diglycerides could attract seed-carrying behavior of ant in ant–seed interaction[183,184]. Moreover, a potential toxicity of rac-1(3)-palmitoyl glycerol (**84**) has been reported. This compound can induce hypothermia, however this was only a sign of toxicity, not the immediate cause of serious situation[185]. Additional biological activities of glycerides to animal needed to be investigated further.

4 Summary

BLM-guided purification of channel-forming compound

Insect herbivory on plants is a complex interaction between several organisms, various chemical factors and fine tuned plant signaling cascades. The oral secretion (OS) from insect larvae contains a "pool" of chemicals which could trigger diverse plant defense reactions. Especially, the oral secretion from lepidopteran larvae showed channel-forming activity in the black lipid membrane (BLM) assay, which was common for several lepidopteran species. Therefore this PhD work mainly concentrated on the discovery of new elicitor(s) which have the channel-forming activity, and further investigate the corresponding functions in plant defense. Here, a porin like protein (PLP) has been partially purified through diverse column chromatography and identified as a channel-forming compound present in the OS of *S. littoralis* larvae. Following the BLM-guided fractionation of 10 mL OS (collected from 500 larvae in the 4th instar stage) and proteomic analysis of several BLM active fractions, the identified peptides (ATIAGTYAFGPAK and TDAYFNLAYAK) were matched to the porin type protein derived from Gram-negative *Ralstonia pickettii* 12J by stringent database searching of MS/MS spectra (MASCOT) and homology-based approach (*de novo* MS BLAST). Due to the limited amount of OS, it was impossible to get the pure PLP from the final active fraction. Fortunately, the commercially available porin α-hemolysin (α-HL, **41**) showed comparable BLM activity compare to the crude oral secretion and active fractions. This further confirmed the interpretation of proteomic data and indicated that the porin-like protein (PLP) from OS is one of the factors responsible for the channel-forming activity.

Biological functions of α-HL (41) in plant defense reactions

In order to investigate the role of membrane potential (V_m) changes and the cross-talk between plant responses in the plant–insect interactions, α-HL (**41**) was applied to mimic the PLP activity. In parallel, the plant defense inducing activities of α-HL (**41**) were compared with that of alamethicin (**42**), a channel forming peptide which induces plant defense reactions. This provided more information about the structure–activity relationship between the different channel-forming compounds. α-HL (**41**) induced the ion flux (K^+, Ca^{2+}) in BLM assay and up-regulation of the transcription level of *CML42*, comparable to PLP-containing fraction.

OS showed multiple activities, but could not induce Ca^{2+} flux in BLM assay. The induced plant defense activities of α-HL (**41**) and alamethicin (**42**) are summaried in **Table 6**.

Microbial origin?

The proposed bacterial origin of the PLP suggested that the bacteria in insect gut might play an important role in plant–insect interactions. Therefore we try to identify the channel formation activity from the secretion of gut bacteria. *Enterococcus mundtii* and *Clostridium* sp. were the major organisms among the commensals in 4th instar *S. littoralis* larvae. The fermentation broth of the wild-type *C. cellulolyticum* exhibited the channel-forming activity in the BLM assay, indicating that the gut microorganisms could contribute to the plant membrane potential change. Further investigation demonstrated that channel-forming proteins may be the candidate for this effect.

Chemical components from oral secretions of *S. littoralis* larvae

Due to the various origins of chemical components within the insect gut, the metabolites in insect OS are highly diverse. They might come from diet, secreted by insect themselves or from gut microbes. The OS was the main source of chemical elicitors from the insect, like volicitin (**14**). More chemical components present in the oral secretion were investigated, in order to better understand the function of chemical factors in the plant–insect interactions. From aqueous phase of OS after CH_2Cl_2 extraction, 12 oleanene type saponins (**46–57**) were identified using a combination of liquid chromatography, HPLC-MS and NMR spectroscopy, which weren't digested in the insect gut. Oleanen type saponins were the major components in bean seeds, which were used for the insect diet. They exhibit diverse biological activities as reported in the literature. However the biological functions of these compounds in plant–insect interactions need to be investigated further. Using headspace VOC collection and GC-MS for OS analysis, three alkanens pentadecane (**61**), tetradecane (**62**) and heptadecane (**63**) were identified, with pentadecane (**61**) being the most abundant.

Chemical investigation on the white secretion on the inner lid of pitcher plant *Nepenthes lowii*

As a side project, the chemical composition of white secretions from carnivorous pitcher plant *N. lowii* has been analyzed. Mature *N. lowii* produced very large pitcher, which can carry mountain tree shrews (*Tupaia montana*). The tree shrew defecates into the pitcher thereby providing the nitrogen source for the pitcher plant, while feeding on exudates secreted by glands on the inner surface of the pitcher lid. After analysis of the chemical components of this white secretion by NMR and GC-MS, 48 compounds have been identified, including three sugars D-(+)-glucose (**64**), D-(−)-fructose (**65**) and D-(+)-sucrose (**66**), 16 fatty acids (**67–82**), 11 monoglycerides (**83–93**), 18 diglycerides (**94–111**) and three triglycerides (**112–114**). Understanding the biological relevance of chemical components of the white secretions will be very useful for further investigation of the ecological relationship between pitcher plant and tree shrews.

5 Zusammenfassung

BLM-geleitete Reinigung von kanalbildenden Verbindungen

Herbivorie von Insekten an Pflanzen ist eine sehr komplexe Interaktion zwischen verschiedenen Organismen, zahlreichen chemischen Faktoren und fein geregelten pflanzlichen Signalkaskaden. Das Oralsekret (OS) von Insektenlarven ist ein ‚pool' für chemische Substanzen, die verschiedene pflanzliche Abwehrreaktionen auslösen können. Im Besonderen zeigt das OS von Lepidopteren-Larven typischerweise kanalbildende Aktivität im ‚black lipid membrane (BLM) assay'. Im Fokus der vorliegenden Doktorarbeit lag daher hauptsächlich das Auffinden von neuen Substanzen mit kanalbildenden Aktivitäten und Untersuchungen zur ihren Funktionen in der pflanzlichen Abwehr. Aus dem OS von *S. littoralis* Larven konnte mittels verschiedener chromatographischer Methoden ein ‚porin-like protein' (PLP) partiell gereinigt und als kanalbildende Verbindung identifiziert werden. Nach BLM-geleiteter Fraktionierung von 10 mL OS (von 500 Larven im 4. Larvenstadium gesammelt) und proteomischer Analyse verschiedener BLM-aktiver Fraktionen zeigte eine Polypeptid-Aminosäuresequenz nach MASCOT und *de novo* MS BLAST Auswertung Homologie zu einem Porin des Gramnegativen Bakteriums *Ralstonia pickettii* 12J. Aufgrund der limitierten Menge an der hochgereinigten Fraktion war es unmöglich reines PLP hieraus zu isolieren. Allerdings zeigte ein käufliches Porin, α-Hämolysin (α-HL, **41**) eine zum ungereinigten OS und den aktiven Fraktionen vergleichbare BLM Aktivität. Dies bestätigte die Daten aus der Proteom Analyse und zeigte, dass das PLP aus dem OS in der Tat zumindest einen Faktor darstellt, der für die kanalbildende Aktivität verantwortlich ist.

Biologische Funktionen von α-Hämolysin (41) in pflanzlichen Verteidigungsreaktionen

Um die Rolle des Membranpotentials (V_m) und den ‚cross-talk' zwischen verschiedenen pflanzlichen Reaktionen in Pflanze-Insekten Interaktionen zu untersuchen, wurde α-Hämolysin (**41**) als Mimik der PLP Aktivität eingesetzt. Parallel wurden die abwehrinduzierenden Akivitäten von α-HL (**41**) mit denen von Alamethicin (**42**), einem kanalbildenden und Pflanzenabwehr induzierenden Peptid, verglichen. Dies lieferte zusätzliche Informationen über Struktur-Aktivitäts-Beziehungen hinsichtlich der verschiedenen Kanalbildner. Ver-

gleichbar mit d er PLP-Fraktion induzierte α-HL (**41**) Ionenflüsse (K$^+$, C a^{2+}) i m B LM a ssay und e rhöhte de n T ranscript-Level von *CML42*. OS z eigte ve rschiedene Aktivitäten, konnt e aber k einen C a^{2+} Fluss im BLM assay induzieren. Die von α-HL (**41**) b eziehungsweise Alamethicin (**41**) ausgelösten Pflanzenabwehraktivitäten sind in Tabelle 6 zusammengefasst.

Mikrobieller Ursprung?

Der sehr wahrscheinlich bakterielle Ursprung von PLP lässt vermuten, dass Bakterien des Insektendarms eine wichtige Rolle in den Wechselwirkungen zwischen Pflanzen und Insekten spielen könnten. Deshalb wurde versucht sekretierte, kanalbildende Aktivitäten bei Darmbakterien zu finden. Die häufigsten Bakterien bei *S. littoralis* des 4. Larvenstadiums sind *Enterococcus mundtii* und *Clostridium spec*. Im Fermentationsmedium von *C. cellulolyticum* konnte in der Tat kanalbildende Aktivität im BLM assay gezeigt werden, was nahelegt, dass Darmbakterien zu den Membranpotential-Änderungen in den Pflanzen beitragen konnten. Weitere Untersuchungen bestätigten, dass tatsächlich kanalbildende Proteine Kandidaten dafür sein könnten.

Chemische Verbindungen im Oralsekret von *S. littoralis* Larven

Aufgrund de r unt erschiedlichen Q uellen für c hemische V erbindungen i m Insektendarm s ind die Metaboliten im OS sehr verschieden. Sie können aus der Diät stammen, von den Insekten selbst oder von Darmbakterien sekretiert werden. OS war die Hauptquelle für chemische Signalsubstanzen von Insekten, w ie da s V olicitin (**14**). U m di e F unktion von c hemischen V erbindungen in der Interaktion zwischen Pflanze und Insekt besser zu verstehen, wurden weitere Komponenten im OS unt ersucht. In der w ässrigen Phase von O S nach CH$_2$Cl$_2$ Extraktion konnten nach Flüssigkeitschromatographie, HPLC-MS und NMR Spektroskopie 12 Oleanen-Typ S aponine (**46–57**) i dentifiziert w erden. D iese w aren ni cht i m Insektendarm a bgebaut worden. Oleanen-Typ Saponine sind die Hauptkomponenten in Bohnensamen, die die Grundlage für die Insektendiät bilden und besitzen laut Literatur verschiedene biologische Aktivitäten. A llerdings mü ssten diese bi ologischen Funktionen i n P flanze-Insekten W echselwirkungen noch genauer untersucht werden. Darüber hinaus konnten mittels VOC Anreicherung und nachfolgender GC-MS Analyse in OS drei flüchtige Alkane identifiziert werden, das dominierende Pentadecan (**61**), sowie Tetradecan (**62**) und Heptadecan (**63**).

Chemische Untersuchung eines weißen Sekrets vom inneren Deckel der Kannenpflanze *Nepenthes lowii*

Im Rahmen seines Seitenprojektes wurde ein weißes Sekret vom inneren Deckel der karnivoren Kannenpflanze *N. lowii* analysiert. Ausgewachsene *N. lowii* Pflanzen produzieren sehr große Kannen, die das Spitzhörnchen *Tupaia montana* tragen können. Während dieses Spitzhörnchen das weiße Sekret vom inneren Kannendeckel leckt, kotet es in die Kanne und liefert dadurch eine Stickstoffquelle für die Kannenpflanze. Nach NMR und GC-MS Analyse der chemischen Verbindungen des weißen Sekrets konnten 48 Substanzen identifiziert werden. Darunter waren drei Zucker zu finden, D-(+)-Glukose (**64**), D-(−)-Fruktose (**65**) und D-(+)-Saccharose (**66**), 16 Fettsäuren (**67**–**82**), 11 Monoglyceride (**83**–**93**), 18 Diglyceride (**94**–**111**) und drei Triglyceride (**112**–**114**). Das Verständnis der biologischen Relevanz der verschiedenen Komponenten des weißen Sekrets kann im Hinblick auf weitere Untersuchungen zur ökologischen Wechselwirkung zwischen den Kannenpflanzen und Spitzhörnchen hilfreich sein.

6 Experimental Section

6.1 Material and equipments

6.1.1 Small molecular analysis

Sephadex LH20 (17-0090-01) gel material was purchased from GE Healthcare (Uppsala, Sweden). Analytical thin layer chromatography (TLC) plates (Kieselgel 60 F254) were purchased from Merck Chemicals (Darmstadt, Germany). The separated compounds were stained by 10% H_2SO_4-EtOH and heating.

Liquid chromatography mass spectrometry (LC-MS) was performed either with an Agilent HP 1100 system coupled with Thermo Finnigan LCQ instrument with ESI source and 3-dimensional ion trap analyser, or with a Dionex UltiMate 3000 HPLC system coupled to a Thermo Finnigan LTQ instrument with ESI source and linear ion trap analyser.

Analytical columns: Grom-Sil 120 ODS-3 CP (125 mm × 2 mm) column and Phenomenex Gemini (5µ C18 110Å 250 mm × 2 mm) column. Semi-preparative column: Phenomenex Gemini (5µ C18 250 mm× 10 mm) column. HPLC fractions were collected with Gilson Fraction Collector FC206.

Gas chromatography mass spectrometry (GC-MS) was performed with a Thermo Finnigan Trace MS 2000 series (Thermoquest, D-63329 Egelsbach, Germany) and a Thermo Scientific ITQ Series quadrupole ion trap, equipped with a Phenomenex ZB-5 (15 m × 0.25 mm, 0.25 µm) column. Mass spectra were measured in electron impact (EI) positive mode at 70 eV. LC-MS and GC-MS data were analyzed using the Xcalibur software (v2.0.7).

Volatile organic compounds (VOC) were collected with the "closed loop stripping" (CLS) technique, or with solid phase microextraction (SPME) techniques. For CLS miniature rotary pumps were purchased from Fürgut (D-88139, Aitrach). VOC were absorbed on 1.5 mg of activated carbon filters (charcoal), with length 60 mm, and diameter 5 mm, from le Ruisseau de Montbrun (F-0935 Daumazan sur Arize, France).

The zNose[100] was purchased from Electronic Sensor Technology (Newbury Park, CA, USA). The instrument comprised a programmable collecting device (suction pump connected to a Tenax®-trap with 30 mL/min air flow for concentration of compounds prior to analysis) linked to a miniaturized gas chromatography equipped with a stainless steel column (1 m,

DB-5, film thickness 0.25 μm, ID 0.25 mm) and a very sensitive surface acoustic wave quartz micro-balance detector (SAW) mounted on a thermal electric element. The detector temperature could be adjusted between 0 ^{o}C – 140 ^{o}C to obtain maximum sensitivity for the analytes. Lower temperature provided enhanced sensitivity but failed to desorb the compounds, however higher temperature decreased the sensitivity but the linear dynamic range was extended. Helium served as carrier gas (flow rate 3 mL/min).

NMR spectra were recorded with an AV 400, AV 500 and Avance DRX 500 spectrometer (Bruker). The chemical shift was specified as δ in ppm, the coupling constant J in Hz. The chemical shifts were relative to the solvent served as an internal standard: CDCl$_3$ δ_H = 7.26 ppm, δ_C = 77.70 ppm; CD$_3$OD δ_H = 3.31 ppm, δ_C = 49.00 ppm.

Authentic standard sugars: D-(+)-glucose (**64**), D-(−)-fructose (**65**) and D-(+)-sucrose (**66**) were purchased from Sigma-Aldrich (USA), lauric acid (**67,** C12:0), myristic acid (**68,** C14:0), palmitic acid (**69**, C16:0), arachidic acid (**71,** C20:0), lignoceric acid (**73,** C24:0) and palmitoleic acid (**74,** C16:1 n = 7), oleic acid (**79**, C18:1 n = 9), *cis*-11-eicosenoic acid (**80**, C20:1 n = 9), nervonic acid (**81**, C24:1 n = 9) and linoleic acid (**82**, C18:2 n= 6) were obtained from Sigma. Organic solvents (acetonitrile, methanol, ethanol, acetone, ethyl acteate, chloroform, dichloromethane and hexane) were purchased from Merck Chemicals (Darmstadt, Germany). Silylated fatty acids mixture (Cat. No. 722307), containing TMS capric acid (C10:0), TMS myristic acid (**68**-TMS, C14:0), TMS stearic acid (**70**-TMS, C18:0), TMS behenic acid (**72**-TMS, C22:0)), was purchased from Macherey-Nagel (Düren, Germany). *N*-methyl-*N*-trimethylsilyl-trifluoroacet-amide (MSTFA) was obtained from Macherey-Nagel (Düren, Germany).

6.1.2 Protein chemistry

Sephadex G-25 (fine, 17-0032-01), G-75 (17-0050-01), DEAE Sephadex A-25 (17-0170-01), and CM Sephadex C-25 (17-0210-01) gel materials were purchased from GE Healthcare (Uppsala, Sweden).

Vivaspin 3KD, 5KD, 30KD MWCO PES were purchased from Sartorius stedim (Göttingen, Germany).

PD-10 desalting columns were purchased from GE Healthcare (Amersham, United Kingdom).

The pronase enzyme (Cat. No. 165921) was purchased from Roche (Mannheim, Germany).

Fast protein liquid chromatography (FPLC) was performed using the ÄKTA Explorers 10 system (GE Healthcare). The ÄKTA system was equipped with Superdex 75 HR 10/30 column (10 mm × 300 mm, Pharmacia Biotech) for size exclusion and Resource Q 1 mL (3.2 mm × 30 mm, Pharmacia Biotech) for anion exchange. Fractions were collected with 96-deep well plate (2 mL). The protein signal was detected by UV at 280 nm. Data were analyzed by UNICORN software Version 3.2.

1D SDS-PAGE electrophoresis was performed on Mini-Protean®TetraCell from BIO-RAD, staining with 0.1% Coomassie-Brilliant-Blue R250 (Applichem) within 45% ethanol und 10% acetic acid in water, destaining with 20% ethanol, 10% acetic acid in water. Protein molecular weight marker (SM0431) was purchased from Fermentas.

LC-MS/MS for Proteomic analysis was performed with a nanoAcquity nanoUPLC system (Waters, Manchester, UK) with Symmetry C18 trap-column (20 × 0.18 mm, 5 µm particle size) and nanoAcquity analytical C18 column (200 mm × 75 µm ID, C18 BEH 130 material, 1.7 µm particle size). MS/MS was performed with the nanoelectrospray source of a Synapt HDMS tandem mass spectrometer (Waters, Manchester, UK). Acquired spectra were baseline subtracted, smoothed, deisotoped, and lockmass-corrected using ProteinLynx Global Server Browser (PLGS) v2.5 software (Waters, Manchester, UK). Processed MS/MS spectra were searched against NCBInr database (updated on September 11, 2011, containing 15,270,974 sequence entries) using MASCOT v2.3 software installed on a local server and connected to PLGS as a search engine.

6.1.3 Real-Time PCR

Trizol reagent was purchased from Invitrogen (Darmstadt, Germany) and stored at 4 $^{\circ}$C until use. TURBO DNA-free Kit was obtained from Ambion (Austin, USA). Oligo-dT$_{18}$ primers and RiboLock RNase Inhibitor were purchased from Fermentas (Germany). Omniscript cDNA synthesis kit was purchased from Qiagen (Germany). Brilliant QPCR SYBR green Mix was purchased from Agilent Technology (USA).

6.2 Biological materials

Eggs of *S. littoralis* larvae were acquired from Bayer CropScience AG (Monheim, Germany) and reared on the agar-based artificial diet. Artificial diet was prepared as follows: ground white beans (500 g) were soaked overnight in water (1200 mL) and ascorbic acid (9 g), parabene (9 g), aq formaldehyde (4 mL, 36.5%), and agar (75 g), boiled in 1000 mL of H_2O, were added. After cooling, the mixture solidified to a white waxy solid[50]. Individual plastic cages with the diet and the larvae were kept at 23–25 $^{\circ}C$ under a light-dark regime with 16 h of illumination.

Transgenic soybean 6.6.12 cell lines carrying the stable integrated plasmid *pGN Aequ/neo2* and expressing apoaequorin were grown and used to reconstitute aequorin as described[85].

The *CML42* expression experiments with *A. thaliana* were conducted using Columbia ecotype (Col–0, wild type). Seeds were imbibed for 3 days at 4 $^{\circ}C$ and subsequently transferred to a growth chamber under 16-h light/8-h dark photoperiod at 22 $^{\circ}C$. Transgenic *A. thaliana* (Col) expressing cytosolic apoaequorin were used for $[Ca^{2+}]_{cyt}$ measurement. Plants were grown vertically in Hoagland's medium with 1% agar for 14 days.

Lima bean (*P. lunatus*) L. cv Ferry Morse var Jackson Wonder Bush plants were grown from seeds in a plastic pot using sterilized potting soil at 23 $^{\circ}C$ with 60% humidity and 270 μE m^{-2} s^{-1} during a 16-h photoperiod.

The white secretion of pitcher plant *N. lowii* were obtained from the Botanical Garden, University of Bonn and stored at −20 $^{\circ}C$ until use.

6.3 Collection of oral secretions

Oral secretions from 4th-instar *S. littoralis* larvae were collected with pipette by gently squeezing the larva with a forceps behind the head which caused immediate regurgitation. Fresh oral secretions were collected during afternoon, due to relatively more OS regurgitated by the insect larva during afternoon. Secretions were stored at −80 $^{\circ}C$ until use. Normally 20 μL OS could be collected from each larva per time. Before use, harvested samples were centrifuged at 16,000 × g for 30 min at 4 $^{\circ}C$ to remove particles from the rest of diet.

6.4 Elicitor isolation

6.4.1 Vivaspin molecule cut-off separation

After centrifugation, 500 μL clear supernatant of OS was applied to the Vivaspin 500 with different molecule cut-off (3 KD, 5 KD and 30 KD). The centrifugal force was adjusted according to the advice provided by manufactor for 30 min. After separation by centrifugation, two parts (filtrated and non-filtrated part) were obtained according to the molecular size. The 500 μL final volumn was obtained for each part by adding H_2O in order to adjust the same concentration as before separation, and following by the BLM activity test. Vivaspin 30 KD was used to concentrate fractions after column chromatography.

6.4.2 Heat denaturation

The crude supernatant was kept at room temperature for 1 d or heated for 4 h at 100 °C respectively, followed by the BLM activity test in order to evaluate the stability of the sample after high temperature denaturation.

6.4.3 Pronase digestion

The pronase enzyme[186] (Cat. No. 165921), purchased from Roche (Mannheim, Germany), was applied according to manufactor's guide. Fresh pronase stock solution was prepared by adding pronase powder to water at 10 mg/mL. The reaction system with 0.05% SDS was prepared as described in **Table 9** at 37 °C for 16 h, and stopped by freezing at –20 °C. Due to the interference of tiny amount SDS in BLM assay, an altenative digestion protocol without SDS was estabilished (**Table 10**).

Table 9. Pronase digestion protocol with SDS

Positive control	*Enzyme control*	*Enzyme treatment*
	25 μL 10% SDS	25 μL 10% SDS
	25 μL 2M Tris pH 7.5	25 μL 2M Tris pH 7.5
	50 μL 10 mg/mL pronase	50 μL 10 mg/mL pronase
20 μL OS		20 μL OS
480 μL H_2O	400 μL H_2O	380 μL H_2O

Table 10. Pronase digestion protocol without SDS

Positive control	Enzyme control	Enzyme treatment
	25 µL 200 mM CaCl$_2$	25 µL 200 mM CaCl$_2$
	25 µL 2M Tris pH 7.5	25 µL 2M Tris pH 7.5
	50 µL 10 mg/mL pronase	50 µL 10 mg/mL pronase
20 µL OS		20 µL OS
480 µL H$_2$O	400 µL H$_2$O	380 µL H$_2$O

6.4.4 Organic solvent extract

300 µL supernatant of insect OS was extracted with 3×300 µL CH$_2$Cl$_2$. CH$_2$Cl$_2$ extract were combined, and the solvent was removed by a stream of argon. The residue was redissolved into ACN to reach a concentration of 10 mg/mL. The aqueous phase was completely dried, and followed by adding 300 µL H$_2$O into the residue. 10 µL CH$_2$Cl$_2$ extract and aqueous phase were applied into BLM assay respectively.

6.4.5 BLM-guided purification

10 mL supernatant from the crude OS accumulated from 500 larvae was extracted with 3×20 mL CH$_2$Cl$_2$ and centrifuged at 16,000 g for 10 min to get two clear layers. The CH$_2$Cl$_2$ phase containing non-polar organic compounds was kept for further use after removing the organic solvent at 10 mg/mL in H$_2$O. The channel-active (BLM-assay) aqueous phase was submitted to Sephadex G25 column chromatography (2 cm $\times$ 46 cm, GE, Sweden) using H$_2$O for elution. Seven fractions (15 mL each) were obtained according to the molecular size. The combined active fractions Fr. 2 to Fr. 4 were concentrated in vacuo. The residues were redissolved in water (5 mL) and further separated on Sephadex G75 (2 cm $\times$ 46 cm, GE, Sweden) using H$_2$O for elution. Channel-active subfractions Fr. 3 to Fr. 7 (15 mL each) were analyzed by 12% SDS-PAGE gel electrophoresis and 13 individual bands were submitted to proteomic analysis. Alternatively, the combined active fractions were separated on DEAE Sephadex A25 (2 cm $\times$ 46 cm, GE, Sweden) using a stepwise gradient elution of 50 mM Tris buffer (pH 7.5) (Fr. 1), followed by continued elution with the same buffer (50 mM Tris buffer, pH 7.5) containing 0.2 M KCl (Fr. 2), 0.4 M KCl (Fr. 3), 0.6 M KCl (Fr. 4), 0.8 M KCl (Fr. 5), and 1.0 M KCl (Fr. 6). The fraction volume was 300 mL each. After concentration on a Viva spin filter (30 KD, Sartorius, Germany) and dissolving the residue in water, the sample was further desalted by passing through PD-10 Sephadex G25 column (Amersham, United Kingdom). The chan-nel-active fractions from 0.2 M KCl to 0.6 M KCl (Fr. 2 to Fr. 4) were combined and submit-

ted to a second DEAE Sephadex A25 column chromatography using gradient elution from 50 mM Tris buffer (pH 7.5) to 0.6 M KCl in 50 mM Tris buffer (pH 7.5). The fraction volume was 300 mL each. The BLM activity was mainly found in Fr. 3, eluted with 0.2 M KCl in 50 mM Tris buffer (pH 7.5), but also in Fr. 4 (eluted with 0.3 M KCl) and in Fr. 5 (eluted with 0.4 M KCl). Fraction 3 was analyzed by 12% SDS-PAGE gel for the proteomic analysis by mass spectroscopy. The pooled active fractions from Fr. 3 to Fr. 5 were finally separated using ÄKTA AIEX Resource Q−1mL column chromatography (**Table 11**) using a linear gradient from phase A (50 mM Tris buffer with pH 7.5) to phase B (1.0 M KCl in 50 mM Tris buffer with pH 7.5). The gradient elution volume was 20 column volumes (CV) (2 − 12 min), with a flow rate of 2.0 mL/min and UV detection at 260 nm and 280 nm and collected by a coupled fraction collector (1 mL each). The following active fraction Fr. 6 was subjected to proteomic analysis. The purification chart was outlined in **Scheme 2**.

Table 11. ÄKTA-AIEX purification method

Eluent	*Flow rate*	*UV detector*	*Gradient*	*Fractionation*
A:50 mM Tris pH 7.5 B:1.0 M KCl, 50 mM Tris pH 7.5	2.0 mL/min	260 nm 280 nm	0-2.0 min (100% A) 2.0-12.0 min (0-100% B) 12.0-15.0 min (100% B) 15.0-20.0 min (100% A)	Fr. 1 (A1–A3) Fr. 2 (A4–A6) Fr. 3 (A7–A9) Fr. 4 (A10–A11) Fr. 5 (A12–B2) Fr. 6 (B3–B5) Fr. 7 (B6–B9) Fr. 8 (B10–C2)

6.5 Planar lipid bilayer membrane (BLM) assay

Stable lipid bilayers[93] were formed from a solution of 1,2-diacyl-*sn*-glycero-3-phosphatidylcholine Type IV–S (soybean, Sigma, USA) at 20 mg/mL in heptane by delivering the solution from a plastic tip across a 500 μm or 800 μm hole in a 10 mm diameter teflon cylinder placed into a small glass beaker (15 mL) filled with buffer (10 mM Tris/HCl, containing 200 mM KCl at pH 9.2). Thickness of the teflon cylinder wall was about 1 mm. The brush technique of Mueller and colleagues[187] was used for the BLM formation, the process of the BLM formation was monitored online, and the bilayer area was estimated by the amplitude of the rectangular shape current pulses generated by the 10 mV tooth-shape voltage pulses applied to the membrane via two Ag–AgCl electrodes connected by agar bridges. Currents were recorded under voltage-clamp conditions with a Low Noise Current Preamplifier, Model SR 570 (Stanford Research System, Sunnyvale, USA). Current signals (filtered at 30

Hz) were digitized with a National Instruments (Austin, USA) PCI-6024E card; data were stored and analyzed with Strathclyde Electrophysiology Software WinEDR V 2.7.7 (John Dempster, University of Strathclyde, Glasgow, UK).

The process of the artificial bilayer membrane formation normally took about 2 min. After the membrane had been formed, 10 µL crude OS or desalted fractions were added to the *cis*-compartment and gently stirred. The increase of current indicated the channel-forming activity. Both *cis*- and *trans*-compartments were filled with the same buffer at pH 9.2 representing the pH of the insects' OS. α-HL (**41**) was dissolved at 0.1 mg/mL in 10 mM Tris/HCl (pH 8.0) and 10 µL were applied to the *cis*-compartment to evaluate the channel forming activity. To determine the selectivity for Ca^{2+} ions, 100 mM $Ca(NO_3)_2$ was used instead of 200 mM KCl in 10 mM Tris/HCl (pH 9.2) and 20 µL α-HL (**41**) solution was added to the *cis*-compartment.

6.6 SDS-PAGE electrophoresis

12% SDS-PAGE gel was prepared following the protocol presented in **Table 12** and **Table 13**. 15 µL sample solution was mixed with 5 µL loading buffer and cooked at 100 °C for 5 min. After cooling to room temperature, 20 µL sample solution was loaded onto the gel. 1D SDS-PAGE electrophoresis was performed using the Mini-Protean®TetraCell (BIO-RAD), under 100 V for 15 min and then 150 V for 45 min. The gel was stained over night with 0.1% Coomassie-Brilliant-Blue R250 in 45% ethanol und 10% acetic acid in water, and destained 5 h with 20% ethanol, 10% acetic acid in water.

Table 12. Buffer system of SDS-PAGE electrophoresis

Separation gel buffer (TGP) 4X	Stacking gel buffer (SGP) 4X	Running buffer	Loading buffer
1.5 M Tris-HCl pH 8.8 0.4% SDS	0.5 M Tris-HCl pH 6.8 0.4% SDS	33 g Tris 144 g glycin 10 g SDS 1 L H_2O 10 × dilution	0.125 M Tris-HCl pH 6.8 4% SDS 20% glycerol 0.02% bromophenol blue 0.2 M dithiothreitol H_2O to 10 mL

Table 13. 12% SDS-PAGE gel preparation method

Stacking Gel	Separating Gel
1.0 mL PAM	4.5 mL PAM
2.5 mL SGP 4X	3.75 mL TGP 4X
6.5 mL H_2O	6.75 mL H_2O
100 µL APS	150 µL APS
10 µL TEMED	15 µL TEMED

6.7 Sample preparation for LC-MS/MS analysis

6.7.1 Gel electrophoresis and in-gel digestion of proteins

15 µL aliquots of desalted fractions were mixed with 5 µL of loading buffer (**Table 13**) and denaturated for 5 min at 100 ºC. The samples were loaded onto 12% SDS-PAGE and subjected to electrophoresis. Gels were stained with Coomassie Brilliant Blue and protein bands of interest were cut. After reduction (10 mM dithiothreitol for 30 min at 56 ºC) and alkylation (55 mM iodoacetamide for 20 min at room tempeture in the dark), proteins were in-gel digested as described[188]. Destained, washed, and dehydrated gel pieces were rehydrated for 60 min in 0.5 µM solution of porcine trypsin (Promega) in 25 mM ammonium bicarbonate buffer at 4 ºC and then digested overnight at 37 ºC. The tryptic peptides were extracted from gel pieces with extraction buffer (75% MeCN/5% HCOOH) and the extracts were dried in a vacuum centrifuge. For LC-MS analysis, samples were reconstructed in 10 µL aqueous 1% HCOOH.

6.7.2 LC-MS/MS analysis

Depending on staining intensity, 5 to 8 µL of the samples were injected into a nanoAcquity nanoUPLC system (Waters, Manchester, UK). After desalting and concentrating on a Symmetry C18 trap-column (20 × 0.18 mm, 5 µm) at a flow rate of 15 µL/min (mobile phase: aqueous 0.1% HCOOH) the peptides were separated on a nanoAcquity analytical C18 column (200 mm × 75 µm ID, C18 BEH 130 material, 1.7 µm) using an increasing MeCN gradient at a flow rate of 0.350 µL/min; buffer A (aqueous 0.1% HCOOH) and buffer B (100% MeCN with 0.1% HCOOH) were linearly mixed in a gradient from 1% to 55% phase B over 60 min, increased to 95% B over 5 min, held at 95% B for 5 min and decreased to 1% B over 1 min.

The eluted peptides were transferred through a metal-coated nanoelectrospray tip (Picotip, 50 × 0.36 mm, 10 μm internal diameter, New Objective, Woburn, USA) into a high resolution time-of-flight mass spectrometer (Synapt HDMS, Waters, Manchester, UK) operated in V-mode with a resolving power of at least 10,000 FWHM.

LC-MS data were collected in positive mode using data-dependent acquisition (DDA); the acquisition cycle consisted of a survey scan covering the range of *m/z* 400–1500 Da followed by MS/MS fragmentation of the four most intense precursor ions collected over a 1 s interval in the range of *m/z* 50–1700 Da. The data acquisition was controlled using MassLynx v4.1 software. A 650 fmol/μL human Glu-fibrinopeptide B in 0.1% HCOOH/MeCN (1:1 v/v) was infused at a flow rate of 0.5 μL/min through the reference NanoLockSpray source every 30 seconds to compensate for mass shifts in MS and MS/MS fragmentation mode.

6.7.3 Data processing and protein identification

Acquired spectra were baseline subtracted, smoothed, deisotoped, and lockmass-corrected using ProteinLynx Global Server Browser (PLGS) v2.5 software (Waters, Manchester, UK). PKL-files of MS/MS spectra were generated and searched against NCBInr database (updated on September 11, 2011) using MASCOT v2.3 software installed on a local server. Mass tolerances for precursor and fragment ions were 15 ppm and 0.03 Da, respectively. Other search parameters were: instrument profile, ESI-Trap; fixed modification, carbamidomethyl (cysteine); variable modification, oxidation (methionine), deamidation (asparagine, glutamine); up to 1 missed cleavage were allowed. The following criteria were used to select for confident protein identifications: at least three peptides with peptide ion scores above 25, or one or two peptides with peptide ions scores of 50 or better.

In parallel, MS/MS spectra were sequenced *de novo* using PLGS software after removing the spectra of common background proteins (human keratins and porcine trypsin). A 0.002 Da mass deviation for *de novo* sequencing was allowed and sequences with a ladder score (percentage of expected y- and b-ions) exceeding 40 were subjected for sequence-similarity searching using the MS BLAST program installed on an in-house server. *De novo* predicted peptides were searched against Insecta sub-database (downloaded from NCBInr on October 21, 2011) as well as against complete NCBInr database (updated on August 10, 2011) under described settings: scoring Table, 100; Filter, none; Expect, 100; matrix, PAM30MS; ad-

vanced options, no-gap-hspmax100-sort_by_totalscore-span1. Statistical significance of hits was evaluated according to MS BLAST scoring scheme[189].

6.8 Measurement of cytosolic Ca²⁺

Aequorin was reconstituted from apoaequorin expressed in the transgenic soybean cells *in vivo* with 5 μM synthetic coelenterazine on a shaker (300 rpm) in the dark for 3–24 h. Ca^{2+}-specific luminescence (470 nm) was measured in a final volume of 100 μL using Luminoskan TL Plus (Labsystems, Thermo, Helsinki, Finland) Version 2.0 as described[190]. Treatments (**Table 14**) with OS were performed by adding 10 μL sample to the cell suspension culture, and active fractions by adding 5 μL. Experiments with α-HL (**41**) were performed with 20 μL solutions containing 0.05 and 0.1 mg/mL in 10 mM Tris/HCl pH 8.0 buffer. Experiments with ALA (**42**) were performed with 20 μL solutions at the concentration of 0.01 and 0.1 mg/mL in aqueous 1% MeOH solution. Mixing time for the addition of any sample was 5–7 s. At the end, the residual aequorin was completely discharged by adding 100 μL of 100 mM $CaCl_2$ in 10% EtOH and 2% Triton X100. The resulting luminescence was used to estimate the total amount of aequorin present in various experiments in order to determine the rate of aequorin consumption for the calculation of the cytosolic Ca^{2+} concentration.

Table 14. Sample information of $[Ca^{2+}]_{cyt}$ measurement in soybean cell

Compound	Sample information	Negative control
OS and fractions	10 μL crude OS	10 μL H_2O
	5 μL aqueous phase after CH_2Cl_2 extraction	
	5 μL active fraction from G25 CC	
	5 μL active fraction from G75 CC	
	5 μL active fraction from A25-1ˢᵗ CC	
	5 μL active fraction from A25-2ⁿᵈ CC	
	5 μL final active fraction	
Recombination	10 μL crude OS	10 μL H_2O
	10 μL aqueous phase after CH_2Cl_2 extraction	
	10 μL 10 mg/mL CH_2Cl_2 extract in H_2O	
	20 μL recombination sample	
α-HL (41)	20 μL 0.05 mg/mL α-HL (**41**) in buffer	20 μL 10 mM Tris/HCl pH 8.0
	20 μL 0.1 mg/mL α-HL (**41**) in buffer	
ALA (42)	20 μL 0.01 mg/mL ALA (**42**) in 1% MeOH	20 μL 1% MeOH
	20 μL 0.1 mg/mL ALA (**42**) in 1% MeOH	

Ca^{2+} measurements in transgenic *A. thaliana* (Col) expressing cytosolic apoaequorin were performed by Dr. Vadassery[97]. Plant seedlings were grown in MS media for 3 weeks[191], one

leaf disc was transferred into a well of a 96 well plate containing 100 μL of reconstitution solution with 10 μM coelenterazine and incubated overnight. Bioluminescence counts in *Arabidopsis* were recorded at 5 sec intervals for 20 min as relative light units (RLU/sec) with a microplate luminometer (Luminoscan Ascent, Version 2.4, Thermo Fischer Scientific, Germany). After a 1-min background reading, the sample solution (**Table 15**) was manually added to the well and readings in RLU for 20 min. Calibrations were performed by estimating the amount of aequorin remaining at the end of experiment by discharging all remaining aequorin in 0.1 M $CaCl_2$, 10% ethanol, and the counts were recorded for 10 min. The luminescence counts obtained were calibrated using the equation[233]: $pCa = 0.332588 (-\log k) + 5.5593$, where k was a rate constant equal to luminescence counts per second divided by total remaining counts.

Table 15. Sample information of $[Ca^{2+}]_{cyt}$ measurement in *A.thaliana* leaves

Compound	Sample information	Negative control
OS	25 μL crude OS (1:1) in buffer	25 μL H_2O
Fraction	25 μL CH_2Cl_2 extract in H_2O	25 μL H_2O
α-HL (41)	25 μL 0.1 mg/mL α-HL (**41**) in buffer	25 μL 10 mM Tris/HCl pH 8.0
ALA (42)	25 μL 0.1 mg/mL ALA (**42**) in 1% MeOH	25 μL 1% MeOH

6.9 Apoplastic voltage measurement

Experimental setup and equipment for the measurements of apoplastic voltage changes with *V. faba* plants was the same as described.[12,81] Voltage measurements and OS treatments were performed either locally on the same leaf at a distance of approximately 2.5 cm or systemically on different leaves at a distance of about 25 cm. The leaf tip was submerged in a buffer (2.5 mM MES/KOH, pH 5.7, 2 mM KCl, 1 mM $CaCl_2$, 1 mM $MgCl_2$, 50 mM mannitol), which was grounded with a reference electrode attached to a slightly wounded leaf area covered with buffer (10 mM Tris/HCl, pH 8.0). When the initial apoplastic voltage had recovered (10–20 min), the buffer was removed and OS (1:1 diluted with buffer) was added for measurement. The hyperpolarization of the apoplast of plant cell resembled the depolarization of the symplast. This work has been operated by Dr. Jens B. Hafke from Justus-Liebig University in Giessen.

6.10 Phytohormone measurements

Phytohormone levels were measured as described previously.[24] Two of the *A. thaliana* leaves of a whole plant were wounded by manual pattern wheel damage to obtain around 26 holes on each leaf (six vertical motions on either side of the leaf). 40 µL sample solution was applied into all wounded sites immediately. Sample information is present in **Table 16**. Crude OS supernatant was diluted 1:1 (v/v) using 10 mM Tris/HCl pH 8.0 buffer, the final active fraction was dissolved in the same buffer after buffer exchange with a PD–10 column, α-HL (**41**) was dissolved in the same buffer with the concentration of 0.05 mg/mL, and ALA (**42**) was dissolved in 1% MeOH of 0.1 mg/mL. The experiment was controlled by applying 40 µL 10 mM Tris/HCl pH 8.0 buffer and 1% MeOH onto the wounded sites under the same degree of damage. Five time points (0 min, 30 min, 45 min, 60 min and 90 min) were chosen to check the phytohormone levels. Every control and treatment time point had at least two parallel reduplicates. After treatment, the leaves were gently covered by aluminum foil and immediately frozen in liquid nitrogen, then stored at –80 °C until use.

Table 16. Sample information of phytohormones measurement in *A.thaliana* leaves

Compound	Sample information	Negative control
OS	20 µL/leaf crude OS (1:1 v/v) in buffer	20 µL/leaf 10 mM Tris/HCl pH 8.0
Fraction	20 µL/leaf final active fraction	20 µL/leaf 10 mM Tris/HCl pH 8.0
α-HL (41)	20 µL/leaf 0.05 mg/mL α-HL (**41**) in buffer	20 µL/leaf 10 mM Tris/HCl pH 8.0
ALA (42)	20 µL/leaf 0.1 mg/mL ALA (**42**) in 1% MeOH	20 µL/leaf 1% MeOH

Plant material was transferred into small tubes with zirconia beads (mixture of 2.0 mm and 0.7 mm size) and immediately frozen in liquid nitrogen. After homogenization using a Peqlab, 1.5 mL MeOH containing 4 µL/mL internal standard solution (9,10-D$_2$-9,10-dihydro-jasmonic acid, D$_4$-salicylic acid, D$_6$-abscisic acid at 10 ng/mL in MeOH; JA-[^{13}C$_6$]Ile at 2 ng/mL in MeOH) was added to extract phytohormones. After centrifugation at 13,000 g for 20 min at 4 °C, the supernatant was transferred into new Eppendorf tubes, and the pellets were extracted by additional 0.5 mL MeOH without internal standard for 30 min at 4 °C. Extracts were combined and dried under vacuum. Finally, the MeOH extract was dissolved in 500 µL MeOH and the clear supernatant was submitted to HPLC-MS analysis. Quantification of JA (**1**), SA (**2**), (−)-JA-L-Ile (**3**), (+)-7-*iso*-JA-L-Ile (**4**) and *cis*-OPDA (**5**) had been performed by Dr. Reichelt[87] (Department of Biochemistry, Max-Planck Institute for Chemical Ecology).

6.11 RNA isolation and quantitative PCR of *CML42 in A. thaliana* leaves

The t ranscriptional level o f *CML42* was m easured a s de scribed pr eviously[24]. O ne of t he *A. thaliana* leaves in the whole plant was wounded manually by pattern wheel to get around 26 holes on each leaf (six vertical motions on either side of the leaf), and 20 μL test solution were immediately applied into all wounded spots. C rude OS supernatant w as di luted (1:1) using 10 mM Tris/HCl at pH 8.0. The active fraction (3 × 1 mL) obtained from ion exchange chromatography was first concentrated and dissolved in Tris buffer (0.5 mL, 10 mM Tris/HCl at pH 8.0). A sample of α-HL (**41**) was dissolved in the same buffer at 0.05 mg/mL and ALA (**42**) was dissolved in 1% MeOH at 0.1 mg/mL. 20 μL 10 mM T ris/HCl pH 8.0 bu ffer and aqueous 1% MeOH solution were applied to the wounded sites as negative control respective-ly. Sample information is presented in **Table 17**. All experiments had at least three replicates. The treated-leaf s amples w ere h arvested a nd i mmediately placed i nto l iquid ni trogen, t hen stored at −80 °C for further use.

Table 17. Sample information of *CML42* transcriptional level measurement

Compound	Sample information	Negative control
OS	20 μL/leaf crude OS (1:1 v/v) in buffer	20 μL/leaf 10 mM Tris/HCl pH 8.0
Fraction	20 μL/leaf final active fraction	20 μL/leaf 10 mM Tris/HCl pH 8.0
α-HL (41)	20 μL/leaf 0.05 mg/mL α-HL (**41**) in buffer	20 μL/leaf 10 mM Tris/HCl pH 8.0
ALA (42)	20 μL/leaf 0.1 mg/mL ALA (**42**) in 1% MeOH	20 μL/leaf 1% MeOH

Frozen leaf material was ground to a fine powder in liquid N_2, total RNA was extracted by 1.0 mL T rizol reagent (Invitrogen, Darmstadt, Germany) according to the manufacturer's guide. Contaminating DNA wa s r emoved b y TURBO DNA-free K it (Ambion, A ustin, U SA), a nd RNA quantity w as e valuated photometrically. 1 μg to tal R NA w as converted in to s ingle-stranded cDNA us ing a mix of oligo-dT$_{18}$ primers using the Omniscript cDNA synthesis kit (Qiagen, Germany). The Real Time PCR was done in an optical 96-well plate on a MX3000P Real-Time P CR D etection S ystem (Stratagene) using th e Brilliant Q PCR S YBR g reen M ix (Agilent) to monitor double-stranded DNA synthesis with ROX as a reference dye included in the PCR master mix[24]. The *CML42* mRNA levels for cDNA probe were normalized using the house-keeping gene *RPS18B* as the reference gene. The normalized fold transcript expression values of *CML42* were c alculated w ith the ΔΔCP equation according to Michael W. Pfaffl's Method[192].

6.12 VOC emission from lima bean leaves

6.12.1 VOC emission assay with charcoal trap

A single plantlet of lima bean (*P. lunatus*) with two developed primary leaves, potted in soil, was placed in the glass desiccators (750 mL). Pot and soil were carefully wrapped with aluminium foil and three larvae (*S. littoralis*) were placed on the leaves. The whole experimental setup was kept at 22 – 24 ^{o}C with a light/dark rhythm of 8 h light, 9 h dark, and 7 h light and started at 1:00 pm. The headspace volatiles were collected for 24 h using charcoal (1.5 mg) traps.

Plantlets of lima bean (*P. lunatus*) with two fully developed primary leaves were cut with razor blades and immediately transferred into brown vials (6 mL) containing 2 mL tap water with the test substance. Sample information is presented in **Table 18**. The whole plantlets were enclosed in glass desiccators (750 mL). Headspace volatiles were collected for 24 h on charcoal (1.5 mg) traps. Setups were kept at 22 – 24 ^{o}C with a light/dark rhythm of 8 h light, 9 h dark, and 7 h light[11] and started at 1:00 pm.

Table 18. Sample information of VOC measurement with charcoal trap in lima bean

Compound	Sample information	Negative control
OS	20 μL crude OS in 2 mL H_2O	2 mL H_2O
Fraction	20 μL final active fraction in 2 mL H_2O	2 mL H_2O
JA (1)	1 mM JA (**1**) solution (1% MeOH in H_2O)	2 mL H_2O
α-HL (41)	20 μL 1.0 mg/mL α-HL (**41**) in 2 mL buffer	2 mL buffer (10 mM Tris/HCl pH 8.0)
ALA (42)	20 μL 1.0 mg/mL ALA (**42**) in 2 mL H_2O	2 mL H_2O

Collected VOC were eluted with CH_2Cl_2 (2 × 20 μL, containing 200 ng/mL 1-bromodecane as internal standard), and directly analyzed by GC-MS. Samples were analyzed on a Finnigan GC Trace MS 2000 series. Mass spectra were measured in electron impact (EI) positive mode at 70 eV. Separation was performed on a Zebron ZB-5ms capillary column (30 m × 0.25 mm i.d. × 0.25 μm; Phenomenex). Helium at a flow rate of 1.5 mL/min served as carrier gas with 1 μL injection under splitless mode. Compounds were eluted under programmed conditions starting at 45 ^{o}C (2 min isotherm) followed by heating at 10 ^{o}C/min to 200 ^{o}C, then at 30 ^{o}C/min to 280 ^{o}C and held 1 min.

6.12.2 VOC emission assay with SpitWorm and zNose

SpitWorm is the combination of MecWorm with a simultaneous delivery of the OS onto the damaged sites. The MecWorm part was setup following the previous report[36]. Intact leaves from whole plantlets were enclosed in a Plexiglas cabinet (approximately 1000 mL) and punctured therein for the time indicated. The leaf was punctured over three days by Mec-Worm, each day started from 9:00 am until 3:00 pm during the photophase according to a 15:9 LD cycle with 3 h after the onset of the light phase. The puncturing process was performed for 6 h with round area around 122 mm^2 for each hole (the interval time of each puncturing event was 5 s). The 220 μL sample solution was delivered per day through thin PTFE tube (50 cm × 0.25 mm I.D.) with the speed of 0.6 μL/min by Harvard PHD 2000 Infusion pump with the simultaneous damage by MecWorm. The sample information is presented in **Table 19**.

Table 19. Sample information of VOC measurement with SpitWorm in lima bean

Compound	*Sample information*	*Negative control*
Control	MecWorm	
OS	SpitWorm	SpitWorm
	OS (10 × dilution with buffer)	10 mM Tris/HCl pH 8.0 buffer
α-HL (41)	SpitWorm	SpitWorm
	α-HL (**41**) (0.1 mg/mL in buffer)	10 mM Tris/HCl pH 8.0 buffer
ALA (42)	SpitWorm	SpitWorm
	ALA (**42**) (0.1 mg/mL in 1% MeOH)	1% MeOH

VOC emission was monitored by zNose[107,108]. The zNose (model 4100; Electronic Sensor Technology) was connected to the cabinet via a stainless steel needle attached to the Luer-inlet on the instrument. Prepurified air (ZeroAir generator [Parker Hannifin Corp.] and an additional charcoal filter) was passed through the plastic cabinet (around 1000 mL) at 40 mL/min. Every 10 min, zNose trapped an aliquot of the headspace volatiles for 60 s on an internal Tenax®-trap (with flow rate at 30 mL/min), followed by separation on the main DB-5 column (1 m × 0.25 mm × 0.25 μm film, Electronic Sensor Technology) under programmed conditions: from 45 ^{o}C to 180 ^{o}C at 10 ^{o}C/s. Helium acts as carrier gas with flow rate at 3 mL/min. The detector (surface acoustic wave detector) of zNose was operated at 40 ^{o}C. Compounds were identified by comparison of the retention times with those of authentic compounds. The amounts of VOC (ocimene (**8**), DMNT (**10**), MeSA (**12**) and TMTT (**13**)) were quantified after calibration with authentic standards and were presented as ng. Calibration for individual compounds (ocimene (**8**), DMNT (**10**), MeSA (**12**) and TMTT (**13**)) was

achieved with a heated desorber tube (glass tube, temperature controlled: $50 - 300$ $^{\circ}$C; 3100 Vapor Calibrator, Electronic sensor Technology, Newbury Park, CA, USA) attached to the Luer-inlet of the zNose. Diluted samples (0.6 µL methanol solution of $1.0 - 40.0$ µg/mL of ocimene (**8**), $5.0 - 40.0$ µg/mL of DMNT (**10**), $5.0 - 40.0$ µg/mL of MeSA (**12**), $1.0 - 10.0$ µg/mL of TMTT (**13**)) were repeatedly injected by a syringe into the heated tube (190 $^{\circ}$C) while the instrument was sampling (10 s, to trap the total amount of the injected solution). Compounds were eluted under programmed conditions: from 45 $^{\circ}$C to 180 $^{\circ}$C at 10 $^{\circ}$C/s. Data from several runs were pooled and treated statistically (average and RSD). The calibration curves for individual compounds were prepared as the function of amount (ng) and intensity (count per second, cts) (**Figure 68**).
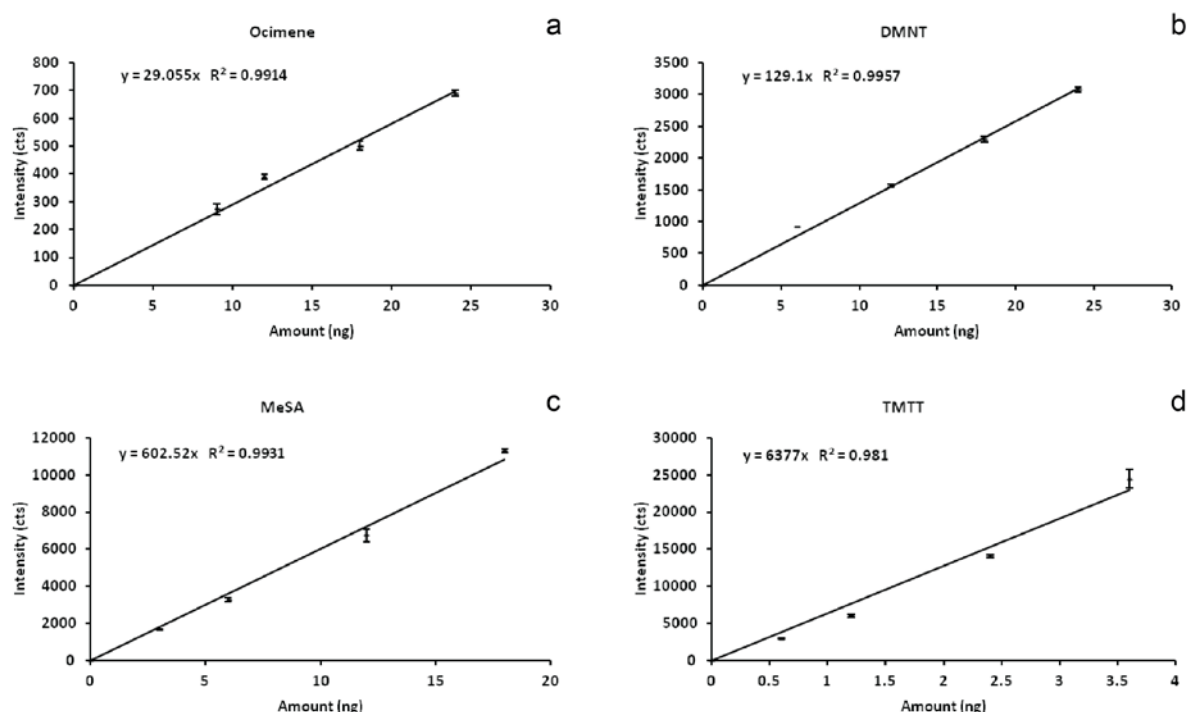
Figure 68. Calibration curves for: (a), ocimene (**8**); (b), DMNT (**10**); (c), MeSA (**12**) and (d), TMTT (**13**). Data represent the mean ± SE, n = 4. Detector response at a constant SAW (surface acoustic wave) temperature (40 $^{\circ}$C) was given in cts (peak area in counts).

6.13 *C. cellulolyticum* strain and culture conditions

Clostridium cellulolyticum DSM 5812 (= ATCC 35319) used in this study was originally isolated by Petitdemange et al. (1984) from decayed grass and was obtained from DSMZ GmbH (Braunschweig, Germany) as a stock culture. The wild type culture was performed by following the literature[107]. It was grown anaerobically[193,194] in serum glass bottles sealed with butyl

rubber stoppers and an aluminium crimps at 37 ^{o}C, without shaking, on medium CM3[195] with cellobiose (6 g/L, Sigma-Aldrich, Schnelldorf) that was modified by replacing KH_2PO_4 and $K_2HPO_4 \cdot 3H_2O$ by 3-(*N*-morpholino)propanesulfonic acid (10 g/L). The pH value of wild type culture is around 7.2. In order to mimic the gut environment, wild type *Clostridium* (50 mL) was incubated together with insect OS (200 μL or 400 μL) under the same culture conditions. This experiment was kindly performed by Dr. Sacha Pidot in Leibniz Institute for Natural Product Research and Infection Biology, Hans Knöll Institute (Jena, Germany).

After harvest, the cells were discarded by centrifugation (5,000 g at 4 ^{o}C for 30 min) and the supernatant was directly submitted to the BLM assay following the described method. The effect of heating was assayed using 100 μL supernatant at 100 ^{o}C for 15 min. 25 mL supernatant was submitted to Viva spin 30KD separation according to the molecular size by centrifugation (16,000 g at 4 ^{o}C for 30 min). The BLM active non-filtrated part (2.5 mL) was subjected to electrophoresis analysis and the fractionation using ÄKTA system coupled with Superdex^{TM} 75 HR 10/30 column eluted by BLM buffer (200 mM KCl, 10 mM Tris/HCl, pH 9.2) at a flow rate of 0.5 mL/min using UV detection (λ = 280 nm). The fractions (0.5 mL) were concentrated 10 times by Viva spin 3KD, and submitted to BLM assay and electrophoresis analysis.

6.14 Identification of saponin analogues

During the purification of channel-forming compounds, a series of glucosides were detected using HPLC-MS analysis in fraction 7 (Fr. 7), which was eluted with H_2O from the Sephadex G25 column chromatography (**Scheme 2**). The HPLC-MS analysis was performed on an Aglient 1100 HPLC coupled with Finnigan LCQ mass spectrometer, and the compounds were separated using a Gemini (2 × 250 mm 5μm C$_{18}$ 110 Å, Phenomenex) column under programmed condition (10% MeCN with 0.5% CH_3COOH over 2 min, 10% to 100% MeCN with 0.5% CH_3COOH over 30 min, 100% MeCN with 0.5% CH_3COOH over 18 min, 0.15 mL/min).

The 1-butanol extract (20 mg) of Fr. 7 was further fractionated by semipreparative reverse-phase HPLC using a Gemini (10 × 250 mm 5 μm C$_{18}$ 110 Å Phemonenex) column. Individual fractions were collected over 1.5 min to afford soyasaponin V (**46**; 2.17 mg, t_R 22.53 min; 40% MeCN in H_2O with 0.5% CH_3COOH over 56 min, 4 mL/min), soyasaponin I (**47**; 2.30 mg, t_R 26.31 min; 40% MeCN in H_2O with 0.5% CH_3COOH over 56 min, 4 mL/min), soya-

saponin II (**48**; 0.99 mg, t_R 33.36 min; 40% MeCN in H_2O with 0.5% CH_3COOH over 56 min, 4 mL/min), sandosaponin A (**54**; 1.69 mg, t_R 42.32 min; 40% MeCN in H_2O with 0.5% CH_3COOH over 56 min, 4 mL/min), dehydrosoyasaponin I (**55**; 1.16 mg, t_R 49.81 min; 40% MeCN in H_2O with 0.5% CH_3COOH over 56 min, 4 mL/min). The purity of the compounds was evaluated using a Grom-Sil ODS-3 CP (2 × 125 mm, 3 µm) C_{18} column under programmed condition (10% MeCN with 0.5% CH_3COOH over 2 min, 10% to 100% MeCN with 0.5% CH_3COOH over 18 min, 100% MeCN with 0.5% CH_3COOH over 10 min, 0.2 mL/min).

ESI parameter: the sheath gas flow rate was 50 arb (arbitrary units), auxiliary gas flow rate was 15 arb, ion spray voltage was 7.00 kV, spray current was 29, capillary tempeture was 200 ^{o}C, capillary voltage was 6.00 V, tube lens offset was 40 V.

100 mg fresh artificial diet was extracted overnight using 2.0 mL H_2O. After centrifugation at 16,000 g for 30 min at 4 ^{o}C, the supernatant was transferred to HPLC-MS analysis under the programmed condition (Phenomenex Gemini 2 × 250 mm 5µm C_{18} 110 Å column, 10% MeCN with 0.5% CH_3COOH over 2 min, 10% to 100% MeCN with 0.5% CH_3COOH over 30 min, 100% MeCN with 0.5% CH_3COOH over 18 min; 0.15 mL/min).

88.3 mg fresh feces from insect larvae feeding on the artificial diet were collected, and extracted overnight by 2.0 mL MeOH. After centrifugation and removing of solvent, 4.72 mg extract was obtained and further dissolved in MeOH, and directly injected into LC-MS for analysis under the programmed condition (Phenomenex Gemini 2 × 250 mm 5µm C_{18} 110 Å column, 10% MeCN with 0.5% CH_3COOH over 2 min, 10% to 100% MeCN with 0.5% CH_3COOH over 30 min, 100% MeCN with 0.5% CH_3COOH over 18 min; 0.15 mL/min).

6.15 SPME analysis of the volatile compounds from OS

VOC from OS of *S. littoralis* larva were collected by solid phase microextraction (SPME) from 100 µL fresh OS placed into 1.5 mL-GC vial for 30 min at room temperature. SPME was equipped with polydimethylsiloxan (PDMS) 100 µm thickness (red/plain) as fiber together with SPME holder 57330-U. The fiber was conditioned at 250 ^{o}C for 30 min before use. VOC from *S. littoralis* larvae were collected from a single live larva (4th instar) located into glass vial (4 mL) for 30 min at room temperature by SPME. One piece of cotton was placed between the larva and the SPME fiber, in order to avoid the possible destruction of fiber by

larva. VOC from artificial diet were collected by the same SPME from 50 mg diet placed into 1.5 mL-GC vial at room temperature for 30 min.

Collected VOC were directly analyzed by GC-MS using a Finnigan GC Trace MS 2000 series. Separation was performed on a Zebron ZB-5ms (15 m × 0.25 mm i.d. × 0.25μm , Phenomenex) capillary column. Individual compounds were eluted under programmed conditions starting at 45 $^{\circ}$C (with 2-min isotherm) followed by heating at 10 $^{\circ}$C/min to 200 $^{\circ}$C, and 30 $^{\circ}$C/min to 280 $^{\circ}$C, and held for 1 min. Helium at a flow rate of 1.5 mL/min served as carrier gas under splitless mode. Mass spectra were measured in electron impact (EI) positive mode at 70 eV. Acquired data were analyzed using the Xcalibur software (v2.0.7) (Thermo Finnigan, USA). Compounds were identified by database searching in the library of the National Institute of Standards and Technology (NIST 2008). Anthentic alkane mixtures (C_8-C_{20}) were analyzed under the same GC-MS condition for comparison the individual mass spectrum and retention times.

6.16 White secretion from *N. lowii*

Sample preparation: 16.8 mg crude white secretion from *N. lowii* were suspended into 1.68 mL H_2O to reach 10 mg/mL solution. 1.0 mL sample solution was mixed well with 1.0 mL MeOH and extracted with 2.0 mL hexane and 2.0 mL CH_2Cl_2 three times respectively. After extraction, the organic solvent was removed by argon, and 0.81 mg hexane extract and 0.40 mg CH_2Cl_2 extract were obtained. These two extracts were combined due to their similar TLC behavior, and dissolved in $CHCl_3$ at a concentration of 10 mg/mL. The remaining aqueous phase was completely dried by argon, and further dissolved in H_2O at a concentration of 10 mg/mL. The sample preparation procedure is presented in **Scheme 3**.

The crude extract, aqueous phase and organic extracts were dried completely and dissolved in deuterated methanol (for crude extract and aqueous phase) or deuterated chloroform (for organic extract) and submitted to ^{1}H NMR analysis.

10 μL organic extract (10 mg/mL), 10 μL aqueous phase (10 mg/mL) and 10 μL crude secretion (10 mg/mL) were transferred into GC-vials with 100 μL insert, and completely dried by argon. The silylation was accomplished by adding 20 μL MSTFA into each vial, and heating at 50 $^{\circ}$C for 2 h. The silylation solution was directly analyzed by GC-MS.

```
                    10 mg/mL mixture
                    (16.8 mg in H₂O)
                          │
                          │ 1:1 MeOH
                          │
              ┌───────────┴───────────┐
              ▼                       ▼
      aqueous (7.26 mg)    hexane extract (0.81 mg)
              │                  DCM extract (0.40 mg)
              ▼                       │
      10 mg/mL in H₂O                 │
              │                       ▼
              │ MSTFA          10 mg/mL in CHCl₃
              ▼                       │
          GC-MS                       │ MSTFA
              │                       ▼
              ▼                     GC-MS
            64-66                     │
                                      ▼
                                   67-114
```
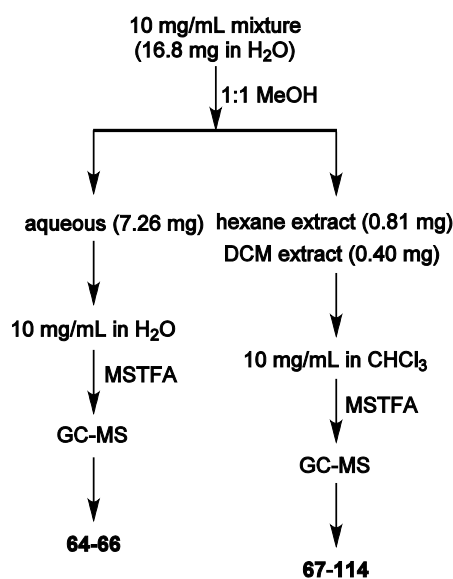
Scheme 3. Analysis of white secretion

Silylated organic extracts were analyzed on Finnigan GC Trace MS 2000 series. Mass spectra were measured in electron impact (EI) positive mode at 70 eV. Separation was performed on a Zebron ZB-5ms capillary column (15 m × 0.25 mm i.d., 0.25 μm; Phenomenex). Helium at a flow rate of 1.5 mL/min served as carrier gas with 1 μL injection under split mode with 15 mL/min split. Compounds were eluted under programmed conditions starting at 60 $^{\circ}$C followed by heating at 6 $^{\circ}$C/min to 300 $^{\circ}$C, and held for 20 min. Silylated aqueous phases and crude secretion were analyzed on the same instrument under modified conditions, which started at 60 $^{\circ}$C followed by heating at 10 $^{\circ}$C/min to 300 $^{\circ}$C and held for 3 min. Acquired data were analyzed using the Xcalibur (Thermo Finnigan, USA) software (v2.0.7).

Sugar analysis: D-(+)-glucose (**64**), D-(+)-fructose (**65**), and D-(+)-sucrose (**66**) (Sigma) were dissolved in H_2O as 1.0 mg/mL stock solution. 10 μL individual sugar solutions were transferred into GC-vial with insert (100 μL) and completely dried by argon, followed by the silylation with 20 μL MSTFA at 50 $^{\circ}$C for 2 h. The silylated products were analyzed directly by GC-MS using the same programmed condition as silylated aqueous phase.

Fatty acid identification: Lauric acid (**67**), myristic acid (**68**), palmitic acid (**69**), arachidic acid (**71**), lignoceric acid (**73**), palmitoleic acid (**74**), oleic acid (**79**), *cis*-11-eicosenoic acid (**80**), nervonic acid (**81**), linoleic acid (**82**) were prepared at 1.0 mg/mL in chloroform as stock solution, respectively. 10 μL individual solutions were transferred into GC-Vial with 100 μL insert and dried completely, following the silylation using 20 μL MSTFA at 50 $^{\circ}$C for 2 h. The silylated products were analyzed directly by GC-MS under the same programmed condition as the silylated organic extract. The fatty acid mixture in MSTFA/n-hexane (containing

TMS capric acid, TMS myristic acid (**68**), TMS stearic acid (**70**), and TMS behenic acid (**72**)) was directly injected into GC-MS under the same programmed condition as silylated organic extract.

Analysis of double bond positions by GC-CI-MS/MS: The methylated sample was prepared according to the procedure reported in literature[196]. 20 µL 10 mg/mL organic extract was treated with an etheral solution of CH_2N_2 (excess). Yellow color has to stay for at least 5 min, followed by a nitrogen stream to remove excess CH_2N_2. The methylation products were then directly submitted into GC-CI-MS analysis.

GC-CI-MS analyses used for determination of double bond position were performed using a Varian 240MS ion-trap mass detector coupled to a Varian 450GC in the internal ionization configuration[197]. A VF-5 ms column (30 m × 0.25 mm ID; 0.25 µm df; Varian Inc. Palo Alto, CA, USA) was used for separation. The split/splitless GC injector was operated at 250 ^{o}C in split mode for electron ionization (EI) or splitless mode for chemical ionization (CI). The GC oven temperature was programmed as follows: 150 ^{o}C for 1 min, 5 ^{o}C/min to 300 ^{o}C, hold 5 min. Helium was used as a carrier gas at a constant flow rate of 1 mL/min. EI spectra were recorded with a mass range of m/z 45–500 at maximum scan rate. CI spectra were recorded using acetonitrile (ACN) as a reagent gas with a mass range of m/z 60–500. CI-MS/MS experiments of $[M + 54]^+$ adducts were conducted with the resonant waveform type for precursor ion excitation, with an isolation window of $m/z = 5$, and 20 ms excitation time. The automatic "q" calculator was used for the determination of precursor ion excitation energy and product ion mass range. All CI measurements were conducted with an ion-trap temperature of 90 ^{o}C, a manifold temperature of 40 ^{o}C, and an ion-source temperature of 160 ^{o}C. Data were analyzed using the MS Workstation software (v6.9.3, Varian Inc., Palo Alto, CA, USA) by Dr. Martin Kaltenpoth (Max Planck Research Group Insect Symbiosis).

6.17 Spectral data summary

Soyasaponin V (**46**), 3 -O-[β-glucopyranosyl(1→2)-β-galactopyranosyl(1→2)-β-glucuronopyranosyl] soyasapogenol B, white powder; t_R 28.22 min; ESI-MS(+): 959 $[M + H]^+$ (100), 1917 $[2M + H]^+$ (10), 797 $[M - 162 + H]^+$ (5), 635 $[M - 162 - 162 + H]^+$ (10), 617 $[M - 162 - 162 - 18 + H]^+$ (6), 441 $[M - 162 - 162 - 18 - 176 + H]^+$ (10), 423 (9), 405 (1); ^{1}H NMR (CD$_3$OD-d_4, 500 MHz) 5.25 (1H, br s, H-12), 4.83 (1H, d, $J = 7.5$ Hz, H-1″), 4.58 (1H, d, $J = 7.5$ Hz, H-1‴), 4.50 (1H, d, $J = 7.5$ Hz, H-1′), 4.14 (1H, d, $J = 11.3$ Hz, H-24α), 3.39

(1H, d, J = 9.5 Hz, H-22), 3.24 (1H, d, J = 11.3 Hz, H-24β), 2.05 (1H, d, J = 12.7 Hz, H-18), 1.24 (3H, s, H-23), 1.12 (3H, s, H-27), 1.01 (3H, s, H-29), 0.98 (3H, s, H-26), 0.92 (3H, s, H-30), 0.91 (3H, s, H-25), 0.83 (3H, s, H-28), 1.64 (1H, m, H-1α), 1.04 (1H, m, H-1β), 2.13 (1H, m, H-2α), 1.82 (1H, m, H-2β), 3.44 (1H, m, H-3), 0.95 (1H, m, H-5), 1.64 (1H, m, H-6α), 1.39 (1H, m, H-6β), 1.55 (1H, m, H-7α), 1.41 (1H, m, H-7β), 1.58 (1H, m, H-9), 1.88 (2H, m, H-11α/11β), 1.76 (2H, m, H-15α/16α), 1.04 (1H, m, H-15β), 1.32 (1H, m, H-16β), 1.75 (1H, m, H-19α), 0.96 (1H, m, H-19β), 1.45 (1H, m, H-21α), 1.33 (1H, m, H-21β), 3.54 (1H, H-2′), 3.79 (1H, H-3′), 3.44 (1H, H-4′), 3.79 (1H, H-5′), 3.75 (1H, H-2″), 3.67 (1H, H-3″), 3.84 (1H, H-4″), 3.79 (2H, H-5″/6″α), 3.72 (1H, H-6″β), 3.28 (1H, H-2‴), 3.39 (1H, H-3‴), 3.36 (2H, H-4‴/5‴), 3.94 (1H, d, J = 12.0 Hz, H-6‴α), 3.75 (1H, H-6‴β). HRESIMS m/z 959.52109 $[M + H]^+$ (calcd. for $C_{48}H_{79}O_{19}$, 959.52101).

Soyasaponin I (**47**), 3-O-[α-rhamnopyranosyl(1→2)-β-galactopyranosyl(1→2)-β-glucuronopyranosyl] soyasapogenol B, white powder; t_R 28.84 min; ESI-MS(+): 943 $[M + H]^+$ (100), 1885 $[2M + H]^+$ (7), 797 $[M - 146 + H]^+$ (17), 635 $[M - 146 - 162 + H]^+$ (10), 617 $[M - 146 - 162 - 18 + H]^+$ (4), 441 $[M - 146 - 162 - 18 - 176 + H]^+$ (13), 423 (9), 405 (1); ^1H NMR (CD$_3$OD-d_4, 500 MHz) 5.24 (1H, br s, H-12), 4.87 (1H, d, J = 7.5 Hz, H-1″), 5.13 (br s, H-1‴), 4.45 (1H, d, J = 9.0 Hz, H-1′), 4.14 (1H, d, J = 11.0 Hz, H-24α), 3.39 (1H, d, J = 8.8 Hz, H-22), 3.19 (1H, d, J = 11.0 Hz, H-24β), 2.05 (1H, d, J = 13.5 Hz, H-18), 1.28 (3H, d, J = 6.0 Hz, H-6‴), 1.26 (3H, s, H-23), 1.12 (3H, s, H-27), 1.01 (3H, s, H-29), 0.97 (3H, s, H-26), 0.92 (3H, s, H-30), 0.90 (3H, s, H-25), 0.83 (3H, s, H-28), 1.65 (1H, m, H-1α), 1.05 (1H, m, H-1β), 2.11 (1H, m, H-2α), 1.82 (1H, m, H-2β), 3.40 (1H, m, H-3), 0.94 (1H, m, H-5), 1.62 (1H, m, H-6α), 1.35 (1H, m, H-6β), 1.56 (1H, m, H-7α), 1.40 (1H, m, H-7β), 1.58 (1H, m, H-9), 1.87 (2H, m, H-11α/11β), 1.77 (1H, m, H-15α), 1.04 (1H, m, H-15β), 1.76 (1H, m, H-16α), 1.31 (1H, m, H-16β), 1.75 (1H, m, H-19α), 0.96 (1H, m, H-19β), 1.45 (1H, m, H-21α), 1.33 (1H, m, H-21β), 3.76 (1H, H-2′), 3.59 (1H, H-3′), 3.44 (1H, H-4′), 3.79 (1H, H-5′), 3.64 (1H, H-2″), 3.54 (1H, H-3″), 3.71 (1H, H-4″), 3.79 (2H, H-5″/6″α), 3.73 (1H, H-6″β), 3.92 (1H, H-2‴), 3.72 (1H, H-3‴), 3.39 (1H, H-4‴), 4.10 (1H, H-5‴). HRESIMS m/z 943.52661 $[M + H]^+$ (calcd. for $C_{48}H_{79}O_{18}$, 943.52609).

Soyasaponin III (**48**), 3-O-[galactopyranosyl(1→2)-glucuronopyranosyl] soyasapogenol B, white powder; t_R 30.84 min; ESI-MS(+): 797 $[M + H]^+$ (100), 635 $[M - 162 + H]^+$ (8), 617 $[M - 162 - 18 + H]^+$ (4), 441 $[M - 162 - 18 - 176 + H]^+$ (20), 423 (18), 405 (1). HRESIMS m/z 797.46744 $[M + H]^+$ (calcd. for $C_{42}H_{69}O_{14}$, 797.46818).

Compound (**49**), 3 -*O*-[galactopyranosyl(1→2)-glucuronopyranosyl]-22-*O*-arabinopyranosyl soyasapogenol B, white powder; t_R 23.27 min; ESI-MS(+): 929 [M + H]$^+$ (100), 951 [M +Na]$^+$ (8), 975 [M +K]$^+$ (8), 797 [M − 132 + H]$^+$ (2), 767 [M − 162 + H]$^+$ (8), 635 [M − 162 − 132 + H]$^+$ (2), 617 [M − 162 − 132 − 18 + H]$^+$ (5), 441 [M − 162 − 132 − 18 − 176 + H]$^+$ (5), 423 (28), 405 (2).

Phaseoside I (**50**), 3 -*O*-[glucopyranosyl(1→2)-galactopyranosyl(1→2)-glucuronopyranosyl]-22-*O*-[glucopyranosyl(1→2)-arabinopyranosyl] soyasapogenol B, white powder; t_R 20.23 min; ESI-MS(+): 1253 [M + H]$^+$ (100), 1091 [M − 162 + H]$^+$ (5), 959 [M − 162 − 132 + H]$^+$ (2), 929 [M − 162 − 162 + H]$^+$ (4), 797 [M − 162 − 162 − 132 + H]$^+$ (0.5), 767 [M − 162 − 162 − 162 + H]$^+$ (1), 635 [M − 162 − 162 − 162 − 132 + H]$^+$ (2), 617 [M − 162 − 162 − 162 − 132 − 18 + H]$^+$ (3), 441 [M − 162 − 162 − 162 − 132 − 18 − 176 + H]$^+$ (2), 423 (7), 405 (1).

Compound (**51**), 3 -*O*-[glucopyranosyl(1→2)-galactopyranosyl(1→2)-glucuronopyranosyl]-22-*O*-arabinopyranosyl soyasapogenol B, white powder; t_R 22.76 min; ESI-MS(+): 1091 [M + H]$^+$ (100), 959 [M − 132 + H]$^+$ (1), 929 [M − 162 + H]$^+$ (3), 797 [M − 162 − 132 + H]$^+$ (1), 767 [M − 162 − 162 + H]$^+$ (5), 635 [M − 162 − 162 − 132 + H]$^+$ (1), 617 [M − 162 − 162 − 132 − 18 + H]$^+$ (1), 441 [M − 162 − 162 − 132 − 18 − 176 + H]$^+$ (2), 423 (8), 405 (1).

Sophoraflavoside I (**52**), 3 -*O*-[rhamnopyranosyl(1→2)-galactopyranosyl(1→2)-glucuronopyranosyl]-22-*O*-[glucopyranosyl(1→2)-arabinopyranosyl] soyasapogenol B, white powder; t_R 20.50 min; ESI-MS(+): 1237 [M + H]$^+$ (100), 1091 [M − 146 + H]$^+$ (3), 1075 [M − 162 + H]$^+$ (2), 943 [M − 162 − 132 + H]$^+$ (6), 797 [M − 162 − 132 − 146 + H]$^+$ (1), 635 [M − 162 − 132 − 146 − 162 + H]$^+$ (1), 617 [M − 162 − 132 − 146 − 162 − 18 + H]$^+$ (1), 441 [M − 162 − 132 − 146 − 162 − 18 − 176 + H]$^+$ (1), 423 (1), 405 (1).

Compound (**53**), 3 -*O*-[glucopyranosyl(1→2)-galactopyranosyl(1→2)-glucuronopyranosyl]-22-*O*-[glucopyranosyl (1→2)-glucopyranosyl] soyasapogenol B, white powder; t_R 19.58 min; ESI-MS(+): 1283 [M + H]$^+$ (100), 1121 [M − 162 + H]$^+$ (5), 959 [M − 162 − 162 + H]$^+$ (8), 797 [M − 162 − 162 − 162 + H]$^+$ (5), 635 [M − 162 − 162 − 162 − 162 + H]$^+$ (5), 617 [M − 162 − 162 − 162 − 162 − 18 + H]$^+$ (3), 441 [M − 162 − 162 − 162 − 162 − 18 − 176 + H]$^+$ (2), 423 (5), 405 (1).

Sandosaponin A (**54**), 3 -*O*-[glucopyranosyl(1→2)-galactopyranosyl(1→2)-glucuronopyranosyl] soyasapogenol E, white powder; t_R 31.04 min; ESI-MS(+): 957 [M + H]$^+$ (100), 795 [M − 162 + H]$^+$ (4), 633 [M − 162 − 162 + H]$^+$ (14), 615 [M − 162 − 162 − 18 + H]$^+$ (8), 439 [M − 162 − 162 − 18 − 176 + H]$^+$ (20), 421 (6), 403 (1).

Dehydrosoyasaponin I (**55**), 3 -*O*-[rhamnopyranosyl (→2) -galactopyranosyl(1→2)-glucuronopyranosyl] soyasapogenol E, white powder; t_R 32.21 min; ESI-MS(+): 941 [M + H]$^+$ (100), 963 [M + Na]$^+$ (13), 795 [M − 146 + H]$^+$ (8), 633 [M − 146 − 162 + H]$^+$ (15), 615 [M − 146 − 162 − 18 + H]$^+$ (8), 439 [M − 146 − 162 − 18 − 176 + H]$^+$ (26), 421 (8), 403 (1).

Soyasaponin A 1 (**56**), 3 -*O*-[glucopyranosyl(1→2)-galactopyranosyl(1→2)-glucuronopyranosyl]-22-*O*-[glucopyranosyl(1→3)-arabinopyranosyl] soyasapogenol A, white powder; t_R 19.13 min; ESI-MS(+): 1269 [M + H]$^+$ (100), 1107 [M − 162 + H]$^+$ (10), 975 [M − 162 − 132 + H]$^+$ (6), 945 [M − 162 − 162 + H]$^+$ (5), 799 [M − 162 − 132 − 176 + H]$^+$ (1), 783 [M − 162 − 162 − 162 + H]$^+$ (1), 651 [M − 162 − 162 − 162 − 132 + H]$^+$ (2), 633 [M − 162 − 162 − 162 − 132 − 18 + H]$^+$ (4), 457 [M − 162 − 162 − 162 − 132 − 18 − 176 + H]$^+$ (4), 439 (7), 421 (3).

Desglucosylsoyasaponin A 1 (**57**), 3 -*O*-[glucopyranosyl(1→2)-galactopyranosyl(1→2)-glucuronopyranosyl]-22-*O*-[arabinopyranosyl] soyasapogenol A, white powder; t_R 21.91 min; ESI-MS(+): 1107 [M + H]$^+$ (100), 975 [M − 132 + H]$^+$ (6), 945 [M − 162 + H]$^+$ (1), 783 [M − 162 − 162 + H]$^+$ (9), 765 [M − 162 − 162 − 18 + H]$^+$ (4), 633 [M − 162 − 162 − 18 − 132 + H]$^+$ (3), 615 [M − 162 − 162 − 18 − 132 − 18 + H]$^+$ (3), 457 [M − 162 − 162 − 18 − 132 − 18 − 176 + H]$^+$ (1), 439 (9), 421 (3).

Pentadecane (**61**), t_R 11.96 min; EI-MS(+): 43 (75), 57 (100), 71 (65), 85 (40), 99 (11), 113 (5), 127 (3), 141 (3), 155 (2), 169 (2), 183 (2), 212 [M$^{+\cdot}$] (3).

Tetradecane (**62**), t_R 10.75 min; EI-MS(+): 43 (84), 57 (100), 71 (58), 85 (34), 99 (8), 113 (2), 127 (2), 141 (2), 155 (2), 198 [M$^{+\cdot}$] (2).

Heptadecane (**63**), t_R 14.24 min; EI-MS(+): 43 (82), 57 (100), 71 (65), 85 (40), 99 (14), 113 (5), 127 (3), 141 (2), 155 (2), 169 (2).

D-(+)-glucose (**64**), ^{1}H NMR (CD$_3$OD-d_4, 400 MHz) 3.12 (1H, dd, J = 8.84, 7.86 Hz, β-H2), 3.26–3.37 (α-H2, α-H5, β-H3, β-H5), 3.62-3.71 (α-H3, α-H6′, β-H6′), 3.76-3.87 (α-H4, α-H6, β-H4, β-H6), 4.47 (1H, d, J = 7.92 Hz, β-H1), 5.10 (1H, d, J = 3.79 Hz, α-H1).

D-(−)-fructose (**65**), ^{1}H NMR (CD$_3$OD-d_4, 400 MHz) 3.48 (1H, d, J = 11.10 Hz, β-pyr-H1′), 3.66 (1H, d, J = 11.20 Hz, β-pyr-H1).

D-(+)-sucrose (**66**), ^{1}H NMR (CD$_3$OD-d_4, 400 MHz) 3.35 (1H, t, J = 9.6 Hz, H4), 3.42 (1H, dd, J = 9.8, 3.8 Hz, H2), 3.60 (1H, d, J = 12.2 Hz, H1′β), 3.64 (1H, d, J = 12.2 Hz, H1′α), 3.70

(1H, t, *J* = 9.6 Hz, H3), 3.73–3.85 (4H, H5, H5′, H6, H6′), 4.02 (1H, m, H4′), 4.09 (1H, d, *J* = 8.3 Hz, H3′), 5.38 (1H, d, *J* = 3.8 Hz, H1)

Lauric acid (C12:0) (**67**) TMS ether, t_R 14.69 min; EI-MS(+): 95 (5), 105 (3), 117 (100), 129 (40), 132 (45), 145 (25), 159 (3), 171 (2), 201 (6), 213 (5), 229 (5), 243 (2), 257 (95), 258 (15), 272 (3).

Myristic acid (C14:0) (**68**) TMS ether, t_R 18.04 min; EI-MS(+): 117 (100), 129 (43), 132 (48), 145 (28), 159 (3), 171 (2), 185 (3), 201 (6), 217 (5), 241 (4), 257 (5), 271 (2), 285 (80), 286 (15), 300 (15).

Palmitic acid (C16:0) (**69**) TMS ether, t_R 21.15 min; EI-MS(+): 117 (100), 129 (43), 132 (50), 145 (33), 159 (5), 171 (3), 187 (3), 201 (8), 215 (2), 229 (2), 243 (3), 257 (2), 269 (5), 285 (5), 299 (2), 313 (77), 314 (15), 328 (5).

Stearic acid (C18:0) (**70**) TMS ether, t_R 24.01 min; EI-MS(+): 96 (25), 110 (10), 117 (100), 129 (70), 129 (70), 132 (20), 145 (40), 180 (13), 185 (13), 199 (12), 222 (18), 264 (12), 295 (2), 311 (3), 325 (2), 339 (73), 340 (20), 354 (5).

Arachidic acid (C20:0) (**71**) TMS ether, t_R 26.63 min; EI-MS(+): 95 (45), 109 (31), 117 (100), 129 (66), 132 (45), 145 (47), 191 (20), 207 (33), 221 (10), 249 (10), 264 (15), 281 (5), 309 (5), 324 (15), 331 (13), 369 (49), 370 (15), 384 (10).

Behenic acid (C22:0) (**72**) TMS ether, t_R 29.12 min; EI-MS(+): 95 (45), 109 (33), 117 (100), 129 (60), 132 (48), 145 (50), 207 (30), 257 (3), 285 (3), 313 (3), 343 (5), 369 (5), 397 (40), 398 (13), 412 (10).

Lignoceric acid (C24:0) (**73**) TMS ether, t_R 31.40 min; EI-MS(+): 95 (83), 109 (52), 117 (100), 129 (76), 145 (55), 155 (28), 191 (80), 207 (80), 239 (30), 244 (60), 253 (20), 281 (15), 313 (10), 348 (8), 382 (5), 397 (5), 412 (3), 423 (15), 425 (20), 426 (9), 440 (7).

Palmitoleic acid (C16:1 *n*-7) (**74**) TMS ether, t_R 20.8 min; EI-MS(+): 117 (100), 129 (68), 132 (15), 145 (32), 171 (5), 185 (8), 199 (10), 213 (2), 227 (2), 236 (10), 311 (56), 312 (10), 326 (5); methyl ester, t_R 15.95 min; EI-MS(+): 55 (100), 67 (75), 81 (70), 96 (66), 110 (30), 123 (22), 134 (12), 141 (16), 152 (20), 166 (8), 194 (15), 207 (8), 218 (13), 236 (25), 268 (12); ACN-CI-MS/MS(+): 166 (10), 180 (25), 194 (15), 206 (12), 220 (10), 238 (8), 252 (24), 266 (8), 290 (100).

cis-11-Octadecenoic acid (C18:1 *n*-7) (**75**) TMS ether, t_R 23.76 min; EI-MS(+): 96 (26), 110 (12), 117 (100), 129 (80), 132 (28), 145 (44), 180 (10), 185 (12), 199 (12), 222 (14), 264 (12), 295 (2), 311 (3), 339 (80), 340 (20), 354 (5); methyl ester, t_R 17.92 min; EI-MS(+): 55 (100), 67 (73), 81 (80), 96 (70), 110 (32), 123 (23), 137 (28), 152 (15), 166 (13), 180 (13), 235 (8), 246 (8), 264 (45), 296 (12); ACN-CI-MS/MS(+): 166 (4), 180 (12), 194 (6), 208 (3), 220 (6), 234 (10), 248 (7), 266 (5), 280 (20), 294 (7), 318 (100).

cis-13-Eicosenoic acid (C20:1 *n*-7) (**76**) TMS ether, t_R 26.40 min; EI-MS(+): 95 (25), 109 (23), 117 (71), 129 (96), 145 (35), 171 (5), 185 (11), 199 (100), 200 (15), 217 (8), 241 (3), 250 (8), 292 (10), 316 (3), 343 (3), 357 (5), 367 (46), 368 (15), 382 (3); methyl ester, t_R 19.71 min; EI-MS(+): 55 (100), 69 (65), 83 (50), 97 (45), 111 (25), 123 (15), 137 (10), 152 (8), 166 (5), 193 (5), 207 (15), 221 (8), 255 (8), 281 (10), 292 (20), 324 (5); ACN-CI-MS/MS(+): 166 (4), 180 (11), 194 (5), 208 (3), 220 (1), 234 (3), 248 (4), 262 (6), 276 (8), 294 (5), 308 (24), 318 (5), 346 (100).

cis-15-Docosenoic acid (C22:1 *n*-7) (**77**) TMS ether, t_R 28.91 min; EI-MS(+): 95 (29), 109 (18), 117 (100), 129 (90), 132 (36), 145 (55), 159 (5), 171 (8), 185 (18), 199 (15), 236 (10), 249 (5), 263 (5), 277 (5), 291 (3), 320 (19), 339 (2), 351 (3), 367 (2), 395 (80), 396 (23), 410 (8); methyl ester, t_R 21.38 min; EI-MS(+): 55 (100), 69 (80), 83 (55), 97 (50), 111 (20), 123 (15), 137 (15), 152 (10), 166 (8), 193 (8), 207 (31), 221 (10), 236 (13), 250 (5), 263 (8), 281 (18), 291 (5), 320 (60); ACN-CI-MS/MS(+): 166 (2), 180 (8), 194 (45), 208 (2), 262 (2), 276 (4), 290 (8), 304 (7), 318 (3), 336 (24), 374 (100).

cis-17-Tetracosenoic acid (C24:1 *n*-7) (**78**) TMS ether, t_R 31.25 min; EI-MS(+): 95 (37), 117 (100), 129 (85), 132 (37), 145 (52), 159 (6), 171 (8), 185 (18), 199 (15), 207 (10), 235 (5), 249 (5), 263 (5), 277 (5), 291 (5), 305 (4), 319 (3), 348 (20), 379 (3), 395 (2), 423 (70), 424 (23), 438 (6); methyl ester, t_R 22.93 min; EI-MS(+): 55 (90), 69 (70), 83 (50), 97 (50), 111 (30), 123 (15), 137 (15), 152 (10), 166 (8), 193 (15), 207 (100), 221 (10), 236 (8), 250 (5), 263 (5), 281 (55), 291 (5), 348 (50); ACN-CI-MS/MS(+): 180 (5), 194 (4), 208 (4), 276 (2), 290 (3), 304 (7), 318 (6), 336 (6), 364 (20), 374 (6), 402 (100).

Oleic acid (C18:1 *n*-9) (**79**) TMS ether, t_R 23.68 min; EI-MS(+): 96 (25), 110 (10), 117 (100), 129 (70), 132 (20), 145 (40), 180 (13), 185 (13), 199 (12), 222 (18), 264 (12), 295 (2), 311 (3), 325 (2), 339 (73), 340 (20), 354 (5); methyl ester, t_R 17.86 min; EI-MS(+): 55 (80), 69 (58), 81 (100), 83 (55), 95 (65), 97 (53), 109 (30), 111 (30), 123 (30), 137 (20), 148 (20), 152 (15), 166 (20), 180 (20), 193 (5), 207 (10), 221 (15), 235 (10), 246 (13), 250 (5), 264 (50), 296 (10);

ACN-CI-MS/MS(+): 149 (3), 163 (3), 180 (4), 194 (12), 206 (17), 208 (32), 220 (18), 222 (17), 234 (8), 252 (28), 266 (10), 290 (5), 301 (7), 318 (8), 316 (10), 318 (100).

cis-11-Eicosenoic acid (C20:1 *n*-9) (**80**) TMS ether, t_R 26.28 min (overlap with **83**); 95 (18), 103 (13), 117 (37), 129 (55), 145 (22), 147 (45), 159 (3), 175 (5), 187 (7), 203 (18), 211 (28), 227 (31), 285 (6), 292 (3), 313 (2), 329 (5), 343 (100), 344 (25), 367 (20), 431 (8); methyl ester, t_R 19.66 min; EI-MS(+): 55 (100), 69 (65), 83 (50), 97 (45), 111 (25), 123 (15), 137 (10), 152 (8), 207 (10), 292 (15); ACN-CI-MS/MS(+):180 (3), 194 (6), 208 (18), 220 (10), 234 (11), 248 (10), 262 (3), 280 (27), 294 (6), 308 (2), 318 (5), 346 (100).

Nervonic acid (C24:1 *n*-9) (**81**) TMS ether, t_R 31.14 min; EI-MS(+): 95 (46), 117 (100), 129 (90), 132 (34), 145 (50), 159 (6), 171 (8), 185 (16), 199 (22), 207 (14), 235 (4), 249 (5), 264 (8), 277 (4), 291 (4), 306 (10), 319 (3), 348 (20), 379 (3), 395 (2), 423 (60), 424 (23), 438 (6); methyl ester, t_R 22.86 min; EI-MS(+): 55 (65), 69 (55), 83 (40), 97 (35), 111 (25), 123 (15), 147 (20), 165 (5), 179 (5), 193 (20), 207 (100), 221 (10), 250 (5), 267 (10), 281 (60), 327 (10), 341 (30), 348 (20), 355 (15); ACN-CI-MS/MS(+): 194 (3), 208 (11), 222 (4), 276 (4), 290 (5), 304 (8), 318 (3), 336 (24), 350 (8), 364 (3), 374 (6), 402 (100).

Linoleic acid (C18:2 *n*-6) (**82**) TMS ether, t_R 23.52 min; EI-MS(+): 95 (88), 109 (50), 117 (100), 129 (88), 135 (48), 149 (30), 163 (15), 178 (30), 187 (13), 201 (10), 215 (5), 220 (25), 234 (8), 262 (55), 283 (2), 309 (2), 337 (95), 338 (23), 352 (5); methyl ester, t_R 17.80 min; EI-MS(+): 55 (43), 67 (100), 81 (95), 95 (65), 109 (20), 121 (15), 135 (15), 150 (15), 165 (10), 179 (5), 193 (20), 262 (10), 294 (15); ACN-CI-MS/MS(+): 150 (6), 164 (10), 178 (9), 192 (21), 204 (13), 206 (20), 218 (13), 232 (5), 236 (7), 246 (6), 250 (13), 264 (8), 276 (8), 278 (23), 288 (10), 292 (13), 306 (8), 314 (20), 316 (100).

Glycerol 1-myristate (**83**) diTMS ether, t_R 26.28 min; EI-MS(+): 95 (18), 103 (13), 117 (37), 129 (55), 145 (22), 147 (45), 159 (3), 175 (5), 187 (7), 203 (18), 211 (28), 227 (31), 285 (6), 292 (3), 313 (2), 329 (5), 343 (100), 344 (25), 367 (20), 431 (8).

Glycerol 1-palmitate (**84**) diTMS ether, t_R 28.71 min; EI-MS(+): 95 (11), 103 (15), 117 (11), 129 (26), 145 (11), 147 (43), 187 (5), 203 (22), 239 (20), 313 (5), 357 (2), 371 (100), 372 (25), 459 (8).

Glycerol 1-stearate (**85**) diTMS ether, t_R 30.98 min; EI-MS(+): 95 (27), 103 (45), 116 (78), 117 (40), 129 (40), 145 (22), 147 (49), 191 (13), 203 (25), 267 (18), 311 (83), 312 (15), 341 (5), 399 (100), 400 (25), 487 (8), 502 (2).

Glycerol 1-behenate (**86**) diTMS ether, t_R 35.18 min; EI-MS(+): 95 (52), 103 (43), 117 (30), 129 (88), 145 (36), 147 (70), 203 (35), 207 (93), 257 (25), 281 (13), 291 (15), 315 (23), 397 (5), 455 (100), 456 (35), 468 (3), 543 (8), 558 (2).

Glycerol 1-lignocerate (**87**) diTMS ether, t_R 37.11 min; EI-MS(+): 95 (38), 103 (40), 129 (85), 147 (55), 191 (18), 203 (28), 207 (100), 218 (8), 423 (3), 451 (2), 483 (60), 484 (20), 571 (5), 583 (2).

Glycerol 1-octadecenoate (**88**) diTMS ether, t_R 30.69 min; EI-MS(+): 95 (23), 103 (50), 129 (100), 147 (68), 191 (5), 203 (30), 218 (10), 257 (13), 265 (14), 307 (5), 339 (5), 397 (58), 410 (8), 485 (6), 500 (3).

Glycerol 1-docosenoate (**89**) diTMS ether, t_R 35.04 min; EI-MS(+): 95 (20), 103 (42), 129 (100), 147 (56), 203 (28), 257 (12), 315 (8), 321 (15), 363 (13), 395 (5), 423 (3), 453 (33), 466 (18), 541 (7), 556 (3).

Glycerol 1-tetracosenate (**90**) diTMS ether, t_R 37.00 min; EI-MS(+): 95 (18), 103 (42), 129 (100), 147 (52), 203 (27), 257 (10), 315 (3), 349 (12), 391 (14), 423 (5), 451 (5), 481 (28), 494 (20).

Glycerol 2-myristate (**91**) diTMS ether, t_R 25.89 min; EI-MS(+): 95 (22), 103 (34), 117 (12), 129 (100), 147 (50), 191 (20), 203 (20), 211 (10), 217 (20), 218 (60), 241 (40), 285 (25), 329 (2), 356 (2), 375 (3), 431 (3).

Glycerol 2-palmitate (**92**) diTMS ether, t_R 28.33 min; EI-MS(+): 95 (22), 103 (40), 129 (100), 147 (55), 191 (25), 203 (25), 217 (15), 218 (78), 313 (22), 385 (5), 403 (3), 459 (3), 484 (2).

Glycerol 2-behenate (**93**) diTMS ether, t_R 35.29 min; EI-MS(+): 103 (20), 117 (16), 119 (100), 129 (13), 133 (96), 147 (26), 190 (16), 204 (15), 207 (93), 321 (3), 353 (5), 455 (3), 468 (2), 543 (5), 558 (3).

Glycerol, 1,2-dilaurate (**94**) TMS ether, t_R 34.59 min; EI-MS(+): 95 (10), 103 (20), 129 (62), 145 (86), 183 (40), 257 (100), 273 (30), 329 (20), 438 (2), 513 (18).

Glycerol, 1-laurate-2-myristate (**95**) TMS ether, t_R 36.52 min; EI-MS(+): 95 (14), 103 (24), 129 (79), 145 (100), 183 (22), 211 (22), 257 (55), 273 (18), 285 (52), 301 (16), 329 (15), 357 (10), 466 (2), 541 (17).

Glycerol, 1-laurate-2-palmitate (**96**) TMS ether, t_R 38.37 min; EI-MS(+): 95 (15), 103 (25), 129 (87), 145 (100), 183 (16), 211 (8), 257 (45), 273 (15), 285 (18), 313 (38), 329 (30), 357 (6), 385 (8), 451 (2), 494 (3), 569 (15).

Glycerol, 1-laurate-2-stearate (**97**) TMS ether, t_R 40.16 min; EI-MS(+): 95 (19), 103 (23), 129 (100), 145 (70), 183 (8), 207 (70), 211 (10), 257 (20), 285 (23), 313 (23), 329 (25), 341 (6), 357 (13), 385 (6), 410 (3), 523 (3), 598 (8).

Glycerol, 1-laurate-2-arachidate (**98**) TMS ether, t_R 42.24 min; EI-MS(+): 95 (16), 103 (13), 129 (60), 145 (23), 183 (18), 207 (100), 257 (15), 281 (15), 313 (8), 329 (13), 357 (8), 385 (5), 411 (10), 439 (6), 467 (2), 521 (2), 626 (3).

Glycerol, 1-laurate-2-octadecenoate (**99**) TMS ether, t_R 40.00 min; EI-MS(+): 95 (13), 103 (15), 129 (100), 145 (30), 183 (11), 257 (30), 273 (5), 329 (45), 339 (12), 255 (3), 367 (2), 410 (5), 520 (2), 596 (6), 611 (2).

Glycerol, 1-laurate-2-eicosenoate (**100**) TMS ether, t_R 42.03 min; EI-MS(+): 95 (18), 103 (16), 129 (100), 145 (25), 183 (8), 207 (92), 253 (13), 257 (13), 281 (13), 285 (16), 329 (12), 339 (10), 357 (25), 410 (5), 439 (3), 548 (3), 624 (5).

Glycerol, 1-laurate-2-docosenoate (**101**) TMS ether, t_R 45.22 min; EI-MS(+): 95 (18), 103 (15), 129 (100), 145 (39), 183 (32), 207 (28), 257 (35), 273 (5), 329 (58), 367 (3), 395 (13), 439 (12), 466 (10), 577 (3), 652 (6).

Glycerol, 1-laurate-2-tetracosenoate (**102**) TMS ether, t_R 49.56 min; EI-MS(+): 95 (18), 103 (15), 129 (100), 145 (35), 183 (13), 207 (50), 257 (23), 281 (8), 329 (50), 349 (8), 357 (5), 423 (10), 439 (3), 467 (3), 494 (6), 605 (3), 680 (5), 695 (2).

Glycerol, 1,3-dilaurate (**103**) TMS ether, t_R 34.88 min; EI-MS(+): 95 (11), 129 (18), 146 (12), 183 (42), 257 (22), 315 (100), 316 (20), 329 (10), 438 (3), 513 (15).

Glycerol, 1-laurate-3-myristate (**104**) TMS ether, t_R 36.82 min; EI-MS(+): 95 (22), 129 (43), 146 (28), 183 (42), 211 (30), 257 (26), 285 (20), 315 (100), 329 (12), 343 (90), 357 (10), 423 (3), 466 (5), 541 (23).

Glycerol, 1-laurate-3-palmitate (**105**) TMS ether, t_R 38.68 min; EI-MS(+): 95 (30), 129 (60), 146 (32), 183 (42), 211 (16), 239 (20), 257 (30), 285 (13), 315 (100), 329 (18), 343 (48), 371 (76), 385 (10), 423 (3), 451 (4), 494 (8), 569 (25).

Glycerol, 1-laurate-3-stearate (**106**) TMS ether, t_R 40.48 min; EI-MS(+): 95 (29), 129 (62), 146 (20), 183 (18), 207 (100), 211 (15), 257 (20), 285 (13), 315 (30), 329 (20), 343 (36), 371 (35), 399 (10), 522 (3), 598 (13), 613 (2).

Glycerol, 1-laurate-3-arachidate (**107**) TMS ether, t_R 42.71 min; EI-MS(+): 95 (15), 129 (34), 183 (8), 207 (100), 257 (8), 281 (15), 315 (6), 329 (5), 343 (8), 357 (4), 371 (13), 399 (3), 439 (2), 467 (2), 549 (2), 626 (3).

Glycerol, 1-laurate-3-octadecenoate (**108**) TMS ether, t_R 40.31 min; EI-MS(+): 95 (45), 129 (100), 146 (24), 183 (45), 207 (48), 257 (46), 264 (25), 281 (6), 315 (75), 329 (63), 367 (6), 397 (45), 410 (10), 449 (3), 477 (3), 520 (7), 521 (3), 596 (15), 611 (2).

Glycerol, 1-laurate-3-eicosenoate (**109**) TMS ether, t_R 42.49 min; EI-MS(+): 95 (24), 129 (56), 146 (10), 183 (10), 207 (100), 257 (10), 285 (13), 315 (9), 329 (7), 343 (20), 357 (18), 397 (15), 410 (5), 425 (3), 439 (3), 449 (2), 467 (2), 549 (5), 624 (6).

Glycerol, 1-laurate-3-docosenoate (**110**) TMS ether, t_R 45.88 min; EI-MS(+): 95 (49), 129 (99), 146 (28), 183 (43), 207 (100), 257 (38), 315 (80), 329 (70), 363 (8), 395 (10), 423 (3), 453 (25), 466 (18), 505 (5), 533 (3), 577 (15), 652 (14), 667 (2).

Glycerol, 1-laurate-3-tetracosenoate (**111**) TMS ether, t_R 50.53 min; EI-MS(+): 95 (31), 129 (60), 146 (15), 183 (20), 207 (100), 257 (20), 281 (15), 315 (38), 329 (36), 349 (6), 357 (5), 391 (5), 399 (5), 423 (4), 453 (3), 466 (3), 481 (10), 494 (9), 533 (3), 562 (3), 605 (8), 680 (6).

Glycerol, 1-laurate-2-caprate-3-laurate (**112**), t_R 42.25 min; EI-MS(+): 133 (14), 155 (40), 183 (60), 207 (100), 229 (10), 253 (10), 257 (20), 281 (22), 298 (5), 311 (10), 397 (3), 411 (20), 439 (10).

Glycerol, 1,2,3-laurate (**113**), t_R 45.17 min; EI-MS(+): 109 (10), 158 (10), 171 (8), 183 (100), 207 (10), 227 (5), 257 (35), 298 (10), 311 (10), 353 (3), 367 (5), 395 (3), 425 (3), 439 (30).

Glycerol, 1-laurate-2-myristate-3-laurate (**114**), t_R 49.35 min; EI-MS(+): 109 (16), 158 (10), 171 (10), 183 (100), 207 (40), 211 (42), 257 (38), 285 (18), 298 (10), 211 (13), 326 (8), 339 (8), 353 (3), 367 (6), 381 (3), 395 (5), 423 (3), 439 (20), 467 (30).

7 Reference list

[1]   Clauss, M. J.; Dietel, S.; Schubert, G.; Mitchell-Olds, T. *J. Chem. Ecol.* **2006**, *32*, 2351-2373.

[2]   Agrawal, A. A.; Petschenka, G.; Bingham, R. A.; Weber, M. G.; Rasmann, S. *New Phytologist* **2012**, *194*, 28-45.

[3]   Paré, P. W.; Tumlinson, J. H. *Plant Physiol.* **1999**, *121*, 325-331.

[4]   Engler, H. S.; Spencer, K. C.; Gilbert, L. E. *Nature* **2000**, *406*, 144-145.

[5]   Fischer, H. M.; Wheat, C. W.; Heckel, D. G.; Vogel, H. *Mol. Biol. Evol.* **2008**, *25*, 809-820.

[6]   Bricchi, I.; Leitner, M.; Foti, M.; Mithöfer, A.; Boland, W.; Maffei, M.E. *Planta* **2010**, *232*, 719–729.

[7]   Kessler, A.; Baldwin, I. T. *Science* **2001**, *291*, 2141-2144.

[8]   Turlings, T. C. J.; Tumlinson, J. H.; Lewis, W. J. *Science*, **1990**, *250*, 1251-1253.

[9]   Maffei, M.; Bossi, S.; Spiteller, D.; Mithöfer, A.; Boland, W. *Plant Physiol.* **2004**, *134*, 1752-1762.

[10]   Maffei, M.; Camusso, W.; Sacco, S. *Phytochemistry* **2001**, *58*, 703-707.

[11]   Engelberth, J.; Koch, T.; Schüler, G.; Bachmann, N.; Rechtenbach, J.; Boland, W *Plant Physiol.* **2001**, *125*, 369-377.

[12]   Zimmermann, M. R.; Maischak, H.; Mithöfer, A.; Boland, W.; Felle, H. H. *Plant Physiol.* **2009**, *149*, 1593–1600.

[13]   Mousavi, S. A. R.; Chauvin, A.; Pascaud, F.; Kellenberger, S.; Farmer, E. E *Nature* **2013**, *500*, 422-426.

[14]   Evans, D. E.; Briars, S. A.; William, L. E. *J. Exp. Bot.* **1991**, *42*, 285-303.

[15]   Leitner, M.; Vandelle, E.; Gaupels, F.; Bellin, D.; Delledonne, M. *Curr. Opin. Plant Biol.* **2009**, *12*, 451-458.

[16]   Orozco-Cardenas, M. L.; Ryan, C. A. *Plant Physiol.* **2002**, *130*, 487-493.

[17]   Jih, P. J.; Chen, Y. C.; Jeng, S. T. *Plant Physiol.* **2003**, *132*, 381-389.

[18]   Orozco-Cardenas, M. L.; Ryan, C. A. *Proc. Natl. Acad. Sci. USA* **1999**, *96*, 6553-6557.

[19]   Bi. J. L.; Felton, G. W. *J. Chem. Ecol.* **1995**, *21*, 1511-1530.

[20]   Mithöfer, A.; Schulze, B.; Boland, W. *FEBS Lett.* **2004**, *4*, 105-118.

[21]   Schmelz, E. A.; Alborn, H. T.; Banchio, E.; Tumlinson, J. H. *Planta* **2003**, *216*, 665-673.

[22]   Fonseca, S.; Chini, A.; Hamberg, M.; Adie, B.; Porzel, A.; Kramell, R.; Miersch, O.; Wasternack, C.; Solano, R. *Nat. Chem. Biol.* **2009**, *5*, 344-350.

[23]   Park, S. W.; Kaimoyo, E.; Kumar, D.; Moser, S.; Klessig, D. F. *Science* **2007**, *318*, 113-116.

[24]   Vadassery, J.; Reichelt, M.; Hause, B.; Gershenzon, J.; Boland, W.; Mithöfer, A. *Plant Physiol.* **2012**, *159*, 1159–1175.

[25]   Hui, D. Q.; Iqbal, J.; Lehmann, K.; Gase, K.; Saluz, H. P.; Baldwin, I. T. *Plant Physiol.* **2003**, *131*, 1877-1893.

[26]   Vadassery, J.; Oelmüller, R. *Plant Signaling & Behavior* **2009**, *4*, 1024–1027.

[27]   Knight, H.; Trewavas, A. J.; Knight, M. R. *Plant J.* **1997**, *12*, 1067–1078.

[28]   Sung, D. Y.; Kaplan, F.; Lee, K. J.; Guy, C. L. *Trends Plant Sci.* **2003**, *8*, 179–187.

[29]   Defalco, T.A.; Bender, K.W.; Snedden, W.A. *Biochem. J.* **2010**, *425*, 27–40.

[30]   Dobney, S.; Chiasson, D.; Lam, P.; Smith, S. P.; Snedden, W. A. *J. Biol. Chem.* **2009**, *284*, 31647–31657.

[31]   Wu, J.; Baldwin, I. T. Annu. Rev. Genet. 2010, 44, 1-24.

[32]   Paré, P. W.; Tumlinson, J. H. *Plant Physiol.* **1999**, *121*, 325-331.

[33]   Koornneef, A.; Pieterse, C. M. J. *Plant Physiol.* **2008**, *146*, 829-844.

[34]   Bricchi, I.; Occhipinti, A.; Bertea, C. M.; Yebelo, S. A.; Brillada, C.; Verrillo, F.; Castro, C. D.; Molinaro, A.; Faulkner, C.; Maule, A. J.; Maffei, M. E. *Plant J.* **2013**, *73*, 14–25.

[35]   Maffei, M. E.; Mithöfer, A.; Arimura, G. I.; Uchtenhagen, H.; Bossi, S.; Mertea, C. M.;Cucuzza, L. S.; Novero, M.; Volpe, V.; Quadro. S.; Boland, W. *Plant Physiol.* **2006**, *140*, 1022–1035.

[36]   Mithöfer, A.; Wanner, G.; Boland, W. *Plant Physiol.* **2005**, *137*, 1160-1168.

[37]   Heil, M. *Curr. Opin. Plant Biol.* **2009**, *14*, 356-363.

[38]   Heil, M.; Ibarra-Laclette, E.; Adame-Álvarez, R. M.; Martínez, O.; Ramirez-Chávez, E.; Molina-Torres, J.; Herrera-Estrella, L. *PLoS One* **2012**, *7*, e30537.

[39]   Mattiacci, L.; Dicke, M.; Posthumus, M. A. *Proc. Natl. Acad. Sci. USA* **1995**, *92*, 2036-2040.

[40]   Morant, A. V.; Jørgensen, K.; Jørgensen, C.; Paquette, S. M.; Sánchez-Pérez, R.; Møller, B. L.; Bak, S. *Phytochem.* **2008**, *69*, 1795-1813.

[41]   Alborn, H. T.; Turlings, T. C. J.; Jones, T. H.; Stenhagen, G.; Loughrin, J. H.; Tumlinsion, J. H. *Science* **1997**, *276*, 945-949.

[42]   Pohnert, G.; Jung, V.; Haukioja, E.; Lempa, K.; Boland, W. *Tetrahedron* **1999**, *55*, 11275-11280.

[43]   Paré, P. W.; Alborn, H. T.; Tumlinson, J. H. *Proc. Natl. Acad. Sci. USA* **1998**, *95*, 13971-13975.

[44]   Spiteller, D.; Boland, W. *Tetrahedron* **2003**, *59*, 135-139.

[45]   Spiteller, D.; Boland, W. *J. Org. Chem.* **2003**, *68*, 8743-8749.

[46]   Spiteller, D.; Oldham, N. J.; Boland, W. *J. Org. Chem.* **2004**, *69*, 1104-1109.

[47]   Truitt, C. L.; Wie, H. X.; Paré, P. W. *Plant Cell* **2004**, *16*, 523-532.

[48]   Gorchein, A. *Biochim. Biophys. Acta* **1973**, *306*, 137-141.

[49]   Kawai, Y.; Yano, I.; Kaneda, K. *Eur. J. Biochem.* **1988**, *171*, 73-80.

[50]   Yagi, H.; Corzo, G.; Nakahara, T. *Biochim. Biophys. Acta* **1997**, *1336*, 28-36.

[51]   Spiteller, D.; Dettner, K.; Boland, W. *Biol. Chem.* **2000**, *381*, 755-762.

[52]   Doss, R. P.; Oliver, J. E.; Proebsting, W. M.; Potter, S. W.; Kuy, S.; Clement, S. L.; Williamson, R. T.; Carney, J. R.; DeVilbiss, E. D. *Proc. Natl. Acad. Sci. USA* **2000**, *97*, 6218-6223.

[53]   Cooper, L. D.; Doss, R. P.; Price, R.; Peterson, K.; Oliver, J. E. *J. Exp. Bot.* **2005**, *56*, 1229-1237.

[54]   Alborn, H. T.; Hansen, T. V.; Jones, T. H.; Bennett, D. C.; Tumlinson, J. H.; Schmelz, E. A.; Teal, P. E. A. *Proc. Natl. Acad. Sci. USA* **2007**, *104*, 12976-12981.

[55]   O'Doherty, I.; Yim, J. J.; Schmelz, E. A.; Schroeder, F. C. *Org. Lett.* **2011**, *13*, 5900-5903.

[56]   Schmelz, E. A.; Carroll, M. J.; LeClere, S.; Phipps, S. M.; Meredith, J.; Chourey, P. S.; Alborn, H. T.; Teal, P. E. A. *Proc. Natl. Acad. Sci. USA* **2006**, *103*, 8894-8899.

[57]   Schmelz, E. A.; Engelberth, J.; Alborn, H. T.; Tumlison, J. H.; Teal, P. E. A. *Proc. Natl. Acad. Sci. USA* **2009**, *106*, 653-657.

[58]   Krol, E.; Trebacz, K. *Ann. Bot.* **2000**, *86*, 449-469.

[59]   Maffei, M. E.; Mithöfer, A.; Boland, W. *Trends Plant Sci.* **2007**, *12*, 310-316.

[60]   Wade, D.; Boman, A.; Wahlin, B.; Drain, C. M.; Andreu, D.; Boman, H. G.; Merrifield, R. B. *Proc. Natl. Acad. Sci. USA* **1990**, *87*, 4761–4765.

[61]   Kourie, J. I.; Shorthouse, A. A. *Am. J. Physiol. Cell. Physiol.* **2000**, *278*, C1063–C1087.

[62]   Saier, M. H. Jr. *J. Membrane Biol.* **2000**, *175*, 165-180.

[63]   Bayley, H. *Nature* **2009**, *459*, 651-652.

[64]   Song, L.; Hobaugh, M. R.; Shustak, C.; Cheley, S.; Bayley, H.; Gouaux, J. E. *Science* **1996**, *274*, 1859-1866.

[65]   Tobkes, N.; Wallace, B. A.; Bayley, H. *Biochemistry* **1985**, *24*, 1915–1920.

[66]   Dinges, M. M.; Orwin, P. M. Schlievert, P. M. *Clin. Microbiol. Rev.* **2000**, *13*, 16-34.

[67]   Gouaux, J. E.; Braha, O.; Hobaugh, M. R.; Song, L.; Cheley, S.; Shustak, C.; Bayley, H. *Proc. Natl, Acad. Sci. U.S.A.* **1994**, *91*, 12828–12831.

[68]   Bashford, C. L.; Alder, G. M.; Fulford, L. G.; Korchev, Y. E.; Kovacs, E.; MacKinnon, A.; Pederzolli, C.; Pasternak, C. A. *J. Membrane Biol.* **1996**, *150*, 37-45.

[69]   Fink, D.; Contreras, M. L.; Lelkes, P. I.; Lazarovici, P. *Cellular Signalling* **1989**, *1*, 387-393.

[70]   Stefureac, R.; Long, Y. T.; Kraatz, H. B.; Howard, P.; Lee, J. S. *Biochemistry* **2006**, *45*, 9172-9179.

[71]   Mueller, M.; Grauschopf, U.; Maier, T.; Glockshuber, R.; Ban, N. *Nature* **2009**, *459*, 726-730.

[72]   Majd, S.; Yusko, E. C.; Billeh, Y. N.; Macrae, M. X.; Yang, J.; Mayer, M. *Curr. Opin. Biotechnol.* **2010**, *21*, 439-476.

[73]   Meyer, C. E.; Reusser, F. *Experientia* **1967**, *23*, 85.

[74]   Pandey, R. C.; Cook, J. C.; Rinehart, K. L. *J. Am. Chem. Soc.* **1977**, *99*, 8469-8483.

[75]   Jen, W. C.; Jones, G. A.; Brewer, D.; Parkinson, V. O.; Taylor, A. *J. Appl. Bacteriol.* **1987**, *63*, 293-298.

[76]   Vodyanoy, I.; Hall, J. E.; Vodyanoy, V. *Biophys. J.* **1988**, *53*, 649-658.

[77]   Müller, P.; Rudin, D. *Nature* **1968**, *217*, 713-719.

[78]   Duclohier, H.; Wróblewski, H. *J. Membrane Biol.* **2001**, *184*, 1-12.

[79]   Rippa, S.; Eid, M.; Formaggio, F.; Toniolo, C.; Béven, L. *ChemBioChem* **2010**, *11*, 2042-2049.

[80]   Engelberth, J.; Koch, T.; Kühnemann, F.; Boland, W. *Angew. Chem. Int. Ed.* **2000**, *39*, 1860-1862.

[81]   Maischak, H.; Zimmermann, M. R.; Felle, H. H.; Boland, W.; Mithöfer, A. *Plant Signaling & Behavior* **2010**, *5*, 988–990.

[82]   Bartram, S.; Jux, A.; Gleixner, G.; Boland, W. *Phytochem.* **2006**, *67*, 1661-1672.

[83]   Chen, F.; D′Auria, J. C.; Tholl, D.; Ross, J. R.; Gershenzon, J.; Noel, J. P.; Pichersky, E. *Plant J.* **2003**, *36*, 577-588.

[84]   Herde, M.; Gärtner, K.; Köllner, T. G.; Fode, B.; Boland, W.; Gershenzon, J.; Gatz, C.; Tholl, D. *Plant Cell* **2008**, *20*, 1152-1168.

[85]   Rippa, S.; Eid, M.; Formaggio, F.; Toniolo, C.; Béven, L. *ChemBioChem* **2010**, *11*, 2042-2049.

[86]   Aidemark, M.; Andersson, C. J.; Rasmusson, A. G.; Widell, S. *BMC Plant Biol.* **2009**, *9*:27.

[87]   Ducrot, P. H.; Milat, M. L.; Blein, J. P.; Lallemand, J. Y. *J. Chem. Soc., Chem. Commu.* **1994**, 2215-2216.

[88]   Goudet, C.; Benitah, J. P.; Milat, M. L.; Sentenac, H.; Thibaud, J. B. *Biophys. J.* **1999**, *77*, 3052-3059.

[89]   Murphy, B.; Anderson, K.; Borissow, C.; Caffrey, P.; Griffith, G.; Hearn, J.; Ibrahim, O.; Khan, N.; Lamburn, N.; Lee, M.; Pugh, K.; Rawlings, B. *Org. Biomol. Chem.* **2010**, *8*, 3758-3770.

[90]   Matsumori, N.; Yamaji, N.; Matsuoka, S.; Oishi, T.; Murata, M. *J. Am. Chem. Soc.* **2002**, *124*, 4180-4181.

[91]   López-Lázaro, M. *Expert Opin. Ther. Targets* **2007**, *11*,1043-1053.

[92]   Arispe, N.; Diaz, J. C.; Simakova, O.; Pollard, H. B. *Proc. Natl. Acad. Sci. U.S.A.* **2008**, *105*, 2610-2615.

[93]   Maischak, H.; Grigoriev, P. A.; Vogel, H.; Boland, W.; Mithöfer, A. *FEBS Lett.* **2007**, *581*, 898–904.

[94]   Lühring, H.; Nguyen, V.D.; Schmidt, L.; Röse. U.S.R. *FEBS Lett.* **2007**, *581*, 5361–5370.

[95]   Benz, R.; Ishii, J.; Nakae, T. *J. Membrane Biol.* **1980**, *56*, 19–29.

[96]   Mithöfer, A.; Ebel, J.; Bhagwat, A. A.; Boller, T.; Neuhaus-Url, G. *Planta* **1999**, *207*, 566–574.

[97]   Vadassery, J.; Ranf, S.; Drzewiecki, C.; Mithöfer, A.; Mazars, C.; Scheel, D.; Lee, J.; Oelmüller, R. *The Plant Journal* **2009**, *59*, 193-206.

[98]   Röse, U. S. R.; Manukian, A.; Heath, R. R.; Tumlinson, J. H. *Plant Physiol.* **1996**, *111*, 487–495.

[99]   Dicke, M.; van Baarlen, P.; Wessels, R.; Dijkman, H. *J. Chem. Ecol.*, **1993**, *19*, 581–599.

[100] Kunert, M.; Biedermann, A.; Koch, T.; Boland, W. *J. Sep.Sci.* **2002**, *25*, 677–684.

[101] Arimura, G.; Köpke, S.; Kunert, M.; Volpe, V.; David, A.; Brand, P.; Dabrowska, P.; Maffei, M. E.; Boland, W. *Plant Physiol.* **2008**, *146*, 965–973.

[102] Ebel, J.; Mithöfer, A. *Planta* **1998**, *206*, 335–348.

[103] Maffei, M.E.; Arimura, G-I.; Mithöfer, A. *Nat. Prod. Rep.* **2012**, *29*, 1288–1303.

[104] Tang, X. S.; Freitak, D.; Vogel, H.; Ping, L. Y.; Shao, Y. Q.; Cordero, E. A.; Andersen, G.; Westermann, M.; Heckel, D. G.; Boland, W. *PLoS ONE* **2012**, *7*, e36978.

[105] Bennik, M. H. J.; Vanloo, B.; Brasseur, R.; Gorris, L. G. M.; Smid, E. J. *Biochim. Biophys. Acta* **1998**, *1373*, 47–58.

[106] Knapp, O.; Maier, E.; Benz, R.; Geny, B.; Popoff, M. R. *Biochim. Biophys. Acta* 2009, *1788*, 2584–2593.

[107] Lincke, T.; Behnken, S.; Ishida, K.; Roth, M.; Hertweck, C. *Angew. Chem. Int. Ed.* **2010**, *49*, 2011–2013.

[108] Cherry, R. J.; Chapman, D.; Graham, D. E. *J. Membrane Biol.* **1972**, *7*, 325-344.

[109] Eisenberg, M.; Hall, J. E.; Mead, C. A. *J. Membrane Biol.* **1973**, *14*, 143-176.

[110] Fonteriz, R. I.; López, M. G.; Garcia-Sancho, J.; Garcia, A. G. *FEBS* **1991**, *283*, 89-92.

[111] Ritov, V. B.; Tverdislova, I. L.; Avakyan, T. Y.; Menshikova, E. V.; Leikin, Y. N.; Bratkovskaya, L. B.; Shimon, R. G. *Gen. Physiol. Biophys.* **1992**, *11*, 49-58.

[112] Matic, S.; Geisler, D. A.; Möller, I. M.; Widell, S.; Rasmusson, A. G. *Biochem. J.* **2005**, *389*, 695-704.

[113] Lee, S.; Badieyan, S.; Bevan, D. R.; Herde, M.; Gatz, C.; Tholl, D. *Proc. Natl. Acad. Sci. U.S.A.* **2008**, *105*, 2610-2615.

[114] Rippa, S.; Adenier, H.; Derbaly, M.; Béven, L. *Chem. Biodivers.* **2007**, *4*, 1360-1373.

[115] Aidemark, M.; Andesson, C. J.; Rasmusson, A. G.; Widee, S. *BMC Plant Biol.* **2009**, *9*, 27-41.

[116] Arimura, G. I.; Ozawa, R.; Kugimiya, S.; Takabayashi, J.; Bohlmann, J. *Plant Physiol.* **2004**, *135*, 1976–1983.

[117] Toniolo, C.; Benedetti, E. *Trends Biochem. Sci.* **1991**, *16*, 350-353.

[118] Matha, V.; Jegorov, A.; Kiess, M.; Brückner, H. *Tissure Cell* **1992**, *24*, 559-564.

[119] Guihard, G.; Falk, S.; Vachon, V.; Laprade, R.; Schwartz, J. L. *Biochemistry* **1999**, *38*, 6164-6170.

[120] Taylor, A. *Proc. N. S. Inst. Sci.* 1986, 36, 27-

[121]   Belmonte, G.; Cescatti, L.; Ferrari, B.; Nicolussi, T.; Ropele, M.; Menestrina, G. *Eur. Biophy. J.* **1987**, *14*, 349–358.

[122]   Menestrina, G. *J. Membrane Biol.* **1986**, *90*, 177-190.

[123]   Bhakdi, S.; Tranum-Jensen, *J. Microbiol. Rev.* **1991**, *55*, 733–751.

[124]   Walev, I.; Martin, E.; Jonas, D.; Mohamadzadeh, M.; Müller-Klieser, W.; Kunz, L.; Bhakdi,S. *Infect. Immun.* **1993**, *61*, 4972–4979.

[125]   Dinges, M. M.; Orwin, P. M.; Schlievert, P. M. *Clin. Microbiol. Rev.* **2000**, *13*, 16–34.

[126]   Noskov, S. Y.; Im, W.; Roux, B. *Biophys. J.* **2004**, *87*, 2299–2309.

[127]   Eichstädt, S.; Gäbler, K.; Below, S.; Müller, C.; Kohler, C.; Engelmann, S.; Hildebrandt, P.; Völker, U.; Hecker, M.; Hildebrandt, J. P. *Cell Calcium* **2009**, *45*, 165–176.

[128]   Hanke, W.; Boheim, G. *Biochim. Biophys. Acta* **1980**, *596*, 456-462.

[129]   Boheim, G. *J. Membrane Biol.* **1974**, *19*, 277-303.

[130]   Curl, C. L.; Price, K. R.; Fenwick, G. R. *J. Sci. Food Agric.* **1988**, *43*, 101–107.

[131]   Rao, G. V.; Rao, P. S.; Tomimori, T.; Kizu, H. *J. Nat. Prod.* **1985**, *48*, 135–138.

[132]   Kitagawa, I.; Yoshikawa, M.; Wang, H. K.; Saito, M.; Tosirisuk, V.; Fujiwara, T.; Tomita, K. *Chem. Pharm. Bull.* **1982**, *30*, 2294–2297.

[133]   Kinjo, J.; Hatakeyama, M.; Udaayama, M.; Tsutanaga, Y.; Yamashita, M.; Nohara, T.; Yoshiki, Y.; Okubo, K. *Biosci. Biotechnol. Biochem.* **1998**, *62*, 429-433.

[134]   Yoshikawa, M.; Wang, H. K.; Kayakiri, H.; Taniyama, T.; Kitagawa, I. *Chem. Pharm. Bull.* **1985**, *33*, 4267–4274.

[135]   Yoshikawa, M.; Shimada, H.; Komatsu, H.; Sakurama, T.; Nishida, N.; Yamahara, J.; Shimoda, H.; Matsuda, H.; Tani, T. *Chem. Pharm. Bull.* **1997**, *45*, 877–882.

[136]   Kitagawa, I.; Taniyama, T.; Murakami, T.; Yoshihara, M.; Yoshikawa, M. *Yakugaku Zasshi* **1988**, *108*, 547–554.

[137]   Miyao, H.; Sakai, Y.; Takeshita, T.; Kinjo, J.; Nohara, T. *Chem. Pharm. Bull.* **1996**, *44*, 1222–1227.

[138]   Kitagawa, I.; Saito, M.; Taniyama, T.; Yoshikawa, M. *Chem. Pharm. Bull.* **1985**, *33*, 1069–1076.

[139]   Lee, S. Y.; Kim, J. S.; Shim, S. H.; Kang, S. S. *Bull. Korean Chem. Soc.* **2011**, *32*, 3650–3654.

[140]   Shiraiwa, M.; Harada, K.; Okubo, K. *Agric. Biol. Chem.* **1991**, *55*, 911-917.

[141] Shimoyamada, M.; Kudo, S.; Okubo, K.; yamauchi, F.; Harada, K. *Agric. Biol. Chem.* **1990**, *54*, 77-81.

[142] Chang, S. Y.; Han, M. J.; Han, S. J.; Kim, D. H. *Biomol. Ther.* **2009**, *17*, 430-437.

[143] Rupasinghe, H. P. V.; Jackson, C. J. C.; Poysa, V.; Berardo, C. D.; Bewley, D. J.; Jenkinson, J. *J. Agric. Food Chem.* **2003**, *51*, 5888-5894.

[144] Wink, M. *Curr. Drug Metab.* **2008**, *9*, 996-1009.

[145] Lee, M. R.; Chen, C. M.; Hwang, B. H.; Hsu, L. M. *J. Mass Spectrom.* **1999**, *34*, 804-812.

[146] Hu, J.; Zheng, Y. L.; Hyde, W.; Hendrich, S.; Murphy, P. A. *J. Agric. Food Chem.* **2004**, *52*, 2689-2696.

[147] Chang, S. Y.; Han, M. J.; Joh, E. H.; Kim, D. H. *J. Pharm. Pharmacol.* **2010**, *52*, 752-756.

[148] Gestetner, B.; Birk, Y.; Tencer, Y. *J. Agric. Food Chem.* **1968**, *16*, 1031-1035.

[149] Hawksworth, G.; Drasar, B. S.; Hill, M. J. *J. Med. Microbiol.* **1971**, *4*, 451-459.

[150] Okubo, K.; Yoshiki, Y. *Adv. Exp. Med. Biol.* **1996**, *405*, 141-154.

[151] Nishida, M.; Hyeon, S. B.; Isogai, A.; Suzuki, A. *Agric. Biol. Chem.* **1981**, *45*, 2637-2638.

[152] Woldemichael, G. M.; Wink, M. *Phytochemistry* **2002**, *60*, 323-327.

[153] Adel, M. M.; Sehnal, F.; Jurzysta, M. *J. Chem. Ecol.* **2000**, *26*, 1065-1078.

[154] Hayashi, H.; Huang, P. Y.; Inoue, K. *Plant Cell Physiol.* **2003**, *44*, 404-411.

[155] Yasuda, T. *Entomol. Exp. Appl.* **1997**, *82*, 349-354.

[156] Severson, R. F.; Rogers, C. E.; Marti, O. G.; Gueldner, R. C.; Arrendale, R. F. *Agric. Biol. Chem.* **1991**, *55*, 2527-2530.

[157] Blom, D.; Fabbri, C.; Connor, E. C.; Schiestl, F. P.; Klauser, D. R.; Boller, T.; Eberl, L.; Weisskopf, L. *Environ. Microbiol.* **2011**, *13*, 3047-3058.

[158] Juniper, B. E.; Robins, R. J.; Joel, D. *The carnivorous plants.* **1989**, pp 86, London, UK: Academic Press.

[159] Clarke, C. M. *Nepenthes of Borneo.* **1997**, Sabah, Malaysia: Natural History Publications (Borneo), Kota Kinabalu.

[160] Moran, J. A. *J. Ecol.* **1996**, *84*, 515-525.

[161] Clarke, C. M.; Bauer, U.; Lee, C. C.; Tuen, A. A.; Rembold, K.; Moran, J. A. *Biol. Lett.* **2009**, *5*, 632-635.

[162] Chin, L. J.; Moran, J. A.; Clarke, C. *New Phytol.* **2010**, *186*, 461-470.

[163]   D′Amato, P. *The savage Garden: cultivating carnivorous plants.* **1998**, Ten Speed Press, Brekeley.

[164]   Phillipps, A.; Lamb, A.; Lee, C. *Pitcher-Plants of Borneo.* **1996**, pp 100, Natural History Publications (Borneo), Kota Kinabalu.

[165]   Oldham, N. J.; Svatoš, A. *Rapid Commun. Mass Spectrom.* **1999**, *13*, 331–336.

[166]   Van Pelt, C. K.; Carpenter, B. K.; Brenna, J. T. *J. Am. Soc. Mass Spectrom.* **1999**, *10*, 1253–1262.

[167]   Michaud, A. L.; Diau, G. Y.; Abril, R.; Brenna, J. T. *Anal. Biochem.* **2002**, *307*, 348–360.

[168]   Bus, J.; Sies, I.; Lie Ken Jie, M. S. F. *Chem. Phys. Lipids* **1976**, *17*, 501-518.

[169]   Curstedt, T. *Biochim. Biophys. Acta.* **1974**, *360*, 12-23.

[170]   Isidorov, V. A.; Rusak, M.; Szczepaniak, L.; Witkowski, S. *J. Chromatogr. A* **2007**, *1166*, 207-211.

[171]   Barber, M.; Chapman, J. R.; Wolstenholme, W. A. *J. Mass Spectrom. Ion Phys.* **1968**, *1*, 98.

[172]   Myher, J. J.; Kuksis, A.; Marai, L.; Yeung, S. K. F.; *Anal. Chem.* **1978**, *50*, 557-561.

[173]   Zöllner, P. *Eur. Mass Spectrom.* **1997**, *3*, 309-315.

[174]   Christie, W. W. *Gas chromatography and lipids: a practical guide.* **1989**, The oily Press, Ayr, Scotland.

[175]   Lauer, W. M.; Aasen, A. J.; Graff, G.; Holman, R. T. *Lipids* **1970**, *5 (11)*, 861-868.

[176]   Moldoveanu. S. C.; Chang, Y. *J. Agric. Food Chem.* **2011**, *59*, 2137-2147.

[177]   Emmons, L. H. Frugivory in treeshrews (*Tupaia*). *American Naturalist* **1991**, *138*, 642-649.

[178]   Erica, H. G.; Fernando, C.; Ruben, R. R.; Francisco, J. A. A. *Planta Med.* **2007**, *73*, 236–240.

[179]   Filomena, C.; Giancarlo, S.; Monica, R. L.; Gianni, S.; Ferruccio, P.; Francesco, M. *Biol. Pharm. Bull.* **2005**, *28*, 1098–1102.

[180]   Lee, J. Y.; Kim, Y. S.; Shin, D. H. *J. Agric. Food Chem.* **2002**, *50*, 2193–2199.

[181]   Philippoussis, F.; Arguin, C.; Mateo, V.; Steff, A. M.; Hugo, P. *Blood* **2003**, *101*, 292–294.

[182]   Cho, K. H.; Hong, J. H.; Lee, K. T. *J. Med. Food* **2010**, *13*, 99-107.

[183]   Marshall, D. L.; Beattie, A. J.; Bollenbacher, W. E. *J. Chem. Ecol.* **1979**, *5*, 335–334.

[184]   Skidmore, B. A.; Heithaus, E. R. *J. Chem. Ecol.* **1988**, *14*, 2185–2196.

[185]   Siddhanti, S. R.; Trumbo, P. R.; Polokoff, R. S.; King, M. W.; Tove, S. B *J. Nutr.* **1987**, *117*, 1671-1675.

[186]   Roche Pronase Cat. No. 165921

[187]   Mueller, P.; Rudin, D. O.; Tien, H. T.; Wescott, W. C. *J. Phys. Chem.* **1963**, *67*, 534–535.

[188]   Shevchenko, A.; Tomas, H.; Havliš, J.; Olsen, J. V.; Mann, M. *Nat. Protoc.* **2006**, *1*, 2856–2860.

[189]   Shevchenko, A.; Sunyaev, S.; Loboda, A.; Bork, P.; Ens, W.; Standing, K. G. *Anal. Chem.* **2001**, *73*, 1917–1926.

[190]   Mithöfer, A.; Mazars, C. *Biol. Proced. Online* **2002**, *4*, 105–118.

[191]   Vadassery, J.; Ranf, S.; Drzewiecki, C.; Mithöfer, A.; Mazars, C.; Scheel, D.; Lee, J.; Oelmüller, R. *Plant J.* **2009**, *59*, 193–206.

[192]   Pfaffl, M. W. *Nucleic Acids Res*. **2001**, *29*, 2002–2007.

[193]   Hungate, R. E. *Methods Microbiol.*, New York Academic, **1969**, *33*, 117-132.

[194]   Miller, T. L.; Wolin, M. J. *Appl. Microbiol.* **1974**, *27*, 985-987.

[195]   Payot, E. S.; Guedon, E.; Cailliez, C.; Gelhaye, E.; Petitdemange, H. *Microbiol.* **1998**, *144*, 375-384.

[196]   Schulze, B.; Lauchli, R.; Sonwa, M. M.; Schmidt, A.; Boland, W. *Anal. Biochem.* **2006**, *348*, 269-283.

[197]   Kroiss, J.; Svatoš, A.; Kalterpoth, M. *J. Chem. Ecol.* **2011**, *37*, 420-427.

8 Appendix

8.1 Spectra Data

8.1.1 MS spectra data

ESI (+)-MS Spectrum of Soyasaponin V (**46**)
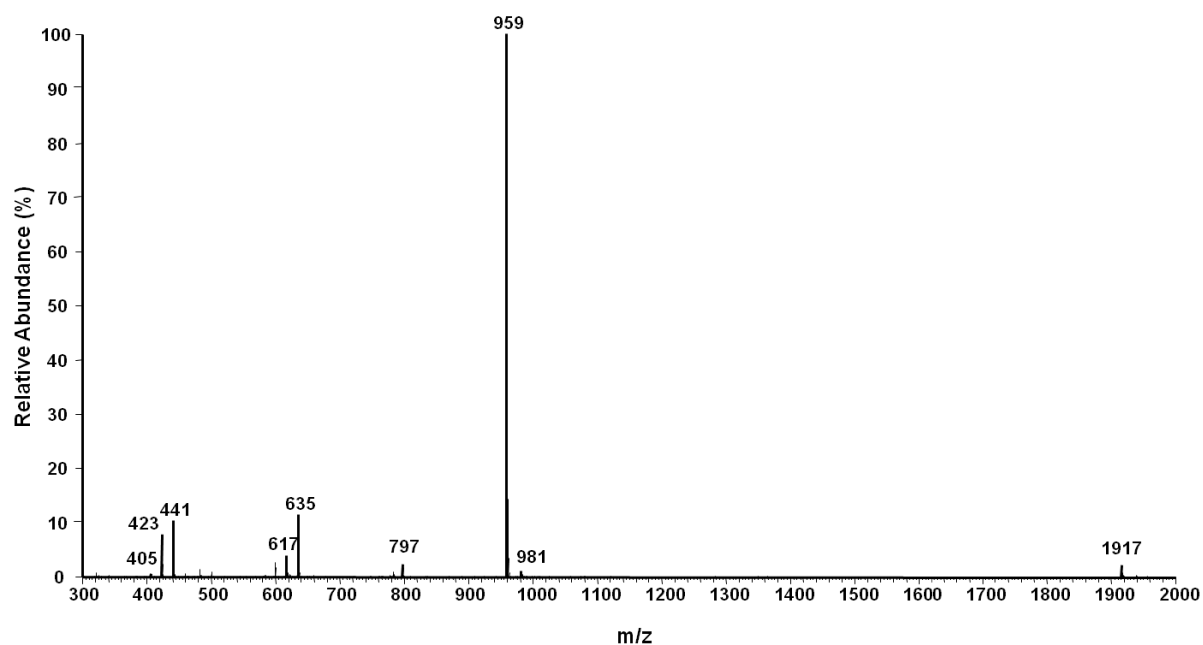
ESI (+)-MS Spectrum of Soyasaponin I (**47**)
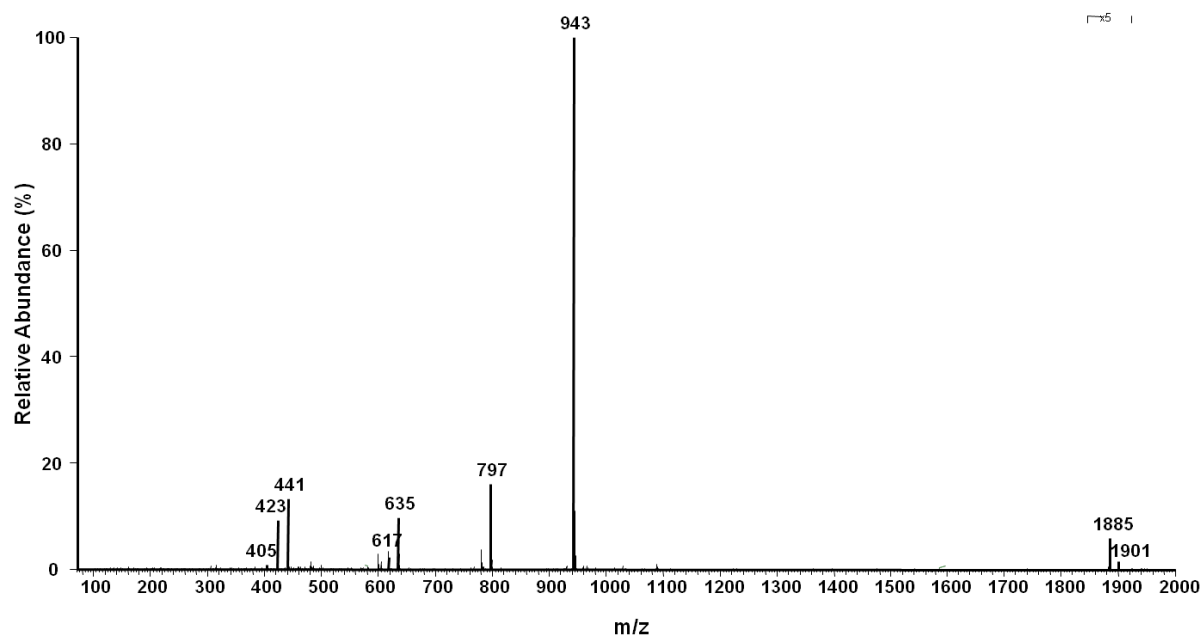
ESI (+)-MS Spectrum of Soyasaponin III (**48**)
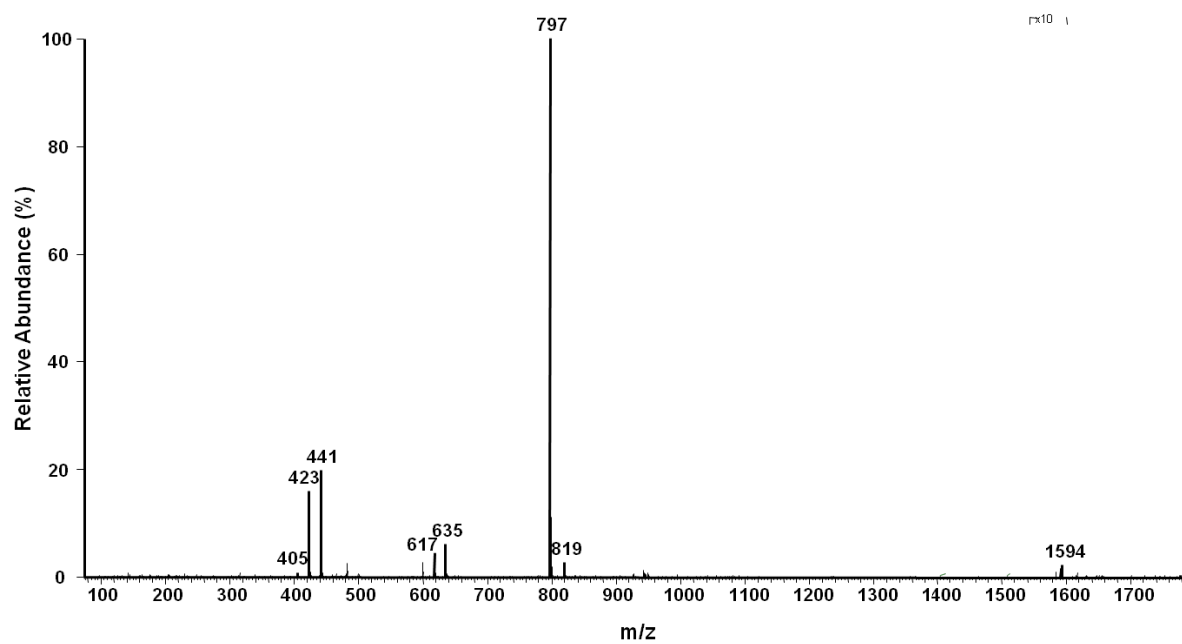
ESI (+)-MS Spectrum of Compound **49**
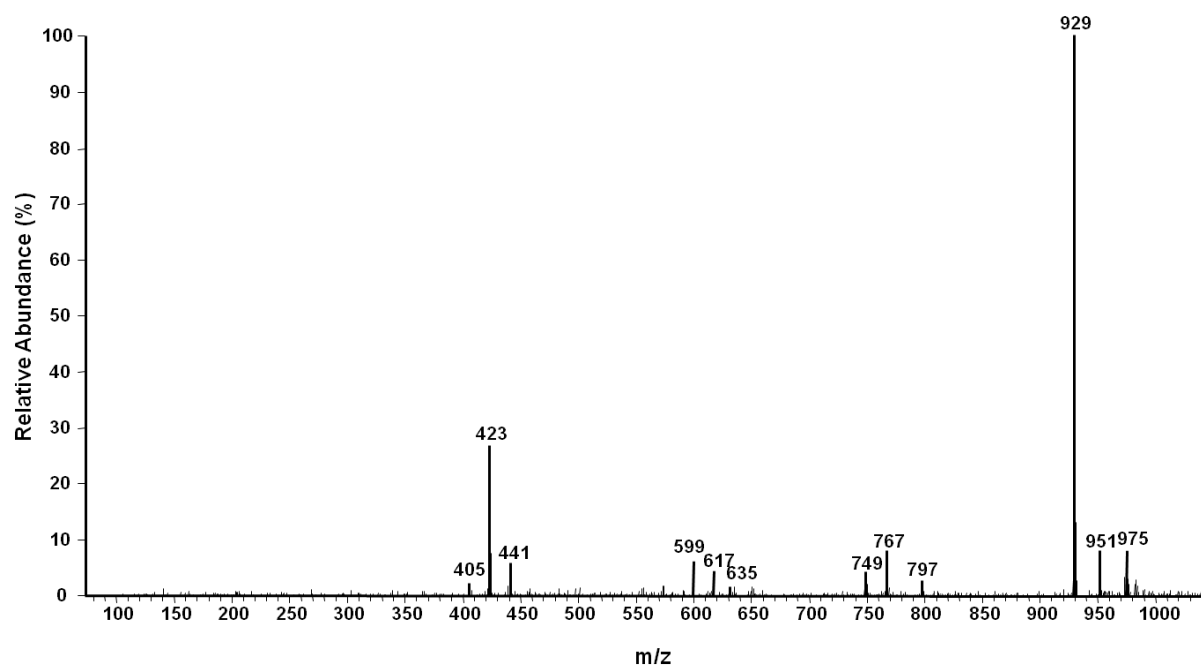
ESI (+)-MS Spectrum of Phaseoside I (**50**)
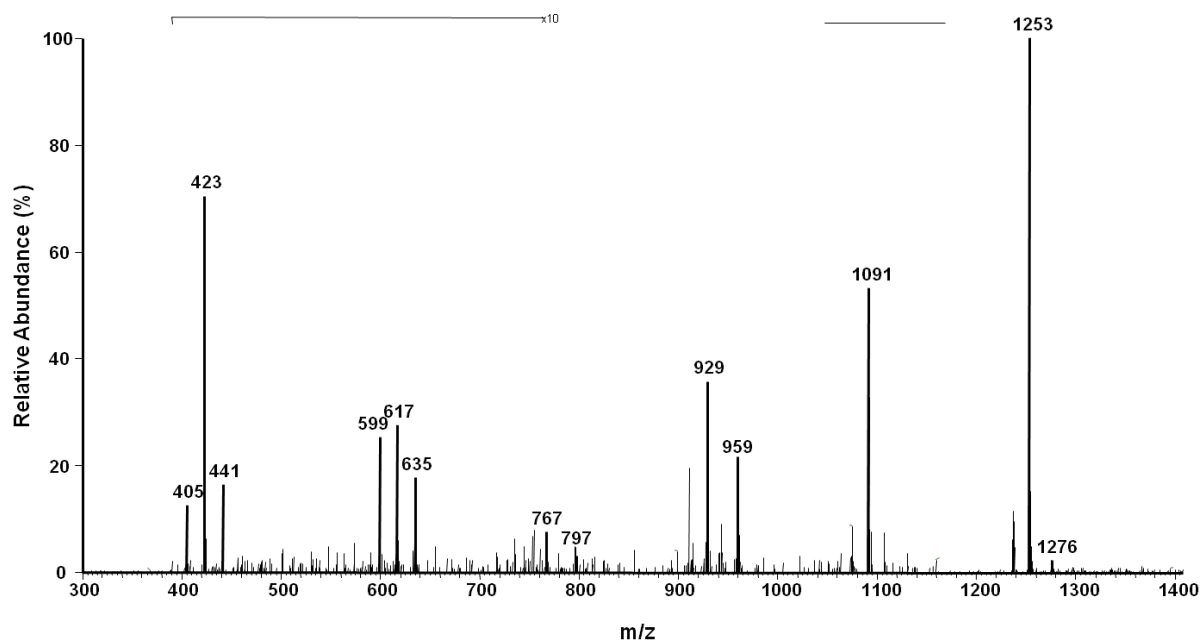
ESI (+)-MS Spectrum of Compound **51**
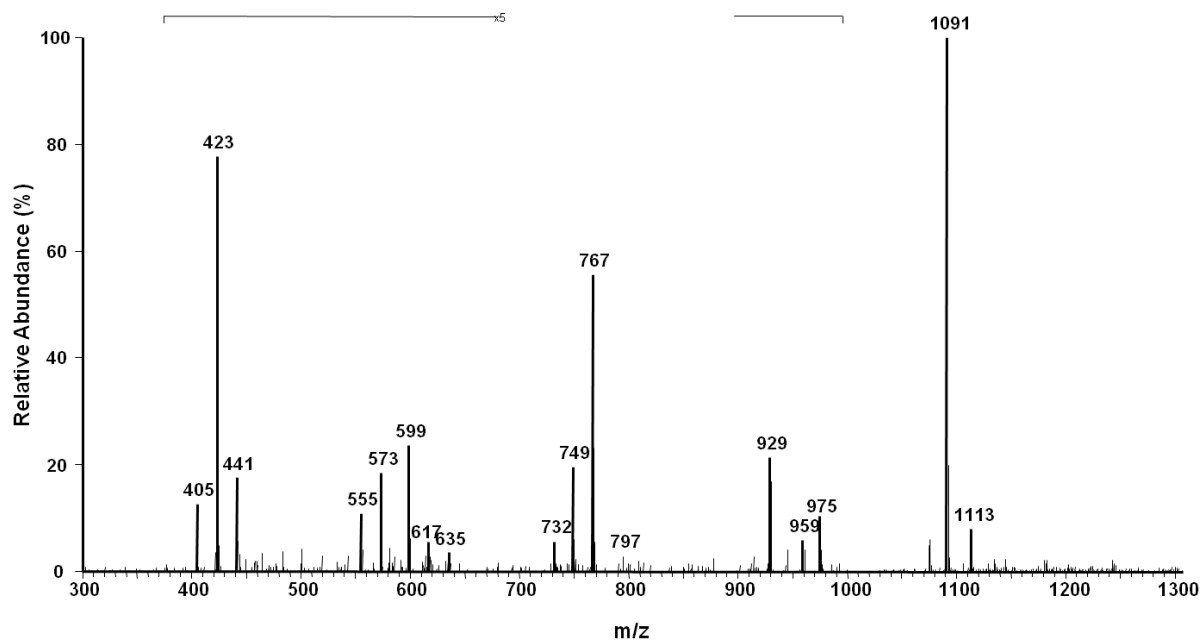
ESI (+)-MS Spectrum of Sophoraflavoside I (**52**)
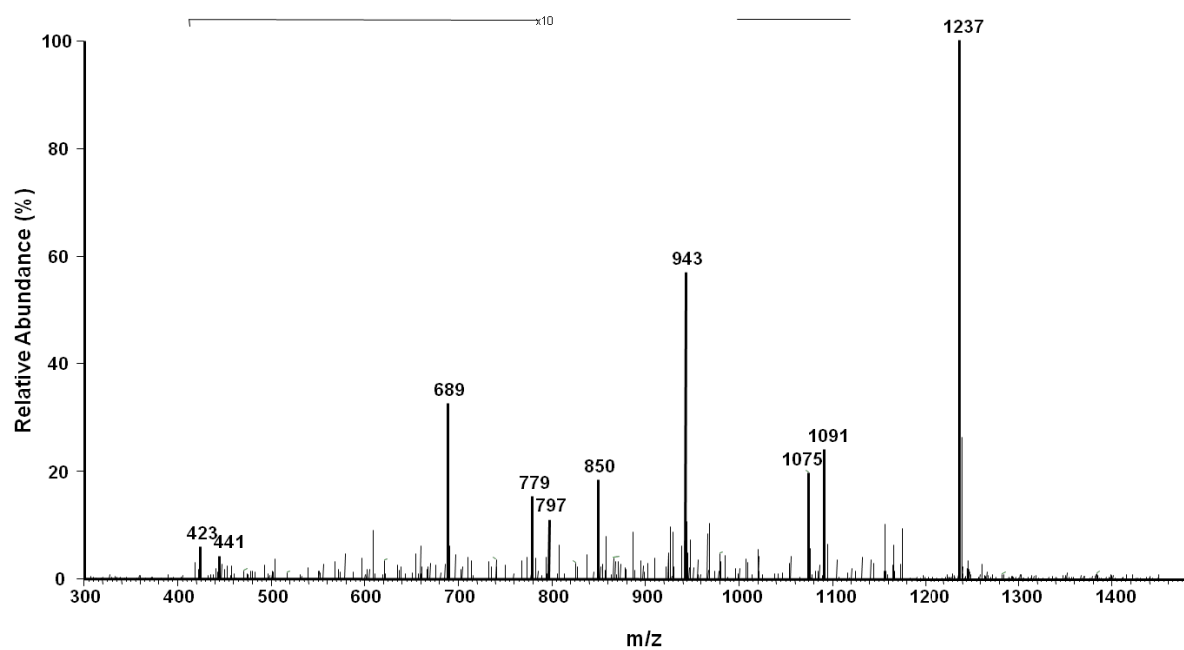
ESI (+)-MS Spectrum of Compound **53**
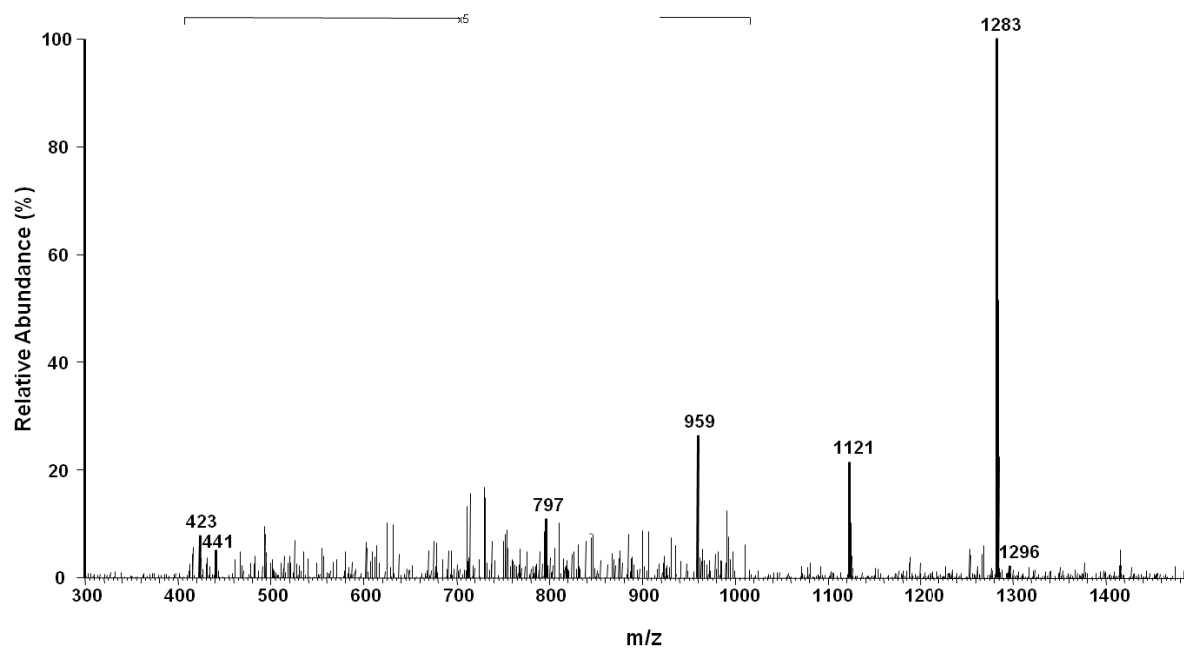
ESI (+)-MS Spectrum of Sandosaponin A (**54**)
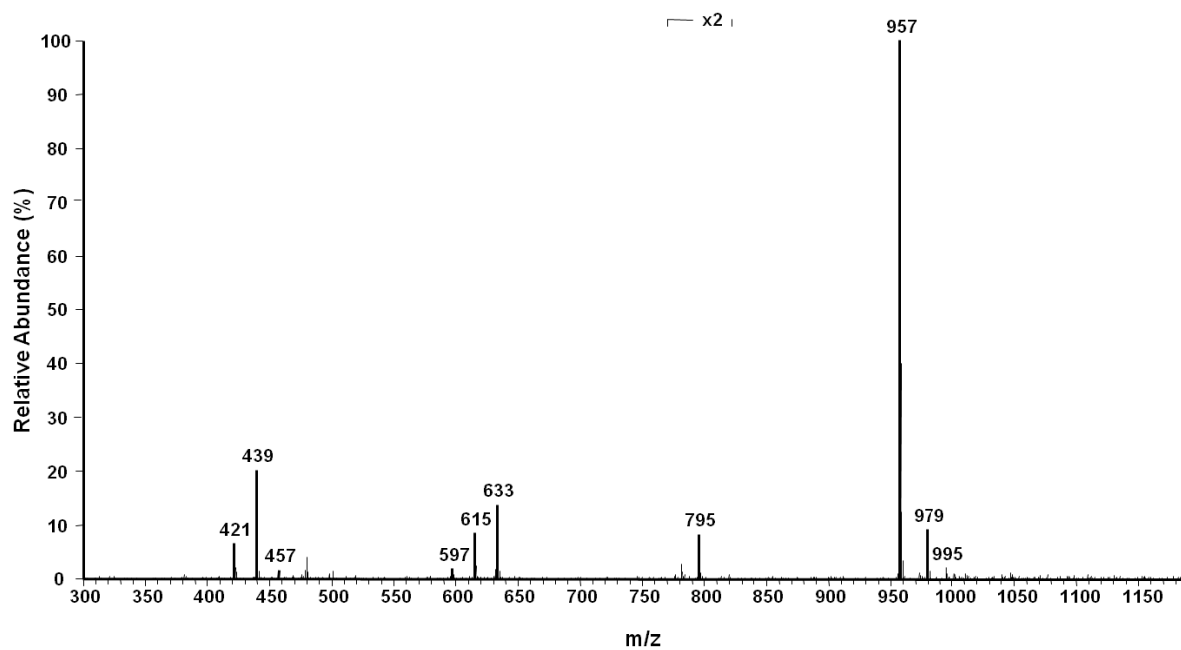
ESI (+)-MS Spectrum of Dehydrosoyasaponin I (**55**)
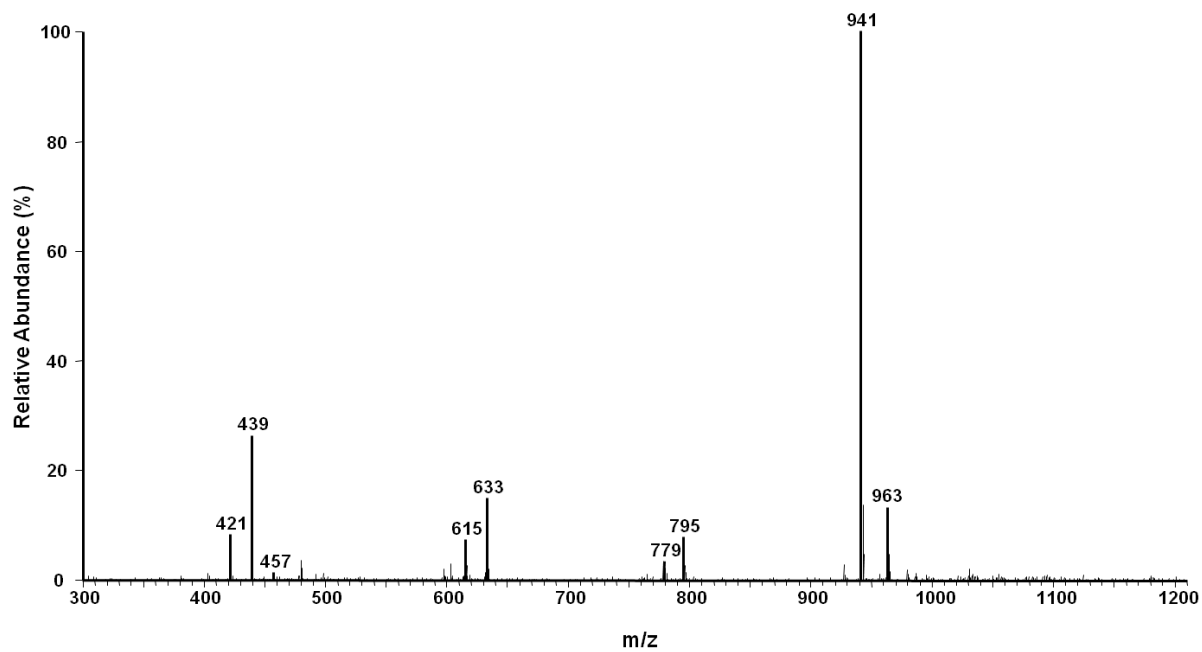
ESI (+)-MS Spectrum of Soyasaponin A1 (**56**)
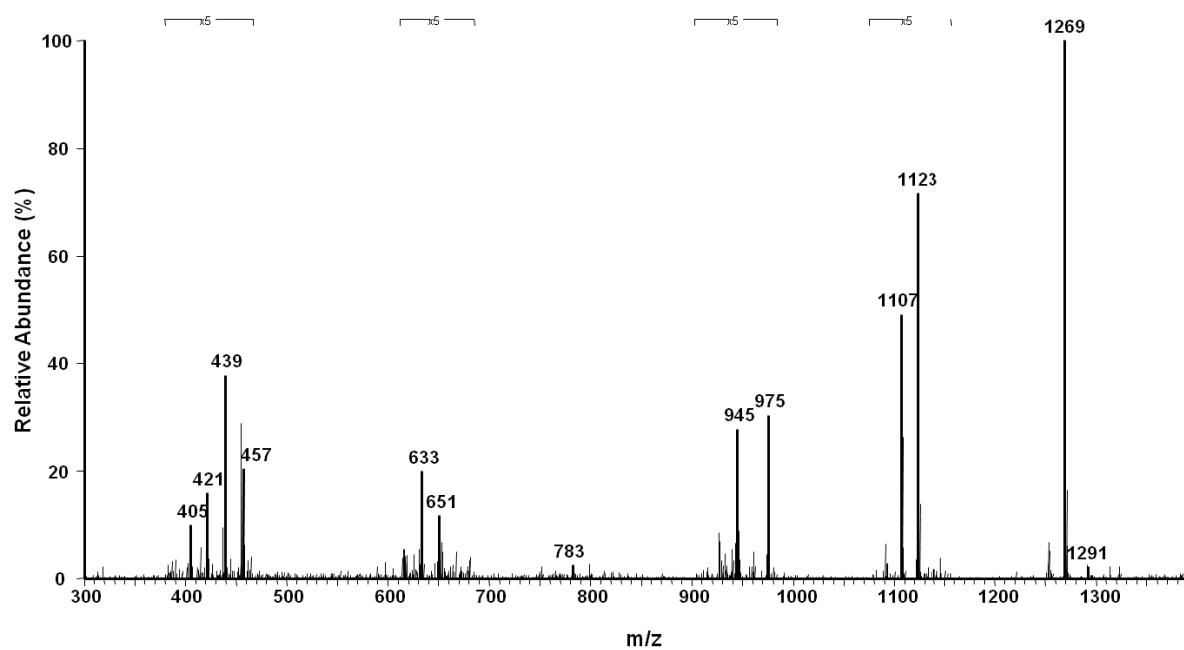
ESI (+)-MS Spectrum of Desglucosylsoyasaponin A1 (**57**)
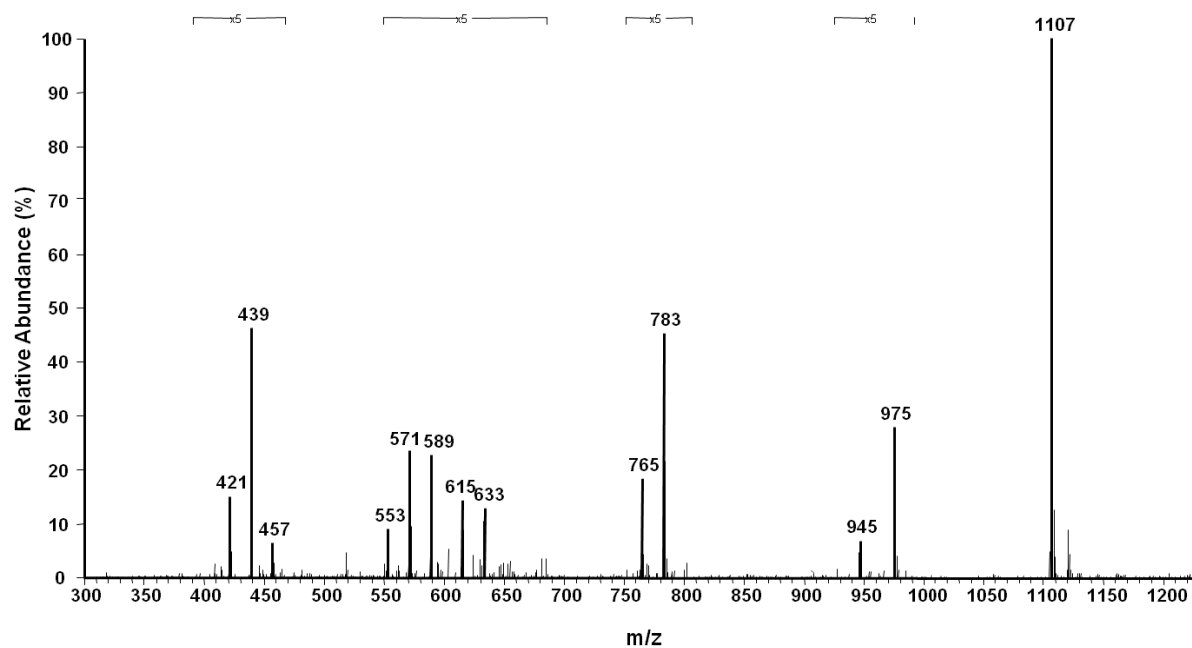
EI (+)-MS Spectrum of Pentadecane (**61**)
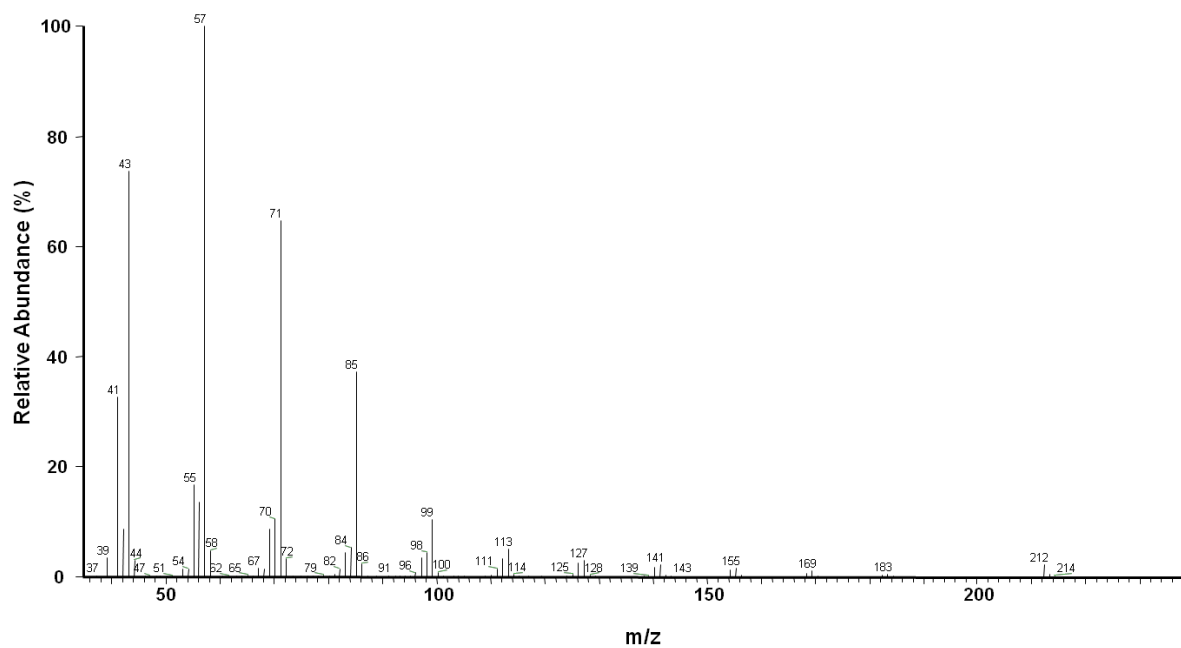
EI (+)-MS Spectrum of Tetradecane (**62**)
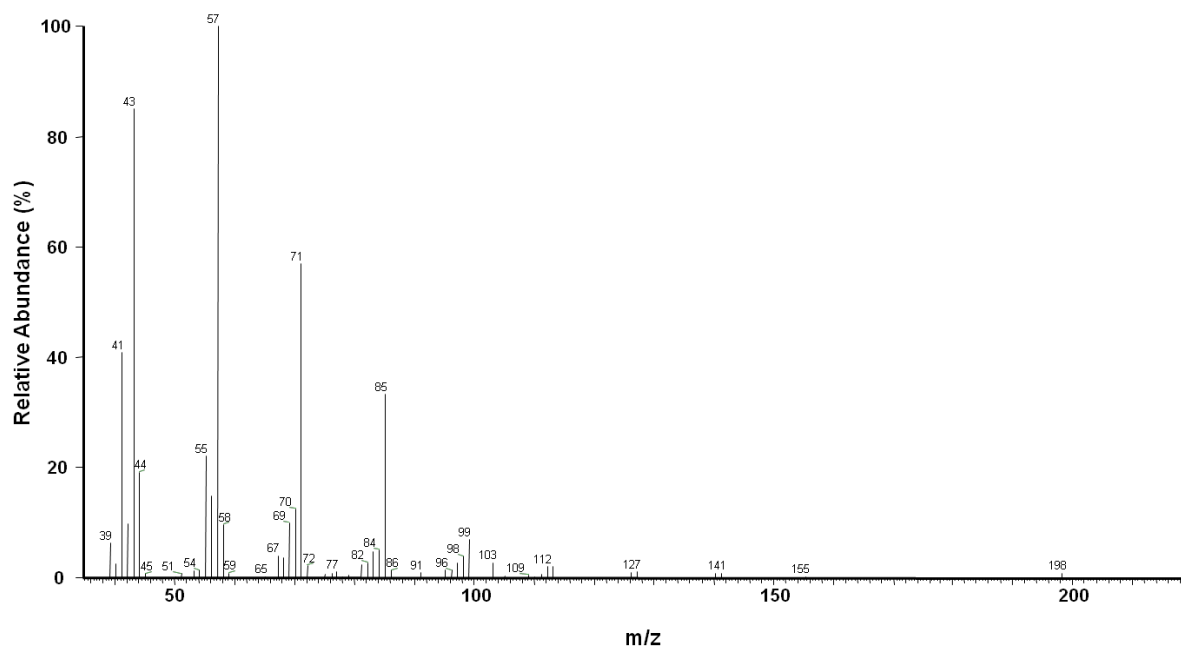
EI (+)-MS Spectrum of Heptadecane (**63**)
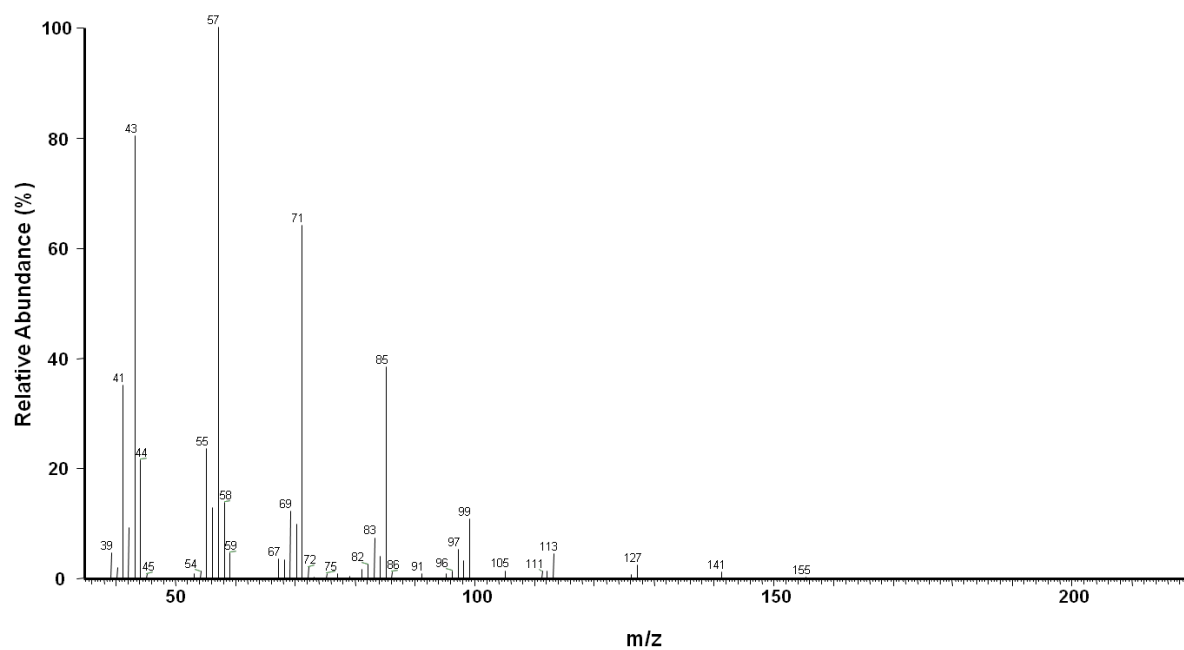
EI (+)-MS Spectrum of Lauric acid (**67**)-TMS ether
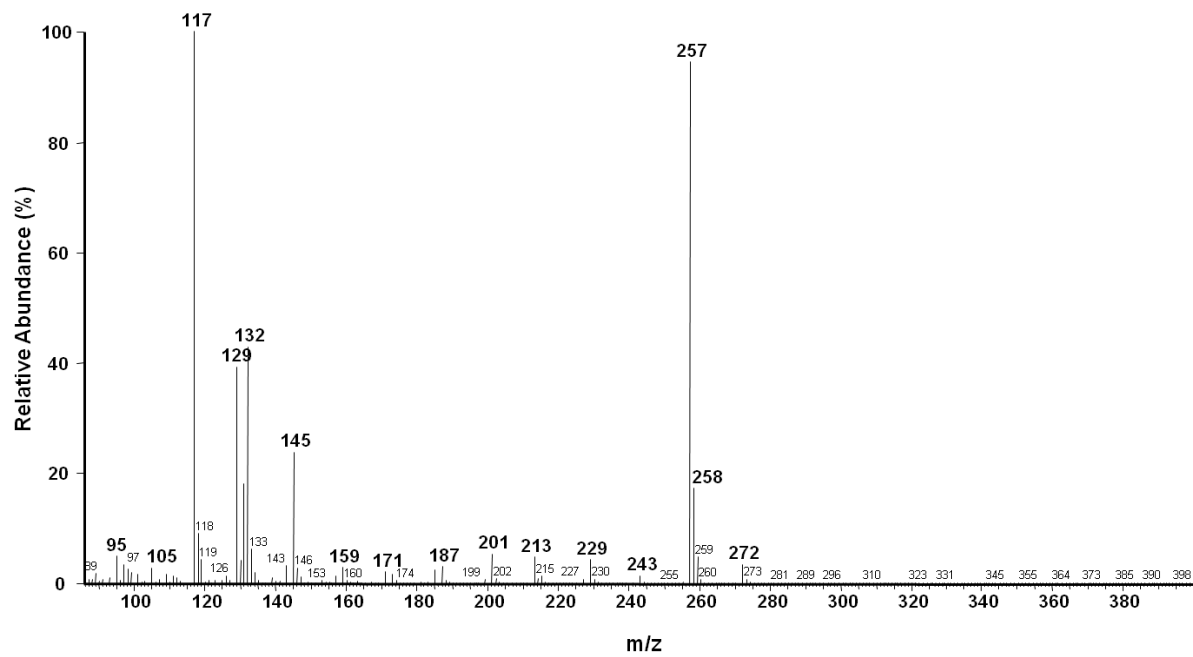
EI (+)-MS Spectrum of Myristic acid (**68**)-TMS ether
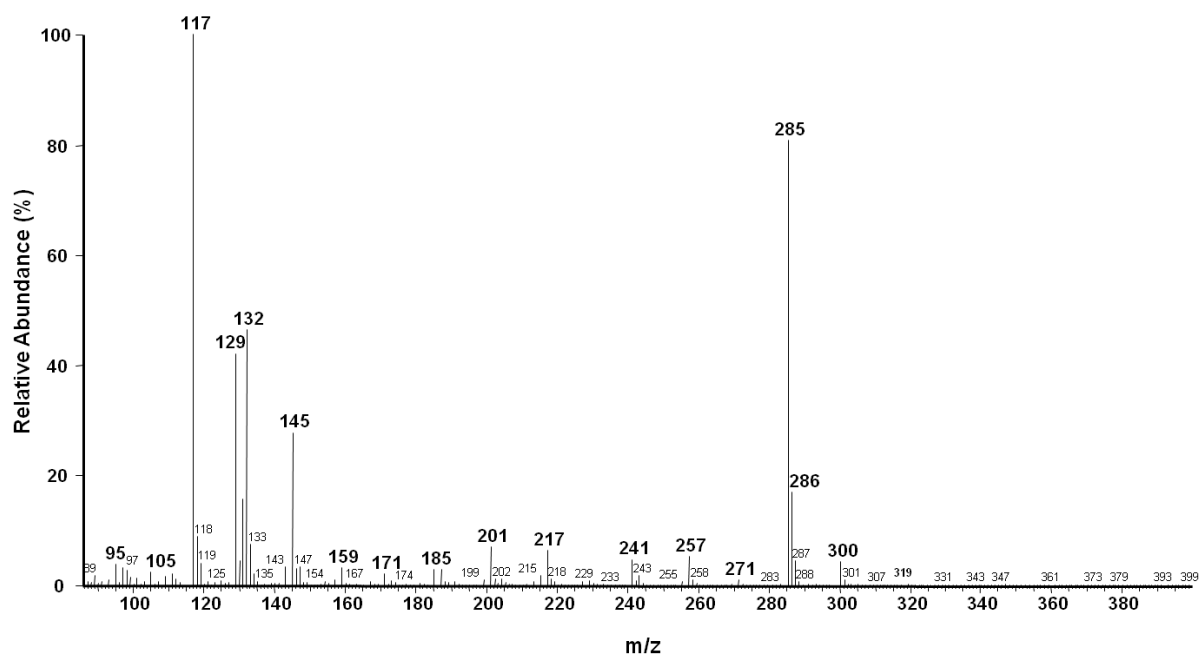
EI (+)-MS Spectrum of Palmitic acid (**69**)-TMS ether
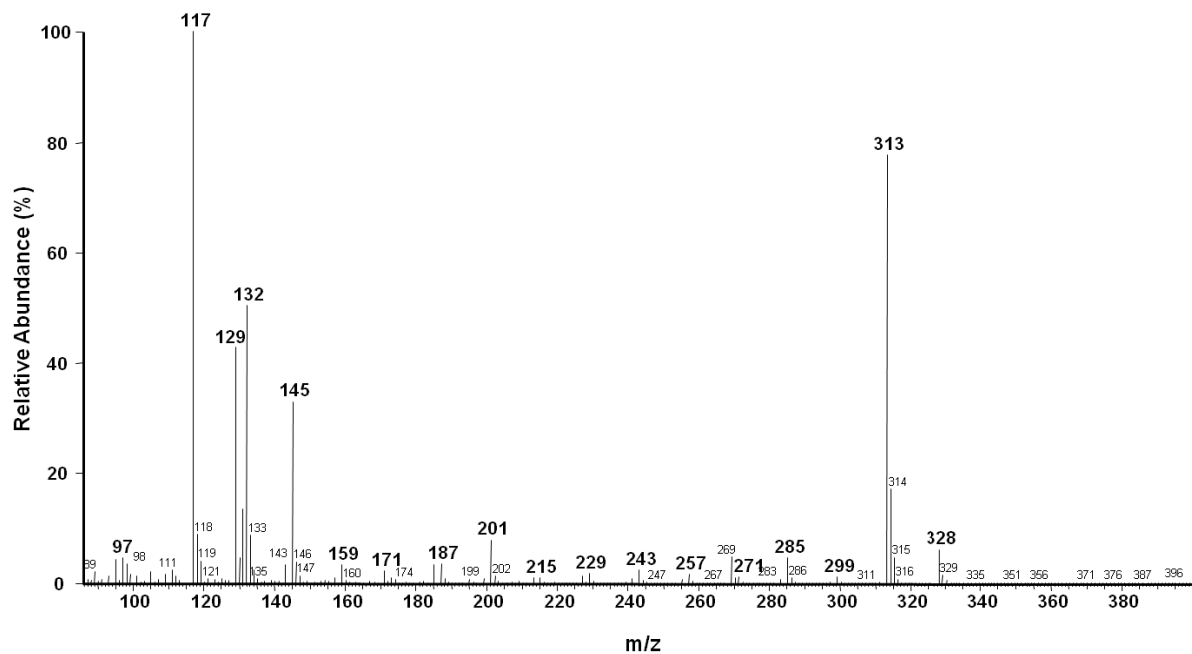
EI (+)-MS Spectrum of Stearic acid (**70**)-TMS ether
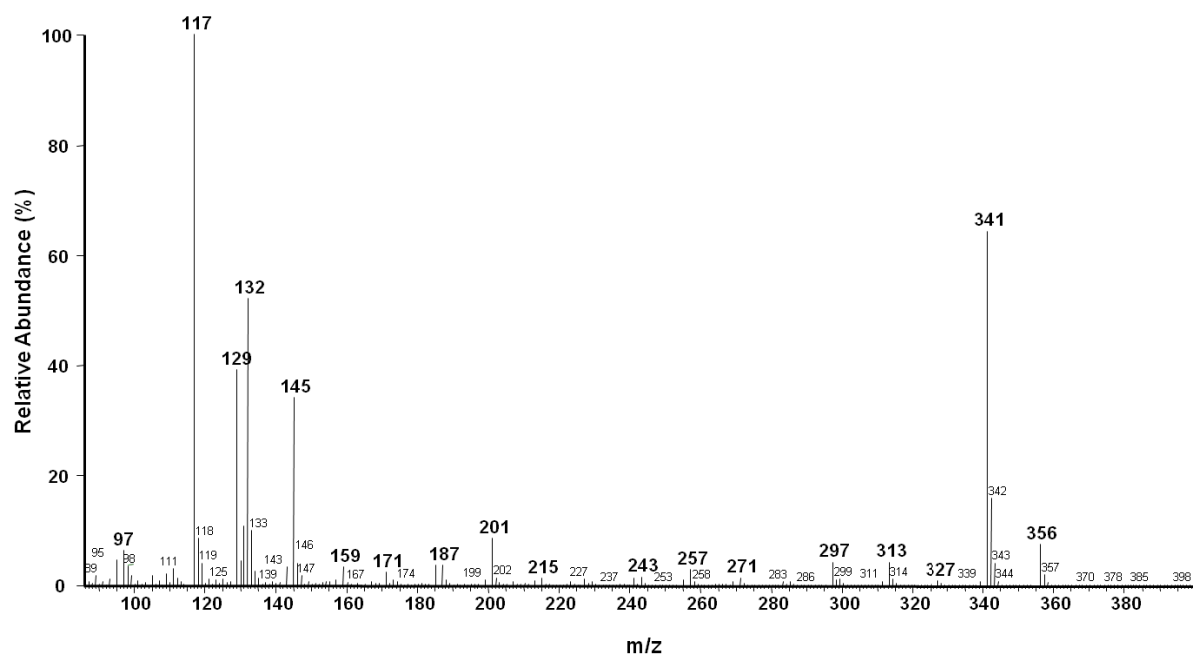
EI (+)-MS Spectrum of Arachidic acid (**71**)-TMS ether
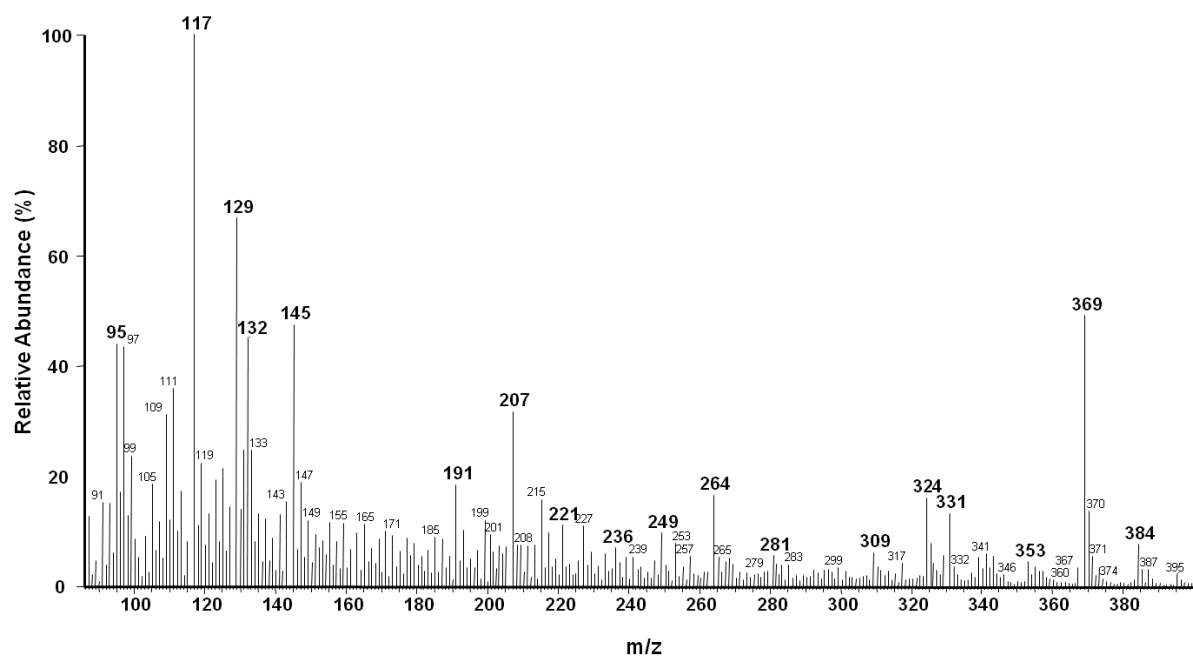
EI (+)-MS Spectrum of Behenic acid (**72**)-TMS ether
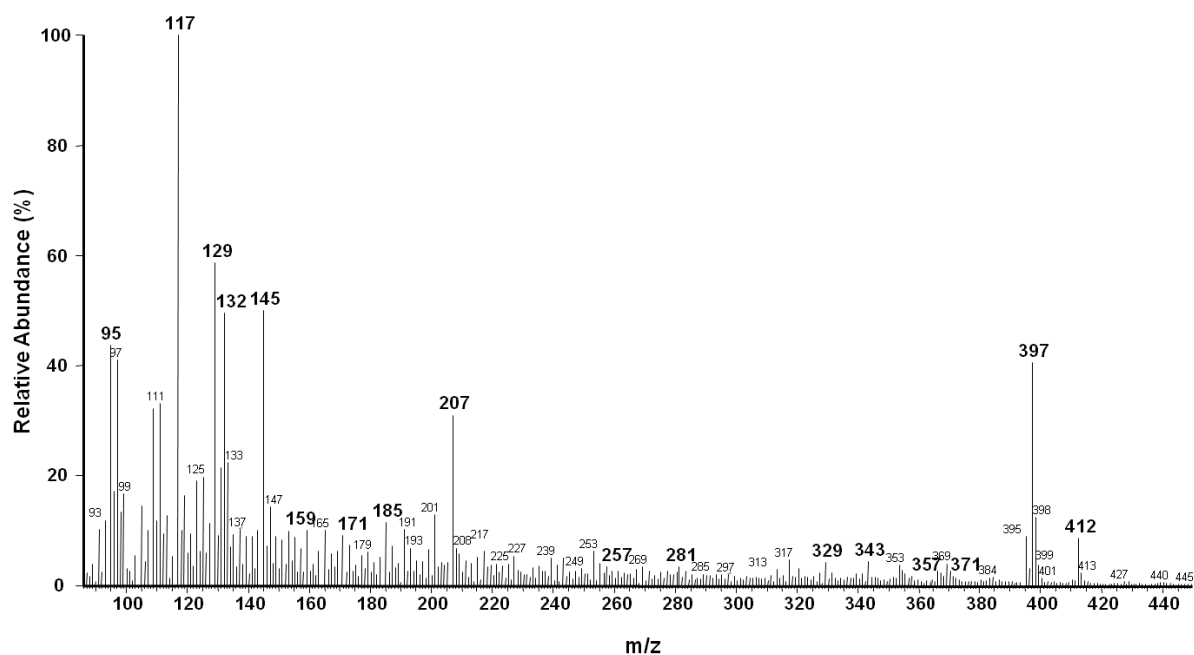
EI (+)-MS Spectrum of Lignoceric acid (**73**)-TMS ether
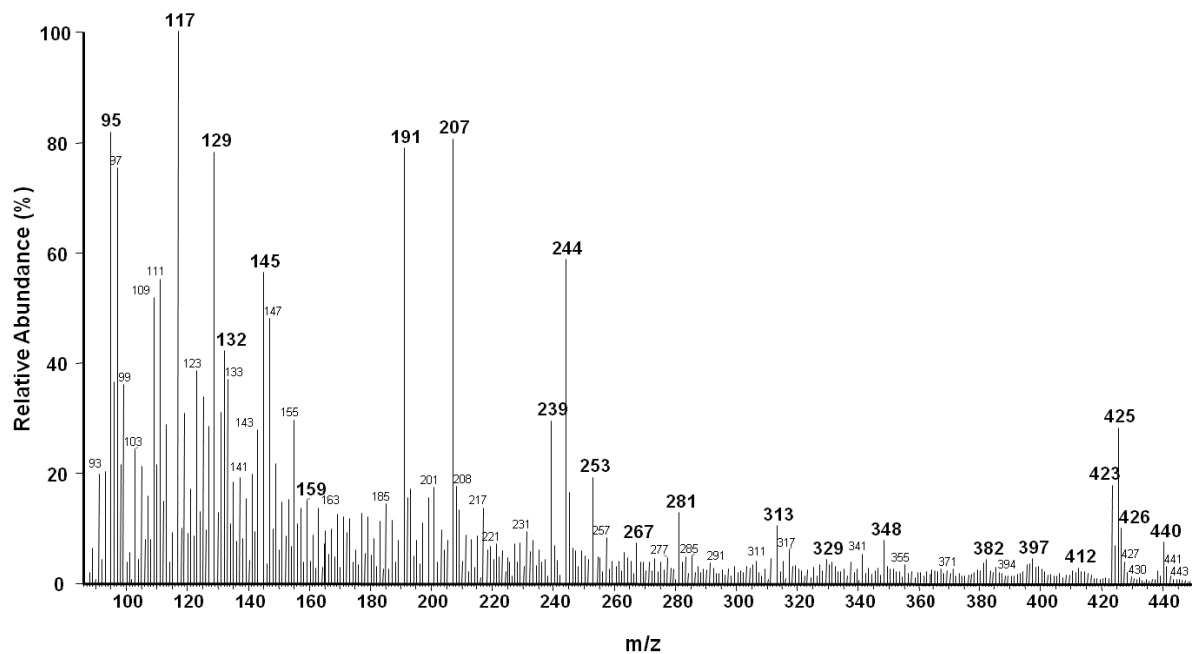
EI (+)-MS Spectrum of Palmitoleic acid (**74**)-TMS ether
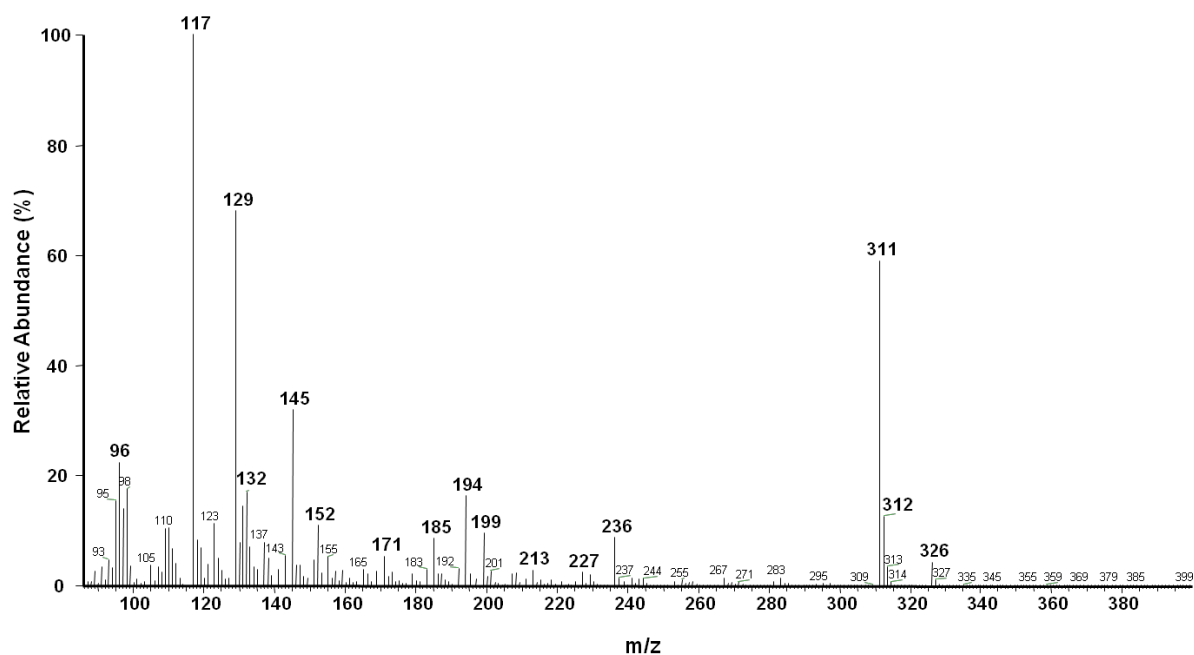
EI (+)-MS Spectrum of *cis*-11-Octadecenoic acid (**75**)/Oleic acid (**79**)-TMS ether
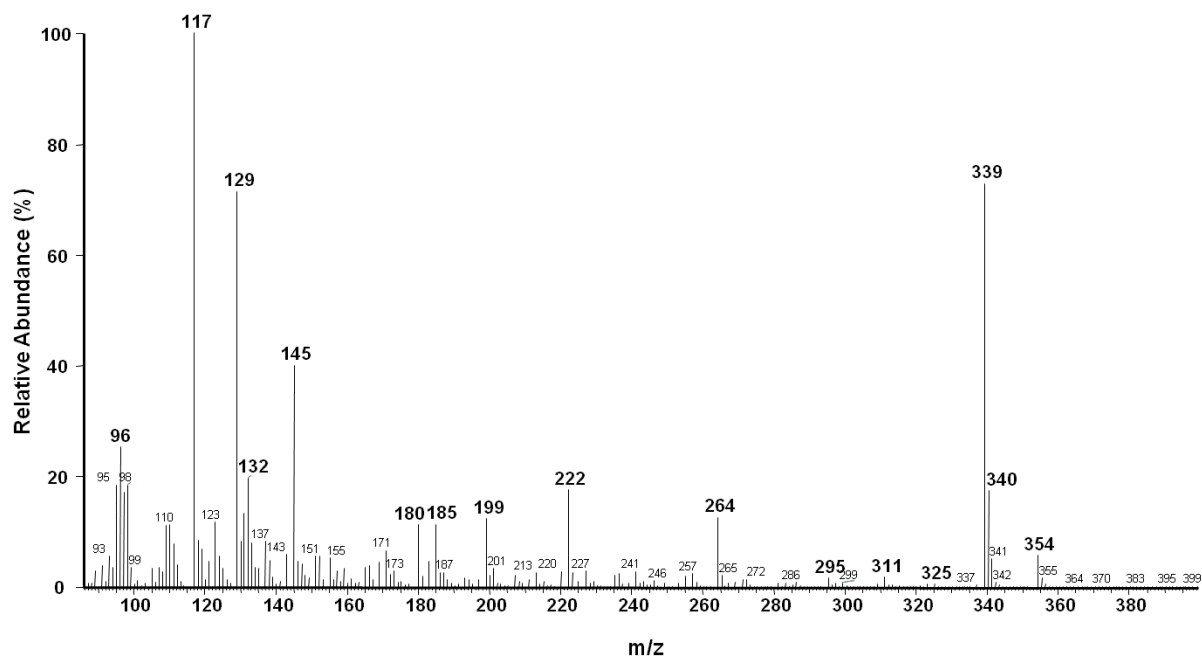
EI (+)-MS Spectrum of *cis*-13-Eicosenoic acid (**76**)/*cis*-11-Eicosenoic acid (**80**)-TMS ether
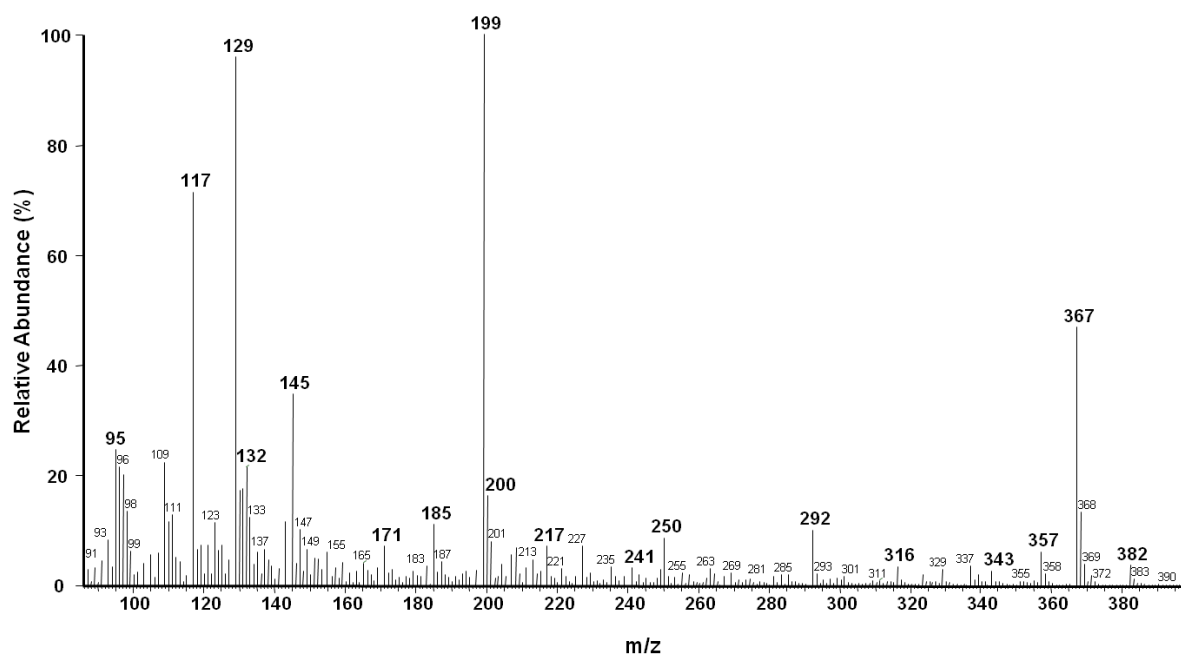
EI (+)-MS Spectrum of *cis*-15-Docosenoic acid (**77**)-TMS ether
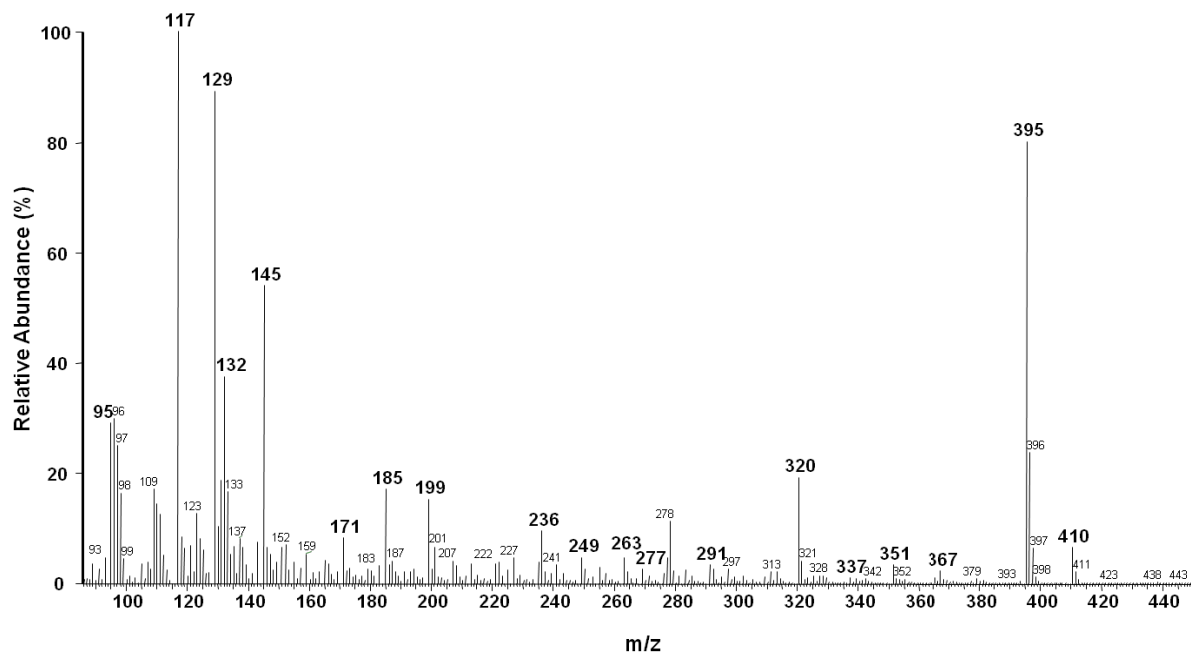
EI (+)-MS Spectrum of *cis*-17-Tetracosenoic acid (**78**)/Nervonic acid (**81**)-TMS ether
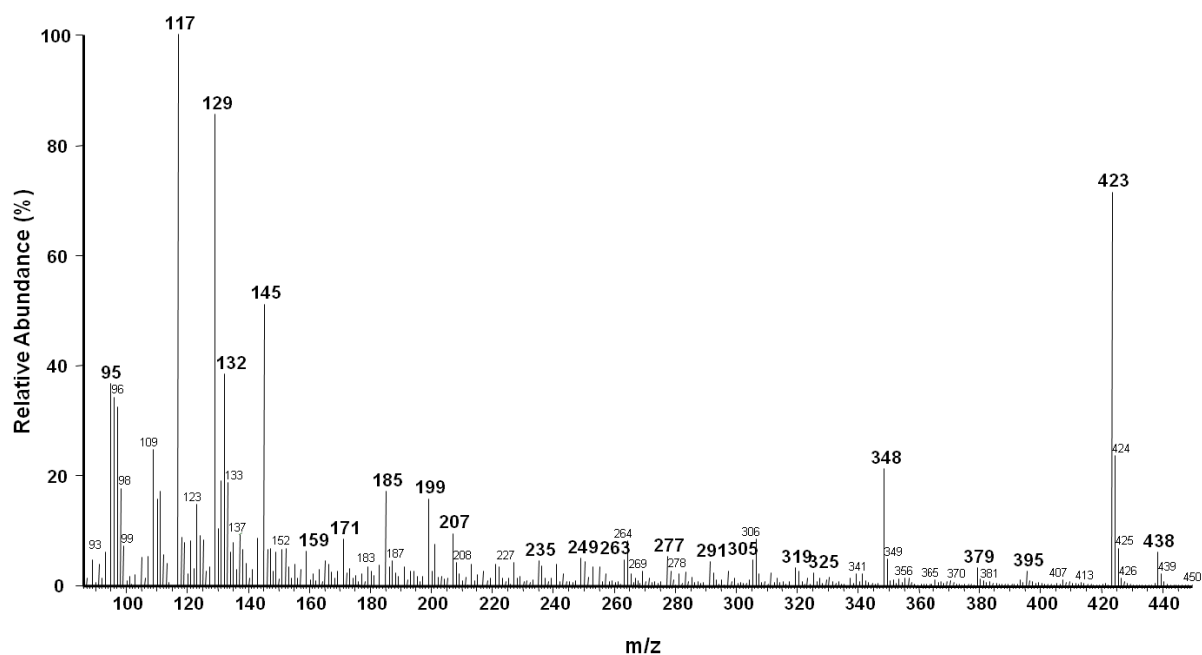
EI (+)-MS Spectrum of Linoleic acid (**82**)-TMS ether
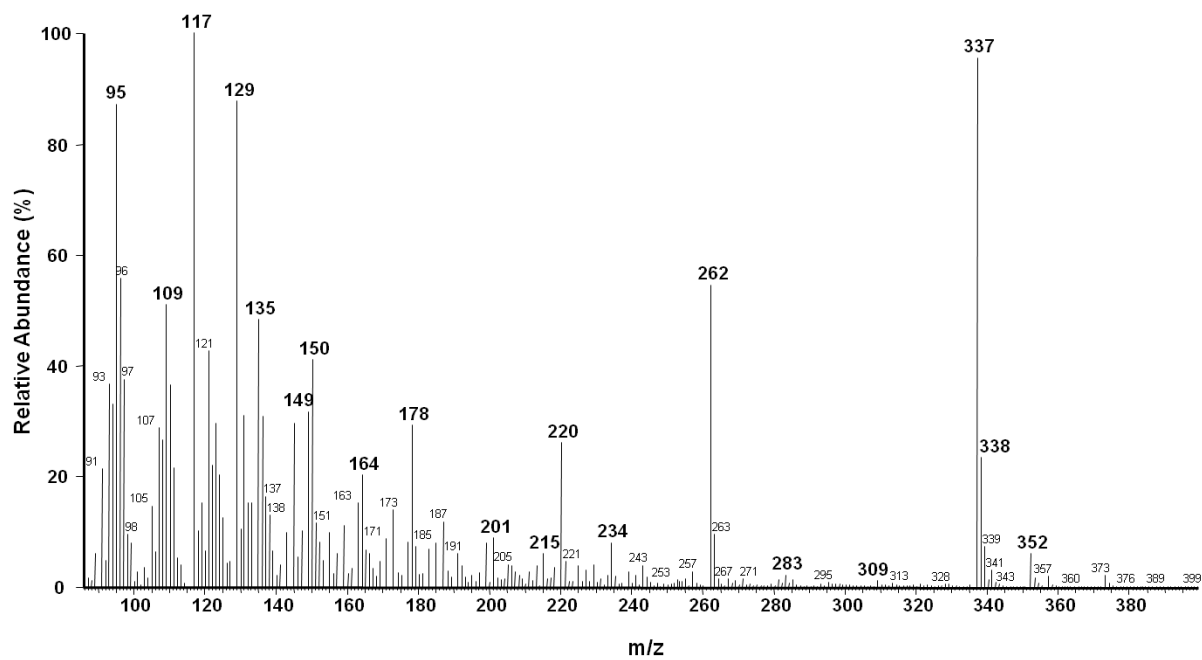
EI (+)-MS Spectrum of Glycerol 1-myristate (**83**)-TMS ether
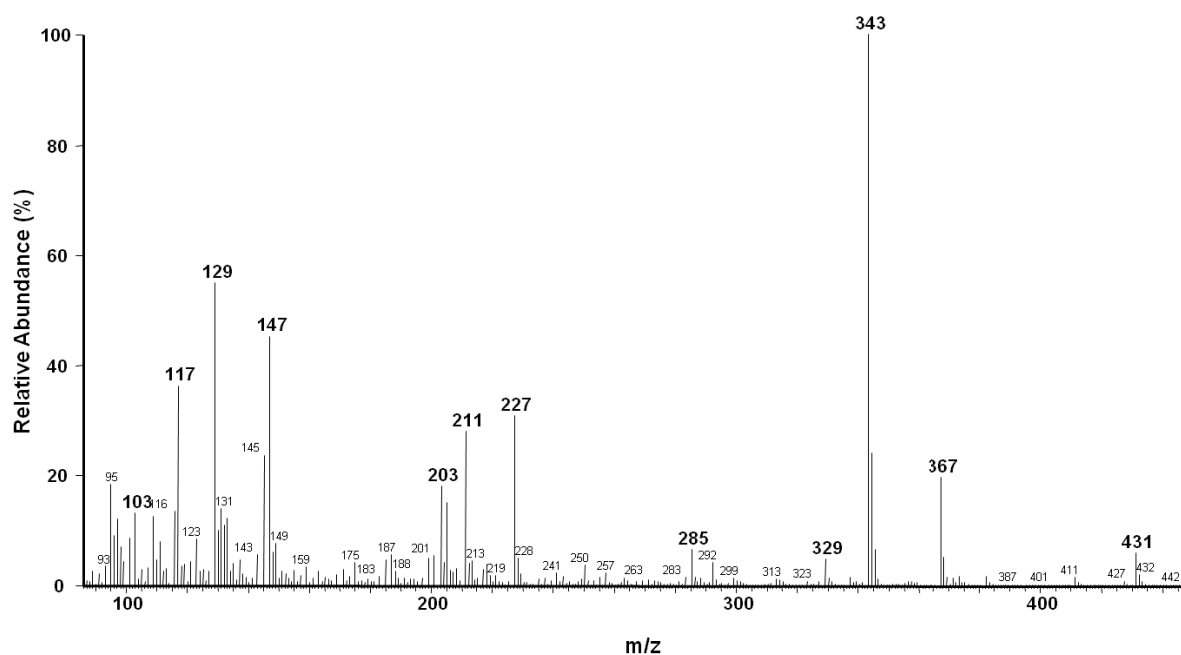
EI (+)-MS Spectrum of Glycerol 1-palmitate (**84**)-TMS ether
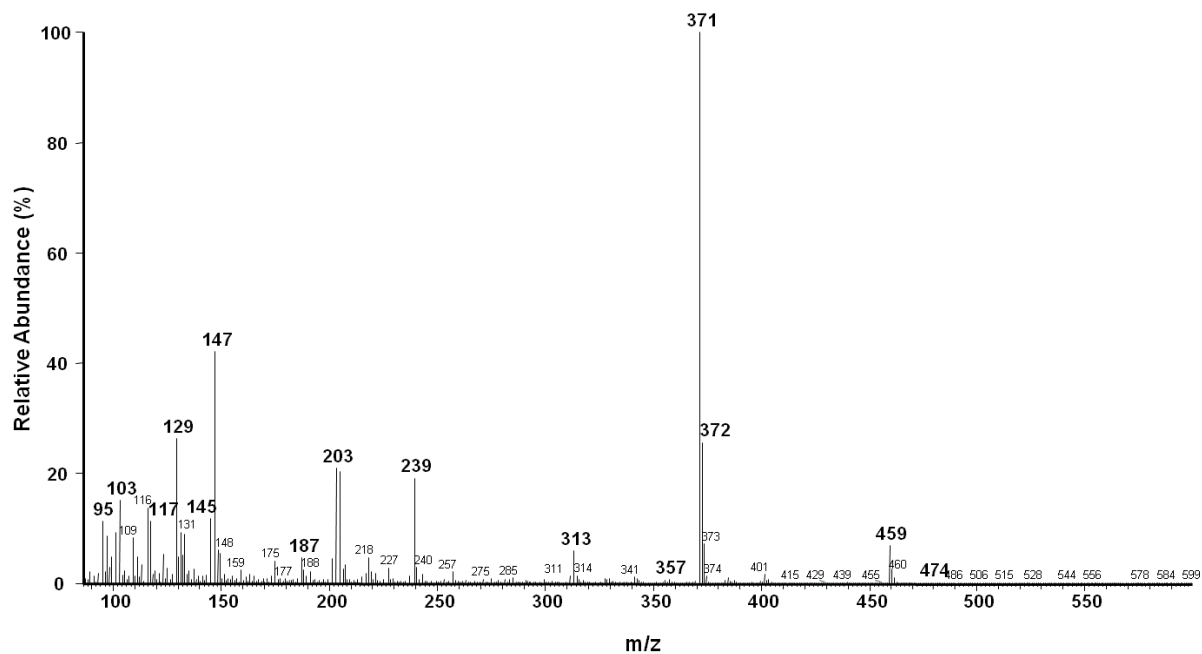
EI (+)-MS Spectrum of Glycerol 1-stearate (**85**)-TMS ether
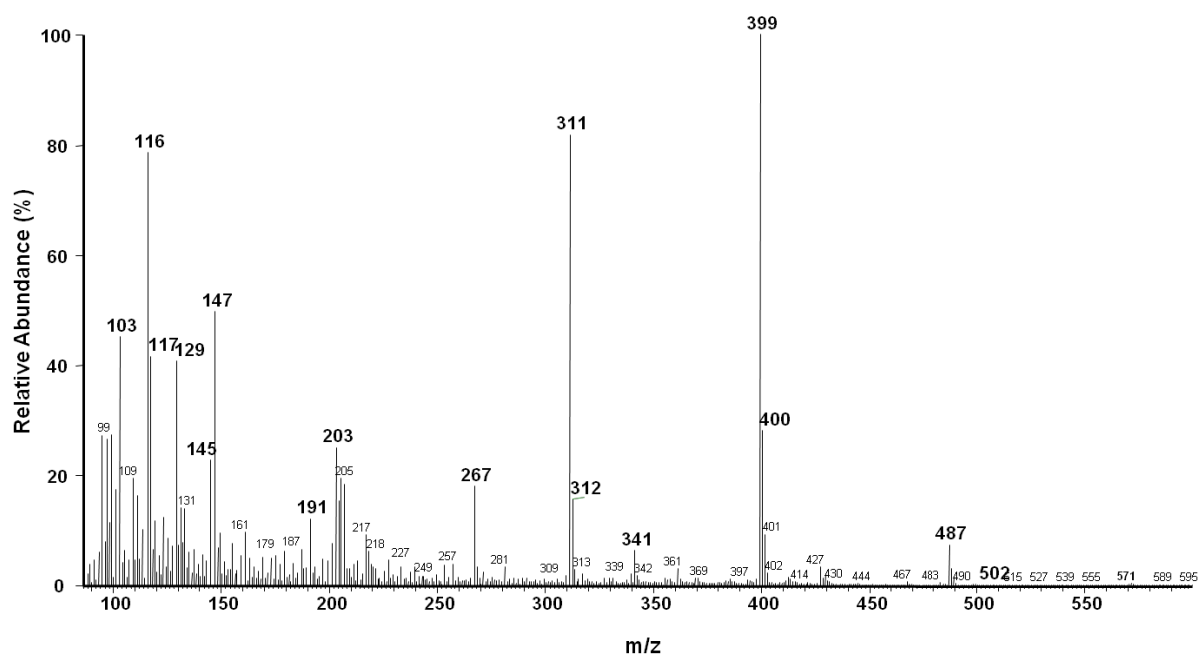
EI (+)-MS Spectrum of Glycerol 1-behenate (**86**)-TMS ether
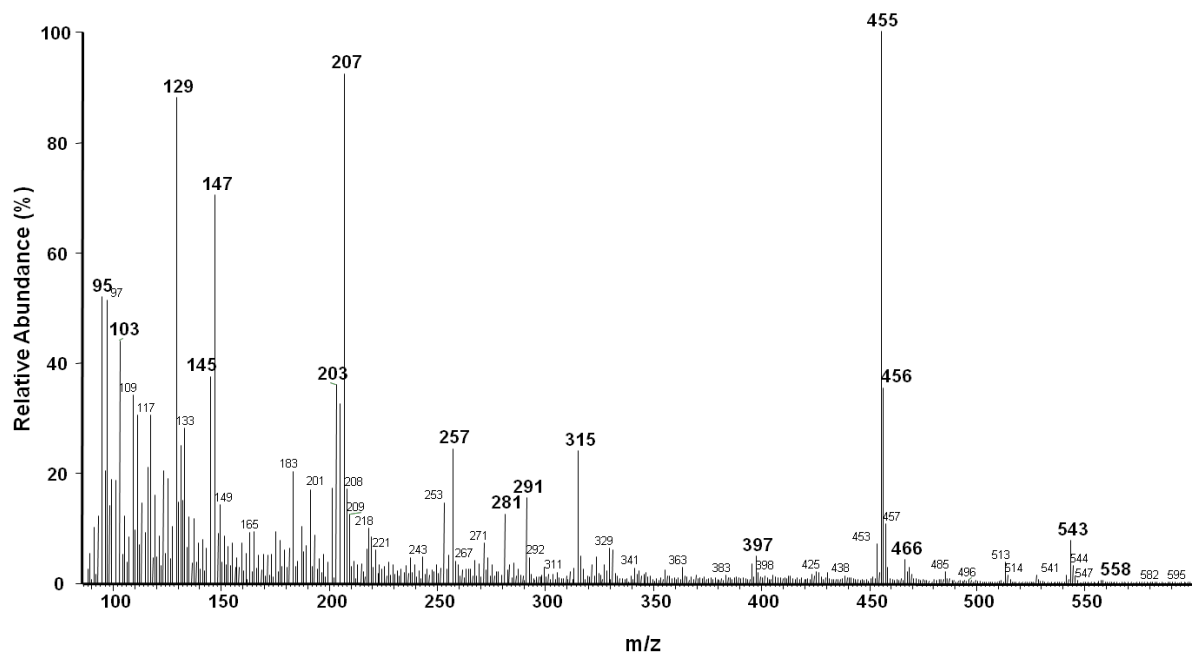
EI (+)-MS Spectrum of Glycerol 1-lignocerate (**87**)-TMS ether
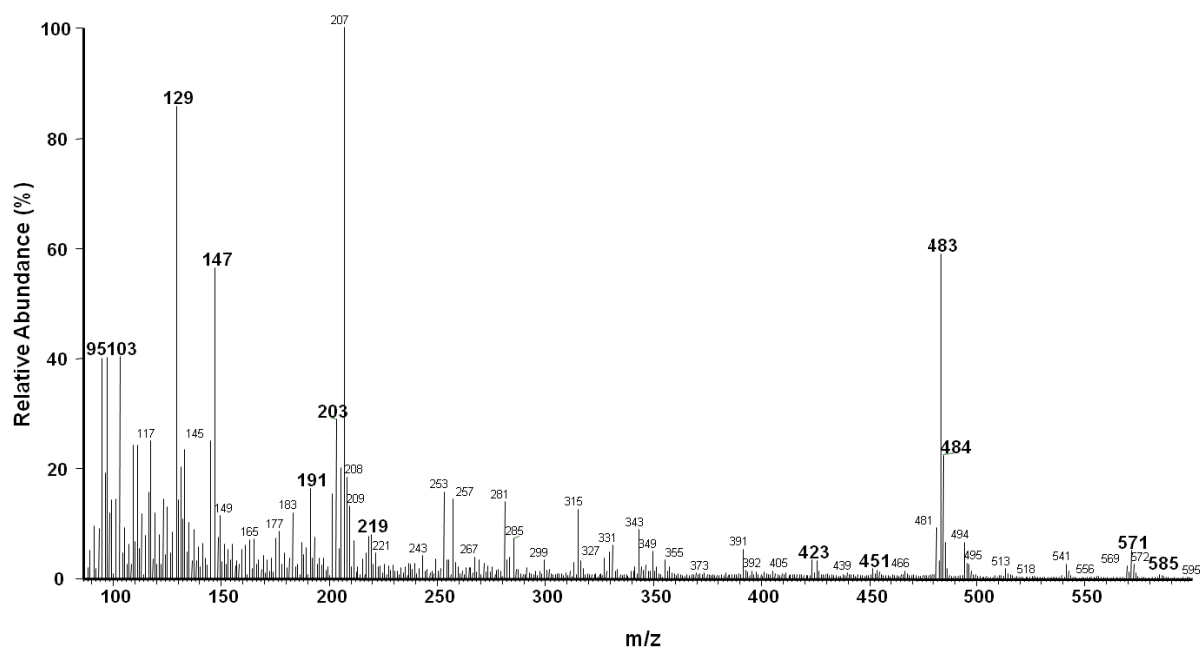
EI (+)-MS Spectrum of Glycerol 1-octadecenoate (**88**)-TMS ether
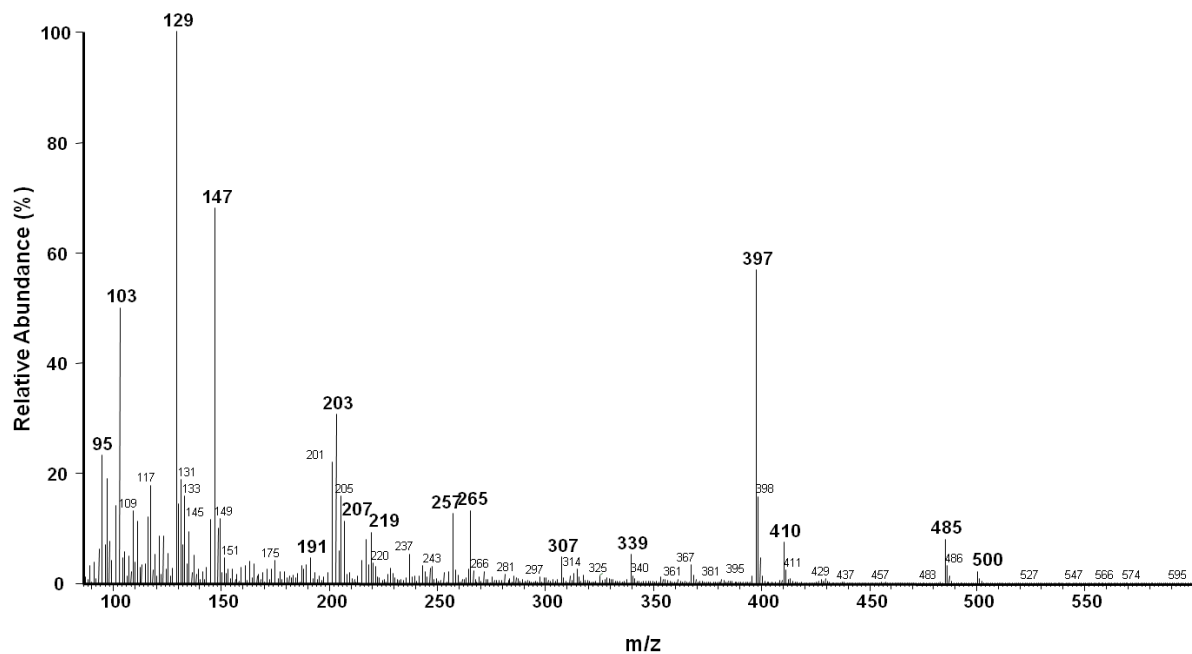
EI (+)-MS Spectrum of Glycerol 1-docosenoate (**89**)-TMS ether
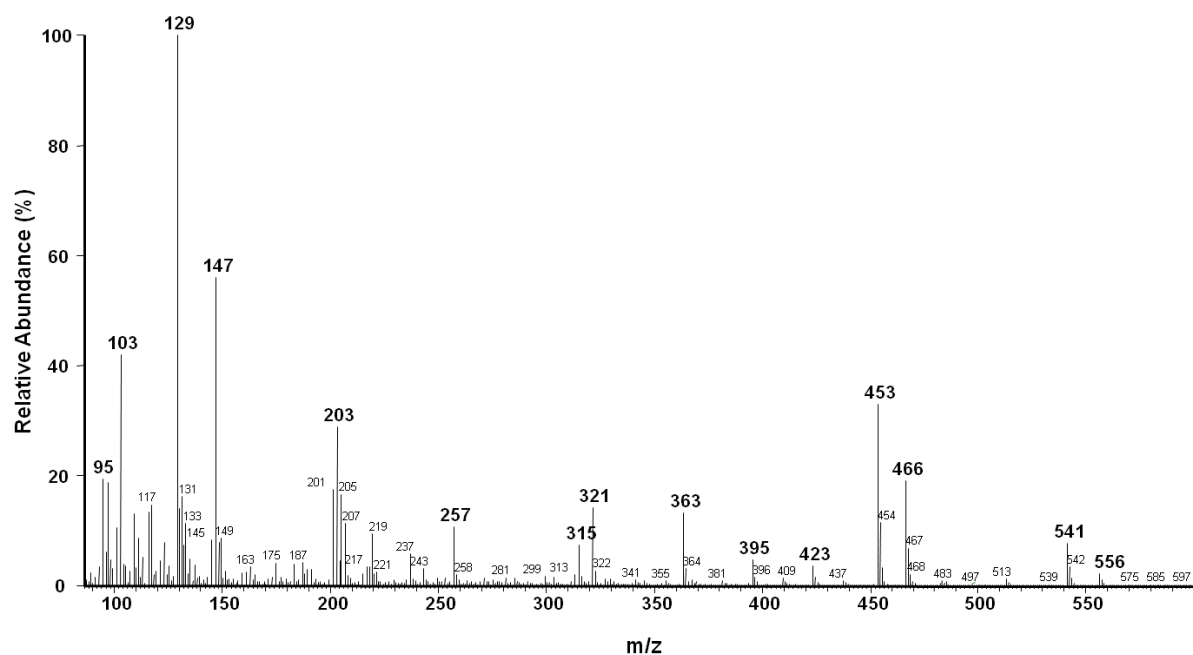
EI (+)-MS Spectrum of Glycerol 1-tetracosenate (**90**)-TMS ether
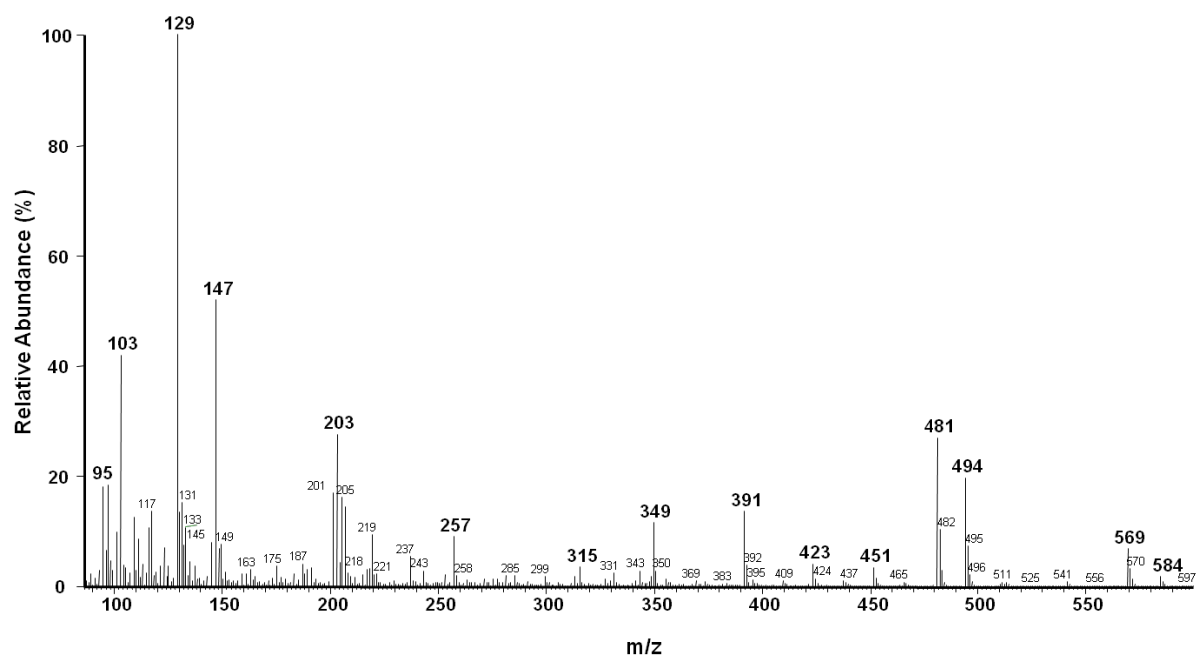
EI (+)-MS Spectrum of Glycerol 2-myristate (**91**)-TMS ether
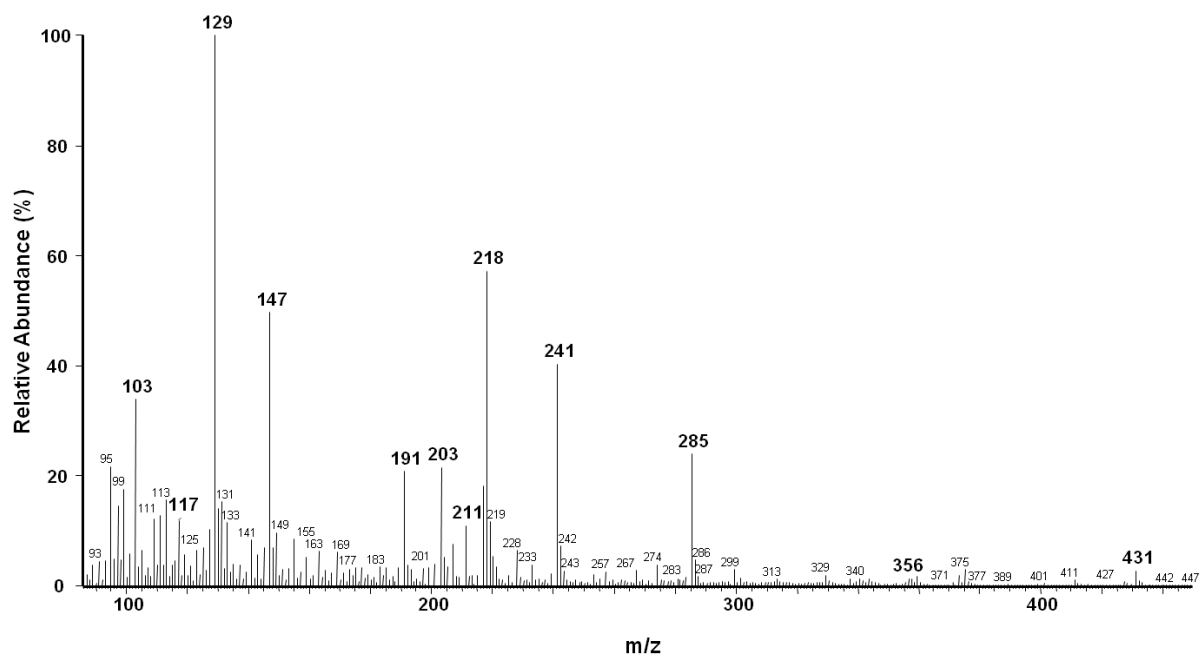
EI (+)-MS Spectrum of Glycerol 2-palmitate (**92**)-TMS ether
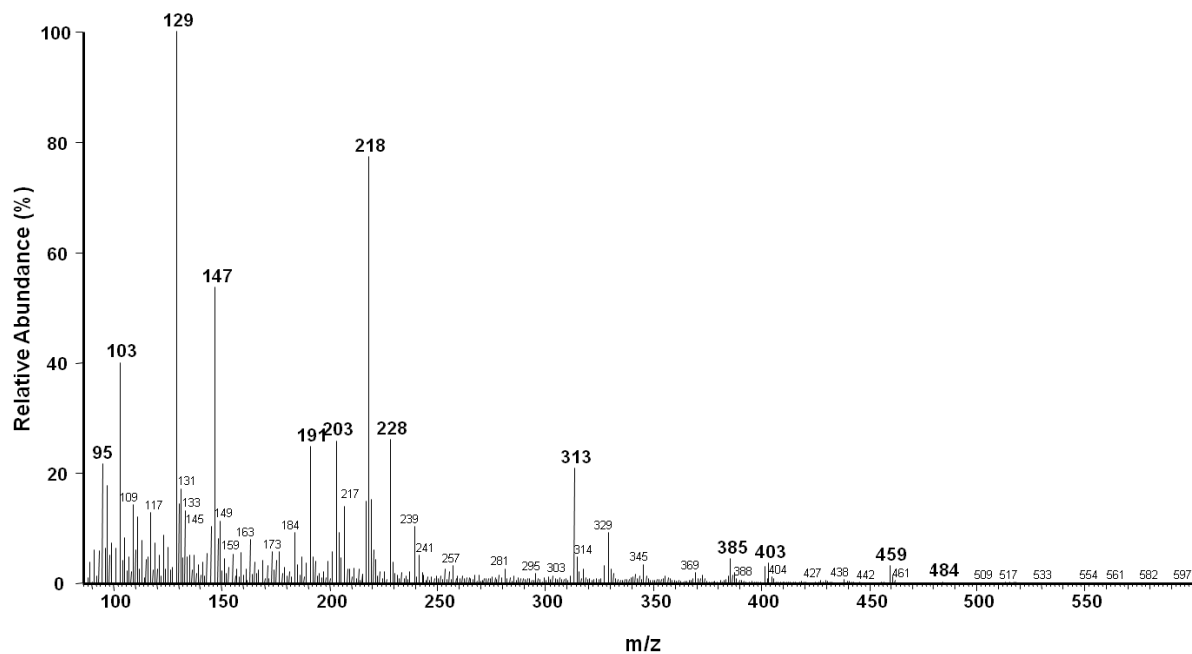
EI (+)-MS Spectrum of Glycerol 2-behenate (**93**)-TMS ether
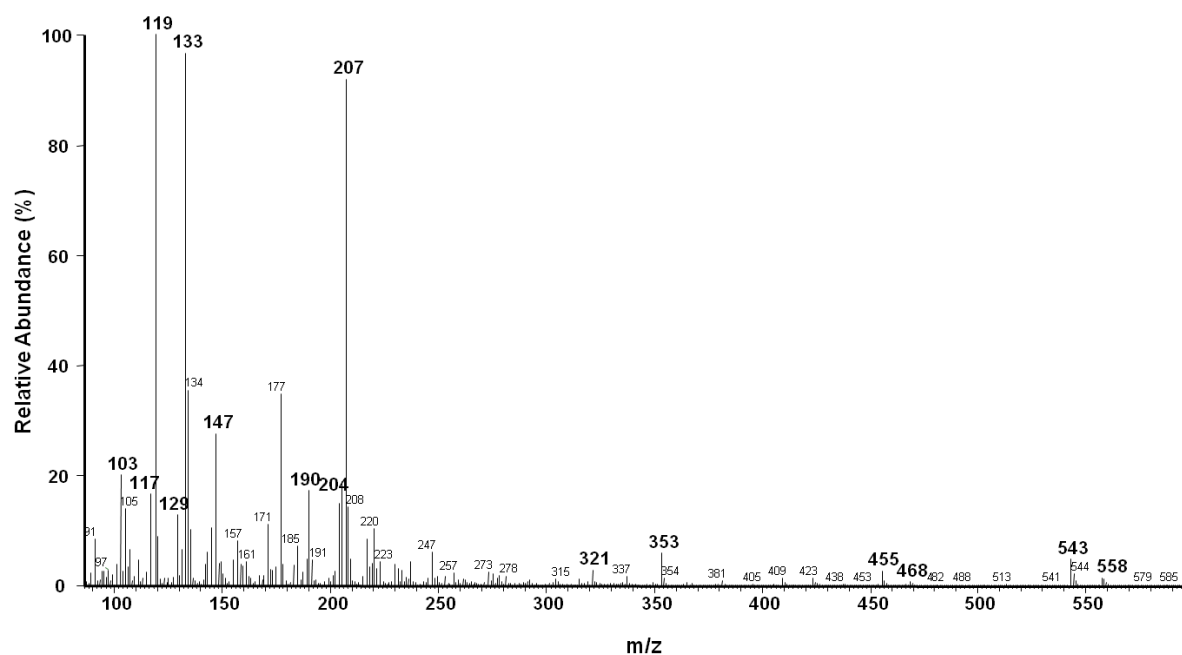
EI (+)-MS Spectrum of Glycerol 1,2-dilaurate (**94**)-TMS ether
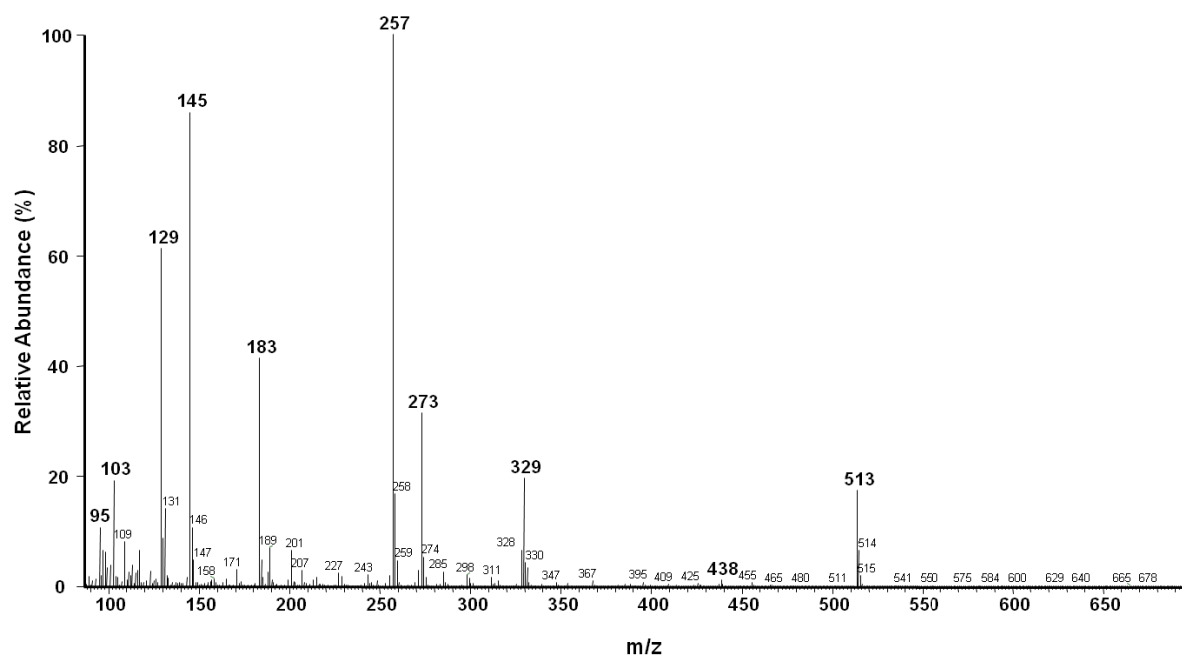
EI (+)-MS Spectrum of Glycerol, 1-laurate-2-myristate (**95**)-TMS ether
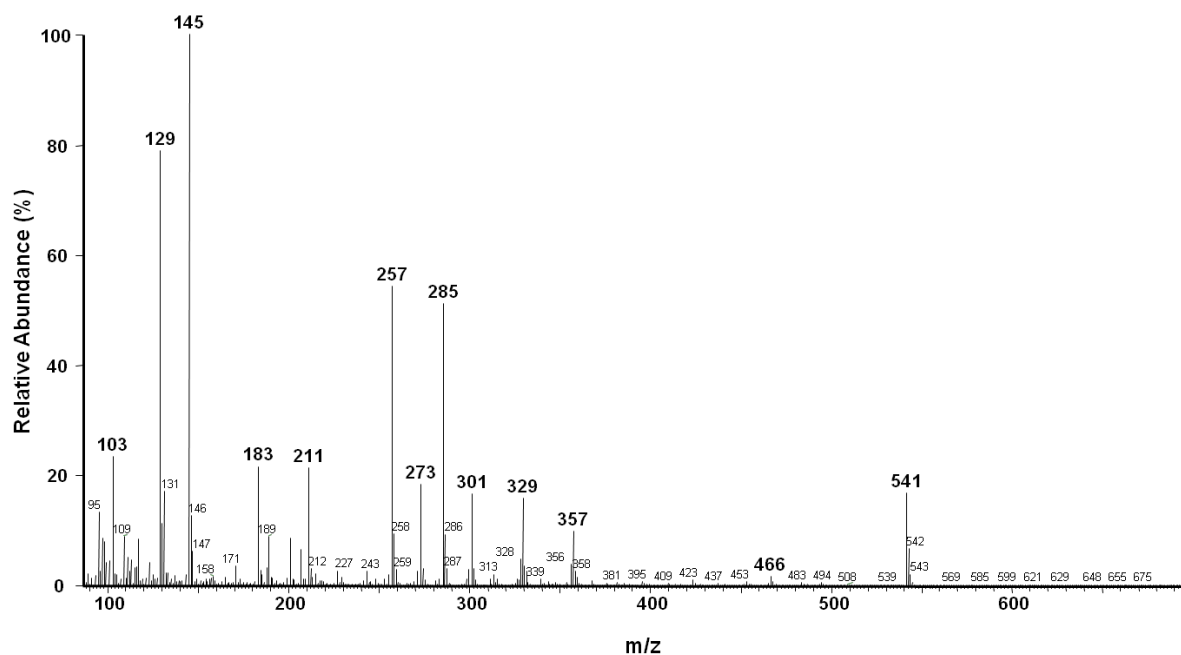
EI (+)-MS Spectrum of Glycerol, 1-laurate-2-palmitate (**96**)-TMS ether
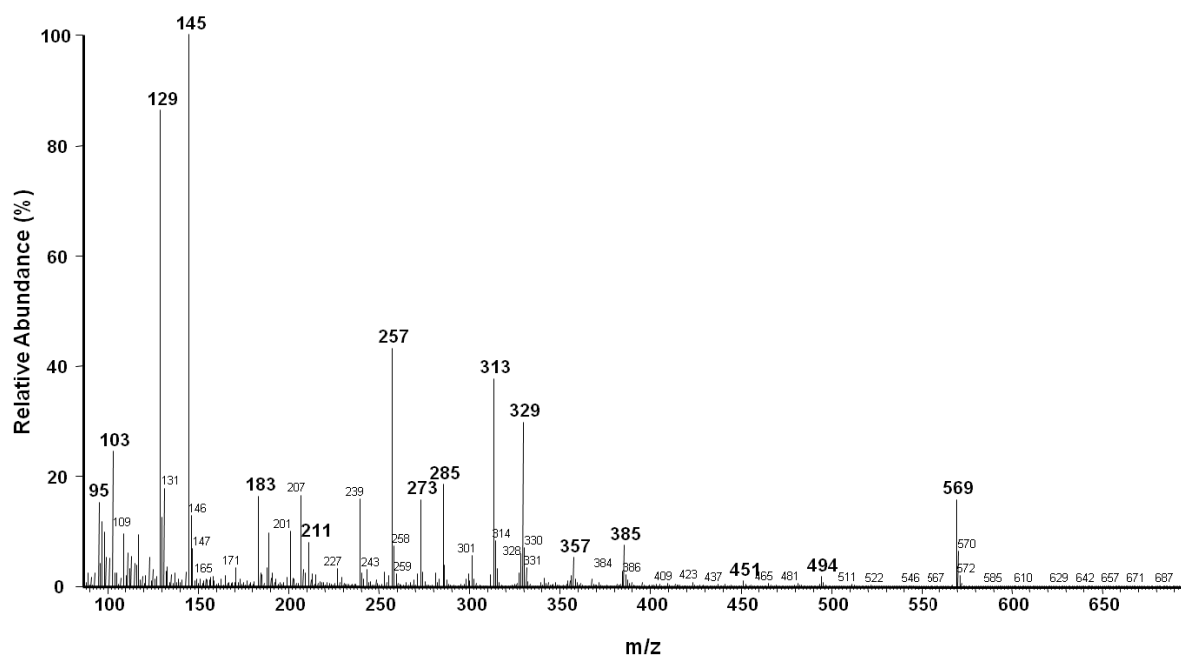
EI (+)-MS Spectrum of Glycerol, 1-laurate-2-stearate (**97**)-TMS ether
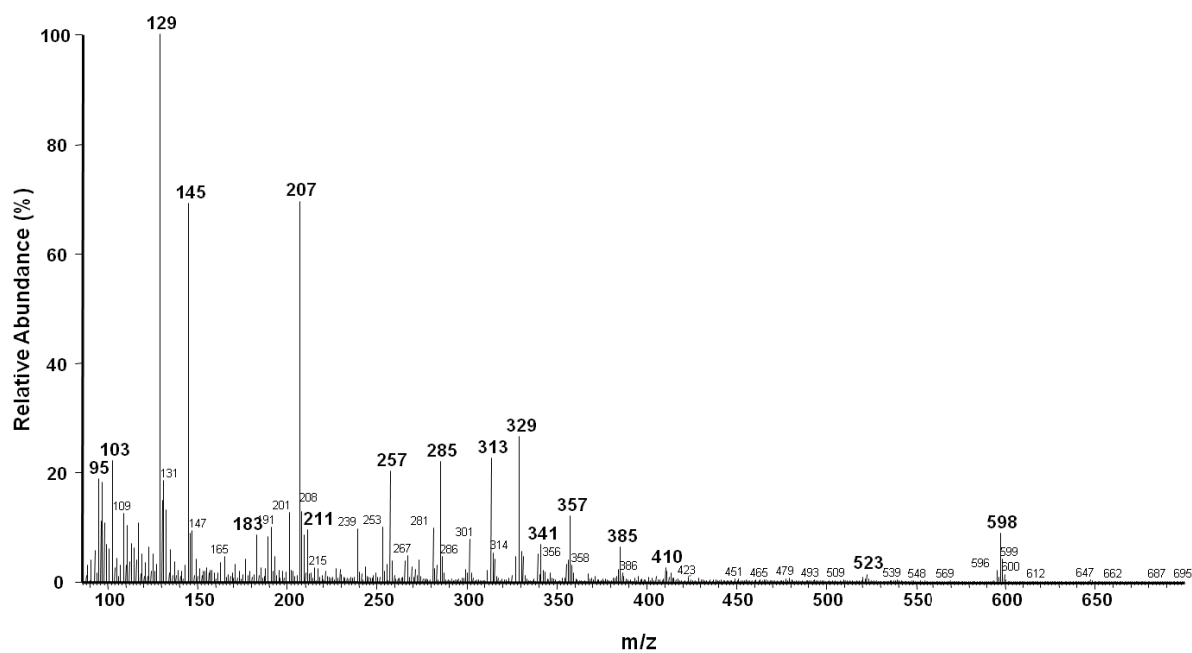
EI (+)-MS Spectrum of Glycerol, 1-laurate-2-arachidonate (**98**)-TMS ether
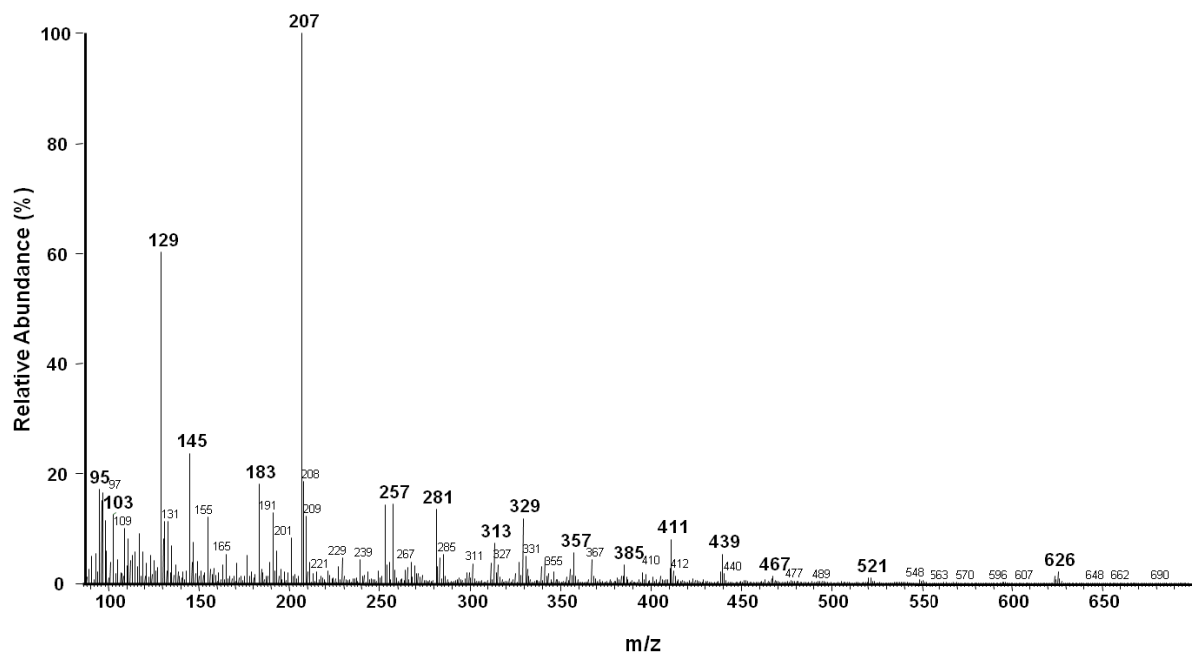
EI (+)-MS Spectrum of Glycerol, 1-laurate-2-octadecenoate (**99**)-TMS ether
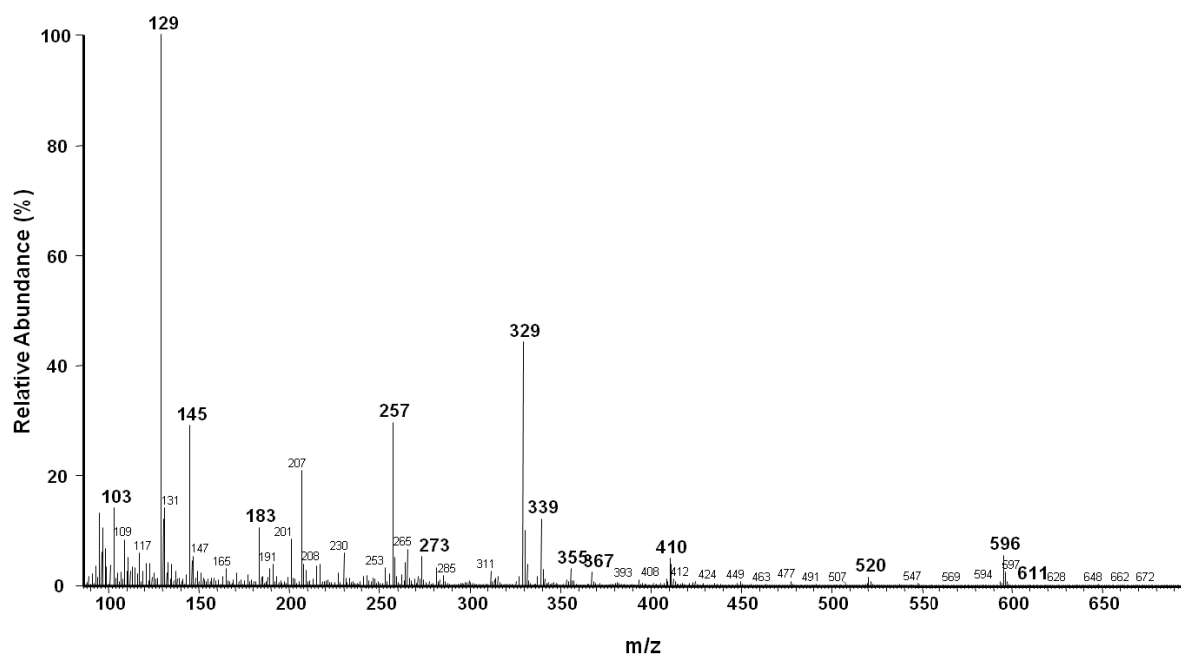
EI (+)-MS Spectrum of Glycerol, 1-laurate-2-eicosenoate (**100**)-TMS ether
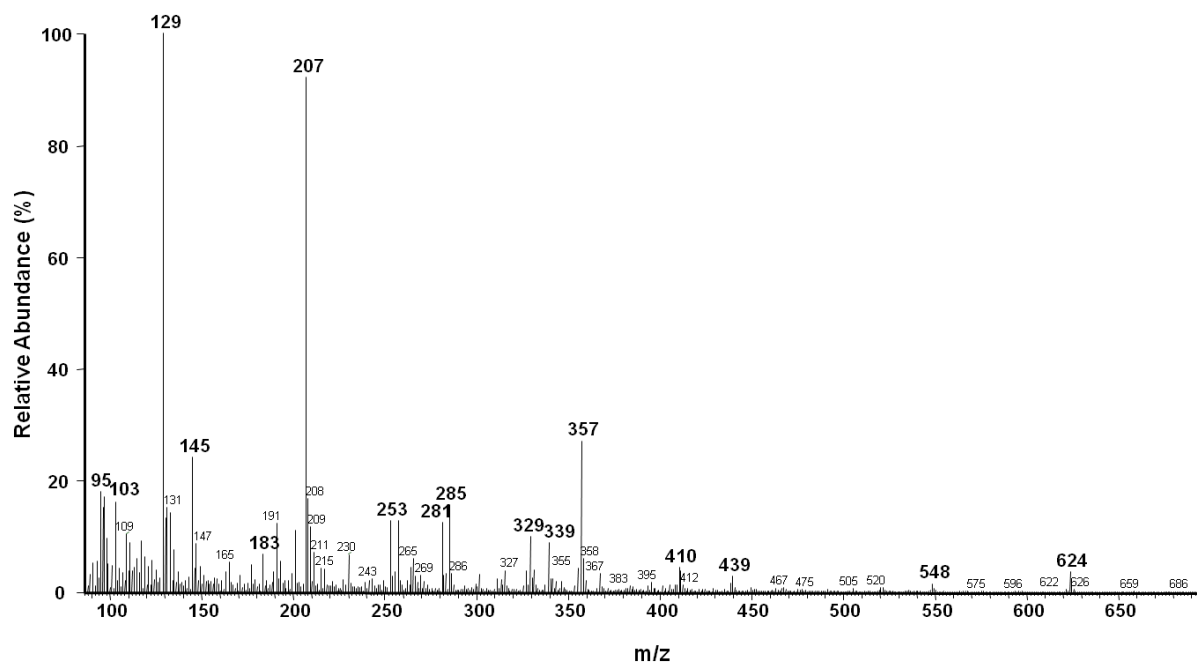
EI (+)-MS Spectrum of Glycerol, 1-laurate-2-docosenoate (**101**)-TMS ether
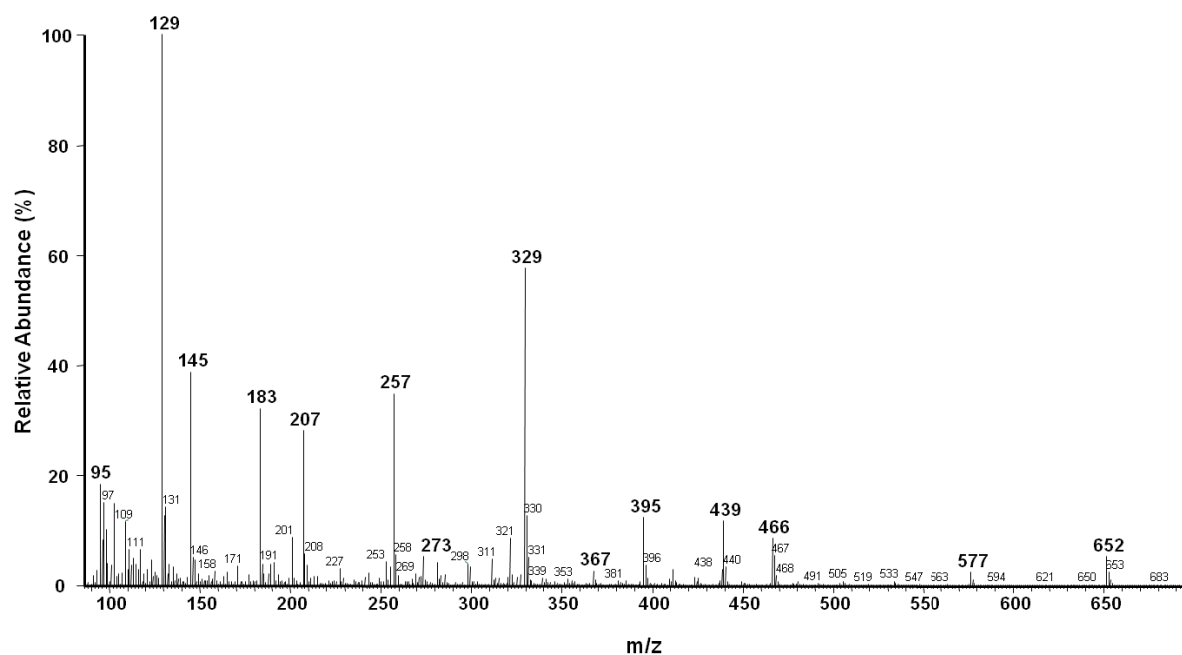
EI (+)-MS Spectrum of Glycerol, 1-laurate-2-tetracosenoate (**102**)-TMS ether
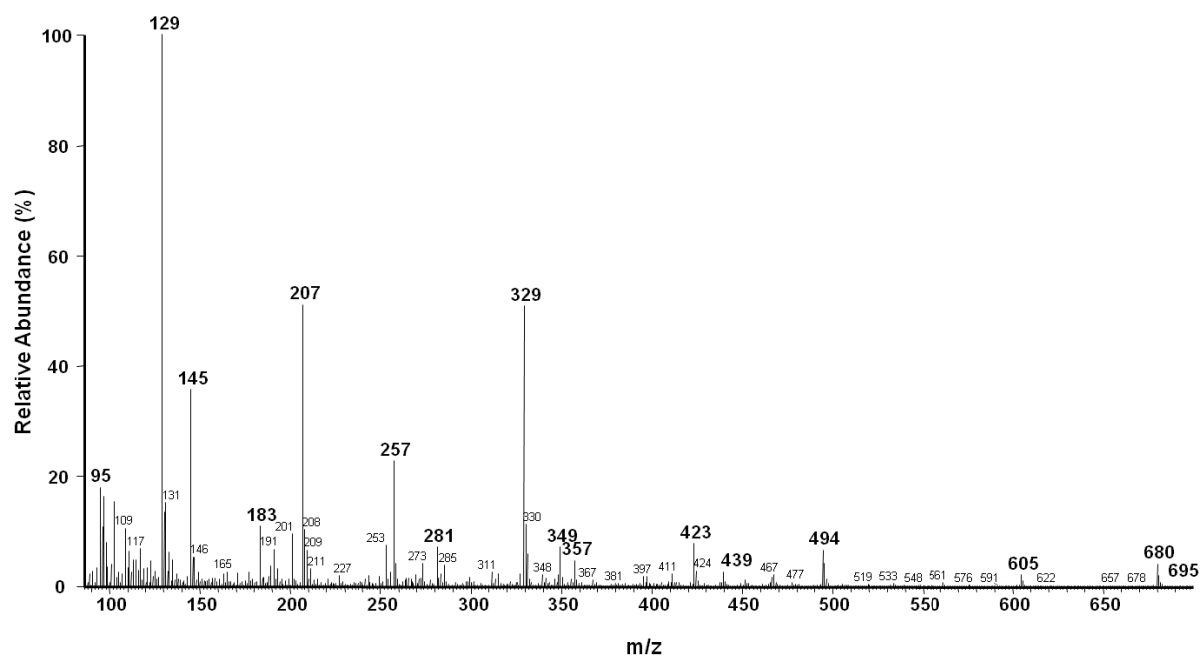
EI (+)-MS Spectrum of Glycerol, 1,3-dilaurate (**103**)-TMS ether
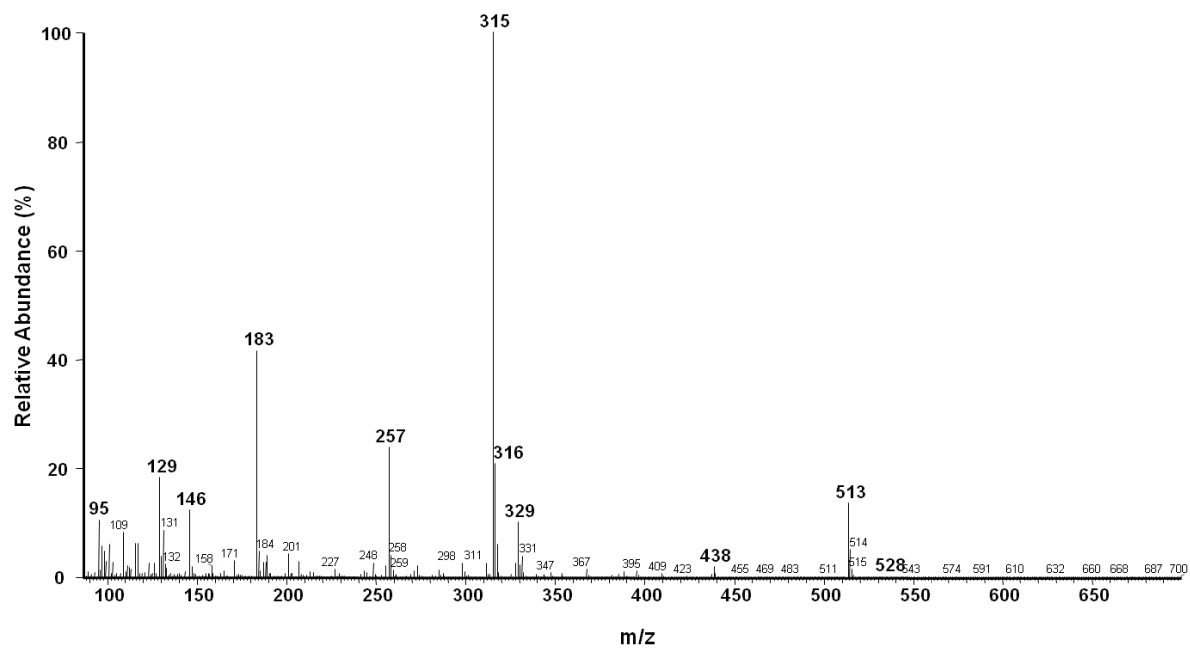
EI (+)-MS Spectrum of Glycerol, 1-laurate-3-myristate (**104**)-TMS ether
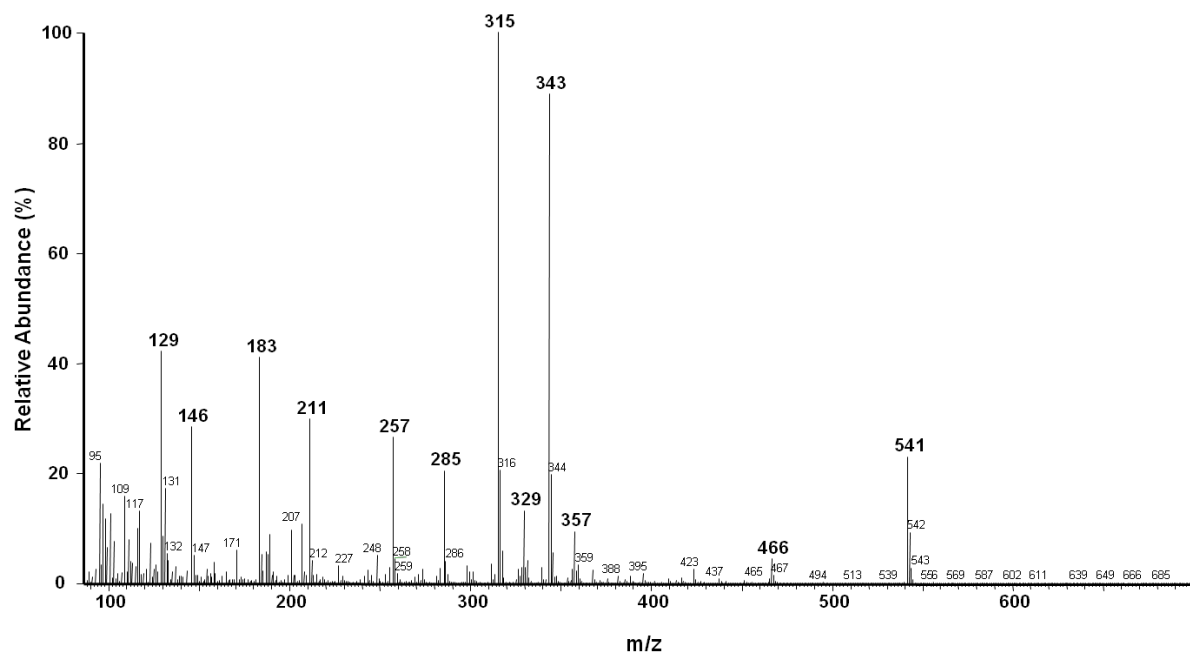
EI (+)-MS Spectrum of Glycerol, 1-laurate-3-palmitate (**105**)-TMS ether
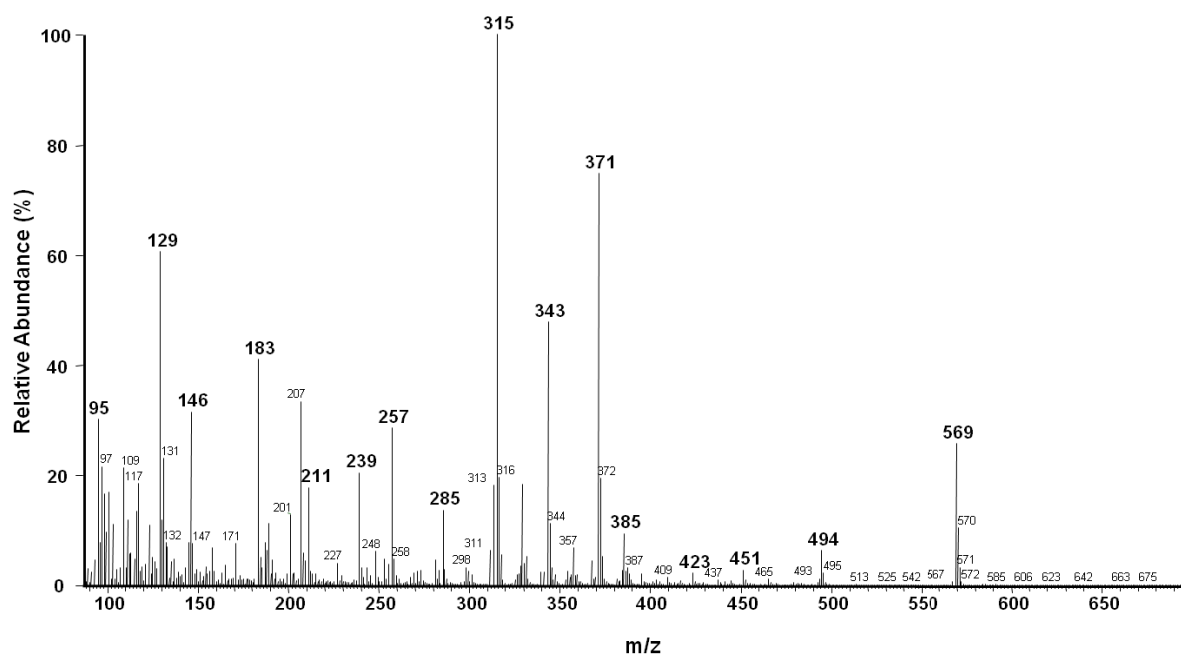
EI (+)-MS Spectrum of Glycerol, 1-laurate-3-stearate (**106**)-TMS ether
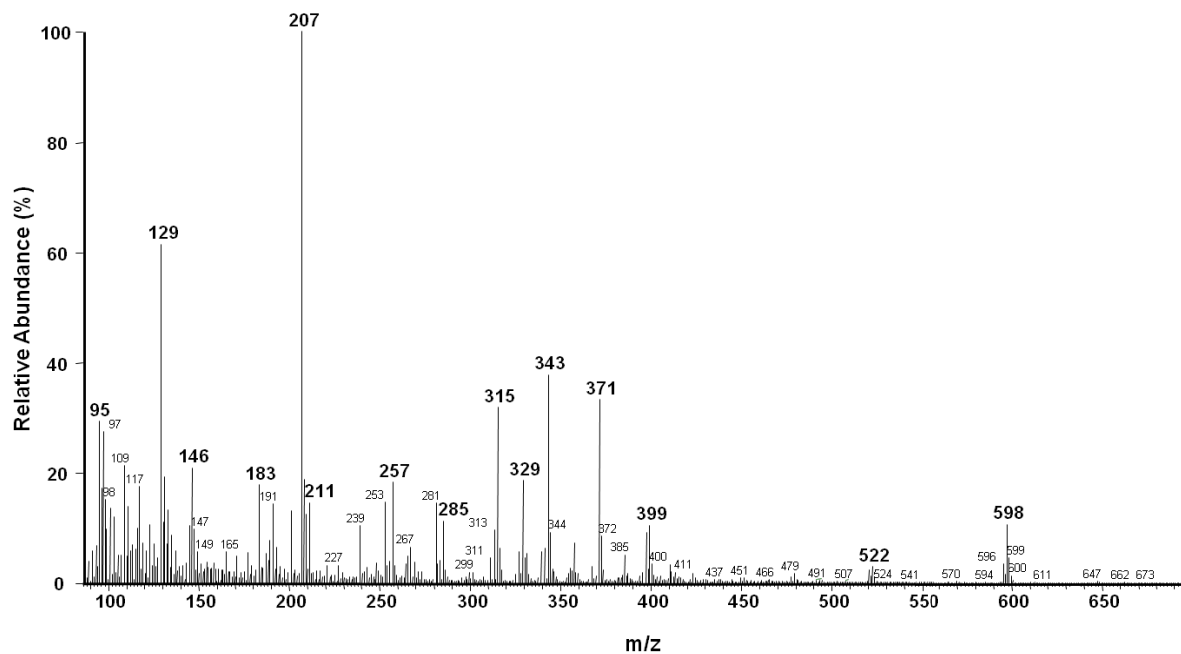
EI (+)-MS Spectrum of Glycerol, 1-laurate-3-arachidonate (**107**)-TMS ether
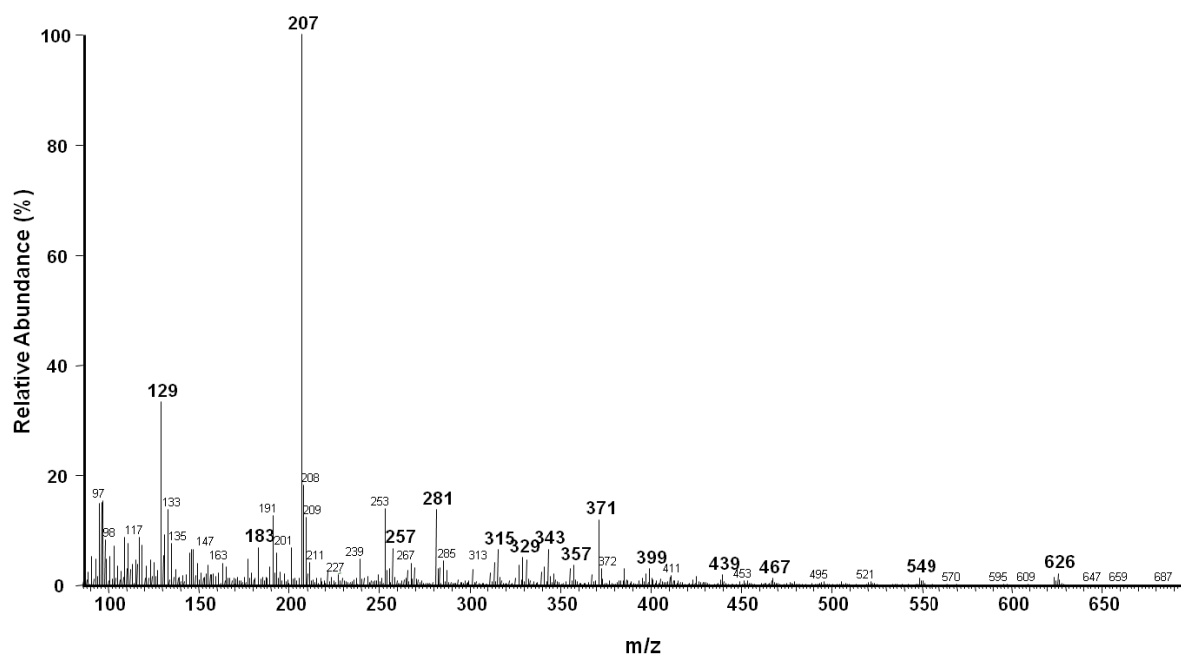
EI (+)-MS Spectrum of Glycerol, 1-laurate-3-octadecenoate (**108**)-TMS ether
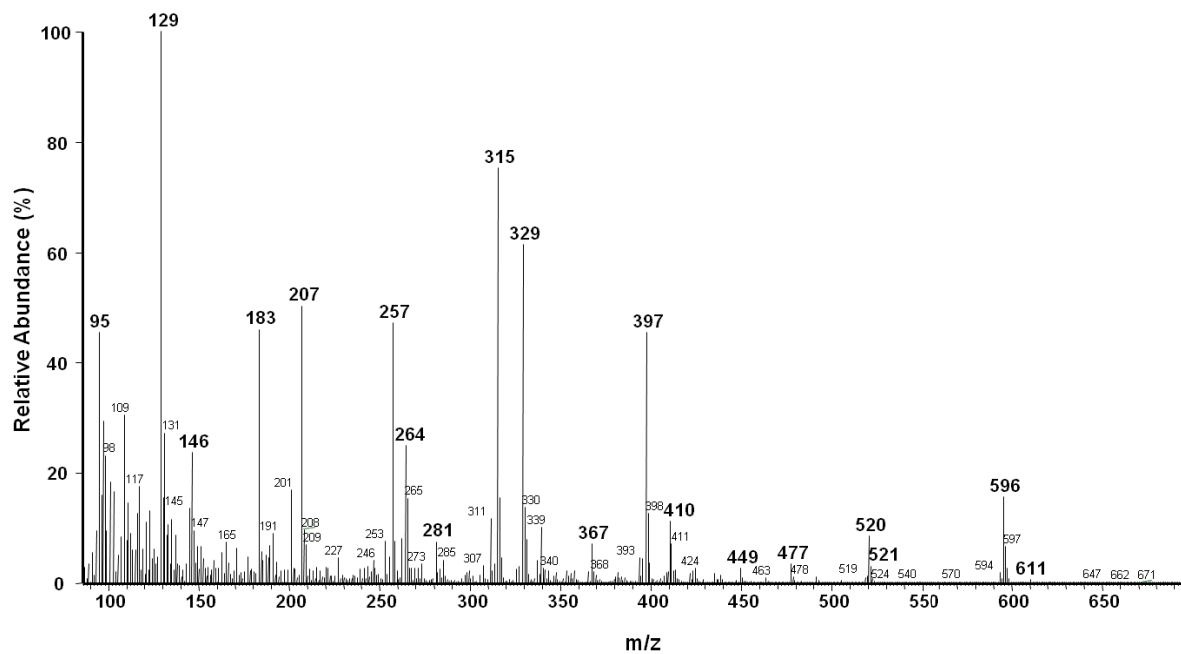
EI (+)-MS Spectrum of Glycerol, 1-laurate-3-eicosenoate (**109**)-TMS ether
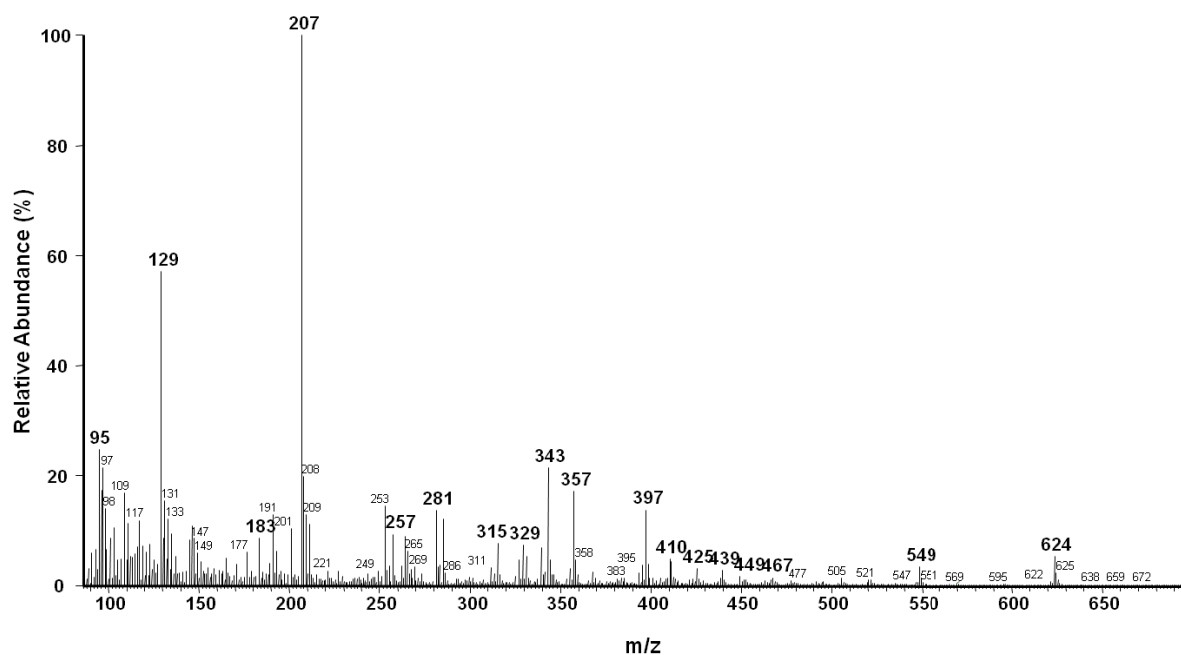
EI (+)-MS Spectrum of Glycerol, 1-laurate-3-docosenoate (**110**)-TMS ether
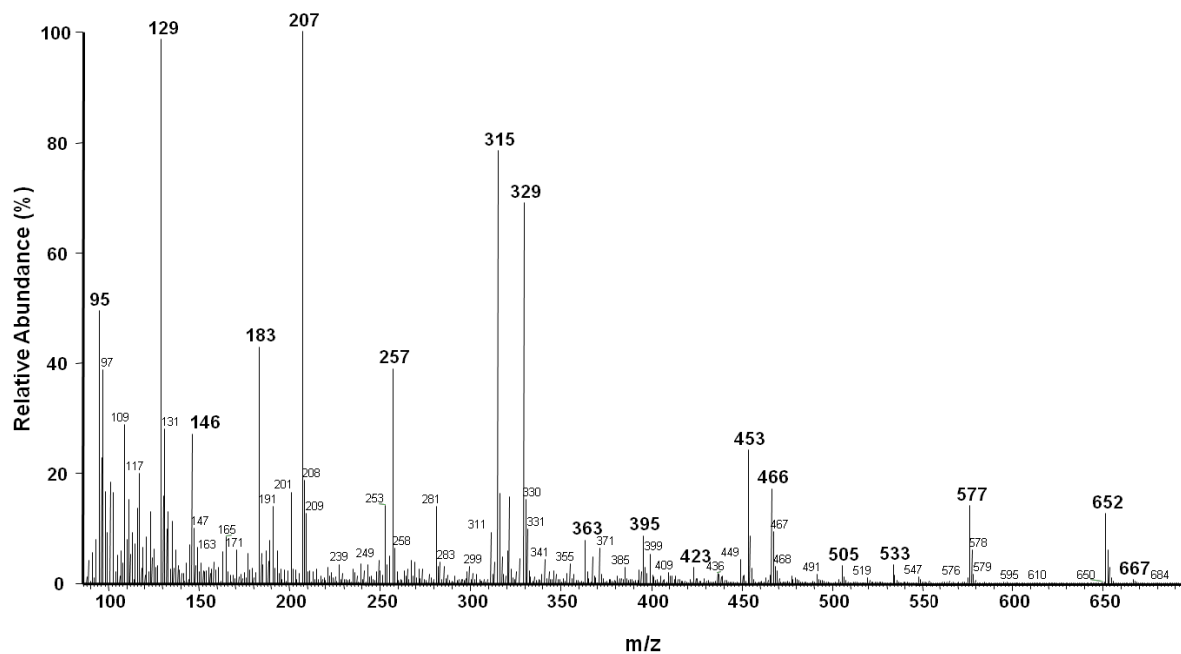
EI (+)-MS Spectrum of Glycerol, 1-laurate-3-tetracosenoate (**111**)-TMS ether
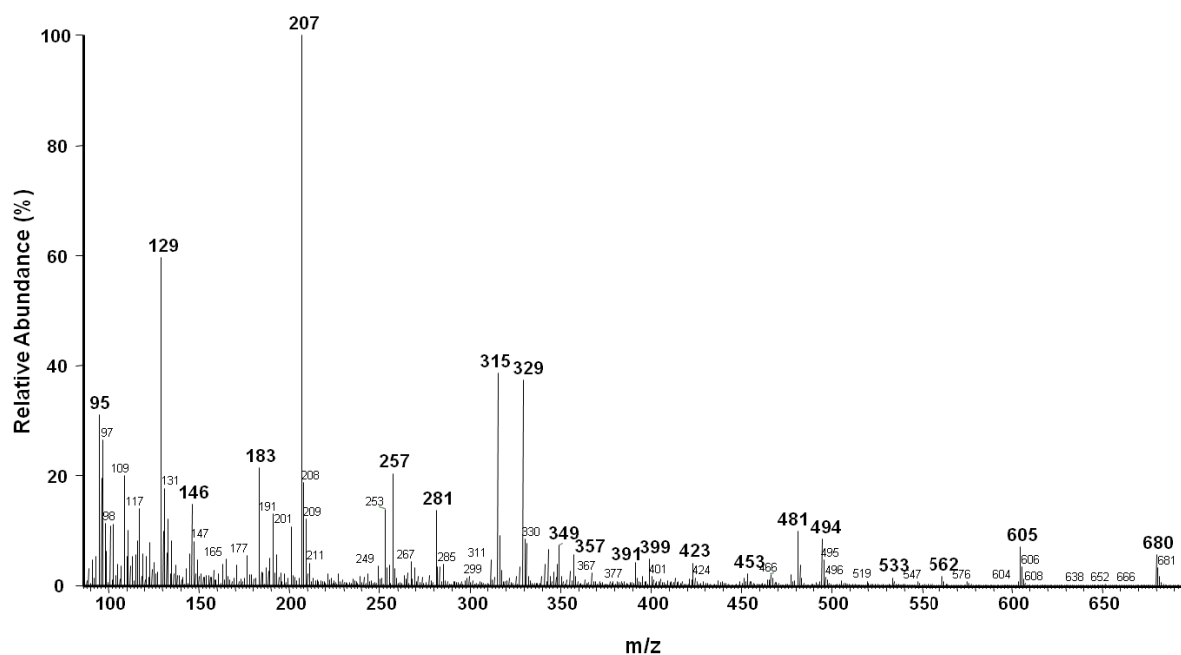
EI (+)-MS Spectrum of Glycerol, 1-laurate-2-caprate-3-laurate (**112**)
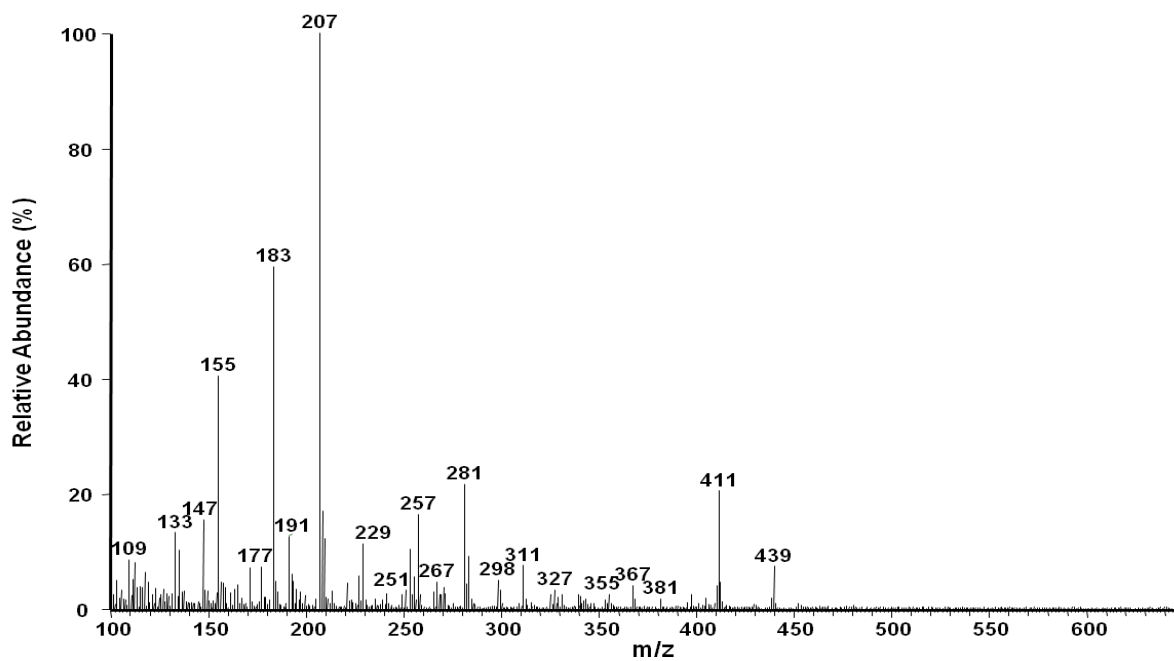
EI (+)-MS Spectrum of Glycerol, 1,2,3-laurate (**113**)
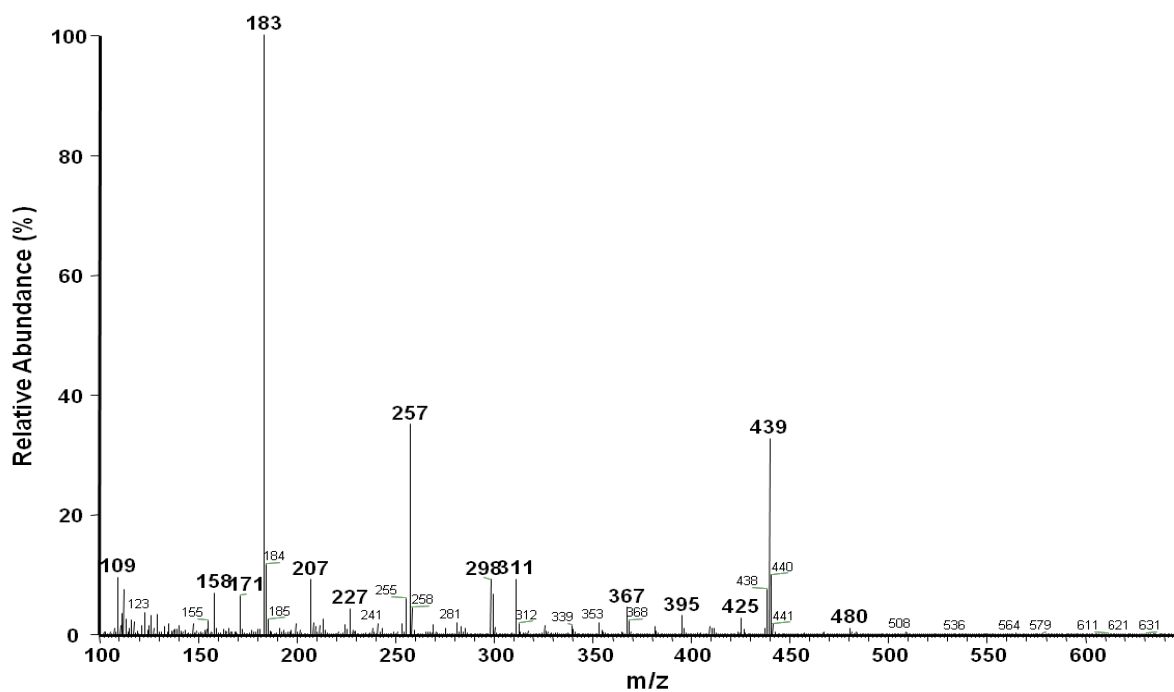
EI (+)-MS Spectrum of Glycerol, 1-laurate-2-myristate-3-laurate (**114**)
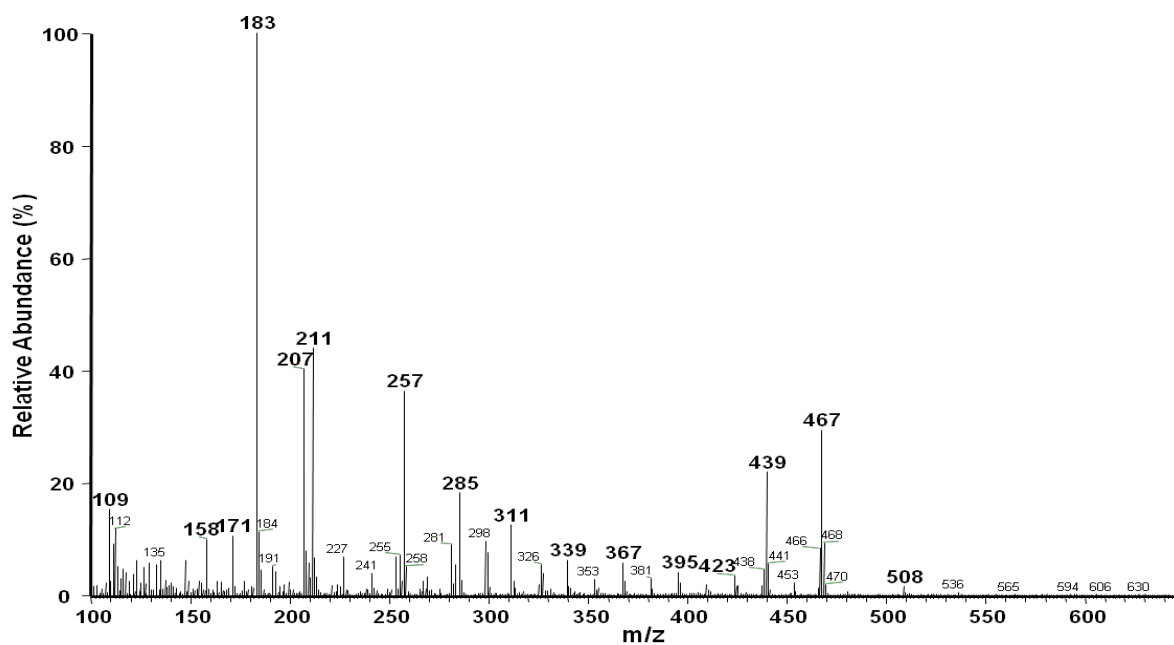
ACN-CI (+)-MS/MS Spectrum of the [M + 54]$^+$ Ion of Palmitoleic acid (**74**)-methyl ester
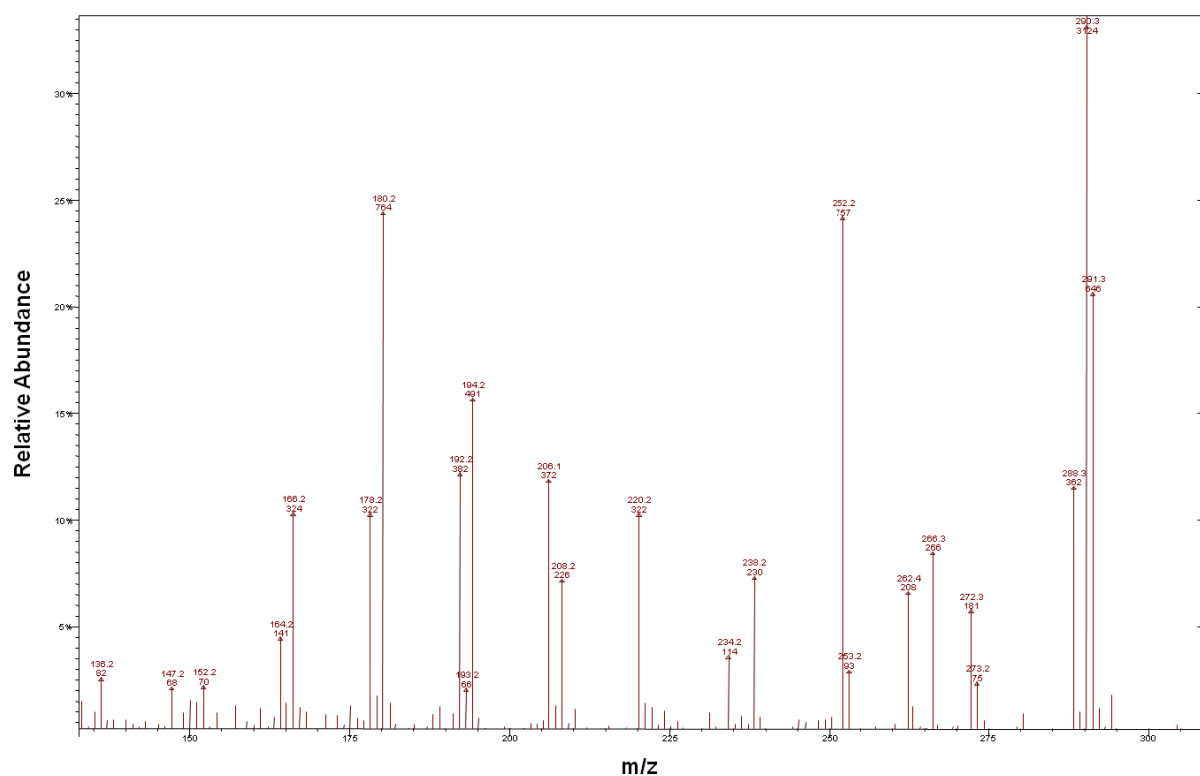

ACN-CI (+)-MS/MS Spectrum of the [M + 54]$^+$ Ion of *cis*-11-Octadecenoic acid (**75**)-methyl ester
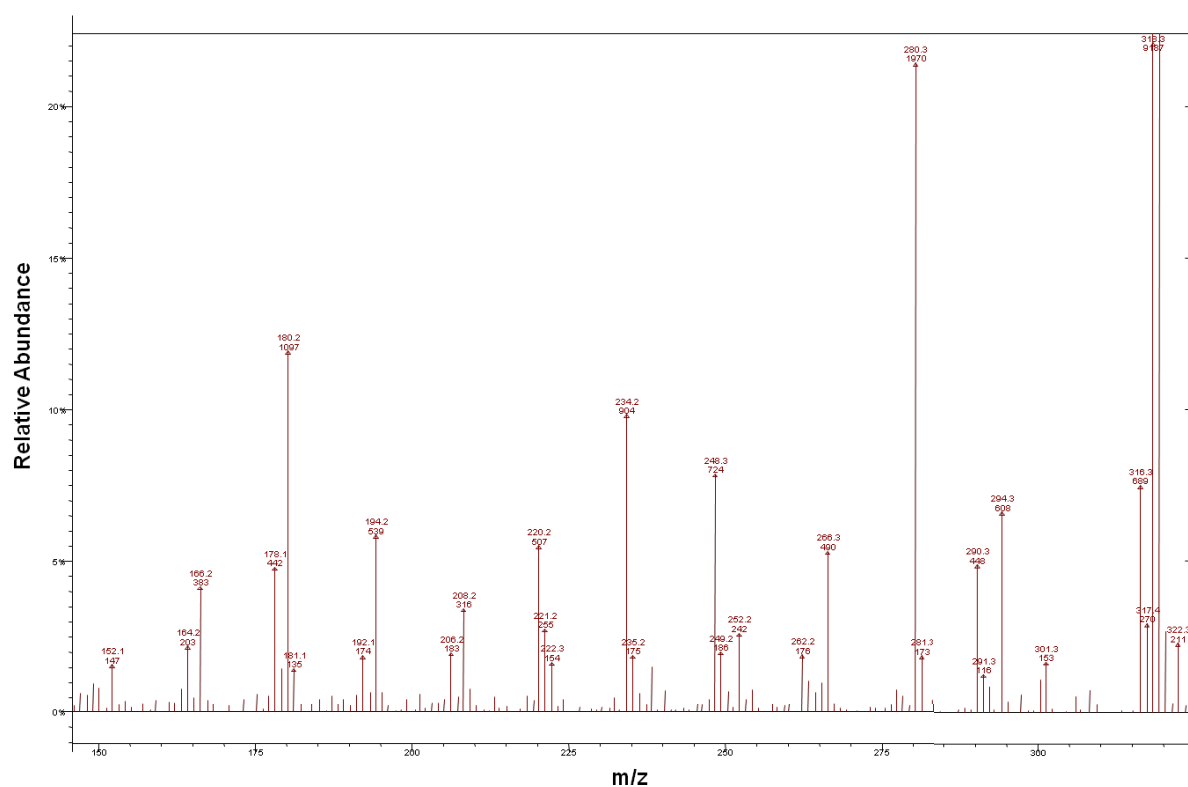
ACN-CI (+)-MS/MS Spectrum of the [M + 54]$^+$ Ion of *cis*-13-Eicosenoic acid (**76**)-methyl ester
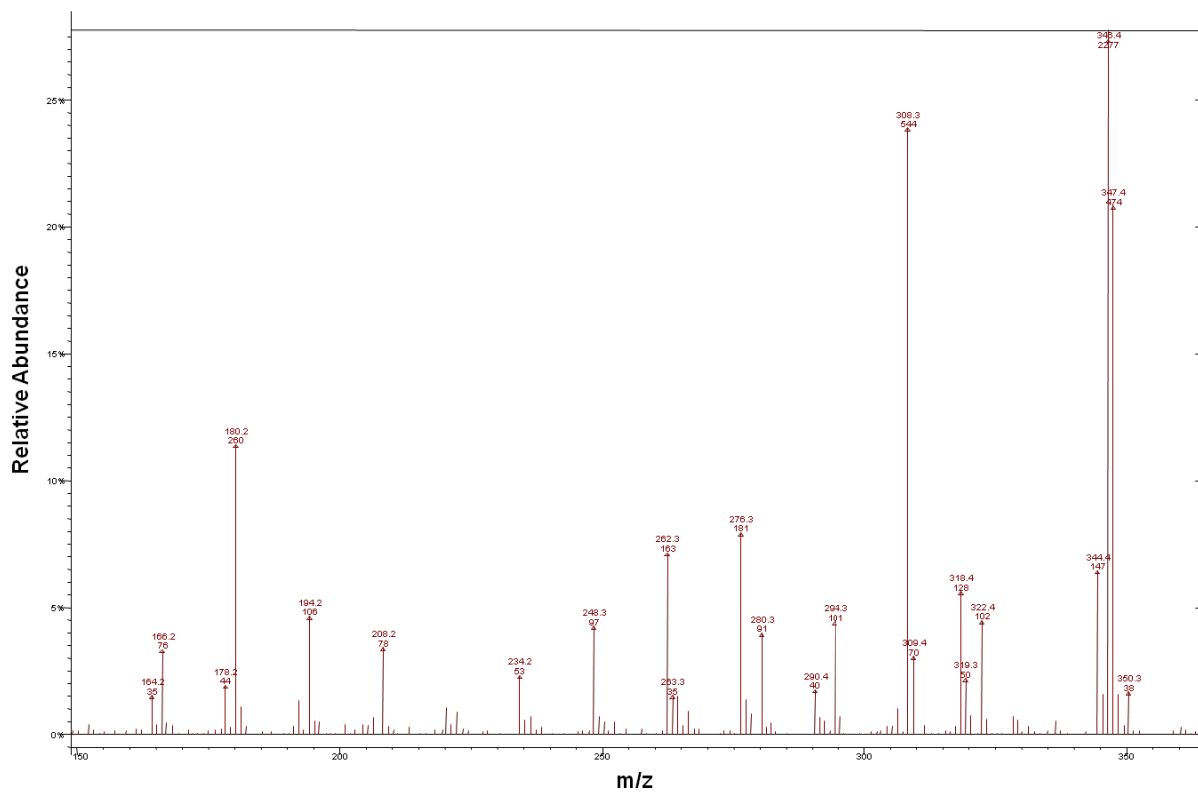
ACN-CI (+)-MS/MS Spectrum of the [M + 54]$^+$ Ion of *cis*-15-Docosenoic acid (**77**)-methyl ester
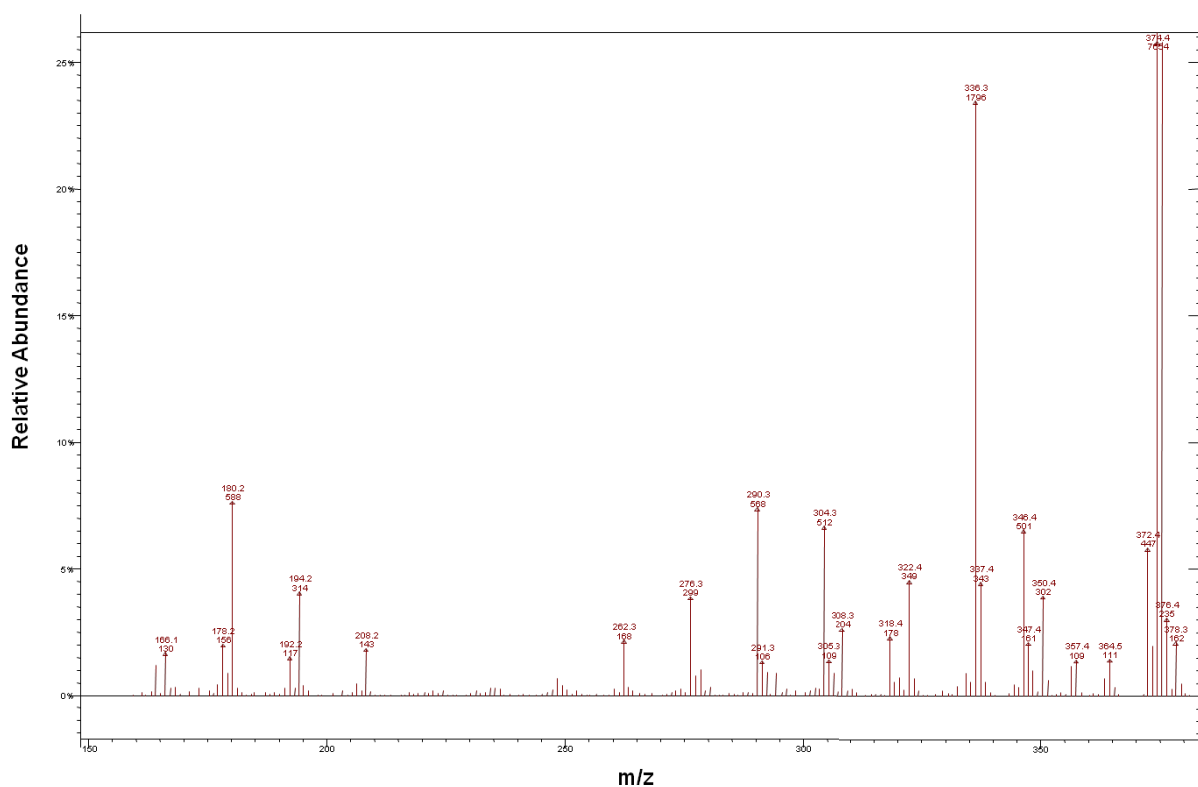
ACN-CI (+)-MS/MS Spectrum of the [M + 54]$^+$ Ion of *cis*-17-Tetracosenoic acid (**78**)-methyl ester
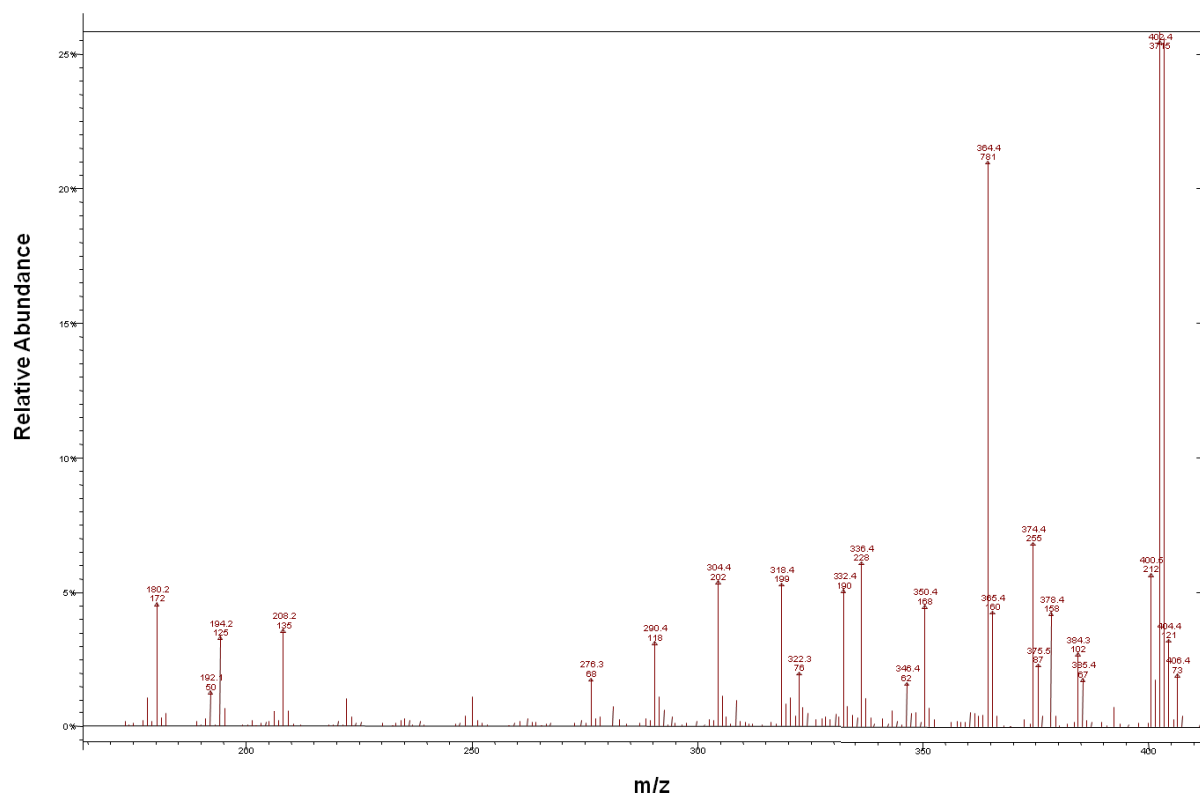
ACN-CI (+)-MS/MS Spectrum of the [M + 54]$^+$ Ion of Oleic acid (**79**)-methyl ester
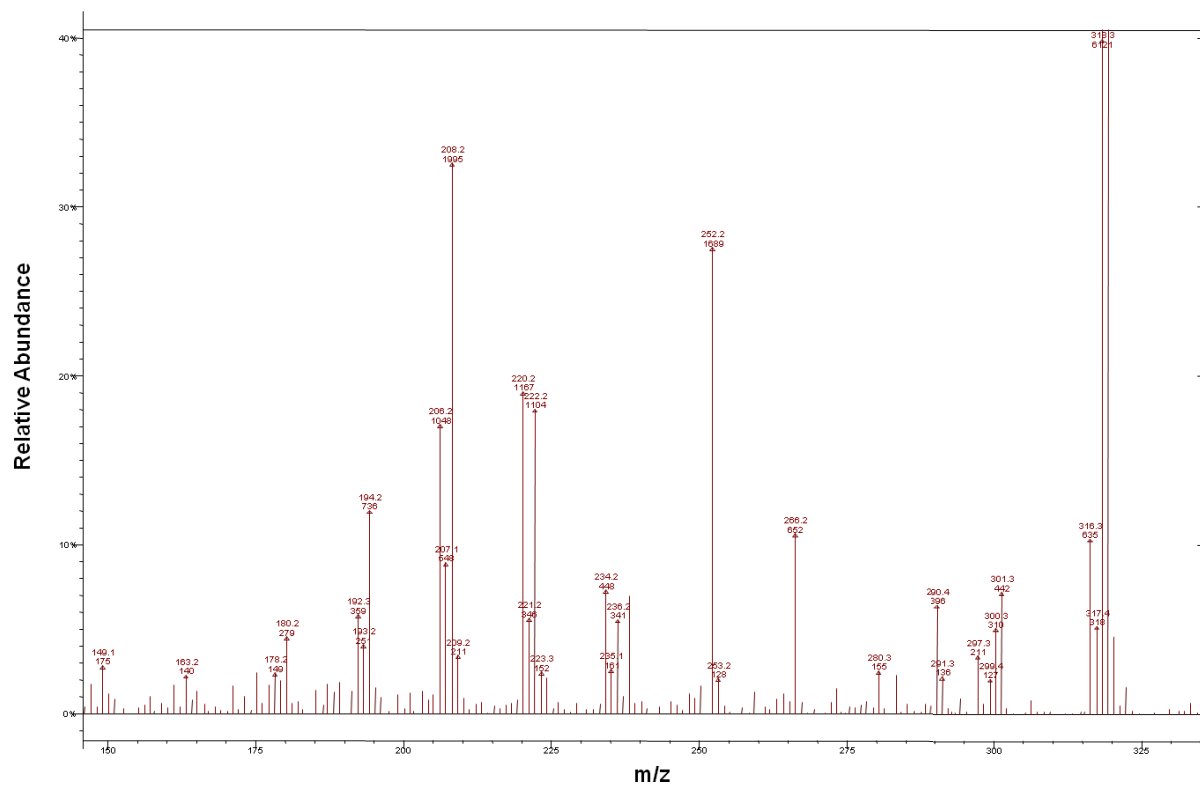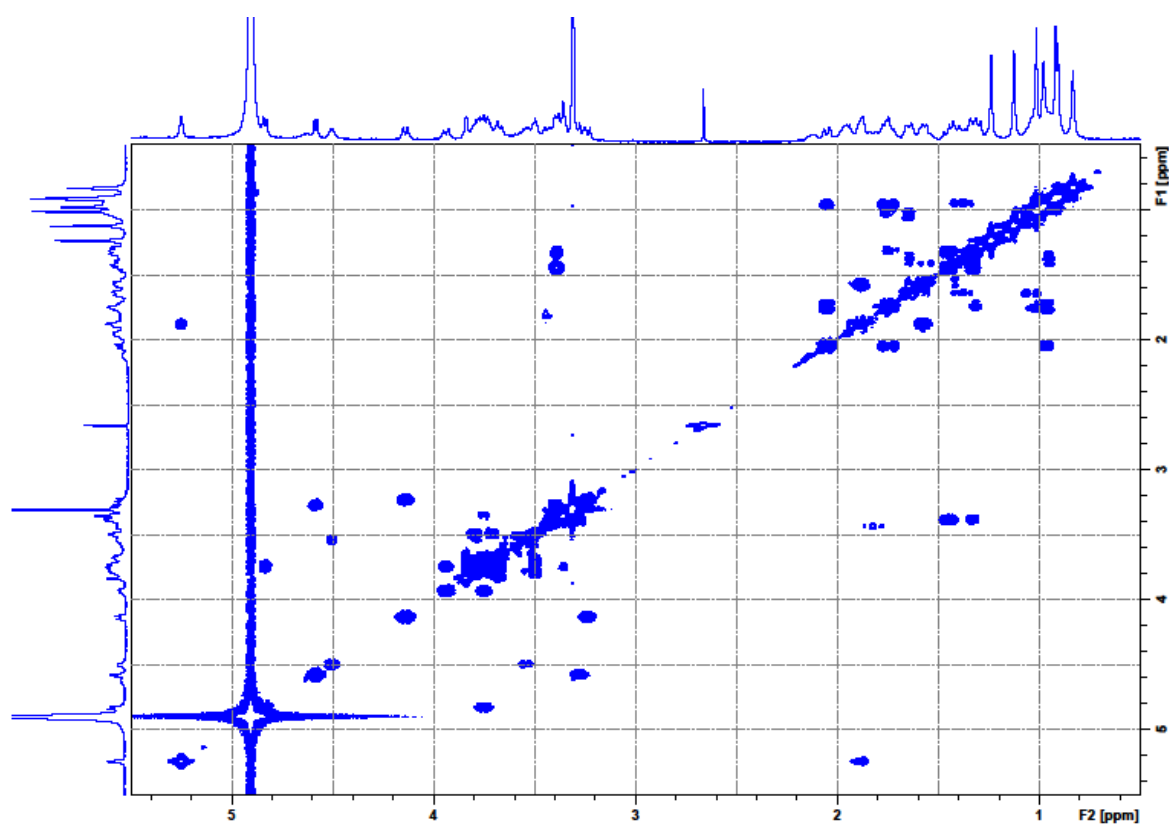
ACN-CI (+)-MS/MS Spectrum of the [M + 54]$^+$ Ion of *cis*-11-Eicosenoic acid (**80**)-methyl ester
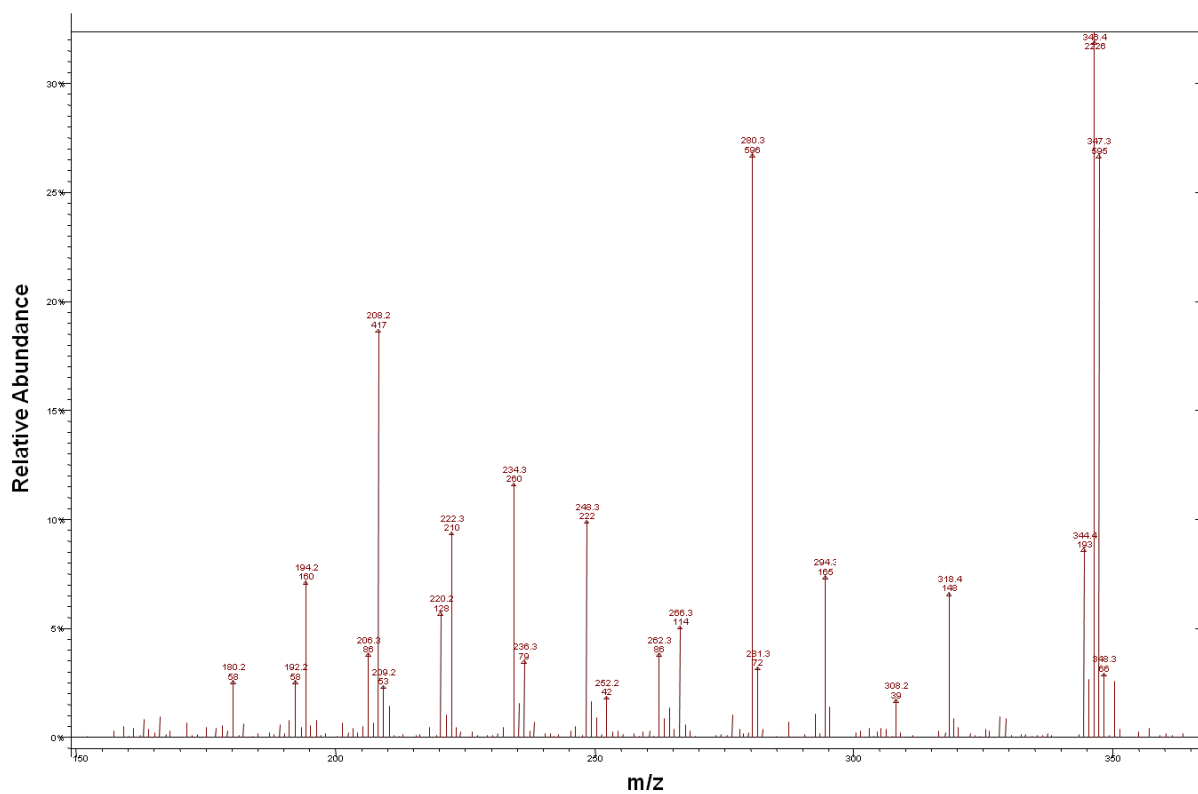
ACN-CI (+)-MS/MS Spectrum of the [M + 54]$^+$ Ion of Nervonic acid (**81**)-methyl ester
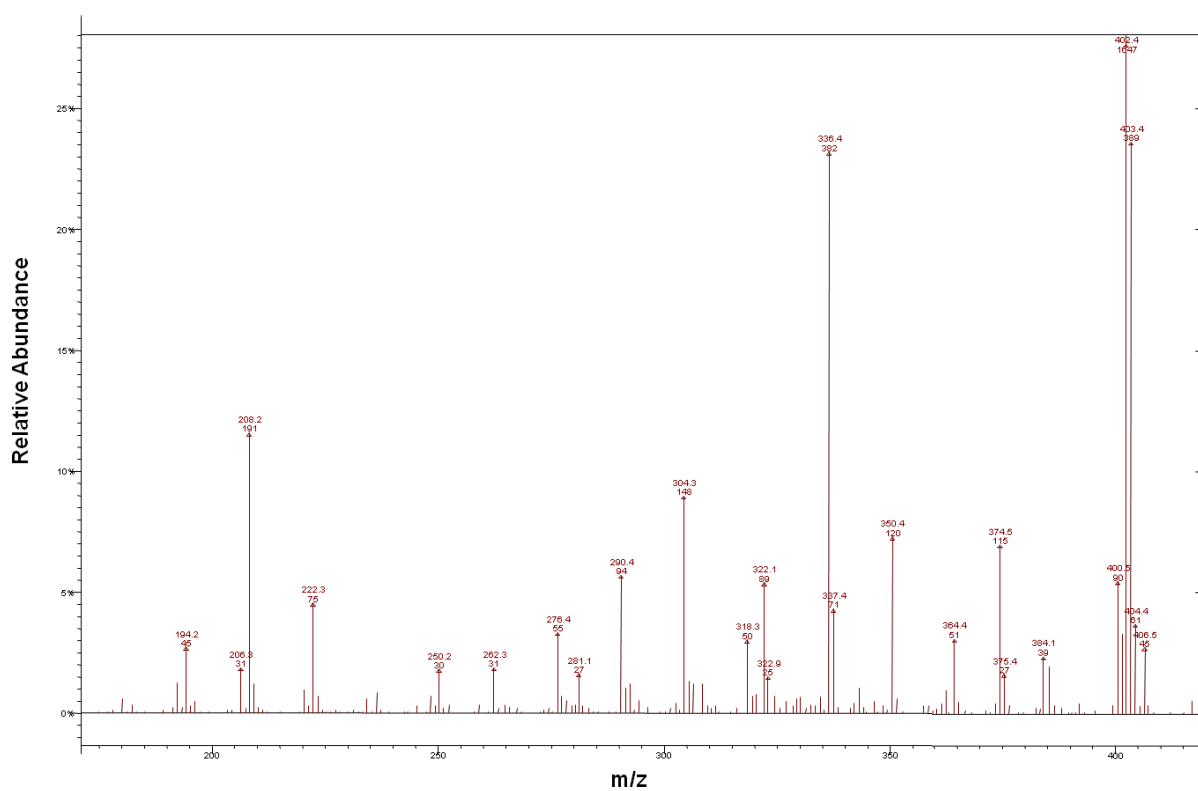
ACN-CI (+)-MS/MS Spectrum of the [M + 54]$^+$ Ion of Linoleic acid (**82**)-methyl ester
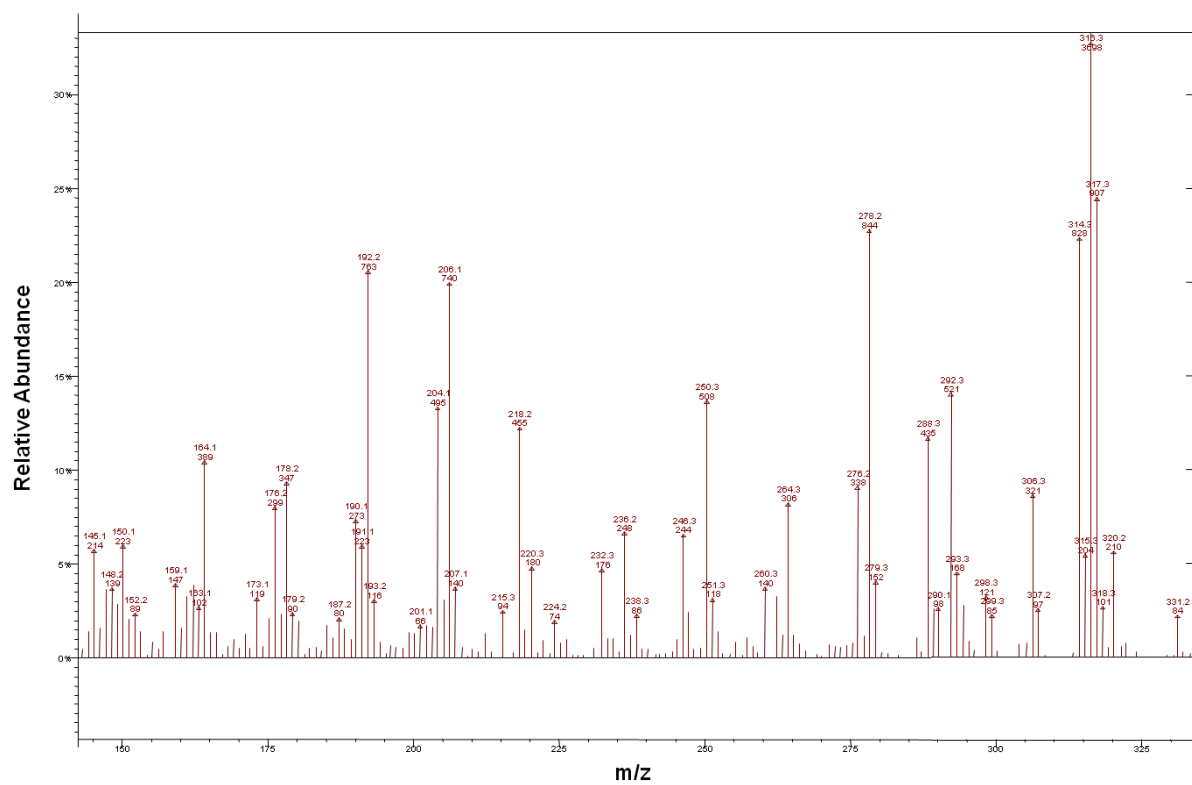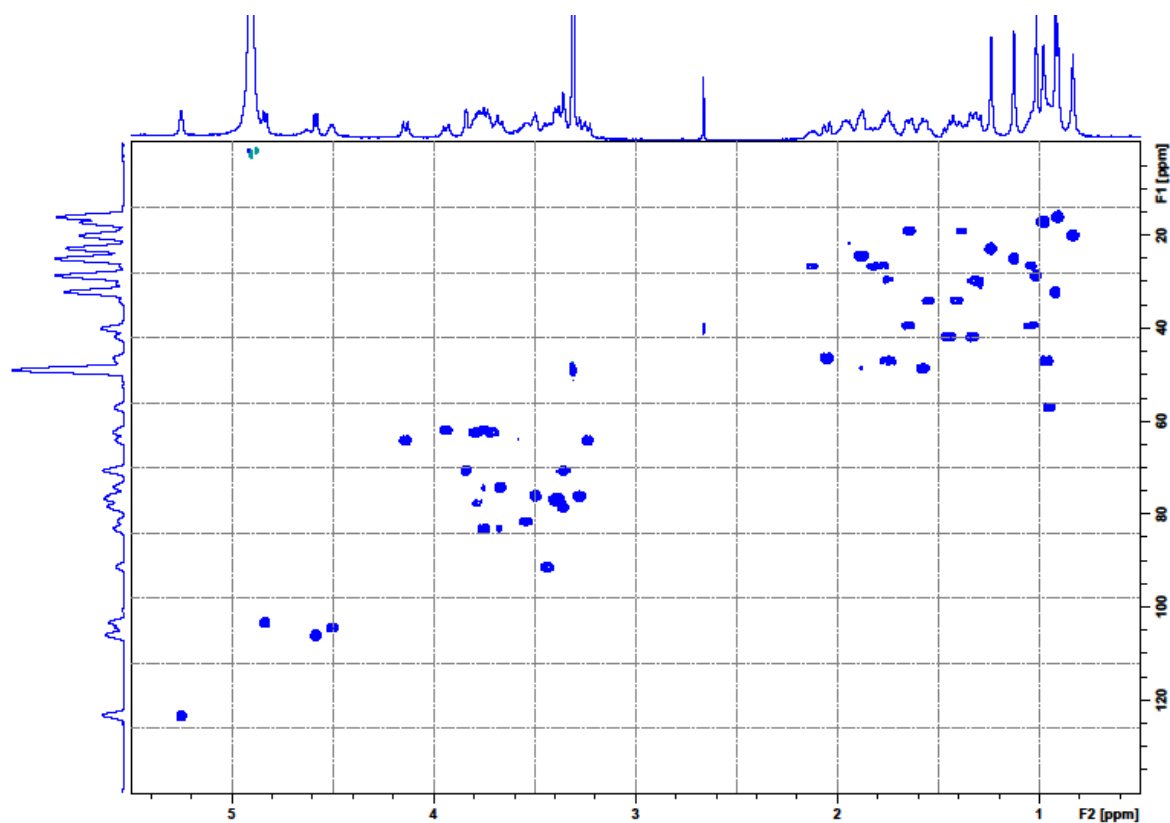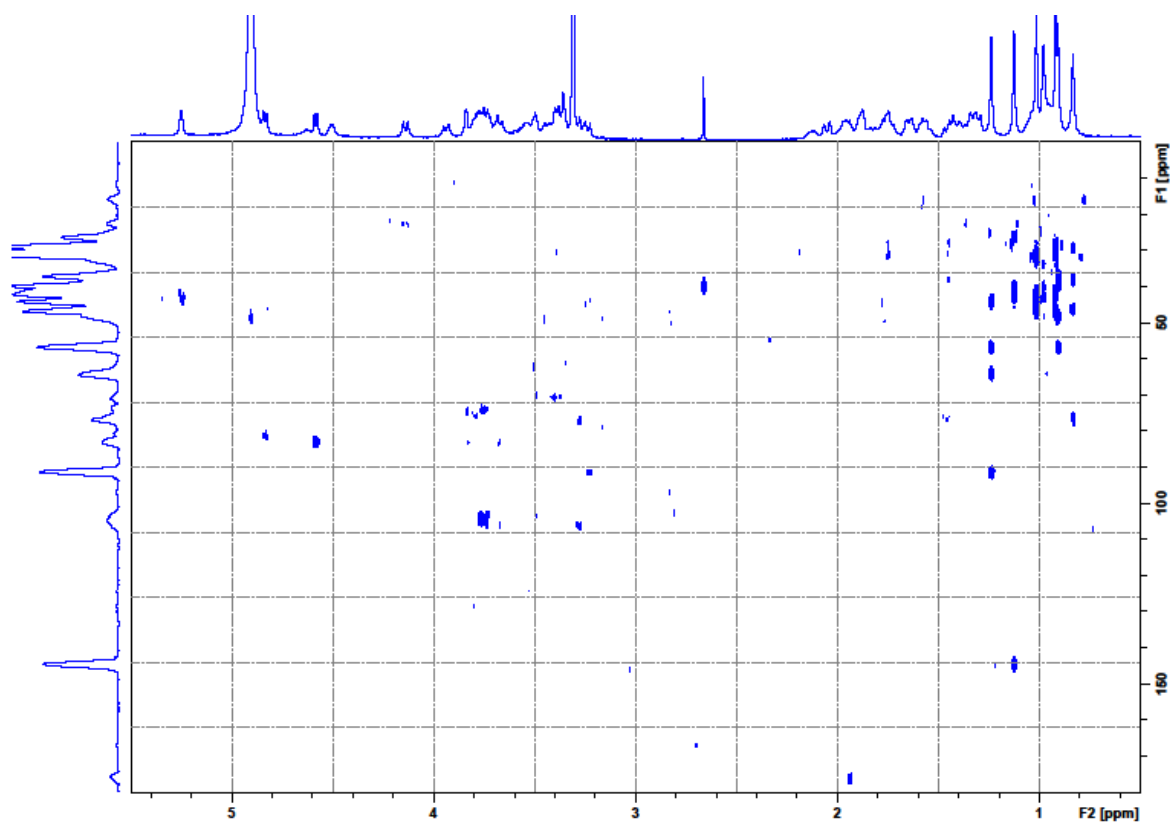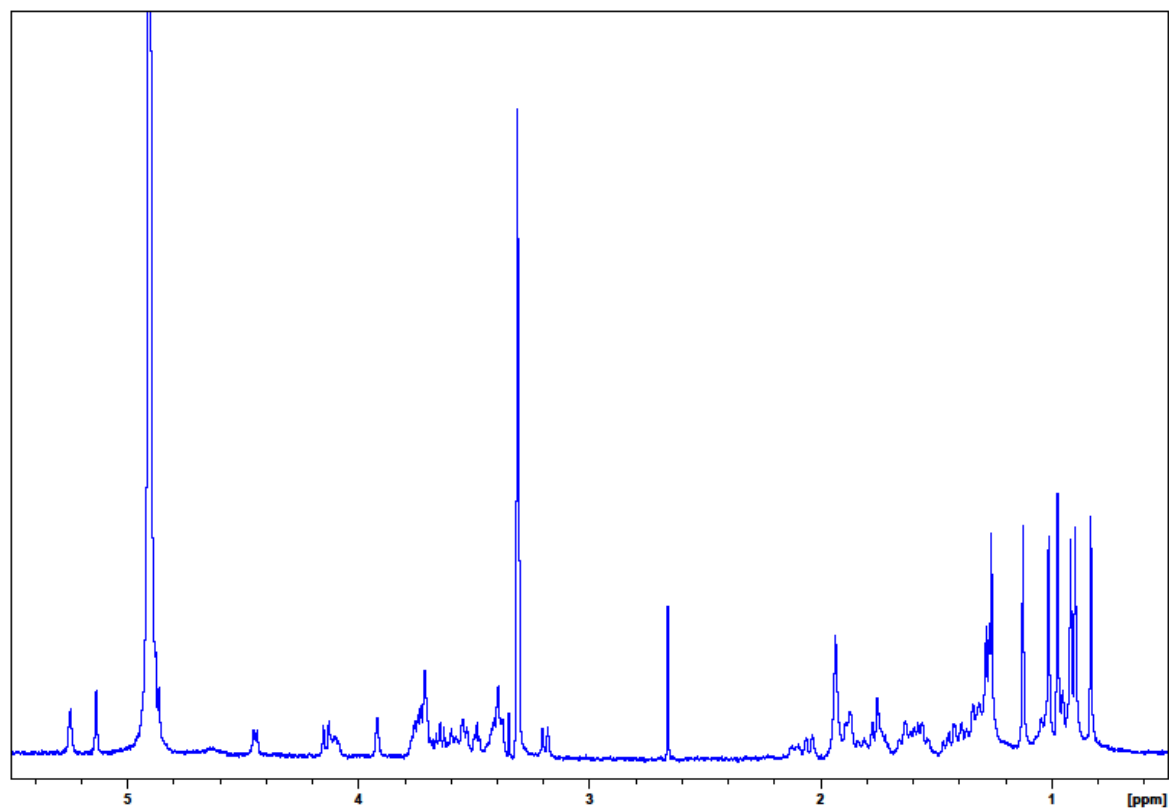
8.1.2 NMR spectra data

^{1}H NMR Spectrum of Soyasaponin V (**46,** 500 MHz, CD$_3$OD-d_4)
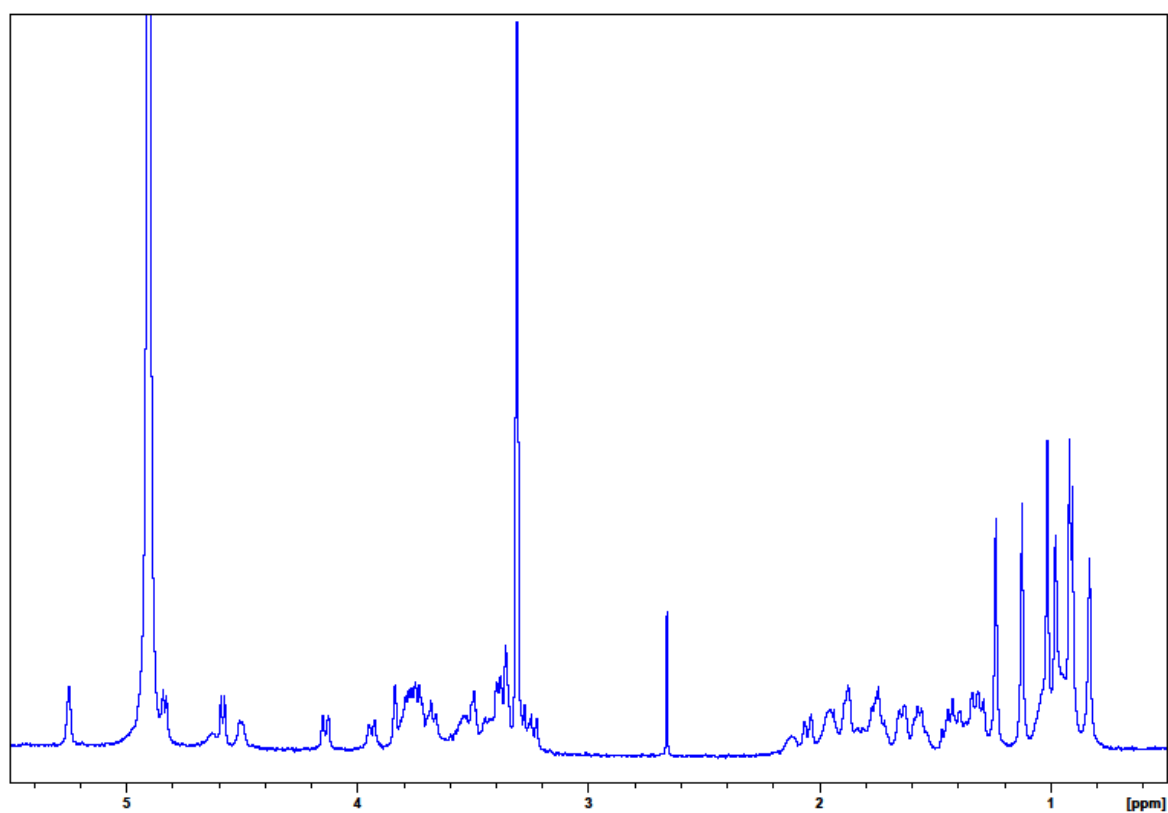
^{1}H-^{1}H COSY Spectrum of Soyasaponin V (**46,** 500 MHz, CD$_3$OD-d_4)

HSQC Spectrum of Soyasaponin V (**46,** 500 MHz, CD$_3$OD-d_4)

HMBC Spectrum of Soyasaponin V (**46,** 500 MHz, CD$_3$OD-d_4)

ROESY Spectrum of Soyasaponin V (**46,** 500 MHz, CD$_3$OD-*d*$_4$)
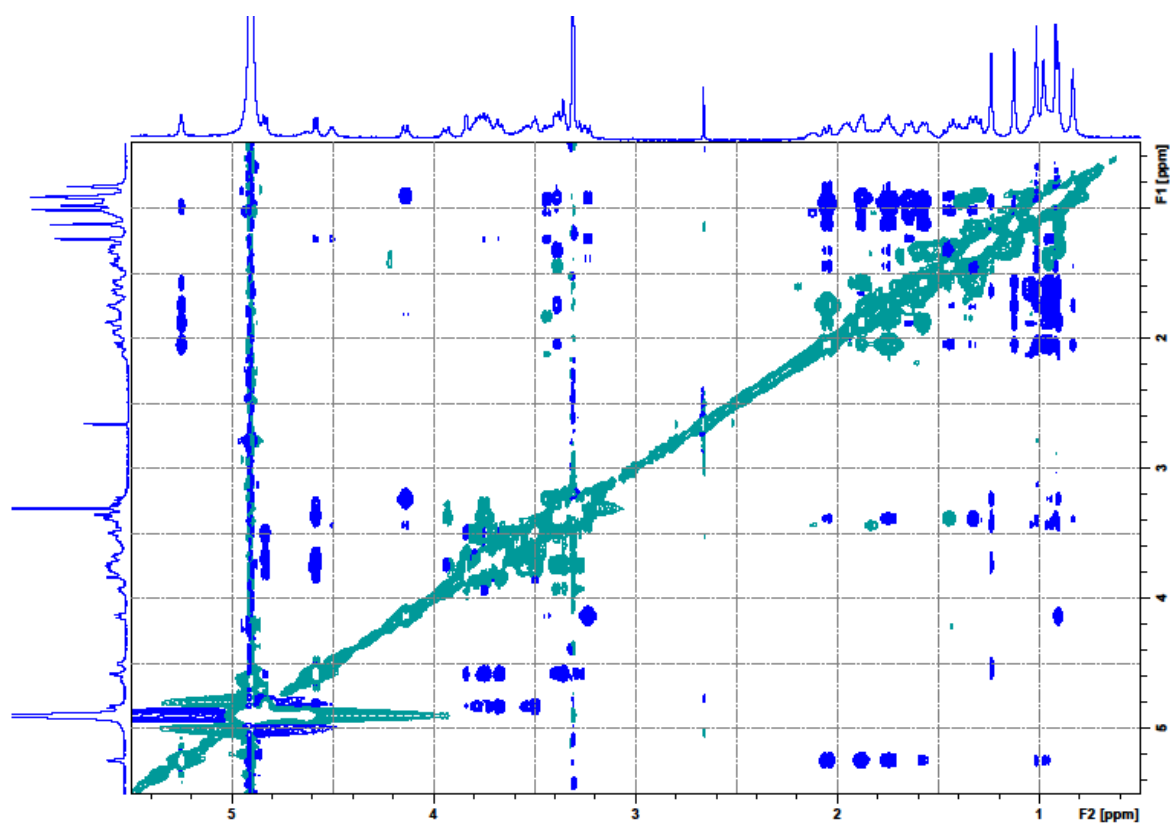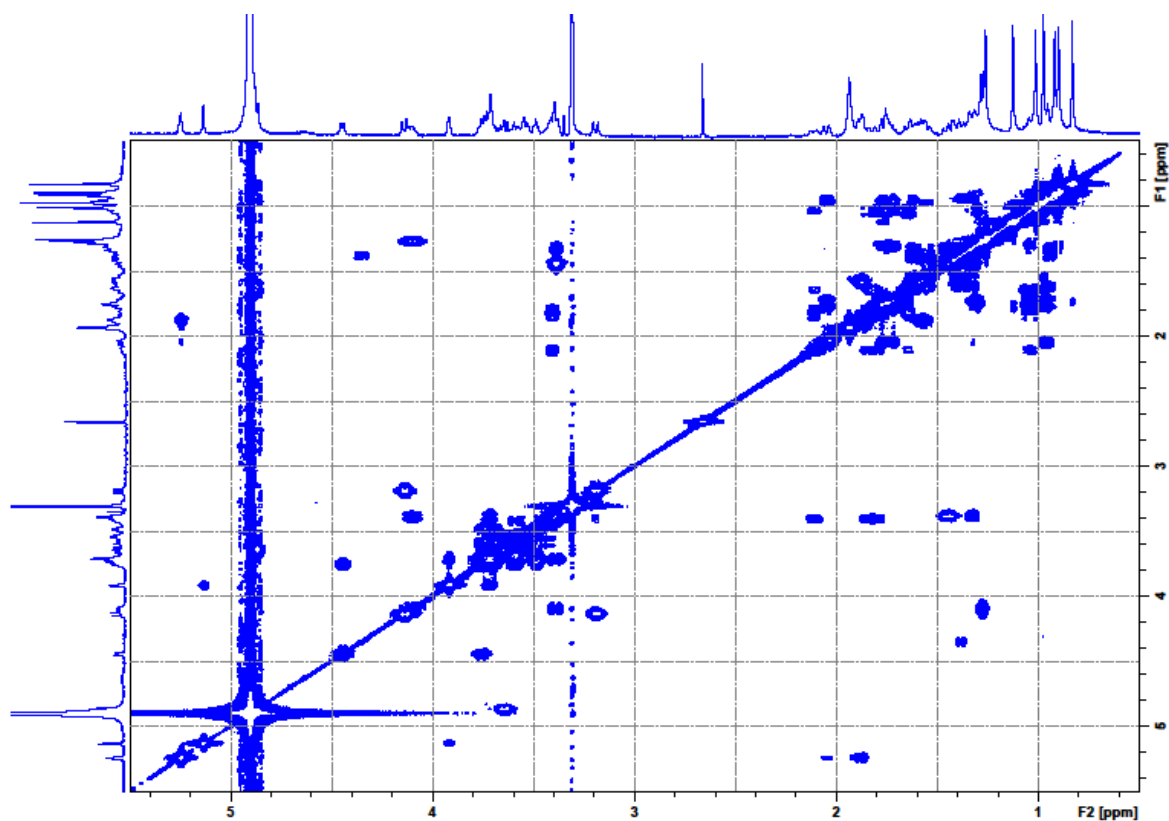

^{1}H NMR Spectrum of Soyasaponin I (**47,** 500 MHz, CD$_3$OD-*d*$_4$)

^{1}H-^{1}H COSY Spectrum of Soyasaponin I (**47,** 500 MHz, CD$_3$OD-d_4)

HSQC Spectrum of Soyasaponin I (**47,** 500 MHz, CD$_3$OD-d_4)

HMBC Spectrum of Soyasaponin I (**47,** 500 MHz, CD$_3$OD-d_4)
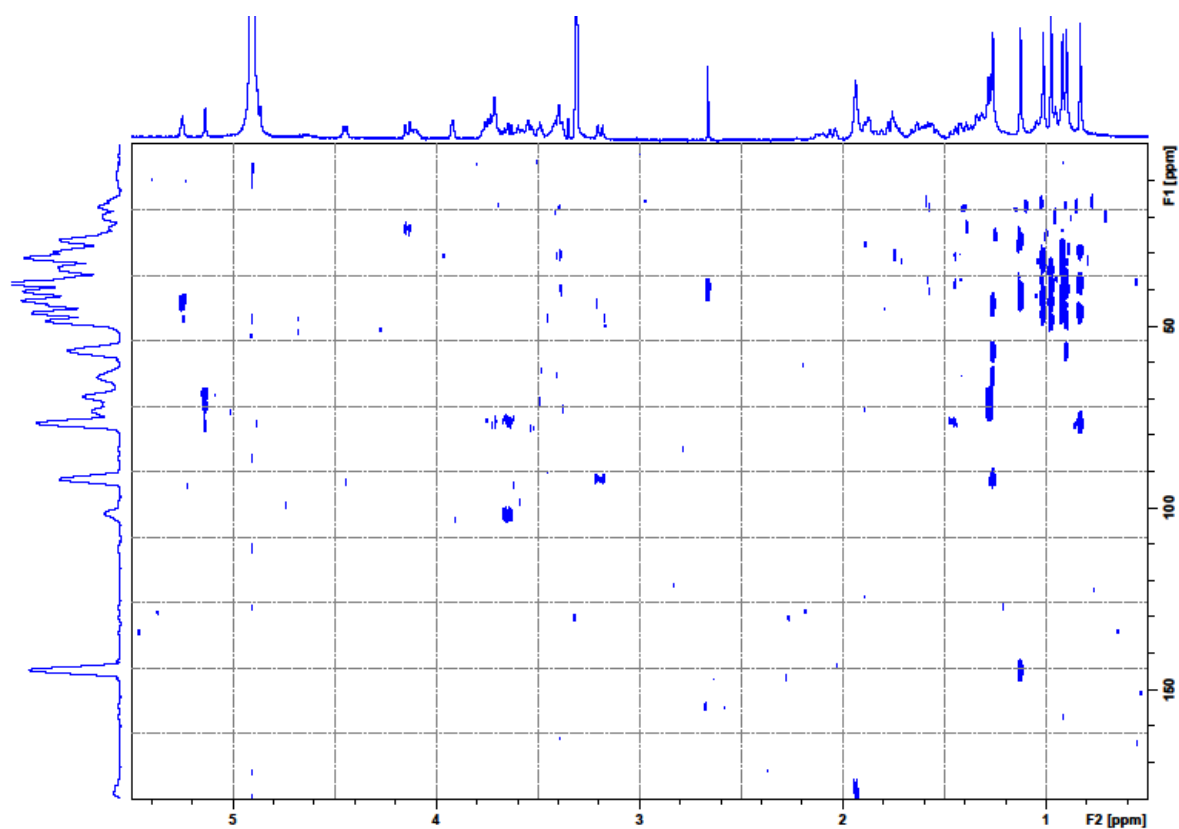
ROESY Spectrum of Soyasaponin I (**47,** 500 MHz, CD$_3$OD-d_4)
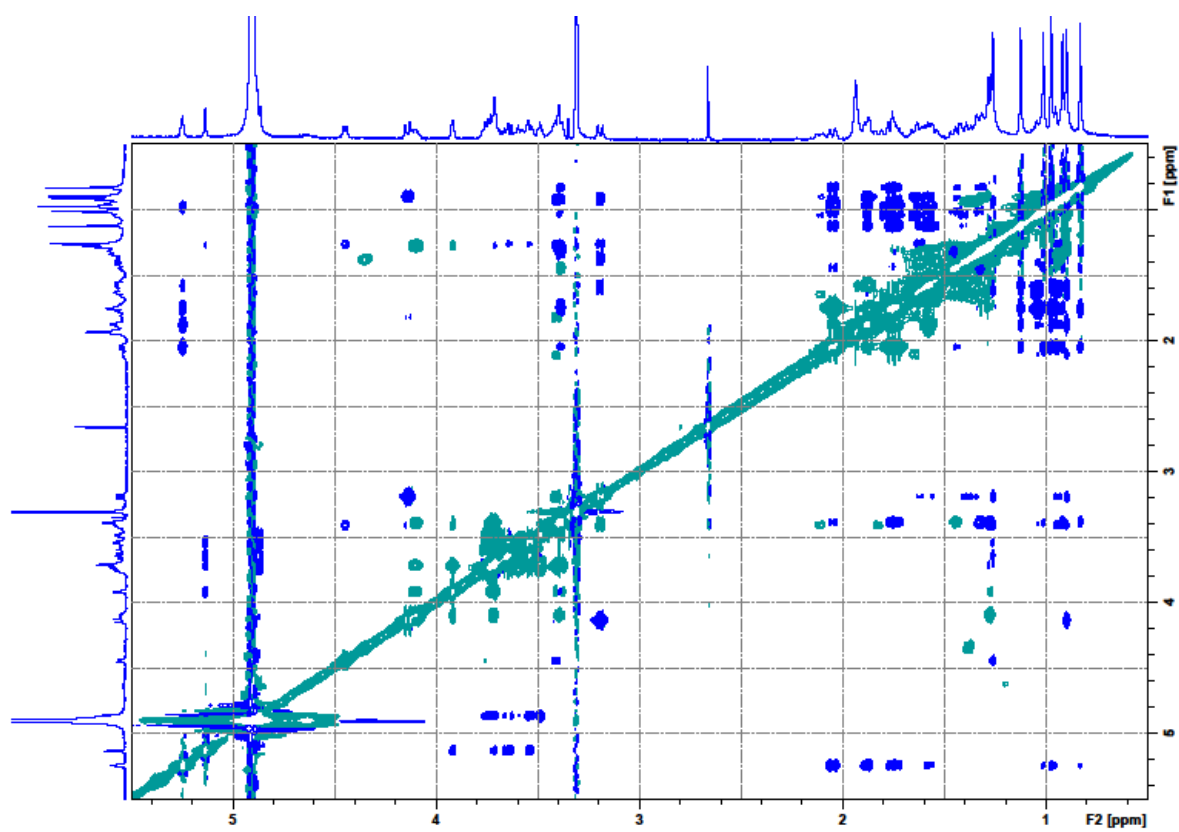
^{1}H NMR Spectrum of Crude White Secretions (500 MHz, CD$_3$OD-d_4)
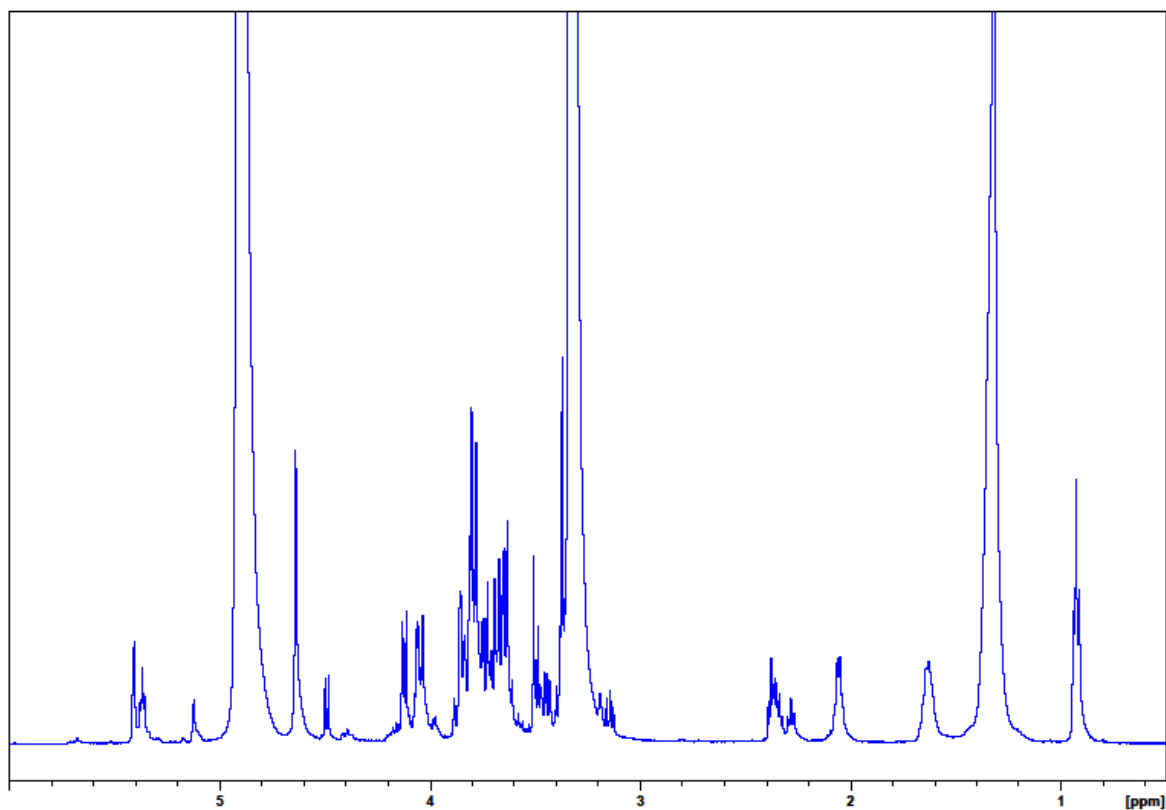
^{1}H NMR Spectrum of Organic Extract of White Secretions (500 MHz, CDCl$_3$-d_1)
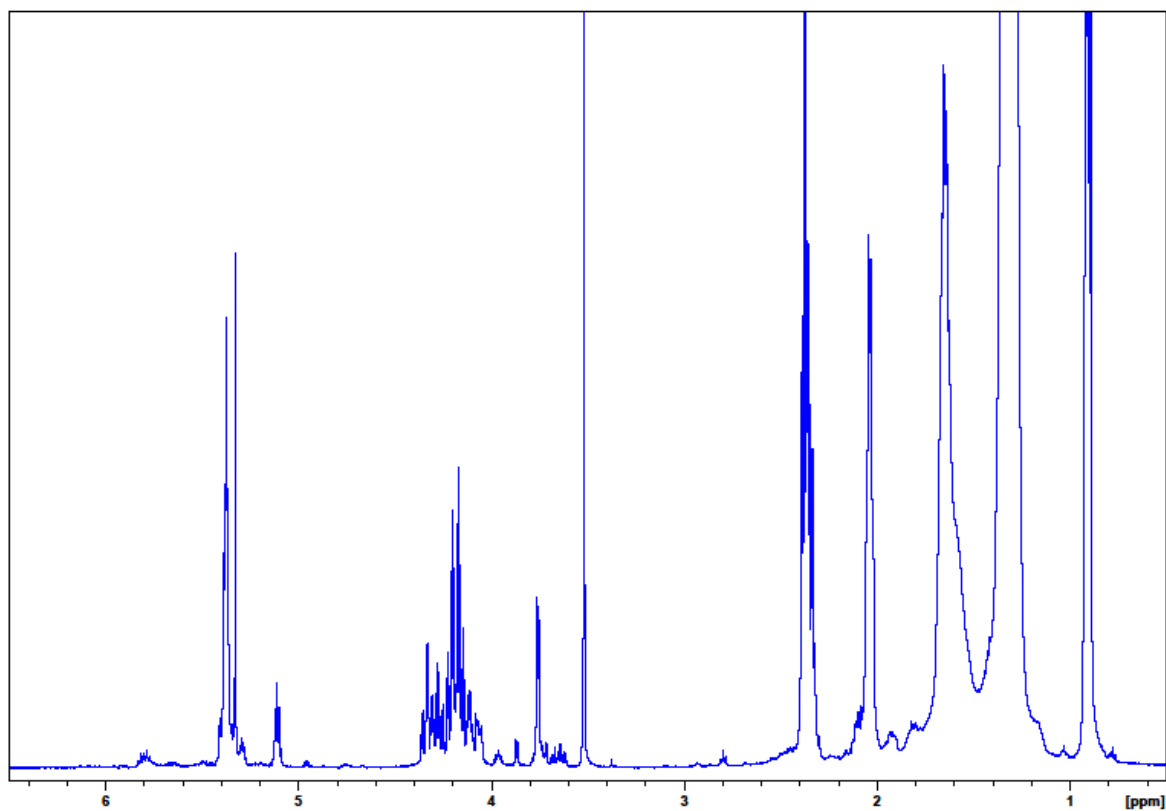
HSQC Spectrum of Organic Extract of White Secretions (500 MHz, CDCl$_3$-d_1)
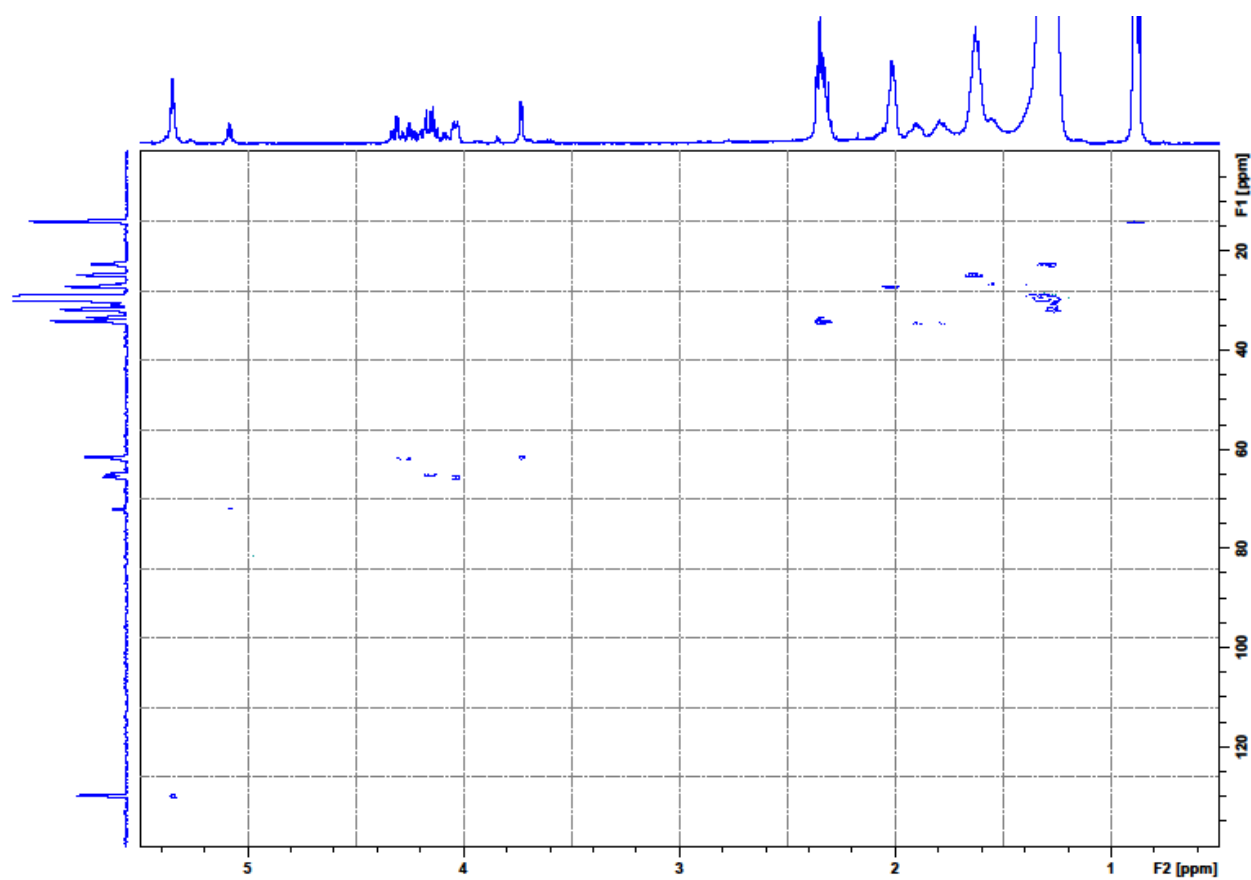
^{1}H NMR Spectrum of Aqueous Phase of Crude White Secretion (500 MHz, CD$_3$OD-d_4)
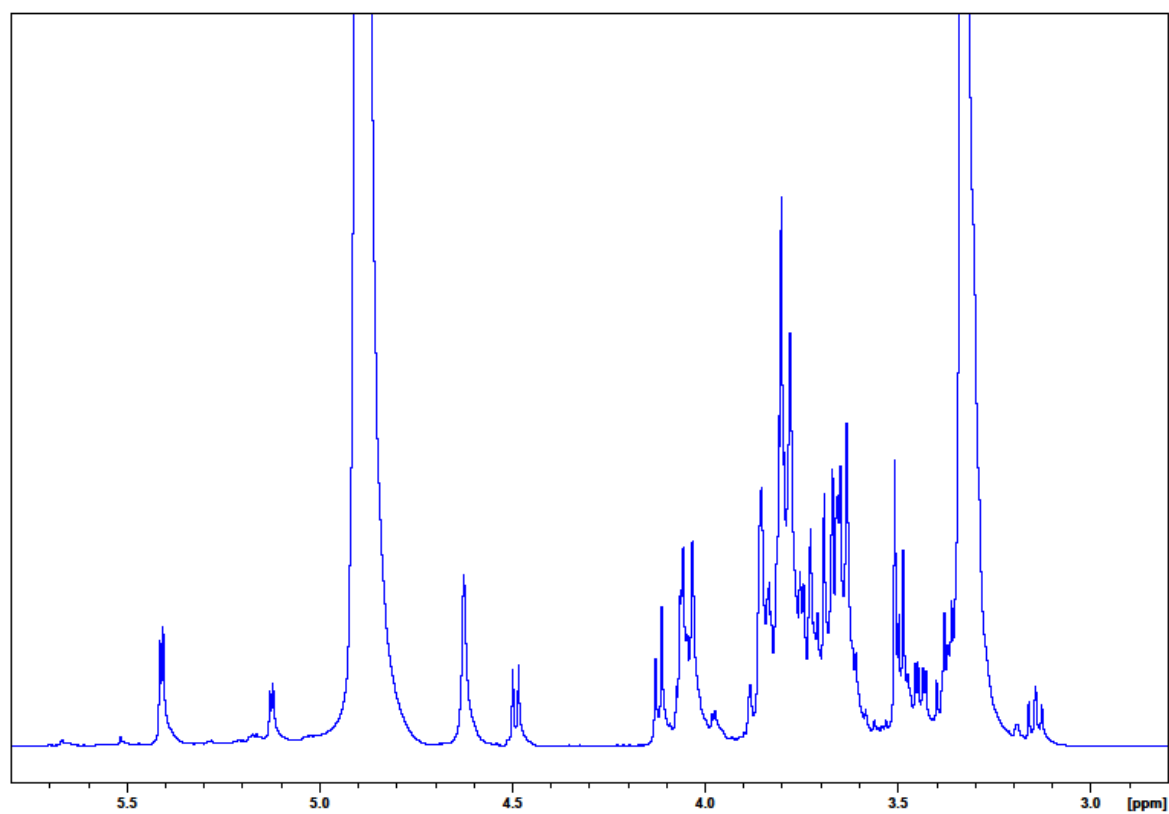
^{1}H NMR Spectrum of D-(+)-Glucose (**64**, 400 MHz, CD$_3$OD-d_4)
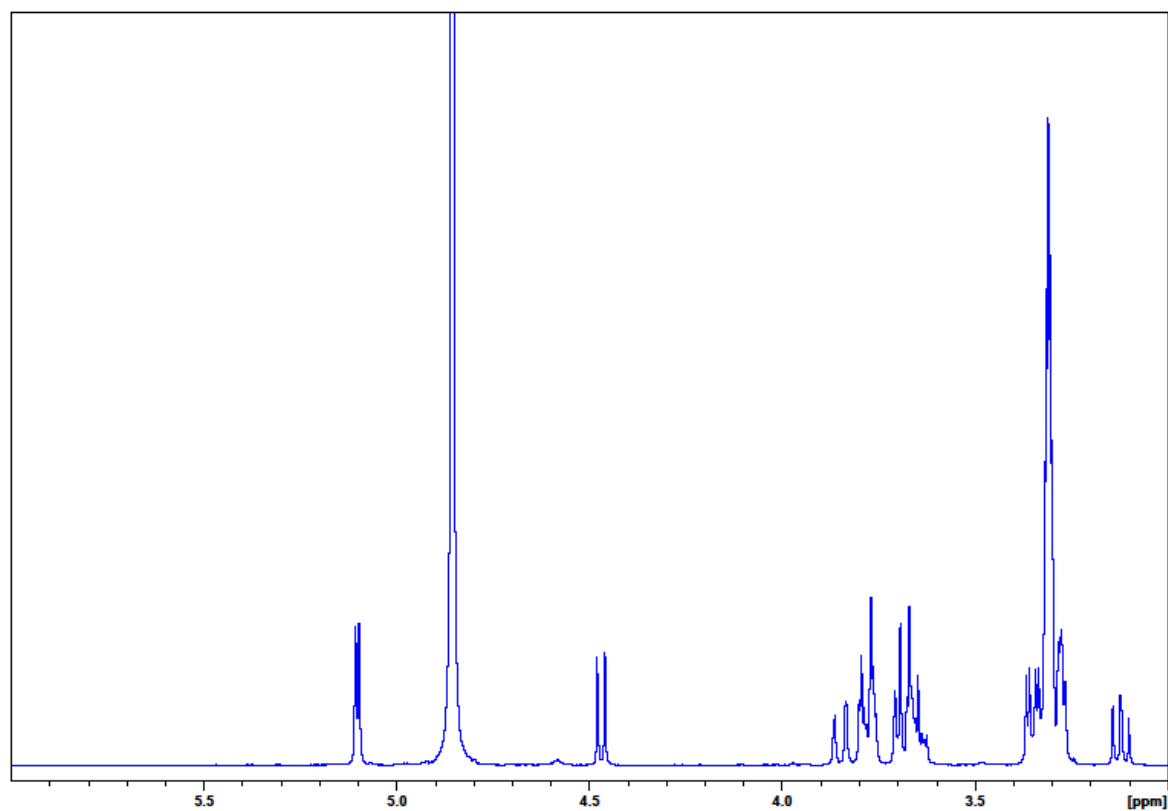
^{1}H NMR Spectrum of D-(−)-Fructose (**65**, 400 MHz, CD$_3$OD-d_4)
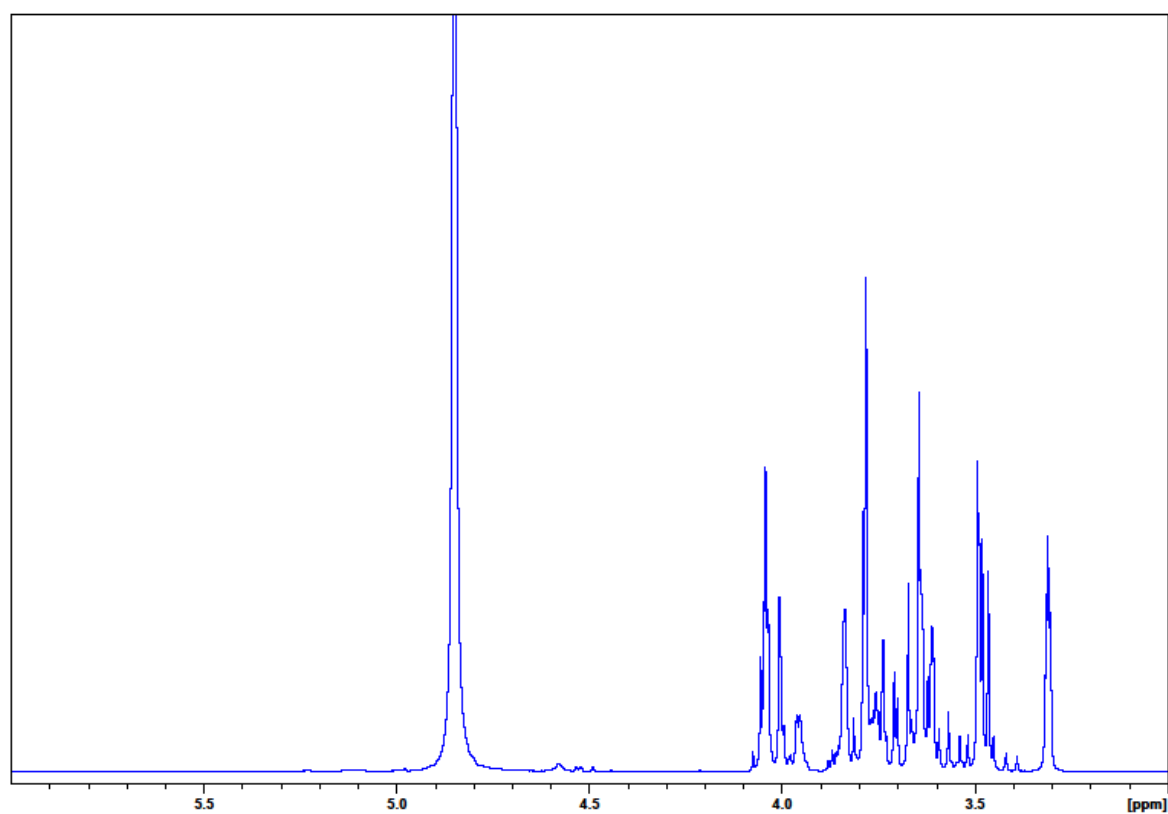
^{1}H NMR Spectrum of D-(+)-Sucrose (**66**, 400 MHz, CD$_3$OD-d_4)

Table S1. NMR Spectroscopic Data for Soyasaponin V (**46**) and in Soyasaponin I (**47**) in CD$_3$OD-d_4

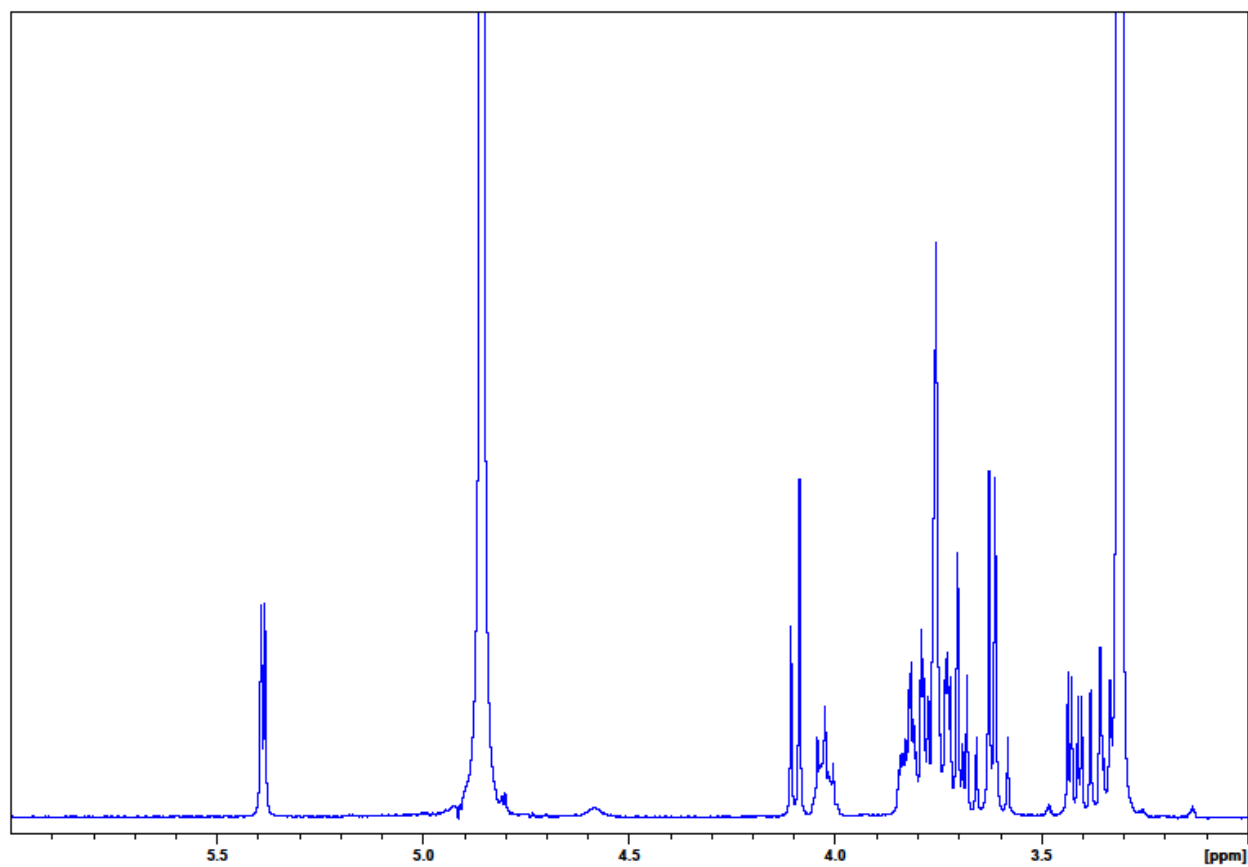|	Soyasaponin V (**46**)			Soyasaponin I (**47**)		
position	^{1}H (J in Hz)	^{13}C	ROESY	^{1}H (J in Hz)	^{13}C	ROESY
aglycon						
1α	1.64, m	39.5		1.65, m	39.6	
1β	1.04, m			1.05, m		
2α	2.13, m	26.7		2.11, m	26.8	
2β	1.82, m			1.82, m		
3	3.44, m	91.4	23	3.40, m	92.2	23
4		44.1			44.1	
5	0.95, m	57.2	9, 23	0.94, m	57.1	9, 23
6α	1.64, m	19.1		1.62, m	19.0	
6β	1.39, m			1.35, m		26
7α	1.55, m	34.0		1.56, m	34.1	
7β	1.41, m			1.40, m		
8		40.2			40.4	
9	1.58, m	48.7	5, 27	1.58, m	48.6	5, 27
10		37.0			36.8	
11α	1.88, m	24.4	25, 26, 27	1.87, m	24.6	25, 26
11β	1.88, m			1.87, m		
12	5.25 br s	123.5	15α, 18, 27, 29	5.24, br s	123.4	18
13		144.8			144.6	
14					43.6	
15α	1.76, m	43.2	12	1.77, m	26.6	27
15β	1.04, m			1.04, m		26, 27, 28
16α	1.76, m	26.7		1.76, m	29.5	
16β	1.32, m			1.31, m		
17		38.1			38.2	
18	2.05, d (12.7)	46.5	12, 26 27, 28, 29	2.05, d (13.5)	46.4	12, 26, 27, 28, 29
19α	1.75, m	47.1	27, 30	1.75	47.1	27, 30
19β	0.96, m			0.96		
20		31.2			31.1	
21α	1.45, m	41.9		1.45	41.9	
21β	1.33, m			1.33		
22	3.39, d (9.5)	76.1	28, 29	3.39, (8.8)	76.7	28, 30
23	1.24, s	22.9	3, 5	1.26, s	23.5	3, 5
24α	4.14, d (11.3)	64.2		4.14, d (11.0)	64.1	25
24β	3.24, d (11.3)			3.19, d (11.0)		25
25	0.91, s	16.2	11, 24α, 24β	0.90, s	16.2	11, 24α, 24β, 28
26	0.98, s	17.3	11, 18, 28	0.97, s	17.2	6β, 11, 15β, 18, 25, 28
27	1.12, s	25.2	5, 9, 11, 12, 18, 19α	1.12, s	25.1	9, 11, 15α, 15β, 18, 19α
28	0.83, s	20.1	18, 22, 26	0.83, s	20.1	15β, 18, 22, 25, 26
29	1.01, s	28.8	12, 18, 22	1.01, s	28.8	
30	0.92, s	32.3	19α	0.92, s	32.3	19α, 22
Sugar						
glcA				glcA		
1′	4.50, d (7.5)	104.5		4.45, d (9.0)	105.3	

2'	3.54	81.6	3.76	76.9	
3'	3.79	77.8	3.59	78.1	
4'	3.44	73.8	3.44	73.8	
5'	3.79	76.5	3.79	76.5	
6'		172.2		172.2	
gal			gal		
1''	4.83, d (7.5)	103.4	4.87, d (7.5)	101.9	
2''	3.75	83.3	3.64	77.8	
3''	3.67	74.3	3.54	76.0	
4''	3.84	70.6	3.71	71.7	
5''	3.79	71.4	3.79	71.4	
6''α	3.79	62.4	3.73	61.9	
6''β	3.72		3.71		
glu			rha		
1'''	4.58, d (7.5)	106.2	5.13, br s	102.0	
2'''	3.28	76.1	3.92	72.0	5''', 6'''
3'''	3.39	76.8	3.72	71.6	5''', 6'''
4'''	3.36	78.6	3.39	73.9	
5'''	3.36	70.8	4.10	69.3	2''', 3'''
6'''α	3.94, d (12.0)	62.1	1.28, d (6.0)	17.9	2''', 3'''
6'''β	3.75				

8.2 Proteomics Data

Table S2. Proteiomic analysis of active fractions (Fr. 3-7) from Sephadex G75. (a) Proteins identified using stringend database searching (MASCOT) and (b) Proteins hit by homolog-based database searching (MS BLAST)

	MASCOT DB searching (a)					MS BLAST searching (b)				
Spot	**Accession number**	**Description**	**Organism**	**matched peptides**	**MASCOT Score**	*de novo* **peptides**	**Accession number**	**Description**	**Organism**	**matched peptides**	**MS Blast Score**
1	ACU00133	chymotrypsin-like protein precursor	*Spodoptera litura*	4	160	122	ACU00133	chymotrypsin-like protein precursor	*Spodoptera litura*	17	928
	ABU96714	trypsin-like serine protease	*Spodoptera litura*	2	84		ABU96714	trypsin-like serine protease	*Spodoptera litura*	8	528
	NP_959390	pantoate-beta-alanine ligase	*Mycobacterium avium* subsp. *paratuberculosis* K-10	1	64		ABP96915	serine protease 2	*Helicoverpa armigera*	4	256
	ACI32818	beta-1,3-glucanase	*Spodoptera littoralis*	1	58						
2	ACU00133	chymotrypsin-like protein precursor	*Spodoptera litura*	2	118	121	ABU96714	trypsin-like serine protease	*Spodoptera litura*	14	776
	ACI32818	beta-1,3-glucanase	*Spodoptera littoralis*	3	108		ADA83701	chymotrypsin	*Helicoverpa armigera*	15	737
	ABR88248	trypsin T5	*Heliothis virescens*	2	98		ADI32887	serine protease	*Helicoverpa armigera*	12	667
	XP_001649432	clip-domain serine protease	*Aedes aegypti*	1	65						
	ABU96714	trypsin-like serine protease	*Spodoptera litura*	1	56						
3	AAA99534	phaseolin	*Phaseolus vulgaris*	7	324	137	ACU00133	chymotrypsin-like protein precursor	*Spodoptera litura*	14	821
	ABU96714	chymotrypsin-like protein precursor	*Spodoptera litura*	2	174		CAA07611	trypsin precursor	*Lacanobia oleracea*	11	578
	ABR88248	trypsin T5	*Heliothis virescens*	1	66		AAA99534	phaseolin	*Phaseolus vulgaris*	8	481

	ABR88239	chymotrypsin-like protease C9	*Heliothis virescens*	1	55						
4	P07219	phaseolin, alpha-type	*Phaseolus vulgaris*	7	324	70	CAA26718	alpha-type phaseolin precursor	*Phaseolus vulgaris*	9	658
	ABW37094	trypsin-like proteinase	*Heliothis virescens*	2	116		ABU96714	trypsin-like serine protease	*Spodoptera litura*	5	327
	AAG51530	dessication-related protein	*Arabidopsis thaliana*	2	110		ABN09090	desiccation-related protein PCC13-62 precursor	*Medicago truncatula*	4	289
							ACI32818	beta-1,3-glucanase	*Spodoptera littoralis*	3	175
							AAO75039	chymotrypsin precursor	*Spodoptera frugiperda*	3	171
5	P07219	phaseolin, alpha-type	*Phaseolus vulgaris*	17	831	116	AAA99534	phaseolin	*Phaseolus vulgaris*	16	1119
	AAG51530	dessication-related protein	*Arabidopsis thaliana*	2	141		ABR88252	trypsin SP2c	*Heliothis virescens*	8	472
	ACI32818	beta-1,3-glucanase	*Spodoptera littoralis*	1	63		ABN09090	desiccation-related protein PCC13-62 precursor	*Medicago truncatula*	4	246
							CAA72956	trypsin-like protease	*Helicoverpa armigera*	4	205
							XP_002021058	trypsin-like serine protease	*Drosophila persimilis*	3	188
							ABR28478	beta-1,3-glucanase	*Spodoptera frugiperda*	2	135

6	P07219	phaseolin, alpha-type	*Phaseolus vulgaris*	7	302	41	CAA26718	alpha-type phaseolin precursor	*Phaseolus vulgaris*	8	588
	ACI32818	beta-1,3-glucanase	*Spodoptera littoralis*	1	63		XP_002081034	trypsin-like serine protease	*Drosophila simulans*	6	282
	ABW37094	trypsin-like proteinase	*Heliothis virescens*	1	64						
7	AAA99534	phaseolin	*Phaseolus vulgaris*	12	560	102	CAA36853	alpha-phaseolin	*Phaseolus vulgaris*	15	975
	ABW37094	trypsin-like proteinase	*Heliothis virescens*	1	64		ABU98624	protease	*Helicoverpa armigera*	6	341
							CAA72958	chymotrypsin-like protease	*Helicoverpa armigera*	7	334
							XP_002026437	trypsin-like serine protease	*Drosophila persimilis*	5	231
							ZP_04189170	haloacid dehalogenase-like hydrolases	*Bacillus cereus* AH1271	1	77
8	P07219	phaseolin, alpha-type	*Phaseolus vulgaris*	3	131	89	ACR15970	serine protease 1	*Mamestra configurata*	10	569
	ABU96714	trypsin-like serine protease	*Spodoptera litura*	1	88		AF233728	AiC2 chymotrypsinogen	*Agrotis ipsilon*	6	325
	XP_001649432	clip-domain serine protease	*Aedes aegypti*	1	72		AAC04316	phaseolin	*Phaseolus vulgaris*	5	325
							ZP_01045748	secreted hemolysin-type calcium-binding bacteriocin	*Nitrobacter* sp. Nb-311A	4	192
							YP_002947474	succinate dehydrogenase, cytochrome b subunit	*Variovorax paradoxus* S110	1	74

9	P07219	phaseolin, alpha-type	*Phaseolus vulgaris*	3	163	103	ACU00133	chymotrypsin-like protein precursor	*Spodoptera litura*	16	804
	ABU96714	trypsin-like serine protease	*Spodoptera litura*	2	141		ABR88245	trypsin T3a	*Heliothis virescens*	10	513
	ABW37094	trypsin-like proteinase	*Heliothis virescens*	2	98		CAA36853	alpha-phaseolin	*Phaseolus vulgaris*	6	365
10	P35042	trypsin CFT-1	*Choristoneura fumiferana*	1	69	83	ABU98624	protease	*Helicoverpa armigera*	9	497
	ABW37094	trypsin-like proteinase	*Heliothis virescens*	1	64		AAP97394	alpha-amylase 3	*Diatraea saccharalis*	3	163
	AAO75039	chymotrypsin precursor	*Spodoptera frugiperda*	1	64		NP_001177563	odorant receptor 183	*Nasonia vitripennis*	3	156
	P07219	phaseolin, alpha-type	*Phaseolus vulgaris*	2	62		EDW41759	glutamyl-tRNA synthetase	*Drosophila sechellia*	1	76
11	CAD28836	phytohemagglutinin	*Phaseolus vulgaris*	3	226	118	P15231	leucoagglutinating phytohemagglutinin	*Phaseolus vulgaris*	9	601
	AAG51530	dessication-related protein	*Arabidopsis thaliana*	2	183		ABN09089	desiccation-related protein PCC13-62 precursor	*Medicago truncatula*	9	561
	YP_001900764	porin Gram-negative type	*Ralstonia pickettii 12J*	3	155		AAN10048	high molecular weight root vegetative storage protein precursor	*Medicago sativa*	7	390
	P07219	phaseolin, alpha-type	*Phaseolus vulgaris*	3	152		EDS41410	trypsin eta	*Culex quinquefasciatus*	5	236
							ACD28332	porin Gram-negative type	*Ralstonia pickettii 12J*	3	163
							AEK35552	amidase	*Corynebacterium*	2	121

	8								*variabile* DSM 44702		
							AAV33657	chymotrypsin-like	*Helicoverpa punctigera*	2	113
12	AAG51530	dessication-related protein	*Arabidopsis thaliana*	2	65	19	AAF74740	trypsin precursor AiJ5	*Agrotis ipsilon*	2	149
13	CAD28836	phytohemagglutinin	*Phaseolus vulgaris*	2	174	69	CAF25189	carboxypeptidase precursor	*Helicoverpa armigera*	9	476
	AAG51530	dessication-related protein	*Arabidopsis thaliana*	2	126		ACD28493	porin Gram-negative type	*Ralstonia pickettii 12J*	6	402
	ABU98614	alpha-amylase	*Helicoverpa armigera*	1	73		AEA76309	alpha-amylase	*Mamestra configurata*	6	343
	ABW37094	trypsin-like proteinase	*Heliothis virescens*	1	62		ABN09090	desiccation-related protein PCC13-62 precursor	*Medicago truncatula*	6	342
							CAJ34351	phytohemagglutinin precursor	*Phaseolus vulgaris*	5	295
							ACT15362	trypsinogen 2	*Takifugu obscurus*	4	194

Table S3. Proteiomic analysis of active fractions (Fr. 3) from 2nd DEAE A25. (a) Proteins identified using stringend database searching (MASCOT) and (b) Proteins hit by homolog-based database searching (MS BLAST)

Spot	MASCOT DB searching (a)					MS BLAST searching (b)					
	Accession number	Description	Organism	matched peptides	MASCOT Score	*de novo* peptides	Accession number	Description	Organism	matched peptides	MS Blast Score
14	AAU95561	DING protein	*Solanum tuberosum*	2	134	85	ACR16004	serine protease 2	*Mamestra configurata*	7	413
	P00761	GLP-binding protein 1b	*Solanum tuberosum*	1	89		BAA92940	yieldin precursor	*Vigna unguiculata*	7	340
							AAU95561	DING protein	*Solanum tuberosum*	5	300
							YP_609556	glycosyl transferase MigA	*Pseudomonas entomophila* L48	3	155
							CAD28837	phytohemagglutinin	*Phaseolus vulgaris*	2	118
							YP_004557 786	ornithine cyclodeaminase/mu-crystallin	*Sinorhizobium meliloti* AK83	1	81
15	AAU95561	DING protein	*Solanum tuberosum*	3	158	56	BAA92940	yieldin precursor	*Vigna unguiculata*	5	255
	AAG51530	dessication-related protein	*Arabidopsis thaliana*	2	94		AAA33760	phytohemagglutinin prepeptide	*Phaseolus vulgaris*	3	152
	ZP_00944567	outer membrane porin protein 32 precursor	*Ralstonia solanacearum* UW551	1	59		YP_259866	alkaline phosphatase L	*Pseudomonas fluorescens* Pf-5	1	79
							AAF24227	trypsin-like PiT2c	*Plodia*	1	79

							precursor	*interpunctella*		
16	YP_00287066 0	amino acid ABC transporter substrate-binding protein	*Pseudomonas fluorescens* SBW25	6	288	68	AAU95561	DING protein	*Solanum tuberosum*	5	326
	AAU95561	DING protein	*Solanum tuberosum*	4	206		BAG79074	amino acid ABC transporter substrate binding component	*Escherichia coli* SE11	6	318
	AAG51530	dessication-related protein, putative	*Arabidopsis thaliana*	2	111		ABN09089	desiccation-related protein PCC13-62 precursor	*Medicago truncatula*	4	242
	YP_00190076 4	porin Gram-negative type	*Ralstonia pickettii* 12J	2	96		ACD28332	porin Gram-negative type	*Ralstonia pickettii* 12J	2	176
	CAD28673	phytohemagglutinin	*Phaseolus vulgaris*	1	63		BAA92940	yieldin precursor	*Vigna unguiculata*	3	163
							BAG00096	precorrin-2 methyltransferase	*Microcystis aeruginosa* NIES-843	1	77
							BAB62584	pentatricopeptide (PPR) repeat-containing protein-like	*Oryza sativa* Japonica Group	1	76
17	ZP_05133826	alkaline phosphatase L	*Stenotrophomon as* sp. SKA14	5	265	139	AAY92032	alkaline phosphatase L	*Pseudomonas fluorescens* Pf-5	19	1100
	AAO72974	GLP-binding protein 1b	*Solanum tuberosum*	3	196		ABN09090	desiccation-related protein	*Medicago truncatula*	8	465

AAU95561	DING protein	*Solanum tuberosum*	3	149		PCC13-62 precursor			
					EEN90397	alkylhydroperoxidase AhpD	*Rhodococcus erythropolis* SK121	1	74

Table S4. Proteiomic analysis of final active fraction. (a) Proteins identified using stringend database searching (MASCOT) and (b) Proteins hit by homolog-based database searching (MS BLAST)

	MASCOT DB searching (a)					MS BLAST searching (b)					
Spot	Accession number	Description	Organism	matched peptides	MASCOT Score	*de novo* peptides	Accession number	Description	Organism	matched peptides	MS BLAST Score
18	AAA99534	phaseolin	*Phaseolus vulgaris*	15	578	128	AAC04316	phaseolin	*Phaseolus vulgaris*	12	732
	YP_001900764	porin	*Ralstonia pickettii* 12J	3	132		AAV33657	chymotrypsin-like	*Helicoverpa punctigera*	5	322
	AAG51530	dessication-related protein, Ferritin-like superfamily	*Arabidopsis thaliana*	2	121		AAF24228	trypsin-like PiT2c precursor	*Plodia interpunctella*	2	117
	ACR15984	serine protease 25	*Mamestra configurata*	2	105		ABR88252	trypsin SP2c	*Heliothis virescens*	1	100
							AAF74743	trypsin precursor Hz8	*Helicoverpa zea*	1	85
							AEL24137	Peptidase_M14N E-CP-C_like	*Cyclobacterium marinum* DSM 745	1	75

Table S5. Proteiomic data of B4 and B5 by MS^E analysis.

No.	Accession number	BLAST	Description	MW	Organism	Conserved domains
1	B8I1Q1	YP_002507666	hypothetical protein Ccel_3398	974 AA	*Clostridium cellulolyticum* H10	
2	B8I5P3	YP_002504690	hypothetical protein Ccel_0323 ACL74710	332 AA 332 AA	*Clostridium cellulolyticum* H10 *Clostridium cellulolyticum* H10	GGGtGRT superfamily GGGtGRT superfamily
3	B1QED9	EDT80554	clp protease	230 AA	*Clostridium botulinum* NCTC 2916	Clp_protease_like signal peptide peptidase SppA
4	C0DBK6	EEG51381 WP_007719749	SH3 domain protein, partial hypothetical protein, partial	169 AA 169 AA	*Clostridium asparagiforme* DSM 15981 *Clostridium asparagiforme*	Bacterial SH3 domain

8.3 List of abbreviations

(–)-JA-L-Ile	(-)-jasmonoyl-L-isoleucine
(+)-7-*iso*-JA-L-Ile	(+)-7-iso-jasmonoyl-L-isoleucine
1D SDS-PAGE	One dimention sodium dodecylsulfate polyacrylamide gel electrophoresis
ABA	Abscisic acid
AcOH	Acetic acid
Aib	α-aminoisobutyric acid
AIEX	Anion exchange
ALA	Alamethicin
AOS	Active oxygen species
APS	Ammoniumperoxydisulfat
arb units	Arbitrary units
BLAST	Basic local alignment search tool
BLM	Black lipid membrane
CC	Column chromatography
CD_3OD	Deuterated methanol
$CDCl_3$	deuterated chloroform
cDNA	Complementary DNA
cis-OPDA	*cis*-(+)-12-oxo-phytodienoic acid
CLS	Closed loop stripping
CML42	Calmodulin like protein 42
cts	Count per second
CV	Column volume
DCM	Dichloromethane
DDA	Data dependent acquisition
DMNT	4,8-Dimethylnona-1,3,7-triene
DTT	Dithiothreitol
EtOAc	Ethyl acetate
EtOH	Ethanol
FA	Formic acid
Gln	L-Glutamin
Glu	L-Glutamine acid
HAMP	herbivore-associated molecular patterns
JA	Jasmonic acid
KD	Kilo dalton
MeCN	Acetonitril

MeOH	Methanol
MeSA	Methyl salicylic acid
MSTFA	*N*-methyl-*N*-trimethylsilyl-trifluoroacetamide
MWCO	Molecular weight cut off
NCBI	National center for biotechnology information
NCBInr	NCBI non-redundant protein database
NIST	National Institute of Standards and Technology
OGA	Oligogalacturonic acid
OS	Oral secretion
PAM	Acrylamid/bisacrylamid (40%) Rotiphorese
pCa	Concentration of calcium ion
PDMS	Polydimethylsiloxan
PLGS	ProteinLynx Global Server Browser
PLP	Porin-like protein
RLU	Relative light units
RT-PCR	Real time polymerase chain reaction
SA	Salicylic acid
SAW	Surface acoustic wave
SE	Standard error
SGP	Stacking gel buffer
SPE	Solid phase extraction
SPME	Solid phase microextraction
TEMED	N,N,N,N-tetramethylendiamin
TGP	Separation gel buffer
TLC	Thin layer chromatography
TMS	Trimethylsilyl
TMTT	4,8,12-Trimethyltrideca-1,3,7,11-tetraene
V_m	Membrane potential
VOC	Volatile organic compound
α-HL	α-Hemolysin
NMR	Nuclear magnetic resonance
^{1}H NMR	Proton nuclear magnetic resonance
^{13}C NMR	Carbon nuclear magnetic resonance
MHz	Megahertz
δ	Chemical shift in NMR
ppm	Parts per million (chemical shift)

J	Coupling constant
Hz	Hertz (frequency)
s	Singlet
br d	Broad doublet
d	Doublet
dd	Doublet of doublet
t	Triplet
m	Multiplet
HPLC	High performance liquid chromatography
LC-MS	Liquid chromatography-mass spectrometry
RP-C18	Reverse phase-C18
FPLC	Fast protein liquid chromatography
GC-MS	Gas chromatography-mass spectrometry
FWHM	Full width at half maxium
EI-MS	Electron impact-mass chromatography
ESI	Eletrospray ionization
MS/MS	Tandem mass spectrometry
MW	Molecular weight
amu	Atomic mass unit
TIC	Total ion current chromatography
EIC	Extract ion current chromatography
t_R	Retention time
m/z	Mass-to-charge ratio

8.4 List of publications and talks

8.4.1 List of publications

H. Hu ; **H. Gu o**; E . Li; X. Liu; Y . Zhou; Y . C he   Decaspirones F−I, Bioactive Secondary Metabolites from t he S aprophytic Fungus *Helicoma v iridis J . N at. P rod.* **2006**, *69*, 1672 - 1675.

H. Gu o; H. Hu; S. Liu; X. Liu; Y . Zhou; Y . Che B ioactive *p*-Terphenyl Derivatives from a *Cordyceps*-Colonizing Isolate of *Gliocladium* sp. *J. Nat. Prod.* **2007**, *70*, 1519-1521.

Y. Chen and **H. Guo**, Z. Du, X. Liu, Y. Che and X. Ye Ecology-based screen identifies new metabolites from a *Cordyceps*-Colonizing f ungus a s c ancer c ell p roliferation i nhibitors a nd apoptosis inducers *Cell Prolif.* **2009**, *12*, 838-847.

H. Guo, B. Sun, H. Gao, S. Niu, X. Liu, X. Yao, and Y. Che Trichocladinols A-C, Cytotoxic Metabolites from a *Cordyceps*-Colonizing A scomycete *Trichocladium opa cum Eur. J. Org. Chem.* **2009**, *32*, 5525-5530.

H. Guo, B. Sun, H. Gao, X. Chen, S. Liu, X. Yao, X. Liu, Y. Che Diketopiperazines from the *Cordyceps*-colonizing fungus *Epicoccum nigrum J. Nat. Prod.* **2009**, *72*, 2115-2119.

Huijuan Guo, Natalie Wielsch, Jens B. Hafke, Aleš Svatoš, Axel Mithöfer, Wilhelm Boland A por in-like pr otein f rom or al s ecretions of *Spodoptera l ittoralis* larvae i nduces d efense-related early events in plant leaves. *Insect Biochem. Mol. Biol.* **2013**, *43*, 849-858.

Yongqi S hao, **Huijuan G uo**, Stefan B artram, Wilhelm B oland   In vi vo P yro-SIP a ssessing active gut microbiota of cotton leafworm, *Spodoptera littoralis*. (under revision)

8.4.2 List of posters and talks

Talks

1. **H. Guo**, A. Mithöfer, W. Boland; Isolation, Purification, and Structural Elucidation of A ctive C ompounds f rom Insect Tissue. 4 [th] ILRS S ymposium 20 11, A ltes Schloss, Dornburg, Germany, March 7, 2011.

2. **H. Gu o**, A . M ithöfer, W. B oland; C hemical Investigation of C hannel-Forming Compound f rom Lepidopteran Larvae. 5 [th] ILRS Symposium 2012, R osensäle, Friedrich-Schiller-Universität Jena, Germany, March 13, 2012.

3. **H. Gu o**, A . M ithöfer, W. B oland; C hemical Investigation of C hannel-Forming Compound from L epidopteran Larvae. 6th ILRS S ymposium 2013, H KI-Center for Systems Biology of Infection, Jena, Germany, March 13, 2013.

4. **H. Guo**, A. Mithöfer, W. Boland; Elicitor-Active and Channel-Forming Compounds in th e O ral S ecretions o f th e P lant P est S podoptera litto ralis. 4 5th PhD w orkshop Naturstoff: Chemie, Biologie und Ökologie, April 12, 2013

Posters

1. **H. Gu o**, S . B artram, A . M ithöfer, W . B oland; C hemical I nvestigations on I on Channel F orming C ompounds f rom O ral S ecretions of H erbivorous Lepidopteran Larvae. J SMC/ILRS S ymposium 2009, M ain B uilding, Friedrich-Schiller-Universität Jena, Germany, October 12, 2009

2. **H. Gu o**, N. Wielsch, J. B. Hafke, A. S vatoš, A. Mithöfer, W. Boland; A porin-like protein from or al s ecretions of *Spodoptera littoralis* larvae i nduces d efense-related early ev ents i n p lant l eaves. 7th Central a nd E astern E uropean P roteomics Conference (C EEPC), Abbe C enter B eutenberg a nd Max P lanck Institute f or Chemical Ecology, Jena, Germany , October 13-16, 2013

8.5 Curriculum Vitae

Name: Huijuan Guo

Date of Birth: 28.11.1983

Place of Birth: Datong, China

Nationality: Chinese

Education

08/2009-   Doctoral T hesis i n c hemistry unde r t he s upervision of P rof. D r.
                      Wilhelm Boland

                      Max-Planck-Institute for Chemical Ecology, Jena, Germany

                      Co-supervised by Prof. Dr. Georg Pohnert

                      Friedrich-Schiller-Universität Jena, Germany

> *Chemical Investigations on Channel-Forming Compounds from Oral Secretions of Herbivorous Lepidopteran Larvae*

> *Chemical I nvestigations on W hite Se cretions of P itcher P lant Nepenthes lowii*

> *MALDI-TOF A nalysis o f O ligogalacturonic A cids (OGAs) as the "Damage Self-Recognition" elicitors*

09/2004-07/2007   Master T hesis i n na tural pr oduct c hemistry unde r t he s upervision of
                      Prof. Dr. Yongsheng Che

                      Institute of M icrobiology, C hinese A cademy of Sciences, B eijing,
                      China

> *Screening and C hemical Investigations of B ioactive Se condary Metabolites from Entomogenous Fungi*

09/2000-07/2004   Bachelor i n B iotechnology a t S henyang A griculture U niversity,
                      Shenyang, China

> *Bioactive Peptides Analysis from Beans extract*

Work Experience

07/2007-07/2009   Research assistant w ith P rof. D r. Y ongsheng C he i n I nstitute of
                      Microbiology, Chinese Academy of Sciences, Beijing, China

> ➢ *Screening and Chemical Investigations of Bioactive Secondary*
>   *Metabolites from Entomogenous Fungi*
> ➢ *HPLC instruments maintenance and troubleshooting*
> ➢ *Setup of crude extracts, fractions, and pure compounds library*
> ➢ *Coordinate biological activity evaluation (cooperation)*

Jena, den 29.10.2013

9 Acknowledgement

My supervisor Prof. Dr. Wilhelm Boland gave me this kind opportunity to study in Jena and introduced me to the research field of chemical ecology. I would like to thank him from the bottom of my heart for his kind supervision and insistent support. He never gave up my project and me, even when the project was in the bottleneck situation, and finally his kind support helped me complete my PhD thesis. This PhD thesis couldn't be finished without his smart ideas and intensive discussions. I will never forget about his help for review my publication and this thesis. It is my great pleasure to study under his direct supervision.

I would like to thank Prof. Dr. Georg Pohnert as my second supervisor in Friedrich Schiller University, for his kind discussion and nice suggestions about my project.

I would like to thank Dr. Axel Mithöfer from my heart for his kind supervision in many biological models, for example, the gene expression, calcium ion measurement, when this project was in most difficult situation. He introduced me into the plant physiology field. And he helped me translate the summary into German.

Dr. Heiko Maischak firstly introduced me into the eletrophysiology field and showed me the basic experiments about the black lipid membrane assay, how to write the lab journal properly and kind discussion in the beginning of this project, especially many kind suggestions after his PhD study.

I would like to give my appreciation to Dr. Rita Büchler, not only for her kind help in the experiments. She introduced me into the protein chemistry field and her kind character greatly influenced me. I'll never forget her handshake on my first day in Max-Planck Institute. In the daily life, she helped me read contract and translate into English. Her kind help supported me to overcome many difficulties in the beginning of my PhD study in Jena.

I would like to thank Dr. Daniela Schmidt and Dr. Jeannette Kley for their nice discussions about the protein chemistry and proteomic data analysis, and very nice and clear sample preparation for peptide LC-MS/MS analysis, and very interesting discussions about the German-Chinese culture and explaining me the German culture.

I would like to thank Dr. Jyothilakshmi Vadassery for her kind discussions about my project and introduced me into the plant molecular biology. I thank Andrea Lehr and Sandra Scholz for their kind technical support for many experiments, like phytohormone extract and RT-

I would like to thank all the members in bioorganic department. Because of their routine support and the sharing of ideas, many experiments were done very successfully. I would like to thank all the members in our institute. Because of their hard working, we have good working environment and efficient communication. It is extremely important for everyone in our department.

I would like to thank my Chinese friends in Jena. They gave me many help in life and in scientific research.

Finally I would like give my hearty appreciation to my parents and my younger sister. They always support me to study continuously and give me liberty to follow my interest. With their supporting and expectation, I could successfully complete my PhD thesis.

Selbständigkeitserklärung

Ich erkläre, dass ich die vorliegende Arbeit selbständig und unter Verwendung der angegebenen Hilfsmittel, persönlichen Mitteilungen und Quellen angefertigt habe.

Jena, den 29.10.2013